EVALUATING RAIN GARDENS OF DIFFERENT CONFIGURATIONS AND SCM INFILTRATION TESTING METHODS TO DETERMINE RAIN GARDEN DESIGN AND SITE INVESTIGATION RECOMMENDATIONS

By

Zachary Michael Zukowski

Thesis
Submitted to Department of Civil and Environmental Engineering
College of Engineering
Villanova University
in partial fulfillment of the requirements
for the degree of

MASTER OF SCIENCE/DOCTORATE OF PHILOSOPHY

In

Civil Engineering

April, 2016

Villanova, Pennsylvania

EVALUATING RAIN GARDENS OF DIFFERENT CONFIGURATIONS AND SCM INFILTRATION TESTING METHODS TO DETERMINE RAIN GARDEN DESIGN AND SITE INVESTIGATION RECOMMENDATIONS

By

Zachary Michael Zukowski

Approved: _____

Dr. Andrea L. Welker, P.E., M. ASCE
Professor, Department of Civil and Environmental Engineering
Primary Advisor

Approved: _____

Dr. Robert G. Traver, P.E., D. WRE, F. EWRI, F. ASCE
Professor, Department of Civil and Environmental Engineering
Co-Advisor

Approved: _____

Dr. David Dinehart
Professor, Chairman of Department of Civil and Environmental Engineering

Approved: _____

Dr. Gary Gabriele
Drosdick Endowed Dean, Dean of College of Engineering

Note: Approval page is used for personal bound copies only.
This page is not to be submitted electronically

STATEMENT BY AUTHOR

This thesis has been submitted in partial fulfillment of requirements for an advanced degree at the Villanova University.

Brief quotations from this thesis are allowable without special permission, provided that accurate acknowledgment of source is made. Requests for permission for extended quotation from or reproduction of this manuscript in whole or in part may be granted by the head of the major department or the Associate Dean for Graduate Studies and Research of the College of Engineering when in his or her judgment the proposed use of the material is in the interests of scholarship. In all other instances, however, permission must be obtained from the author.

ACKNOWLEDGEMENTS

TABLE OF CONTENTS

LIST OF TABLES

LIST OF FIGURES

NOMENCLATURE

A area of the soil sample (cm^2)

A_{Bur} area of the UMS KSAT burette (cm^2)

A_O area of the underdrain well cap orifice (4.0×10^{-5} m^2)

b coefficient of a fitted exponential function from the UMS KSAT (s^{-1})

C_D coefficient of discharge for the underdrain well cap orifice (0.57, unitless)

g acceleration due to gravity (m/s^2)

H head above the underdrain orifice centerline (m)

H_w head of water provided from water column (cm)

ΔH hydraulic head difference (cm)

$K_{\circ C}$ temperature-corrected hydraulic conductivity (cm/s)

K_s measured saturated hydraulic conductivity from infiltration testing (cm/s)

L length of soil sample (cm)

Q steady-state flow rate from UMS KSAT Mariotte tube (cm^3/s)

Q_{under} outflow through the underdrain well cap with orifice (m^3/s)

R^2 coefficient of determination

r radius of Modified Philip-Dunne infiltrometer (5 cm)

S_P shift parameter for the underdrain well cap orifice (0.05, unitless)

t time required to infiltrate water through a soil sample (s)

t_{max} time required for all of the water to infiltrate from Modified Philip-Dunne infiltromter (s)

t_{med} time required for half of the water to infiltrate from Modified Philip-Dunne infiltromter (s)

V volume of water infiltrated in soil sample (cm^3)

α volumetric water content correlation constant (unitless)

β volumetric water content correlation constant (unitless)

ε_a dielectric permittivity (unitless)

ε_R temperature-corrected dielectric permittivity (unitless)

$\mu_{°C}$ viscosity of water at the temperature measured during infiltration testing (kg/m-s)

μ_T viscosity of water at desired temperature correction (kg/m-s)

τ_{max} parametric value for the Modified Philip-Dunne infiltrometer (unitless)

ABSTRACT

Rain gardens are vegetated stormwater control measures (SCMs) designed to mitigate stormwater runoff volume. The Pennsylvania Department of Environmental Protection (PADEP), and many other states, set guidelines and recommendations for rain garden site design and site investigations many years ago. The design components include soil media, soil media depth, vegetation, loading ratios, and the condition of the bottom of the rain garden. The research conducted in recent years indicates that a review of these guidelines is warranted. In the last 10 years, the dataset and knowledge of the behavior of rain gardens has expanded.

The focus of this study was to:

- Instrument, monitor, and collected data from four different rain gardens to make new recommendations to rain garden design and construction. A major component of focus was soil media, which involved comparing sites with a high sand content (sites which promote infiltration), to native soils (sites with a high fine-grained content which promote vegetation growth and pollutant removal).

- Perform various infiltration testing techniques used to determine hydraulic conductivity for rain garden design and post-construction performance. The results of these tests were compared to determine if methods other than the double-ring infiltrometer can produce accurate hydraulic conductivity values. The PADEP (2006) recommends using the double-ring infiltrometer to measure hydraulic conductivity prior to rain garden design. However, the double-ring infiltrometer is large, requires a lot of time to install and conduct, and uses a lot of water.

In this study, four rain gardens were selected to compare the different design components and determine how they affect hydrologic performance. The Bioinfiltration Fedigan Rain Garden (FRGI), the Bioretention Fedigan Rain Garden (FRGR), the Bioinfiltration Traffic Island (BTI), and the Pavilion Traffic Island (PTI) were all instrumented and investigated to collect soil and hydrologic data. Data from four storms in the Fall of 2015 was collected and analyzed: two were around 2.54 cm, and two were larger storms closer to the 2-year, 24-hour design storm. To make infiltration testing recommendations, two separate studies were conducted. A single-ring infiltrometer technique developed by Princeton Hydro, LLC was performed at the BTI and compared to the recession rate calculated from instrumentation within the pond since 2003. Seven single-ring infiltrometer tests were conducted to determine if the geometric mean of the results compared to the recession rate, which is considered an area-average hydraulic conductivity measurement of the SCM. Another study used a Modified Philip-Dunne infiltrometer built at Villanova University and compared to the double-ring infiltrometer, single-ring infiltrometer, and a laboratory method called the UMS KSAT. Hydraulic conductivity data from this study was also compared to soil laboratory properties to determine if correlations exist between soil classification properties and hydraulic conductivity.

Data obtained from this study determined that:

- Site design recommendations should not be made for the individual design components; rather, rain gardens should be designed as whole systems. Individual components affect each other, so they should be designed for one other to create a cost-effective, well-performing rain garden. For example, rain gardens with higher impervious drainage area-to-infiltration areas may require deeper soil media depths.

- It is recommended that the native interface not be compacted, native vegetation be used at rain gardens, and native soils or soils with a higher-fine grained content be used to save on design and construction costs.

- The age of rain gardens and the presence of fine-grained material does not limit performance or drastically reduce infiltration during rain events.

- It is recommended that other infiltration testing techniques, such as the single-ring infiltrometer or Modified Philip-Dunne infiltrometer, be used instead of the double-ring infiltrometer. Using these methods can save time and water required, which can save site investigation cost. Furthermore, these techniques are faster, so more can be conducted in the same amount of time. This can result in a better understanding of the hydraulic conductivity of the whole site.

- Future research for rain garden study could include optimization of rain garden overflow and outflow measurements, using native soils instead of engineered media, and remediating compacted native soil interfaces and studying the new performance of rain gardens which had these construction issues.

- Future research includes studying spatial variability of hydraulic conductivity at an SCM, a more in-depth analysis of the effect of organic soil on hydraulic conductivity, determining how many tests are required per square area of an SCM, and further optimization and additional testing trials of the Modified Philip-Dunne infiltrometer.

CHAPTER 1.   INTRODUCTION

This research focuses on the impact of geotechnical and hydrological components of rain gardens and how they affect overall performance. The study also seeks to determine how the soil type, soil classification values, and hydraulic conductivity should be considered, tested, and evaluated in rain garden design and post-construction performance analyses. The use of green infrastructure as a mitigation tool has become important in restoring the hydrologic cycle disrupted by developments. Stormwater control measures (SCMs) are used in urban and suburban areas to mitigate elevated runoff volumes and high peak flow in watersheds. Vegetated SCMs support vegetation as a means to improve water quality and evapotranspiration (ET), which is the combined effect of evaporation and transpiration that removes water from the soil and vegetation. Types of vegetated SCMs include constructed stormwater wetlands, bioswales, tree pits, tree trenches, green roofs, and rain gardens. Rain gardens contain either an engineered or native soil and can promote infiltration and ET, and are becoming more common in urban and suburban areas to mitigate non-point source pollution in stormwater runoff from impervious surfaces. This work focuses on determining how the type of soil, as well as other design components of rain gardens, affects performance.

Rain gardens have many soil and design configurations which can affect performance and water flow parameters. Systems that contain an underdrain and a liner are typically called "bioretention" rain gardens because they "retain" the water in the system for ET from plants. Sites without a liner are called "bioinfiltration" rain gardens because they can infiltrate water into the native soil beneath the rain garden, which can then provide recharge to the underlying aquifer. The difference between the typical bioretention and bioinfiltration rain garden is

fundamentally the speed at which the water moves through the system, and its effect on treatment. Clay soils and liners inhibit infiltration through the rain garden system. Rain gardens that contain a liner and an underdrain rely on slow release mechanisms and may promote ET if they have an upturned elbow. Rain gardens without a liner and an underdrain promote infiltration and ET, although rain gardens with a sandier media may favor infiltration because of how fast water can move through the system. Other aspects of rain garden design can affect performance, including impervious drainage area-to-infiltration area, age of the rain garden, depth of surface storage, and soil type. Soils in rain gardens can be engineered media or sand-native soil mixes. Compaction, which can occur accidentally during construction, can also affect the hydraulic performance of a rain garden.

Optimum design of rain gardens and other green infrastructure has been the subject of research in recent years (Heasom et al. 2006; Stander et al. 2010; Jennings et al. (2015)) which largely focuses on optimizing hydrologic performance. The questions that this thesis seeks to answer (from a geotechnical focus) are what rain garden design parameters affect performance, and which factors should be chosen for design recommendations for rain gardens. This study is necessary because most of the current design guidance is almost 10 years old, and SCM understanding has expanded since then and is continuing to expand with further research (Pennsylvania Department of Environmental Protection 2006, Davis et al. 2009). It is hypothesized that better knowledge of rain garden design can reduce costs and increase hydrologic performance, creating an increase in value of the systems.

Optimizing rain garden design largely focuses on increasing hydrologic performance through the application of infiltration characteristics, thereby potentially reducing the size and cost. Infiltration rates are controlled by soil properties such as soil type, grain size distribution, dry

bulk density, and the soil water characteristic curve (SWCC). Therefore, geotechnical aspects of rain gardens such as soil type and hydraulic conductivity must be considered in design and post construction performance measurements. This thesis also seeks to answer how infiltration characteristics can be used to determine rain garden performance, and which infiltration testing techniques can be used in post-construction testing. This is important because determining appropriate infiltration testing techniques can help reduce costs of testing and increase knowledge of rain garden performance. Overall, this study seeks to provide guidance during the rain garden design phase with recommendations for both design and post-construction infiltration testing.

1.1 Pennsylvania Department of Environmental Protection Guidelines

1.1.1 Stormwater Control Measure Introduction

As an example, the Pennsylvania Department of Environmental Protection (PADEP) released the Pennsylvania Stormwater Best Management Practices (BMP) in 2006 to "to provide guidance, options and tools that can be used to protect water quality, enhance water availability and reduce flooding potential through effective stormwater management" (Pennsylvania Department of Environmental Protection 2006). This manual provides design recommendations for rain gardens and other SCMs, referred to as BMPs in the manual. The PADEP BMP manual guidelines were used in this study to compare to current rain gardens. These guidelines were used to measure rain garden performance, as well as determine what additional specifications may increase hydrologic performance. It is important to note that these guidelines were published a decade prior to this study at the time where research on rain garden performance was sparse. Data from studies such as these can provide more information regarding design guidance, enhancing confirming or replacing the guidelines set forth in 2006.

The PADEP (2006) guidelines state that disturbance of natural soil destroys permeability, so volume reduction is necessary in areas of land development. The PADEP (2006) BMP manual states that the 2-year storm event is used in volume control guidelines because designing for a larger event is not feasible (Pennsylvania Department of Environmental Protection 2006). These guidelines are set to "protect stream channel morphology; maintain groundwater recharge; prevent downstream increases in flooding; and replicate the natural hydrology on site before development to the greatest extent possible" (Pennsylvania Department of Environmental Protection 2006). To reduce the volume of runoff generated from impervious surface, the PADEP (2006) recommends using infiltration, capture and reuse, and vegetation that produces ET, with the primary focus being infiltration. For sites that are greater than 4047 m^2 or for sites that do not require a stormwater storage facility, the total runoff volume should not be greater than that produced from the 2-year, 24-hour event. This is because this design "provides a storage capacity to help reduce the increase in peak flow rates for larger runoff events" (Pennsylvania Department of Environmental Protection 2006). Since most of the rainfall in Pennsylvania occurs in less than 2.54 cm events, designing for the 2-year storm will allow for significant infiltration and ET while minimizing overflow (Pennsylvania Department of Environmental Protection 2006). Furthermore, the typical Mid-Atlantic bank full stream flow occurs between a 1-year and 2-year event, and stormwater data for the typical 2-year event is well documented. This design protocol is titled Volume Control Guideline 1.

The PADEP (2006) states that the peak flow rate should not increase for the 1-year event through the 100-year event. As necessary, additional SCMs can be used to control the peak flow rate, but most SCM designs already control the peak flow rate or use volume controlling detention SCMs to reduce peak flow rates (Pennsylvania Department of Environmental Protection 2006). Using

Volume Control Guideline 1, water quality will be adequately addressed if the SCM designed is sized appropriately and removes water at a feasible rate. Using Volume Control Guideline 2, peak flow reductions and water quality improvements will not be addressed. This could also be done by designing secondary vegetated SCMs (Pennsylvania Department of Environmental Protection 2006).

1.1.2 Rain Garden Design

The PADEP defines a rain garden as "an excavated shallow surface depression planted with specially selected native vegetation to treat and capture runoff" (Pennsylvania Department of Environmental Protection 2006). Rain gardens are often used with other SCMs to improve volume and peak flow reductions and water quality improvements. Rain gardens pool water in a pond and allow water to infiltrate with the vegetation providing a filter for various pollutants. Plants within rain gardens promote ET and create root systems which increase infiltration within the soil media (Pennsylvania Department of Environmental Protection 2006). Vegetation improves water quality by taking up pollutants from runoff entering the rain garden. Sediments are removed at the surface of the pond, and infiltrating water is filtered by the media within the rain garden. Water can be stored in the soil media to be used by vegetation or the pond to infiltrate into the media (Pennsylvania Department of Environmental Protection 2006). Figure 1.1 and Figure 1.2 depict a typical rain garden design. These figures represent bioinfiltration rain gardens, since they do not contain a liner and allow free infiltration into the native soil layers and underlying aquifers beneath. Bioretention rain gardens would be similarly designed and contain a liner and an underdrain to remove runoff from the system. These may be necessary in certain situations where infiltration is not desired, such as near slopes, mines, or karst topography (Pennsylvania Department of Environmental Protection 2006).
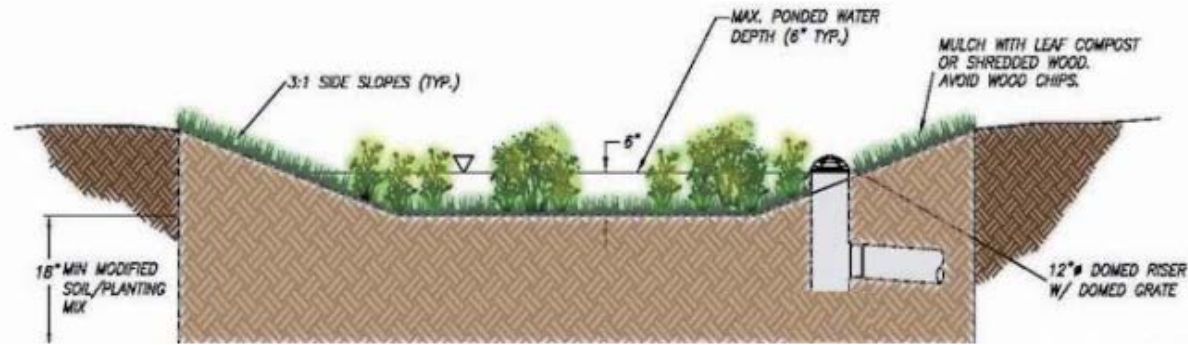
Figure 1.1 A typical rain garden design (Pennsylvania Department of Environmental Protection 2006)
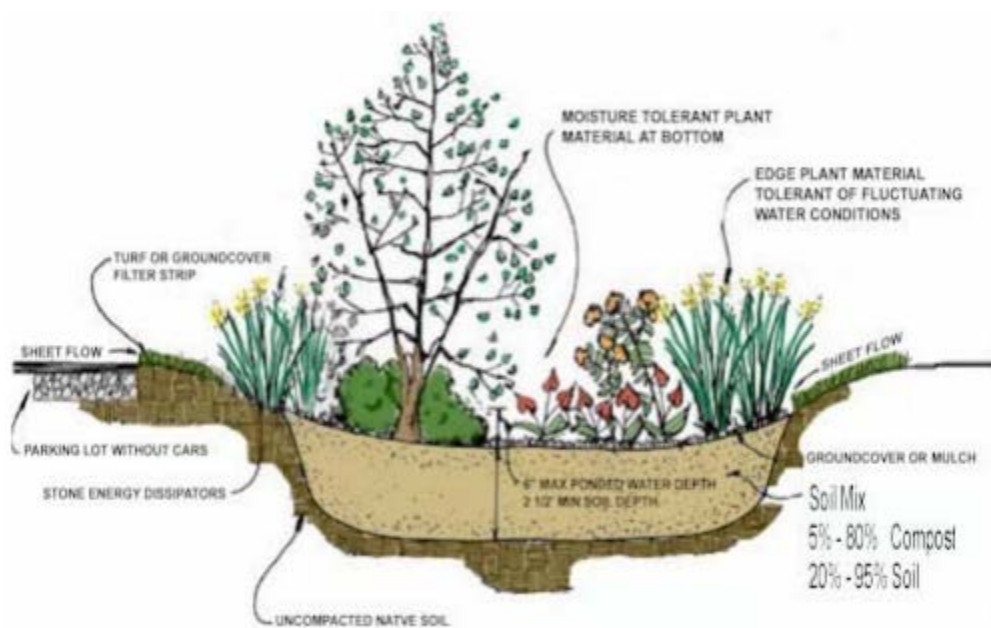
Figure 1.2 A typical rain garden design with a typical soil mix range (Pennsylvania Department of Environmental Protection 2006)

Rain gardens are classified as a Structural SCM because they only mitigate stormwater runoff. Rain gardens (and especially retrofit-designed rain gardens) act to reduce peak flow rates and high runoff volumes that exist due to impervious infrastructure. SCMs that prevent the creation of stormwater runoff are considered Non-Structural SCMs (Pennsylvania Department of

Environmental Protection 2006). Rain gardens can reduce runoff volumes with infiltration and ET, and this ET produced can help replace the portion lost during development, returning the site to its original hydrologic characteristics. Rain gardens can also decrease temperature of stormwater runoff before it reaches local waterways. In addition to the hydrologic improvements, rain gardens improve the aesthetics of a site and provide a natural habitat for a variety of native wildlife (Pennsylvania Department of Environmental Protection 2006).

Pretreatment for rain gardens is considered an option, and flow can enter via sheet flow, trench drains, inlets, curb cuts, and roof leaders, as long as the water enters at a slow enough velocity that erosion does not occur. Once in the pond, water is temporarily stored as it infiltrates into the media and evaporates. Ponding depths are shallow for both safety and aesthetics, yet are deep enough to allow sediments to be removed from the stormwater runoff (Pennsylvania Department of Environmental Protection 2006). The organics within the rain garden act as a filter to improve water quality, protect the engineered media from erosion, and provide plants water to prevent them from wilting. An overflow system, such as a weir box or riser, should be implemented to remove water when the storage of the rain garden is exceeded (Pennsylvania Department of Environmental Protection 2006). This overflow system should provide controlled outflow during larger, more extreme storm events that fill the rain garden system. During these events, water should overflow and move from the pond into the designed overflow system. An underdrain is an optional component of rain gardens, but should be used when liners to remove water from the rain garden when storage is full. Other optional considerations include the use of a gravel or sand bed beneath the engineered media, which can be used to increase the storage volume (Pennsylvania Department of Environmental Protection 2006).

Furthermore, the manual states that rain gardens can be used in a variety of situations, usually for a portion of a site rather than the whole site, including residential and urban environments. Since rain gardens are used in a multitude of situations, including retrofit designs for existing sites, SCM design varies. Generally, native soils beneath rain gardens should have a hydraulic conductivity between 7.06×10^{-5} cm/s and 7.06×10^{-3} cm/s; however, rain gardens designed with an underdrain can be used if the hydraulic conductivity is lower than 7.06×10^{-5} cm/s (Pennsylvania Department of Environmental Protection 2006).

The PADEP (2006) makes the following recommendations for rain garden design:

- Rain gardens should have a maximum impervious drainage area-to-infiltration area of 5:1 and a maximum total drainage area-to-infiltration area of 8:1 (Pennsylvania Department of Environmental Protection 2006).

- Rain gardens should have a maximum ponding time of 72 hours and have a maximum ponding depth of 0.15 m (Pennsylvania Department of Environmental Protection 2006).

- Rain gardens should provide at least 0.45 m of engineered media for vegetation (Pennsylvania Department of Environmental Protection 2006).

- Rain gardens should be at least 0.61 m above the seasonally high water table and minimum depth of bedrock (Pennsylvania Department of Environmental Protection 2006).

- Rain gardens should provide gradual slopes with the maximum being 3:1 and 2:1 being considered acceptable in certain situations (Pennsylvania Department of Environmental Protection 2006).

These design guidelines set forth by the PADEP were created almost 10 years ago and the goal of this study was to update these parameters. The rain gardens selected intentionally do not

follow these exact design components. When placing the rain garden soil, it may be necessary to place more than the minimum or desired depth to account for settlement (Pennsylvania Department of Environmental Protection 2006). Rain garden surficial soils can settle over time, which increases the ponding depth above the design limit unless additional soil is placed.

The PADEP (2006) rain garden soil media design recommendations are as follows:

- The planting media should be a loam soil capable of providing both plant growth and infiltration. Planting soil should be 20%-30% organic material and 70%-80% soil, and storage soils should contain less than 10% clay and 5-10% organic material (Pennsylvania Department of Environmental Protection 2006).

- The soil should contain small amount of clay or fine-grained soils to absorb pollutants and retain water, which is beneficial to vegetation (Pennsylvania Department of Environmental Protection 2006).

- Geotextiles can be used as necessary to protect the structure of the engineered media by preventing the migration of fines through the system, which can change the soil media and clog areas of the rain garden and native soil (Pennsylvania Department of Environmental Protection 2006).

- Shredded mulch or compost depth should be between 5.08 cm and 7.62 cm; larger depths prevent oxygen flow and shallower depths do not prevent erosion (Pennsylvania Department of Environmental Protection 2006). Additionally, wood mulch chips should not be used because they float at the water surface during ponding events (Pennsylvania Department of Environmental Protection 2006).

- Porosity should be considered, since this will dictate the storage within the system. While the storage within engineered media will vary based on soil type and compaction, at least

50% of the total storage must be surface storage volume (Pennsylvania Department of Environmental Protection 2006).

The PADEP BMP manual (2006) defines a rain garden failure as the inability to perform as expected, which can include infiltration, vegetation growth, pollutant removal, and volume and peak flow rate reductions. Failures often occur from compaction, sediment clogging, lack of pretreatment of runoff, improper rain garden maintenance, and poor design components (Pennsylvania Department of Environmental Protection 2006). The PADEP (2006) states that if a rain garden infiltration component fails, it should be designed in such a way that storage and peak flow reductions can still occur during extreme events or smaller frequent rainfall events.

1.1.3 Compaction and Porosity at Rain Gardens

Prior to rain garden construction, it is necessary to determine protected areas and minimal disturbance areas. Protected areas are those which any compaction by disturbance is forbidden, and minimal disturbance areas are those which only necessary traffic and disturbance is permitted (Pennsylvania Department of Environmental Protection 2006). Compaction can result in slower infiltration rates, which hinders the volume of reduction and peak flow rates, as well as water quality improvement measures (Pennsylvania Department of Environmental Protection 2006). Figure 1.3 depicts the difference between loose soil and compacted soil.
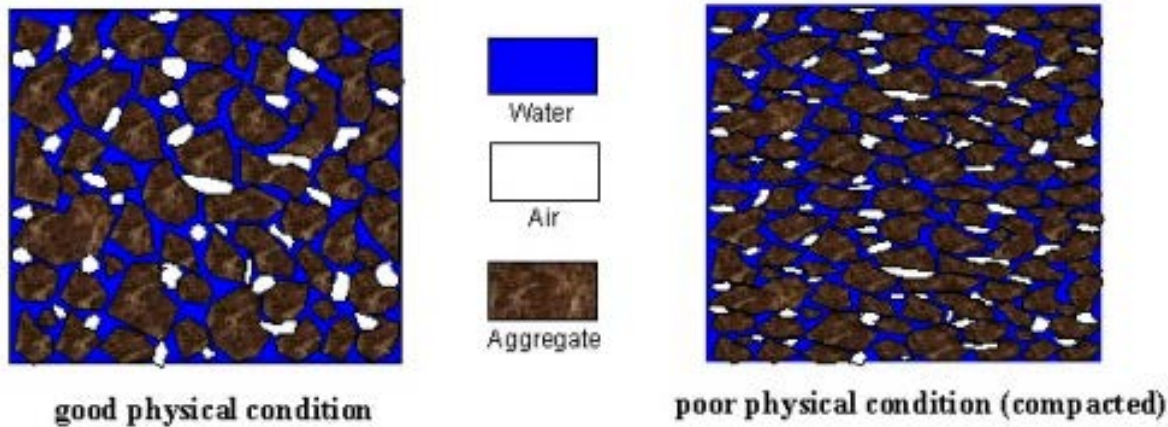
Figure 1.3 The difference between soil in its normal state and a compacted soil (Pennsylvania Department of Environmental Protection 2006)

Compaction during construction can be reduced by marking or fencing off protected and minimal disturbance areas. These areas should also be protected from sediment and erosion (Pennsylvania Department of Environmental Protection 2006). Finally, compaction can be reduced if the engineered media and native soil are tilled at the interface. Placing a small amount of engineered media onto the native soil and tilling the interface can reduce compaction and allow for more infiltration into the native soil (Pennsylvania Department of Environmental Protection 2006). Tilling is the process of mixing and circulating at the appropriate depth to introduce air within the soil, improving infiltration characteristics. Tilling loosens the soil and mixes the two types together, creating a new interface layer. Maintenance within an SCM that could cause compaction should be minimal. Minimizing compaction prior to, during, and after construction at an SCM can reduce costs by reducing the potential for the need to restore soils to a lower-density state, as well as provide a better habitat for vegetation growth (Pennsylvania Department of Environmental Protection 2006). This can especially be the case in rain gardens, when native soils beneath engineered media may need to be restored. This is more costly and more difficult to conduct at deeper depths.

Soils can become compacted from vehicular or foot traffic through the rain garden, or over time due to physical and chemical processes (Pennsylvania Department of Environmental Protection 2006). Compaction reduces porosity, which reduces infiltration the possibility of root growth within the system. Soil amendment types include tilling or mixing with either sand or compost. Mixing with sand can promote infiltration, and adding compost can promote plant growth by releasing nutrients and increasing the water held by the soil (Pennsylvania Department of Environmental Protection 2006). For retrofit SCMs, tilling is the recommended form of soil amendment, and its effect on the soil can be determined by measuring bulk density prior to and after the tilling process (Pennsylvania Department of Environmental Protection 2006). Tilling can only be performed on dry soils, and should not involve the use of equipment that could compact the soils beneath the originally compacted depth, such as disks.

Bulk density testing can be used to quantify the compaction of the soil, which is related to the ability of the soil to absorb water. Bulk density testing should be conducted and used in design of an SCM. Urban areas may have high bulk densities which limit infiltration; however, vegetation and soil improvement procedures can be used to lower bulk density and increase infiltration (Pennsylvania Department of Environmental Protection 2006). Bulk density can be measured in the field or laboratory using many methods and correlate to the soil type. For example, fine-grained materials are not as heavy as coarse-grained materials and thus have a lower bulk density; however, fine-grained materials tend to create a lower hydraulic conductivity. Therefore, it is necessary for field personnel to identify soil types in the field or bring samples to a laboratory for sieve analyses which are used to classify soils (Pennsylvania Department of Environmental Protection 2006).

Macroporosity, which occurs due to plant roots, insects, weathering, freeze-thaw cycles, shrinkage, and chemical processes can increase infiltration (Pennsylvania Department of Environmental Protection 2006). These macropores, while difficult to measure quantitatively, can actively improve infiltration SCMs by providing a means for faster infiltration through the system. Macroporosity can also occur when the soils in the SCM are disturbed during planting and other equipment installation. Since macroporosity can be beneficial to rain gardens, bulk density tests should be used to verify high compaction levels before soil restoration is performed (Pennsylvania Department of Environmental Protection 2006).

1.1.4 Rain Garden Vegetation

Rain gardens should implement native vegetation that requires minimal maintenance and can survive in wet and dry periods. Re-vegetating can be costly and clippings from vegetation can create biomass, which may result in pollutants that effect water quality (Pennsylvania Department of Environmental Protection 2006). Additionally, minimizing the application of pesticides, herbicides, and fertilizers used to maintain non-native species can reduce nitrogen and phosphorus loads at the system. As native vegetation grows, it can provide better runoff volume reductions and peak flow rate reductions than typical landscapes (Pennsylvania Department of Environmental Protection 2006). Over a long period of time, native species can grow to be much stronger and denser, which can increase infiltration and ET at an SCM. Particularly, woodland species reduce volumes and peak flow rates much more than meadow species; however, woodland native vegetation does take longer to grow than meadow vegetation (Pennsylvania Department of Environmental Protection 2006). It is recommended that three species of shrubs and trees be planted and at a shrub-to-tree ratio of 2:1 or 3:1 (Pennsylvania Department of Environmental Protection 2006). The native plants should be tolerant of common pollutants,

such as salt if the rain garden is present in an area where snow occurs during the winter. The PADEP (2006) mention that planting a variety of native species can provide seasonal color and a habitat for local species, but SCMs should be routinely checked for invasive species. Native species should be planted during the final stages of construction, and the vegetation should be flagged or protected as needed to allow for growth (Pennsylvania Department of Environmental Protection 2006). The PADEP (2006) also recommends planting in mid-March through June and mid-September through mid-November.

1.1.5 Rain Garden Maintenance

Maintenance of rain gardens is required as stated by the PADEP (2006). Mulch should be spread when it is deemed necessary or once every 2 or 3 years, and watering may need to occur during dry periods (Pennsylvania Department of Environmental Protection 2006). Twice per year, rain gardens should be inspected for erosion, sediment clogging of the engineered media, and vegetation health (Pennsylvania Department of Environmental Protection 2006). Despite the required maintenance, the cost of rain garden maintenance is generally lower than other SCMs, decreasing the net cost of rain garden construction cost, which is between \$175 and \$245 per cubic meter (Pennsylvania Department of Environmental Protection 2006).

1.1.6 Stormwater Control Measure Site Investigations

The PADEP BMP manual (2006) recommends adequate site investigation and soil evaluation early in the design phase of an infiltration SCM such as a rain garden. After a preliminary site plan is created with potential SCM locations considered, soil evaluation and site investigation should be conducted to amend designs based on the data obtained from field testing and sampling. Soil sampling and identifications should be carried out by a professional with qualifying experience to observe any conditions which may affect SCM performance that could

not be obtained via infiltration testing (Pennsylvania Department of Environmental Protection 2006). Test pits, soil borings, and infiltration tests should be conducted throughout the site to verify previous site knowledge. Risk areas and areas of poor SCM performance should be identified (Pennsylvania Department of Environmental Protection 2006). If a site has a suitable area for an infiltration SCM, it should not be considered for the building program and no exemption should be made to use this area of the site for any other use (Pennsylvania Department of Environmental Protection 2006).

The site investigation process involves background evaluations, test pit observations, infiltration testing, and design considerations (Pennsylvania Department of Environmental Protection 2006). The background evaluation should consider soil maps and geology of the site, which includes previous test pit and soil boring observations. Test pits are considered more appropriate for SCM investigations because they provide a larger visual area than soil borings. Test pits are trenches which are usually dug with a backhoe excavator and are 0.76 m to 0.91 m wide and 1.83 m to 2.29 m deep (Pennsylvania Department of Environmental Protection 2006). Test pits should note soil types and horizons as well as the depth of the water table and the depth of bedrock (Pennsylvania Department of Environmental Protection 2006). It is recommended that infiltration SCMs not exceed 2.29 m in depth; however, in areas of little to no risk, deeper SCMs and deeper test pit evaluations can be considered. Soil samples should be collected from the various soil horizons for laboratory analyses. The PADEP (2006) recommend that test pits and SCMs not be placed near swales, the tope of slopes, and karst topography. The guidelines also recommend that 1 test pit per lot be dug within 7.62 m of the SCM for single-family residential developments, 1 test pit per SCM area or 4047 m^2 be dug for multi-family residential developments, and multiple test pits evenly distributed with 4 to 6 test pits dug per 4047 m^2 of

SCM area for larger infiltration SCMs (Pennsylvania Department of Environmental Protection 2006). The PADEP (2006) recommends that more or less test pits can be dug based on the judgment of the field engineer or the variability of the soil at the site; however, it should be noted that disturbance and compaction by created by test pits could cause adverse effects on SCM performance.

The PADEP (2006) BMP manual recommends conducting a field infiltration test when temperatures are above freezing and not within a day of a rainfall event greater than 1.27 cm. The PADEP (2006) recommends conducting at least one infiltration test at the proposed bottom of the SCM and at least two infiltration tests in each test pit unless the results of the infiltration tests vary greatly. If this is the case, it is recommended to conduct additional infiltration tests and the highest infiltration rate recorded during the testing should be held out of design calculations (Pennsylvania Department of Environmental Protection 2006). The PADEP (2006) recommends using the geometric mean to determine the average hydraulic conductivity values when multiple infiltration tests are performed. Laboratory infiltration tests are not recommended by the PADEP (2006) because they are discreet samples which may not represent the heterogeneity of the site. Testing parameters such as test depths, SCM depth, and number of tests can be modified by the on-site engineer in the field based on judgment.

The PADEP (2006) guidelines outline procedures for double-ring infiltrometer testing and percolation testing. The PADEP (2006) also does mention that other procedures such as the constant head double-ring infiltrometer, constant head permeameter, Guelph permeameter, and casing method can be used. The guidelines recommend using the double-ring infiltrometer for infiltration SCMs because they ensure vertical movement of water through soil while the percolation test method allows water to move in multiple dimensions. The outer ring of the

double-ring infiltrometer prevents water from the inner ring from moving anywhere but in the vertical direction. Percolation testing and other test methods can be used if appropriate formulas are used to calculate hydraulic conductivity.

The double-ring infiltrometer is a two concentric ring system with the inner ring being 50% to 70% of the diameter of the outer ring (Pennsylvania Department of Environmental Protection 2006). These systems can be either purchased or designed and built by engineers that intend to use them. The PADEP (2006) recommends placing a board on the rings and driving them at least 5 cm into the soil. The outer ring should be driven first and the inner ring should be placed into the center of the outer ring and driven next, with the bottom of the two rings being located at the same depth. A presoak period then occurs for 1 hour, with water being added in 0.5 hour increments (Pennsylvania Department of Environmental Protection 2006). Both rings are then filled with a minimum water level of approximately 10 cm, and the drop in water level during the last 0.5 hour interval should be measured to dictate the rest of the testing elements. If the drop in water level within the inner ring is about 5 cm or more during the last 0.5 hour of the presoak period, inner ring measurements are taken every 10 minutes. If the drop in water level is less than 5 cm, measurements of water level in the inner ring are taken every 30 minutes (Pennsylvania Department of Environmental Protection 2006).

The drop in water level in the inner ring is recorded as dictated by the presoak. After each reading is taken, the water levels are filled to the previous height. This procedure is performed until eight readings are recorded or until the rate stabilizes, which occurs when the drop difference between readings is around 0.64 cm for four sequential measurements (Pennsylvania Department of Environmental Protection 2006). The PADEP (2006) states that the drop that

occurs during the eighth reading or the average of the four stabilized readings is considered the infiltration rate for that particular test location.

While other infiltration test methods can be used, the PADEP (2006) strongly makes the case for the double-ring infiltrometer. The guidelines set forth by the PADEP do outline the procedure for the percolation testing method as well; however, for infiltration SCMs such as rain gardens the double-ring infiltrometer is considered to be more accurate in the guidelines. It is necessary to note that this procedure was outlined almost 10 years ago. The American Society for Testing and Materials (ASTM) has since updated the double-ring infiltration testing procedure as well. The double-ring infiltrometer is depicted in Figure 1.4. The double-ring infiltrometer can be difficult to install, use a large amount of time and effort to install and conduct, and requires a large amount of water. Additional test methods which are easier to install, faster to conduct, and use less water have been developed and used since the PADEP guidelines were set forth in 2006.

Figure 1.4 A double-ring infiltration test

1.2 Rain Garden Comparison Study

The guidelines set forth by the PADEP manual were based on limited datasets before SCM literature greatly increased in the 2000s. While much more is known about how SCMs behave than was known in 2006, more knowledge is still necessary. New concepts and ideas that have been investigated since 2006 indicate that studies such as this should be performed to determine new recommendations on rain garden design. Studying rain gardens containing different design components creates a unique opportunity to determine how certain parameters effect hydrologic performance.

To contrast different rain garden design parameters, three rain garden sites were chosen on Villanova University's campus and compared during four storm events that occurred during the fall of 2015. These rain gardens were instrumented with pressure transducers, soil moisture sensors, sharp crested V-notch weirs, volumetric weirs, and other water monitoring systems to determine how they behave hydrologically. The rain gardens chosen have different design aspects including soil media type, impervious drainage area-to-infiltration area ratio, age, compaction of the native soil interface, and the presence of a liner and underdrain. These rain gardens were analyzed and compared to PADEP criteria to determine the importance of specific design components for rain garden design. The first rain garden chosen was the Bioinfiltration Traffic Island, which is the oldest rain garden on Villanova's campus and is depicted in Figure 1.5. The Bioinfiltration Traffic Island has been the subject of many studies (Heasom et al. 2006; Emerson 2008; Emerson and Traver 2008; Gilbert Jenkins et al. 2010; Machusick et al. 2011, and Nemirovsky et al. 2015), and its performance has been monitored continuously since 2003. All of these studies occurred after the PADEP guidance was set forth in 2006. The soil mix is

unique compared to the other sites and impervious drainage area-to-infiltration area is the largest in the study.

Figure 1.5 The Bioinfiltration Traffic Island (photograph courtesy of Villanova Urban Stormwater Partnership)

The Fedigan Rain Gardens were also chosen for this study because they are a rain garden cluster, with one rain garden being a bioretention rain garden and the other being a bioinfiltration rain garden. The Fedigan Rain Gardens have an engineered media with a high sand content, and have the lowest impervious drainage-area-to-infiltration area in this study. The Fedigan Rain Gardens are shown in Figure 1.6. In Figure 1.6, the bioretention rain garden is on the left and the bioinfiltration rain garden is on the right.

Figure 1.6 The Fedigan Rain Gardens (photograph courtesy of Villanova Urban Stormwater Partnership)

Finally, the Pavilion Traffic Island was selected for the comparison study because it was found to be behaving differently than expected. Despite having an engineered media with the most sand of all of the rain gardens in this study, long periods of ponding and a perched water table were observed at the Pavilion Traffic Island, making it behave more like a "failed" rain garden. For this study, the Pavilion Traffic Island was selected to determine design aspects which may have led to this "failure," as well as determining how the rain garden performs despite its limitations. The Pavilion Traffic Island is depicted in Figure 1.7.

Figure 1.7 The Pavilion Traffic Island

1.3 Infiltration Testing Comparison Study

For this part of the study, various infiltration testing techniques were analyzed and compared to determine if testing methods other than the double-ring infiltrometer method described in the PADEP manual can be used to accurately determine hydraulic conductivity at a rain garden. This is important because using an appropriate infiltration testing technique can help create recommendations to improve the design rain gardens and have a better understand the performance of a rain garden post-construction. Determining a feasible alternative to the double-ring infiltrometer can also save cost, time and effort. Much of the data displayed in this portion of the study are currently being considered for publications.

This part of the study aims to make recommendations on infiltration testing at rain gardens by conducting infiltration testing investigations and comparing different methods. The first investigation compared test results from a simple, inexpensive single-ring infiltrometer

conducted at the BTI to the average recession rate at the BTI for its lifetime. The recession rate is how quickly water is drained from the pond after a rain event. This is considered the most accurate hydraulic conductivity measurement of an SCM, since the rain event would act as a large-scale test covering all portions of the SCM. The purpose of this test was to determine if the single-ring infiltrometer could accurately predict the hydraulic conductivity considering that the average recession rate is the average hydraulic conductivity at the BTI. This is done because the single-ring infiltrometer is much more inexpensive purchasing water monitoring equipment. Therefore, if the single-ring infiltrometer is deemed accurate, it can be used as a feasible infiltration testing technique prior to and post-construction of an SCM. Since it is smaller and more inexpensive than the double-ring infiltrometer, more can be conducted in the same amount of time, which allows for more of the SCM to be tested. Figure 1.8 depicts a single-ring infiltration test and Figure 1.9 shows the BTI ponded after a rain event, which provides a large-scale infiltration test.

Figure 1.8 A single-ring infiltrometer test

Figure 1.9 The BTI ponded during a rain event (photograph courtesy of Villanova Urban Stormwater Partnership)

The second investigation aims to compare a many different infiltration testing techniques at the BTI, the FRG, and a native soil site in Upper Moreland Township, PA. The main purpose of the study is to determine if an infiltrometer built at Villanova University compares to field and laboratory hydraulic conductivity testing techniques. If the infiltrometer built at Villanova, known as a Modified Philip-Dunne infiltrometer, compares favorably to the double-ring infiltrometer and other methods, it can be used to determine hydraulic conductivity in place of the much larger double-ring infiltrometer. Figure 1.10 depicts a Modified Philip-Dunne infiltrometer which was built at Villanova University. This infiltrometer is outfitted with electronic components to measure water and collect GPS measurements. This allows the test to be conducted without a field engineer being at the infiltrometer to measure water drop, and allows for ease of plotting test locations afterwards. In addition to the field methods compared, a laboratory method known as the UMS KSAT was used in the study to determine how it compared to the field methods. Figure 1.11 shows the UMS KSAT laboratory testing apparatus. The study used double-ring infiltrometer tests, single-ring infiltrometer tests, Modified Philip-Dunne infiltrometer tests, and UMS KSAT laboratory tests to determine if the Modified Philip-Dunne infiltrometer is an appropriate test method for measuring the hydraulic conductivity of an SCM. Table 1.1 provides the tests conducted at each location. More Modified Philip-Dunne tests can be conducted than the double-ring infiltrometer in the same amount of time because the procedure for the Modified Philip-Dunne infiltrometer is faster to install and requires less water than the double-ring infiltrometer. This allows better understanding of the hydraulic conductivity at an SCM. Furthermore, the addition of electronic measuring components allows for easy data collection, manipulation, and storage.

Figure 1.10 The modified Philip-Dunne infiltrometer (photograph courtesy of Villanova Urban Stormwater Partnership)

Figure 1.11 The UMS KSAT (Decagon Devices 2016)

Table 1.1. The infiltration tests conducted at each site

Test Type	FRG	BTI	Upper Moreland
Double-Ring Infiltrometer	3	-	2
Single-Ring Infiltrometer	-	7	-
Modified Philip-Dunne Infiltrometer	4	2	3
UMS KSAT	2	-	6

The overall goals of this project were to determine how geotechnical and hydrological factors affect rain garden performance, as well as determine how performance measures can be considered for rain garden design and post-construction performance verification. Rain gardens of different designs and various infiltration testing techniques were evaluated in this study. The PADEP (2006) recommendations need to be adjusted based on new knowledge of rain gardens and infiltration testing techniques which have developed within the last 10 years. Data collected in this study was used to make these design and site investigation recommendations to the PADEP (2006) BMP Manual.

CHAPTER 2.   LITERATURE REVIEW

2.1 Rain Garden Performance Factors

There are many factors that influence infiltration at rain gardens. In the beginning of a storm, infiltration rates are typically higher; however, the infiltration rate typically drops during the event and decreases asymptotically. The hydraulic conductivity of the soil, soil suction pressure head, and initial moisture deficit all have an effect on the infiltration of runoff at a rain garden during a storm event. Of these factors, Braga et al. (2007) found that hydraulic conductivity has the greatest effect on infiltration in an infiltration bed, with soil suction pressure head and initial moisture deficit variably effecting infiltration. Braga et al. (2007) also found that the hydraulic conductivity of the flow in an infiltration bed remains constant during each storm event as it moves through the bed. Temperature also has a significant effect on the infiltration rate during storm events. Lin et al. (2003) suggested that there could be a 40% difference in infiltration between summer and winter months due to a change in viscosity. Similarly, Braga et al. (2007) found that infiltration in a basin reduced by 56% in the winter months. Higher temperatures decrease viscosity, leading to more water movement and thus increasing hydraulic conductivity (Braga 2007; Emerson and Traver 2008). Additionally, Constantz (1982) found that a decrease in surface tension due to an increase in temperature can also lead to higher infiltration rates.

The soil water characteristic curve, which is a measure of the matric suction at different levels of saturation of a soil, is also frequently used to determine the unsaturated flow during infiltration. However, at higher saturation, the air phase in an unsaturated soil system becomes discontinuous, making this method less accurate (Bicalho et al. 2000). These discontinuous air pockets are formed when water begins to fill smaller pores first during infiltration, which results

in the larger pores being blocked (Chen et al. 2014). Entrapped air, though hard to predict, can cause dramatic instability in infiltration rates and hydrologic performances with higher entrapped air leading to lower infiltration rates. The amount of entrapped air is a non-linear function based on the lowest degree of saturation that occurs during the wetting-drying cycle, which occurs when the matric suction is highest (Chen et al. 2014). Entrapped air may also be a function of temperature. Hopmans and Dane (1986) found that at higher temperatures, less entrapped air was observed. This, combined with the decrease in viscosity, can act to increase the infiltration rate (Hopmans and Dane 1986). Wang et al. (2010) conducted experiments to determine how infiltration rates changed in an air-confined infiltration test compared to an air-draining infiltration test. In the air-confining tests, it was found that air entrapment increased on average by 7%, and the infiltration rates were up to ten times slower than those observed in air-draining tests infiltration (Wang et al. 2010). Wang et al. (2010) also found that there is a cyclic process of escaping air during infiltration. Infiltration rates increased during periods of air escape, and conversely decreased when air escape stopped (Wang et al. 2010).

Macroporosity within a rain garden can be caused by a number of different processes. Wormholes, freeze-thaw cyclic cracks, and roots can cause macropores which increase infiltration (Weiler 2005). Like entrapped air, the presence of macropores in soils can cause instability in water infiltration into soil. Macropores are typically greater than 1 mm in diameter (Watson and Luxmoore 1986; Luxmoore 1981). Dunn and Phillips (1991) found that flow through macropores can constitute 73% to 83% of flow in the soil matrix during infiltration. Air compression can cause fingering, which can lead to a higher infiltration rate (Wang et al. 2010). In an air-confined infiltration model, Wang et al. (2010) found that fingering occurred and caused an unstable infiltration, while stable flow was observed in the air-draining model. Dual-

porosity models, which consider the water flow caused by macropores and micropores, can be used to determine the hydraulic conductivity (Nachabe 1995). Since water flow through macropores is a function of gravity, one-directional flow as seen in the double-ring infiltrometer test is unnecessary (Nachabe 1995). Considering this and the possible negative impact of driving the double-ring infiltrometer on the soil structure, Nachabe (1995) used a tension infiltrometer to determine the effects of macropores on infiltration. Nachabe (1995) found that the infiltration rate in macropores was 3.6 times that of the soil matrix, with macroporsity decreasing with depth. This is likely because plant roots create macroporosity. If plant roots do not extend to deep depths, the soil matrix likely has a higher homogeneity.

While macroporosity may play a role in infiltration, some have argued that for conservative design, macroporosity should not be considered in determination of soil hydraulic properties for SCM design. Lee et al. (2015) states that while flow from macroporosity may be present in SCMs, it is a reasonable to assume that soil matrix flow dominates when macroporosity data is not available. This is because natural heterogeneity of soil and soil compaction are likely present to limit macropore flow. Furthermore, macroporosity may or may not be present and therefore should not be relied upon in the design phase. Lee et al. (2015) described a method of appropriately filtering soil hydraulic properties from the United States Department of Agriculture (USDA) UNSODA database. This method filtered high saturated hydraulic conductivity values from the database which were deemed to be unrealistic due to macropore-flow. By removing these particular samples from the datasets, the Modified van Genuchten-Mualem model can be used for partially and variably saturated soils (Lee et al. 2015).

Soil compaction also has a great deal of influence on infiltration and drainage, particularly at rain gardens where loose soils are typically required. Soils with higher bulk densities can slow the

infiltration of water. This can occur in the rain garden soil itself or underlying soil. Soil compaction in the underlying layer may be caused by construction activities at the site, or other site activities that could cause soil disturbances. The wetting and drying of soils in a rain garden can cause compaction over a long period of time. A study conducted in New Jersey found that soil texture played a much larger role in the compaction of a rain garden soil than age (Yergeau and Obropta 2013). Yergeau and Obropta (2013) recommend performing soil surveys and classifying soils based on texture when conducting site investigations for rain gardens. However, Yergea and Obropta (2013) do not mention classifying soil by using Atterberg limits or soil plasticity values.

As part of a study with the Environmental Protection Agency (EPA), Stander et al. (2010) studied the effect of the surface area of a rain garden to determine if it had a direct correlation to rain garden performance. In the study, six rain gardens were constructed with identical drainage areas of 1,180 m^2: two with a surface area of 26 m^2, two with a surface area of 53 m^2, and two with a surface area of 106 m^2 (Stander et al. 2010). The rain gardens studied have surface areas of 2%, 4%, and 8% of the drainage area (Stander et al. 2010). Each rain garden had an engineered media which contains 98% sand, <1% silt, <1% clay and around 1% organic material (Stander et al. 2010) The engineered media had a depth of 0.86 m and overlaid a geotextile which separated a gravel layer from the engineered media (Stander et al. 2010). Stander et al. (2010) determined that the rain garden surface area did not play a significant role in rain garden hydrologic performance within the tested storm range (2.00 mm to 30.46 mm of rainfall); however, there was a significant and observable difference in wetting front dynamics between the engineered media and underlying soil.

In one study conducted by Jennings et al. (2015), rain garden algorithms were analyzed using meteorological data to compare typical rain garden designs to the typical storms that occur in Ohio. To do this, Jennings et al. (2015) varied the depth of the rain garden, the loading ratios, and the infiltration characteristics. The authors set the hydraulic conductivity of the system to 1.8×10^{-4} cm/s since this is the typical value recommendations specify; the authors also note that recommendations typically state that sites with a lower hydraulic conductivity should install an underdrain (Jennings et al. 2015). The simulations provided by Jennings et al. (2015) show that rain gardens with this hydraulic conductivity reduce 85% of the runoff volume, and rain gardens with a hydraulic conductivity of 0.9×10^{-4} cm/s still reduce about 75% of the runoff volume and leave ponded water in the system only 30% of the time. Simulations conducted by the authors found that rain gardens with a soil depth of 0.30 m would not increase performance over rain gardens with a soil depth of 0.20 m (Jennings et al. 2015). Jennings et al. (2015) determined that rain gardens with a 0.25 m depth reduced stormwater runoff volume by almost 52%, and rain gardens with a depth of 0.30 m reduced stormwater runoff volume by 96%. Further analyses by Jennings et al. (2015) indicated that an impervious drainage area-to-infiltration area of 3:1 is very conservative, and rain gardens with a loading ratio of 5:1 does not increase performance much more than a rain garden with a loading ratio of 10:1. From the analyses, Jennings et al. (2015) determined that rain gardens with a loading ratio of 10:1 reduced approximately 85% of the runoff volume and a rain garden with a loading ratio of 20:1 reduced approximately 60% of the runoff volume. In fact, the authors state that rain gardens with a loading ratio greater than around 5:1 would not accomplish much more runoff reduction because "overflow is inevitable during heavy rainfall events" (Jennings et al. 2015).

Since all of the simulations provided by Jennings et al. (2015) use the typical lowest recommended hydraulic conductivity of 1.8×10^{-4} cm/s, rain gardens with a higher hydraulic conductivity would perform even better than specified. Jennings et al. (2015) states that rain garden design recommendations are usually too conservative and that a rain garden of any size and depth will benefit stormwater by reducing some volume of runoff. Finally, Jennings et al. (2015) states that recommendations should not treat infiltration as a constant; rather, the hydraulic conductivity should be viewed as a component which can change over time due to the buildup of fine-grained material and organic material in rain gardens.

Schlea et al. (2014) also studied the benefit of rain gardens in terms of volume reduction. The authors used five rain gardens which capture street-side runoff in Ohio to determine how they performed during 38 storm simulations (Schlea et al. 2014). The rain gardens studied by Schlea et al. (2014) ranged in size from 18.3 m^2 to 27.7 m^2, had total drainage areas ranging from 869 m^2 to 3,388 m^2, and had hydraulic conductivity values ranging from 3.7×10^{-4} cm/s to 2.7×10^{-3} cm/s (Schlea et al. 2014). Interestingly, the sites studied by Schlea et al. (2014) had higher fine-grained and organic material than typical rain gardens, with soil compositions consisting of 20%-25% sand, 35%-40% silt, 35%-40% clay, and around 20% organic material. The results of the study indicated that the rain gardens reduced stormwater runoff volume by 37% during 8 storms ranging in size from 0.1 cm to 1.7 cm, and outflow only occurred during 26% of the 38 storms simulated (Schlea et al. 2014).

2.2 Infiltration Modeling and Infiltration Testing

Infiltration modeling can be an accurate way to measure the saturated hydraulic conductivity and infiltration rates. The Green and Ampt equation (Green and Ampt 1911) is an approximate solution to the Richards equation (Richards 1931). The Richards equation (1931) is the partial

differential equation that describes water flow through porous media. The Green and Ampt model assumes that the initial porous media moisture content profile is uniform and that there is a sharp wetting front. Philip (1993) removed the final limitation of the Green and Ampt model, which was that the ponding head is zero. Lee et al. (2013) found that Green and Ampt can be modified to address the profile of an SCM to model infiltration. The area-average depth should be used instead of the maximum depth and the maximum value of the infiltrated depth should be used to represent a maximum possible infiltration rate (Lee et al. 2013). To test the accuracy of the Green and Ampt model, Lee et al. (2013) used an instrumented SCM to record recession rates during two storms and compared these to Green and Ampt values when the matric suction was iterated to 250 cm. The minimum, average, and maximum measured infiltration rate was found to be 0.31 cm/h, 0.65 cm/h, and 1.38 cm/h, respectively (Lee et al. 2013). The Green and Ampt minimum, average, and maximum infiltration rate was found to be 0.55 cm/h, 0.72 cm/h, and 1.10 cm/h, respectively (Lee et al. 2013). With this collected data, Lee et al. (2013) found that Green and Ampt can sufficiently model infiltration in a bioinfiltration SCM if the initial matric suction is known. Lee et al. (2013) also found that in the Green and Ampt model, matric suction and porosity should be varied together with matric suction being the free variable.

There are many types of hydraulic conductivity test methods and testing apparatuses. Fernuik and Huag (1990) conducted hydraulic conductivity testing with three different field methods and compared the results to laboratory testing procedures. Considering that the laboratory testing methods were the true values, this would determine if the hydraulic conductivity testing methods result in accurate hydraulic conductivity measurements. The test methods studied by Fernuik and Huag (1990) included the sealed single-ring infiltrometer, sealed double-ring infiltrometer, and air-entry permeameter. The three infiltration testing techniques were tested on sand-bentonite

liners and a sandy clay liner, then compared to triaxial permeameter tests conducted on soil samples of the liners (Fernuik and Huag 1990). Fernuik and Huag (1990) determine that testing for hydraulic conductivity using the sealed single-ring infiltrometer, the sealed double-ring infiltrometer, and air-entry permeameter resulted in accurate values when compared to the laboratory triaxial permeameter tests. Fernuik and Huag (1990) determined that all the testes produced results ranging within one-quarter of an order of magnitude. The authors noted that the single-ring infiltrometer and air-entry permeameter could be conducted faster than the double-ring infiltrometer and were easier to install (Fernuik and Huag 1990). Fernuik and Huag (1990) concluded that the single-ring infiltrometer and air-entry permeameter gave comparable results to the double-ring infiltrometer and the geometric hydraulic conductivity of ten tests of each method accurately produced the same hydraulic conductivity found by the double-ring infiltrometer test (Fernuik and Huag 1990). This study portrays the concept that other infiltration testing methods which are easier and more inexpensive could potentially be used instead of the double-ring infiltrometer test method.

The Modified Philip-Dunne infiltrometer is another type of single-ring infiltrometer (Ahmed et al. 2011a, Gulliver et al. 2008, Ahmed et al. 2011b, Ahmed et al. 2014, Asleson et al. 2008). Ahmed et al. (2011a) determined that the Modified Philip-Dunne infiltrometer is a relatively fast infiltration testing method that requires less water than other infiltration testing methods. Ahmed et al. (2011a) also state that the method is light and can be conducted with minimal training. The authors found that 30 to 40 Modified Philip-Dunne infiltrometer tests plus some general soil property tests can be tested in a single day by a three-man team (Ahmed et al. 2011a). Ahmed et al. (2011a) classify the Modified Philip-Dunne infiltrometer technique as a method for testing the surficial soils at SCMs; however, they do also note that it can be installed in holes such as test

pits to measure the hydraulic conductivity of deeper layers. The authors also state that many

Modified Philip-Dunne infiltrometer tests should be performed to determine the representative

hydraulic conductivity at a site (Ahmed et al. 2011a). Ahmed et al. (2011a) tested the Modified

Philip-Dunne and the double-ring infiltrometer in a vegetated basin at five locations to determine

if the Modified Philip-Dunne infiltrometer produced similar hydraulic conductivity values. The

authors note that both results produce hydraulic conductivity values in the same order of

magnitude, but the double-ring infiltrometer required more water and time in all five cases.

Ahmed et al. (2011a) do note that the results may not be considered a direct comparison because

the double-ring infiltrometer has a larger footprint due to the larger diameter of the outer ring.

The results of these tests are provided in Table 2.1.

Table 2.1. Modified Philip-Dunne testing results compared to the double-ring infiltrometer
testing results (modified from Ahmed et al. 2011a)

Location	Modified Philip Dunne Infiltrometer			Double Ring Infiltrometer		
	K_{sat} (cm/hr)	Time required to perform the test(hr)	Volume of water required to perform the test (L)	K_{sat} (cm/hr)	Time required to perform the test(hr)	Volume of water required to perform the test (L)
1	7.6	1.1	3.2	4.1	3.1	17
2	2.3	3.0	3.3	2.1	3.6	15.3
3	2.6	1.9	3.3	2.7	2.3	14.5
4	25.1	0.2	3.0	24.5	1.7	27.7
5	12.7	0.5	3.6	4.5	2.1	16.4

Additionally, Ahmed et al. (2011a) used commercial software with the Richards equations for

three-dimensional flow to determine how the software-computed Modified Philip-Dunne

infiltrometer results compared to the software results, as well as the software-computed double-ring infiltrometer results. The software indicated that the hydraulic conductivity results produced for the Modified Philip-Dunne infiltrometer were more accurate compared to the software hydraulic conductivity values than the double-ring infiltrometer (Ahmed et al. 2011a). Thus, from this research, the authors determined the Modified Philip-Dunne infiltrometer can be used to assess the performance of SCMs instead of the much bulkier double-ring infiltrometer.

Ahmed et al. (2011b) used the Modified Philip-Dunne infiltrometer and an infiltration model to determine the spatial variability of hydraulic conductivity in a vegetated swale. Since the hydraulic conductivity was predicted to vary throughout the vegetated swale, it was estimated that 20 measurements were necessary to accurately predict the hydraulic conductivity (Ahmed et al. 2011b). Ahmed et al. (2011b) conducted a field test with the Modified Philip-Dunne infiltrometer and determined that a three-man team could conduct this many tests at a vegetated swale in about a half day, which saves time during site investigations. Data collected from the Modified Philip-Dunne has been used to model cumulative infiltration in swales using the Green Ampt (Mays 2005) equation, which helps determine swale performance and infiltration loss in the SCM (Ahmed et al. 2011b, Ahmed et al. 2014).

Gulliver et al. (2008) used the Modified Philip-Dunne infiltrometer as a tool in an approach to assess low impact development (LID) systems. In the study, Gulliver et al. (2008) propose that SCMs be assessed by a visual inspection, infiltration testing, runoff testing, and monitoring. Gulliver et al. (2008) proposed that infiltration testing can help ensure the system is working during construction and post-construction, develop restoration timetables, and evaluate overall efficiency of the SCM. In the study, eight rain garden sites were evaluated using the Modified Philip-Dunne infiltrometer technique. After testing was complete, each site was evaluated

statistically to determine how many infiltrometer tests would be necessary to accurately predict hydraulic conductivity assuming a 95% confidence interval (Gulliver et al. 2008). The result was that the number ranged from 4 to 34 based on the spatial variability of hydraulic conductivity within a rain garden (Gulliver et al. 2008). These results are provided in Table 2.2. Gulliver et al. (2008) also determined that in two of the three rain gardens test with a synthetic runoff test, the time to drain measured by the Modified Philip-Dunne infiltrometer closely matched the time required to drain the water from the synthetic runoff test. The geometric mean of the Modified Philip-Dunne drain times was the value that closely matched the time needed to drain the water from the synthetic runoff test (Gulliver et al. 2008). These results are produced in Figure 2.1. Gulliver et al. (2008) states that the results provided by the Modified Philip-Dunne infiltrometer are only estimations of the drain time, and are best used to determine areas where hydraulic conductivity in a rain garden may be low due to compaction.

Table 2.2. Number of tests required, N, to predict the hydraulic conductivity within 5%, 10%, and 15% of the mean 95% (modified from Gulliver et al. 2008)

Rain Garden	Size	N	5%	10%	15%
Burnsville	28 m^2	24	56	14	6
RWMWD (4)	29 m^2	4	16	4	2
RWMWD (5)	59 m^2	16	45	11	5
U of M, St. Paul	67 m^2	41	26	6	3
Cottage Grove	70 m^2	20	29	7	3
RWMWD (1)	147 m^2	12	45	11	5
Thompson Lake	278 m^2	30	59	15	7
U of M, Duluth	1350 m^2	34	74	19	8
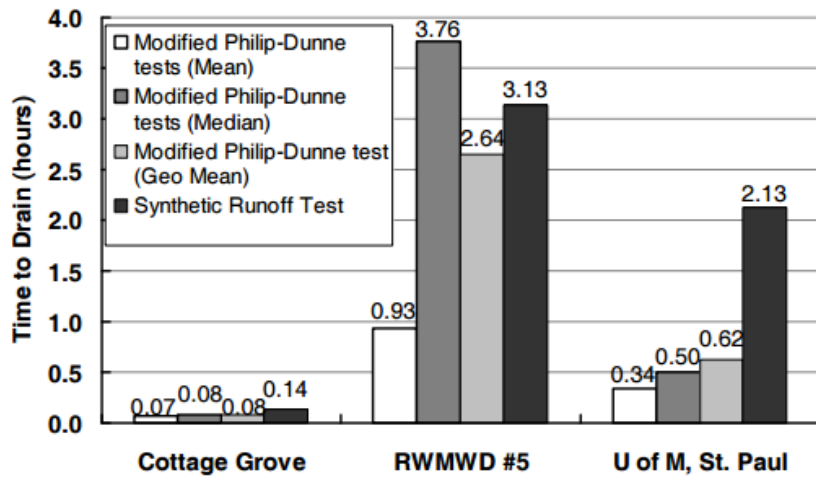
Figure 2.1 Results of the Modified Philip-Dunne infiltrometer testing and synthetic runoff tests (modified from Gulliver et al. 2008)

When conducting infiltration testing, it is important to determine all necessary parameters for proper analyses. Soil type, as well as other soil index properties, should be determined through laboratory testing. Soil-particle analyses are important in understanding infiltration in an SCM (Emerson 2008). Additionally, other aspects of the test play a role in accurately measuring the hydraulic conductivity of soil at an SCM. The ring size, head within the infiltrometer, depth that the infiltrometer is driven into the soil, and temperature of water used in the test all affect the infiltration test (Emerson 2008). Ahmed et al. (2015) found that the geometric mean of the hydraulic conductivity values be used as the overall estimated hydraulic conductivity because results indicated that the hydraulic conductivity is lognormally distributed. The average value of a lognormal distribution is the geometric mean.

CHAPTER 3.   SITE INFORMATION AND INSTRUMENTATION

3.1 Fedigan Rain Gardens

3.1.1   Rain Garden Design and Construction

The Fedigan Rain Gardens (FRG) were constructed in the summer of 2009 as part of Leadership in Energy Efficient Design (LEED) certification renovations to Fedigan Hall, which serves as a sophomore residence hall at Villanova University. These renovations included sensor lighting, geothermal heat, low-flow toilets, and two rain gardens. Since Fedigan Hall does not have a basement, the rain gardens were situated against the building. The bioinfiltration Fedigan Rain Garden (FRGI) is located to the right of Fedigan Hall when facing the entrance and the bioretention Fedigan Rain Garden (FRGR) is located to the left of Fedigan Hall when facing the entrance. Figure 3.1 shows the rain gardens at Fedigan Hall, with the FRGR circled in red and the FRGI circled in blue.

Figure 3.1 The FRGI and the FRGR at Fedigan Hall (Bing Maps 2013)

The rain gardens were constructed similarly, with the major differences being that the FRGR was built with a liner and an underdrain beneath the rain garden and the FRGR has a deeper engineered media depth. Figure 3.2 shows construction of the FRGI, and Figure 3.3 depicts the completed FRGI. Similarly, Figure 3.4 shows construction of the FRGR, and Figure 3.5 shows the completed FRGR. The estimated cost of construction of both rain gardens was around $30,000. Cost of construction was mostly paid for by Villanova University while the instrumentation cost was paid for by the PADEP Growing Greener Grant.

Figure 3.2 Construction of the FRGI at Fedigan Hall (photograph courtesy of Villanova Urban Stormwater Partnership).

Figure 3.3 The completed FRGI at Fedigan Hall (photograph courtesy of Villanova Urban Stormwater Partnership)

Figure 3.4 Construction of the FRGR at Fedigan Hall (photograph courtesy of Villanova Urban Stormwater Partnership)

Figure 3.5 The completed FRGR at Fedigan Hall (photograph courtesy of Villanova Urban Stormwater Partnership)

Additional minor construction elements occurred during 2014 and 2015. Prior to instrumentation installation, conduit was installed to protect wires and cables. Flexible conduit was installed inside the rain garden and polyvinyl chloride (PVC) electrical conduit was installed along Fedigan Hall up to data logger boxes. Figure 3.6 displays conduit being installed at the FRGI and Figure 3.7 depicts conduit installation at the FRGR.

Figure 3.6 Conduit installation at the FRGI

Figure 3.7 Conduit installation at the FRGR

The initial design of the rain gardens called for a maximum of 5:1 impervious drainage area-to-infiltration area ratio. All of the impervious runoff entering the rain gardens comes from the roof of Fedigan Hall. The engineered media used for both rain gardens was designed to contain 85% sand, 10% fines (silts and clays), and 5% organics. Both rain gardens also were designed to have a ponding depth of 0.30 m, and both are designed to empty within 72 hours to mitigate the possibility of mosquito growth at Fedigan Hall. Both rain gardens have a 0.46 m PVC riser for overflow. Within each overflow riser, there is a 0.20 m volumetric weir at the 0.30 m discharge pipe to measure outflow. Outflow is measured when water enters the overflow riser and builds up to the crest of the volumetric weir. As water leaves the riser via the volumetric weir, the flow rate can be measured similarly to the regular V-notch weir at the inlet boxes. Each rain garden also contains a concrete inlet box with a 60° sharp crested V-notch weir to measure inflow. Water from the roof at Fedigan Hall travels to the gutters which take water to the inlet boxes. Figure 3.8 shows one of the inlet boxes and Figure 3.9 shows the overflow riser at the FRGI.

Figure 3.8 A concrete inlet box with a V-notch weir at Fedigan Hall (photograph courtesy of Villanova Urban Stormwater Partnership)

Figure 3.9 The overflow PVC riser, volumetric weir, and discharge pipe (photo credit Villanova Urban Stormwater Partnership). The volumetric weir is located in the discharge pipe that is connected to the overflow riser

The FRGI was designed to have an engineered media depth of 0.46 m. The rain garden was designed to contain a native soil/engineered media interface below the engineered media, followed by native soil. However, during site investigations and instrumentation installation, it was found that the native soil interface is present at approximately 0.35 m. Sieve analyses (ASTM D422) of the engineered media at the FRGI confirmed that the engineered media contained 88% sand, and soil core data found that the media dry bulk density ranged between 1.08 g/cm^3 and 1.39 g/cm^3 with an average value of 1.27 g/cm^3. Soil data for the FRGI can be found in Appendix A. Since no liner or underdrain is present at the FRGI, water infiltrates directly into the native soil where it recharges the groundwater table. The slopes at the FRGI are 3:1 (H:V). Figure 3.10 depicts a design schematic of the FRGI.
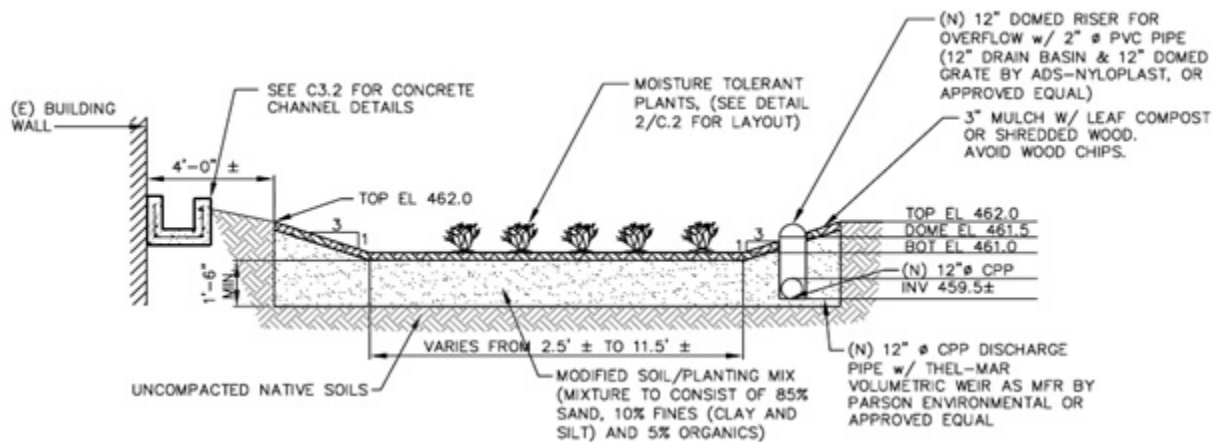
Figure 3.10 Design schematic of the FRGI at Fedigan Hall (drawing courtesy of Blackney Hayes Architects)

The FRGI has an approximate surface area of 92 m^2 and an approximate surface storage volume of 21 m^3. During extremely dry periods, calibrated soil moisture sensors indicate that the engineered media retains around 0.200 (20.0%) volumetric water content. From laboratory testing, the soils are saturated at around 0.400 (40.0%). From soil moisture sensor readings during dry and saturated periods, the void space available during rain events is predicted to be around 0.200 (20%). Half of the area of the roof runoff from Fedigan Hall travels to the rain

garden. The surface area of the roof is approximately 160 m^2, so 80 m^2 of the roof area is dedicated to the FRGI. All of the runoff travelling to the FRGI is impervious runoff. The volume of the soil storage is space is calculated using Equation 3.1, which was provided by the PADEP (2006). This is storage for runoff volume available within the engineered media. When calculating runoff volume, Equation 3.2 is used. Additionally, the amount of water that falls directly into the rain garden is calculated by using Equation 3.3. The total amount of water that travels directly into the rain garden can be calculated by adding the values found from Equation 3.2 and Equation 3.3.

$$\text{Storage Volume} = \text{Rain Garden Surface Area} \times \text{Soil Depth} \times \text{Void Space} \qquad (3.1)$$

$$\text{Runoff Volume} = \text{Impervious Surface Area} \times \text{Rainfall Depth} \qquad (3.2)$$

$$\text{Rain Garden Rainfall Volume} = \text{Rain Garden Surface Area} \times \text{Rainfall Depth} \quad (3.3)$$

The potential void space at the FRGI is 0.20 (20%) based on and the residual volumetric water content of 20% subtracted from the saturated soil volumetric content of 40%. These values were recorded by the soil moisture sensor at the site. Using Equation 3.1, the maximum potential soil storage at the FRGI is approximately 6.44 m^3. This would be the maximum storage available if the soil was dry. Table 3.1 provides the necessary parameters for storage calculations at the FRGI.

Table 3.1. FRGI soil storage and runoff volume calculation values

Rain Garden Surface Area (m^2)	Depth of Engineered Media (m)	Impervious Surface Area (m^2)	Retained Water Content	Saturated Water Content	Maximum Available Void Space	Maximum Soil Storage (m^3)
92	0.35	80	0.200	0.400	0.200	6.44

The FRGR was designed to have an engineered media depth of 0.76 m. The liner is a 0.11 cm ethylene propylene diene monomer (EPDM) liner, and the overflow riser connects to a

perforated PVC underdrain which is around 10 cm in diameter. The liner was designed to be directly below the 0.76 m engineered soil layer. However, during site investigations and instrumentation installation, it was found that the liner is approximately 0.66 m below the ground surface at the FRGR. Sieve analyses (ASTM D422) of the engineered media at the FRGR confirmed that the engineered media contained 89% sand, and soil core data found that the media dry bulk density ranged between 1.09 g/cm^3 and 1.26 g/cm^3 with an average value of 1.19 g/cm^3. Soil data for the FRGR can be found in Appendix A. Figure 3.11 depicts a design schematic of the FRGR. Water that collects in the FRGR system travels through the media and into the underdrain, where it then travels to the overflow riser and exits through the 0.30 m discharge pipe as treated outflow. The slopes at the FRGR are 3:1 (H:V).
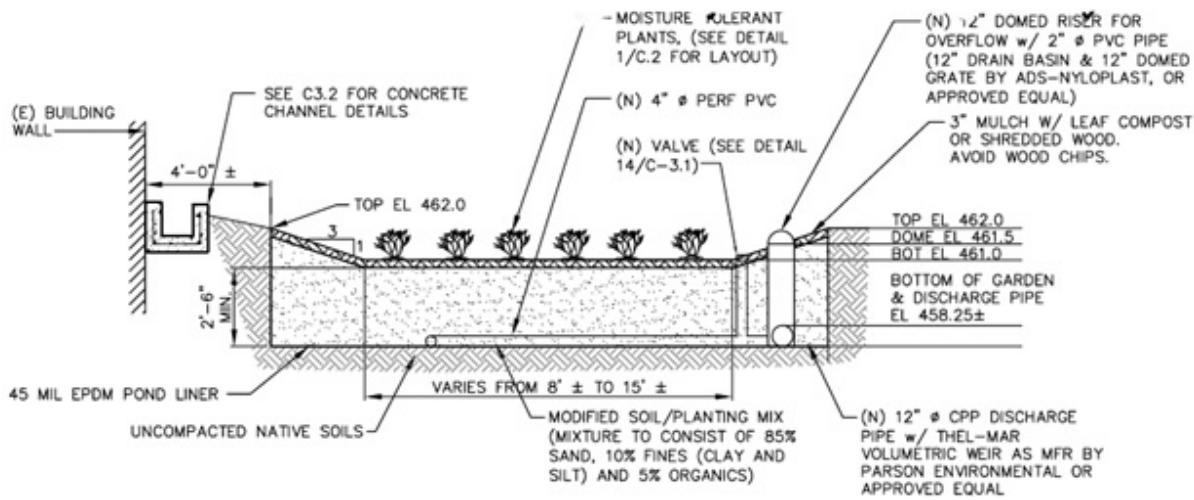
Figure 3.11 Design schematic of the FRGR at Fedigan Hall (drawing courtesy of Blackney Hayes Architects)

The FRGR has an approximate surface area of 79 m^2 and an approximate surface storage volume of 19 m^3. Since the rain garden maintained higher soil moisture contents at deeper depths due to its ability to retain water, the residual volumetric water content could not be determined. However, it is likely similar to the FRGI, since the same engineered media is used at both sites.

Therefore, the same available void space of 0.20 (20%) is expected during storm events. Similar to the FRGI, the FRGR handles 80 m^2 of the roof surface area runoff. The volume of the storage is spaced is calculated using Equation 3.1, which was provided by the PADEP (2006). The runoff volume and storage volumes are calculated in the same was at the FRGI. Using Equation 3.1, the potential soil storage at the FRGR is approximately 10.43 m^3. However, it should be noted it is more difficult to achieve this maximum potential soil storage because the water backs up at the liner and moves slowly through the underdrain system. This means that the soil in the deeper areas of engineered media at the FRGR remains saturated or close to saturated, unlike the engineered at the native soil interface found at the FRGI. Table 3.2 provides the necessary parameters for storage calculations at the FRGR. The runoff volume of rainfall volume that falls directly into the rain garden is calculated in the same way as the FRGI.

Table 3.2. FRGR soil storage and runoff volume calculation values

Rain Garden Surface Area (m^2)	Depth of Engineered Media (m)	Impervious Surface Area (m^2)	Retained Water Content	Saturated Water Content	Maximum Available Void Space	Maximum Soil Storage (m^3)
79	0.66	80	0.200	0.400	0.200	10.43

The rain gardens were inspected quarterly to note bare spaces, invasive species, and debris. These inspections were also used to determine possible deficiencies in plant life, which indicate the need for new plants. The inlet boxes and overflow risers were also inspected quarterly to remove trash, debris, and leaves which may have affected flow rates. Figure 3.12 shows a rain garden with an excessive amount of leaves in the pond, and Figure 3.13 shows leaf removal. The rain gardens were also checked for long periods of ponding, which would indicate soil clogging. However, the runoff was not expected to have a high amount of suspended solids, so clogging was very unlikely.

Figure 3.12 Leaves in the FRGR at Fedigan Hall (photograph courtesy of Villanova Urban Stormwater Partnership)

Figure 3.13 Leaf removal at the FRGI at Fedigan Hall (photograph courtesy of Villanova Urban Stormwater Partnership)

3.1.2 Site Instrumentation

The estimated instrumentation cost for the Fedigan Rain Garden sites was approximately $10,000. The site did not contain any instrumentation to collect samples for water quality testing. All instrumentation data was collected continuously.

3.1.2.1 Pressure Transducers

Currently, there is a Campbell Scientific CS451 pressure transducer located in the pond at the FRGI and the FRGR to measure ponding levels and water temperature in the pond. These pressure transducers are located in PVC pipes in the pond and are connected to junction boxes with terminal blocks. The CS451 pressure transducer operates by detecting pressure and using the known density of water to determine what the height of the water must be to create that amount of pressure. There are also CS451 pressure transducers in each overflow riser to measure outflow along with the 0.20 m volumetric weirs. These pressure transducers are located within perforated PVC pipes to read water levels within the overflow riser. These water levels are used with the known flow equations of the volumetric weirs to determine the flow rate (Thel-Mar 2016). Figure 3.14 displays a Campbell Scientific CS451 pressure transducer and Figure 3.15 shows a volumetric weir. Currently, the inlet boxes are not instrumented with water level measuring devices because some of the gutters that carry water from the roof of Fedigan Hall to the inlet boxes were damaged during this study. The 60° V-notch were put in place to measure inflow; however, leaking gutters could cause inaccurate inflow measurements. An example of the damaged downspouts is shown in Figure 3.16. At the time of this study, gutter repairs were being addressed, and inlet box instrumentation will be addressed after repairs are complete.

Figure 3.14 Campbell Scientific CS451 pressure transducer (Campbell Scientific 2016)

Figure 3.15 An example of a volumetric weir (Thel-mar 2016)

Figure 3.16 A damaged downspout at Fedigan Hall (photograph courtesy of Villanova Urban Stormwater Partnership)

The Campbell Scientific CS451 pressure transducers at the Fedigan Rain Gardens were calibrated every six months, or when data showed that a calibration was required. There was no required pressure transducer setup for rain storm events. Calibration was performed by removing the pressure transducers from their locations and placing them in containers which were gradually filled with water. The output values were required to be reset prior to calibration. This involved setting the "m" value to 1 and the "b" value to 0 in the pressure transducer code. These values follow the standard slope equation, which is provided in Appendix B. Water was filled to five or six points and measured manually, then compared to the level that the pressure transducer indicated at each filling point. The data was then plotted with the pressure transducer readings on the x-axis and measured values on the y-axis. When the points were plotted on a scatter plot, a trendline was made and the equation of the trendline was found. Additionally, the R^2 value was found, and calibration was deemed acceptable if this value was greater than 0.97. Furthermore, calibration points were checked with the new trendline equation. The pressure transducer reading was entered as the "x" value and the new "y" value was determined. This was done and compared to the manual reading for all calibration points. If the error between the manual reading and pressure transducer reading exceeded 10%, it was necessary to re-calibrate the pressure transducer. Figure 3.17 and Figure 3.18 demonstrate the calibration of the pond pressure transducers. Pressure transducer calibrations are provided in Appendix B. An example plot is provided in Figure 3.19.

Figure 3.17 Pressure transducer calibration at the FRG (photograph courtesy of Villanova Urban Stormwater Partnership)

Figure 3.18 A pressure transducer in a calibration container at the FRG (photograph courtesy of Villanova Urban Stormwater Partnership)

y = 2.4501x + 0.6243
R² = 0.9997
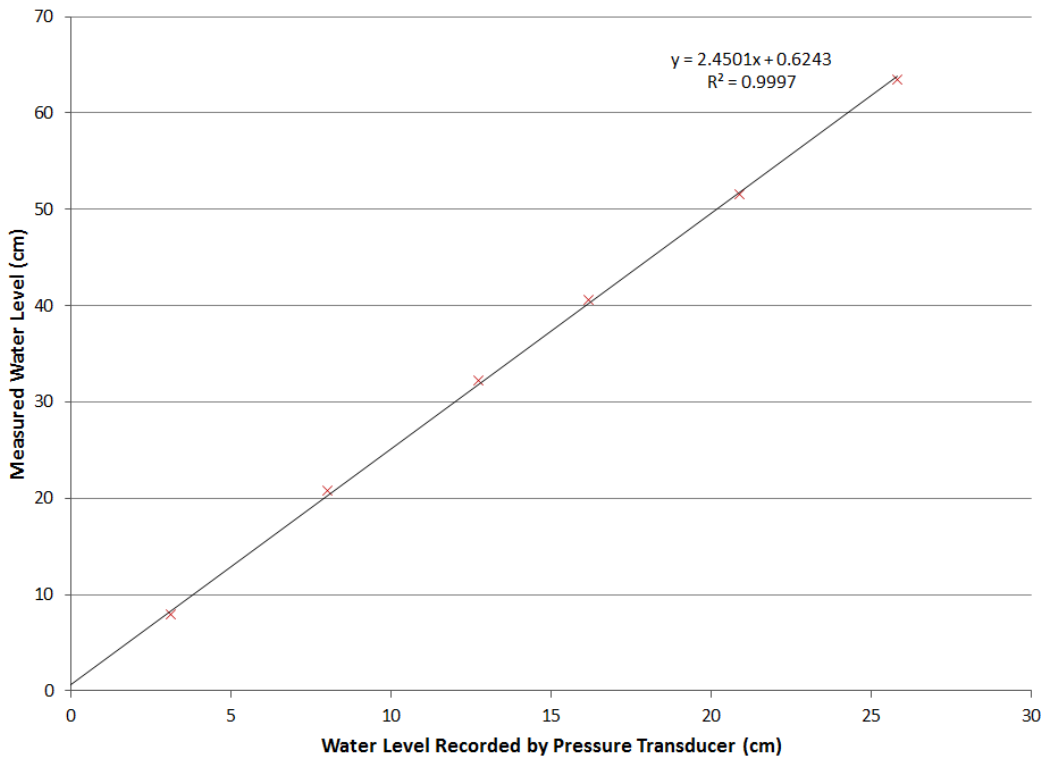
Figure 3.19 An example calibration from the pond pressure transducer at the FRGI

3.1.2.2 Soil Moisture Sensors

Both rain gardens have one Decagon 5TE soil moisture sensor. These sensors are used to measure the volumetric water content, temperature, and conductivity at specific points. The sensor at the FRGI is installed at a depth of 35 cm and the sensor at the FRGI is installed at a depth of 66 cm. This is because the native soil interface at the FRGI is around 35 cm deep and the depth to the liner at the FRGR is approximately 66 cm. These points are particularly important because they provide information on the soil conditions at the points where water exits the rain gardens. At the FRGI, the volumetric water content at the native soil interface provides information on how much water actually infiltrates to the interface and how much is stored in the soil media above it. At the FRGR, the volumetric water content above the liner can be used to determine how much water is retained at this soil depth in a system where water cannot infiltrate

56

into the native soil. Decagon 5TE soil moisture sensors were initially installed at depths of 10 cm, 35 cm, and 66 cm in both rain gardens. However, these were older sensors and the FRGI sensor at 66 cm, the FRGR sensor at 35 cm, and both sensor at 10 cm began malfunctioning. It is proposed to eventually install Stevens HydraProbe II soil moisture sensors at 10 cm, 35 cm, and 66 cm in both rain gardens and remove all of the Decagon 5TE soil moisture sensors. Figure 3.20 depicts the Decagon 5TE soil moisture sensor. When the soil moisture sensors were installed, they were pushed into the soil with minimal lateral movement to prevent shearing of the soil. This shearing could create macroporosity and preferential flow paths for infiltrating water.

Figure 3.20 Decagon 5TE soil moisture sensor (Decagon Devices 2016)

The Decagon 5TE soil moisture sensors needed to be calibrated only once with the specific soil in which they were placed. Soil samples were taken from the depths of sensor placement, and these cores were wetted until the soil was completely saturated. The weight of the sensor was recorded, and the weight of the saturated soil sample was also recorded. Afterwards, the soil moisture sensor was placed into the soil sample and readings of soil moisture were recorded. Periodically, weights of the soil sample were taken as the soil moisture sensor continuously

recorded the volumetric water content. As the soil dried over time, the changes in weight indicated the exact soil moisture of the sample. The dielectric permittivity (ε_a) was recorded with the logger at the points where the weight of the soil and water was recorded manually. This was used with the volumetric water content equation for sands, which is provided in Appendix B. The α and β values were changed using Microsoft Excel's Solver tool, which generated the values which created the smallest error between the volumetric water content found with the measured dielectric permittivity and the volumetric water content found using the weight of the water present in the soil. Plots were then created with calibration curve with the equation using the determined α and β values, and the points of known volumetric water contents determined from the weight of the water within the soil. Soil moisture sensor calibrations are provided in Appendix B. The procedure used to calibrate the Decagon 5TE soil moisture sensors is that used for the calibration of Stevens HydraProbe II soil moisture sensors. This is because the other sites in this comparison study use the Stevens HydraProbe II soil moisture sensors and it was desired to have similar calibrations for a better comparison of the change in soil moisture at each targeted depth.

3.1.2.3 Well Cap with Orifice

A well cap with an orifice has been installed in the FRGR underdrain. The particular well cap used is a 10 cm plastic expansion plug. The calibrated device allows outflow from the underdrain to be measured. A Campbell Scientific CS451 pressure transducer is located behind the well cap to measure water levels. These water levels are used with the calibrated orifice equation to determine flow as shown in Equation 3.4,

$$Q_{underdrain} = 0.565 \times A_0 \times \sqrt{2 \times g \times (H\text{-}0.049)} \qquad (3.4)$$

where $Q_{underdrain}$ is the flow through the underdrain, 0.565 is the coefficient of discharge (C_D), A_O is the area of the orifice (which is 0.4 cm^2), g is the acceleration due to gravity (9.81 m/s^2), H is the head above the centerline of the orifice, and 0.049 is the shift parameter found during calibration.

Figure 3.21 depicts the well cap with an orifice being tested in the lab. The area where the orifice is located is circled in red. The orifice diameter is approximately 0.71 cm, which was determined by testing the well cap at expected flow rates and finding the optimum orifice diameter for accurate low-flow data collection.

Figure 3.21 The well cap with an orifice installed in the testing apparatus

The well cap with an orifice designed for the underdrain was calibrated in the laboratory with the apparatus shown in Figure 3.22. With this apparatus, a Campbell Scientific CS451 pressure

transducer was placed in a piece of perforated PVC pipe while water was added to the drum at a known inflow. This inflow was recorded using an IFM SW Mag Flowmeter in the laboratory. When the pressure transducer stabilized, flow was considered stable, which meant that the inflow rate was equal to the outflow rate. The flow rate and pressure transducer level were recorded at various points when this stabilization occurred. Figure 3.23 demonstrates the well cap laboratory testing, which was done to determine the flow equation for the orifice and the coefficient of discharge.

Figure 3.22 The laboratory apparatus used to test the well cap with an orifice

Figure 3.23 Well cap testing being conducted in the laboratory apparatus

For each stabilized flow rate, the predicted coefficient of discharge was found by using the known recorded flow rate and head above the orifice centerline. After this, the predicted flow rate was found for each point by estimating the coefficient of discharge. The error between the predicted flow rate and known flow rate was found for each point and minimized using the Microsoft Excel Solver tool. This modified the coefficient of discharge and shift parameter appropriately, finding the two values that most accurately predict the flow rate for all of the data points collected. The coefficient of discharge was found to be around 0.56, and a necessary shift parameter of approximately 0.05 was necessary to further reduce the total error. This shift parameter is used to account for pressure transducer zero points, and creates more accurate underdrain flow measurements. While this coefficient of discharge is relatively high, this could be because the well cap is hollow inside. This creates two orifices, with one being located at the

front of the well cap and one being located at the back of the well cap. Figure 3.24 shows the calibration curve created when the well cap was tested three times. In Figure 3.24, the collected stabilized flows at given heads above the centerline of the orifice was plotted with the data that would be provided by the orifice equation with the determined coefficient of discharge and shift parameter. The plot shows that the collected data does closely follow the calibration curve from the equation determined from laboratory testing, validating the coefficient of discharge and shift parameter that accurately predict flow through the orifice in the well cap. The reason the plot does not go through the zero point is because of this added shift parameter. The well cap was installed on the underdrain with a pressure transducer behind it to measure the water level and determine the outflow. The underdrain head levels recorded were used with the orifice equation provided above to determine the underdrain flow at specific times. The pressure transducer wire requires another hole in the well cap; however, this hole is sealed with putty. This well cap does not need to be re-calibrated, but is removed and checked periodically to ensure putty seals are still in place and clogging of the orifice is not occurring. The well cap was inserted into the underdrain and tightened to ensure what was not bypassing the orifice into the overflow riser. The pressure transducer is calibrated similarly as stated above in this section.
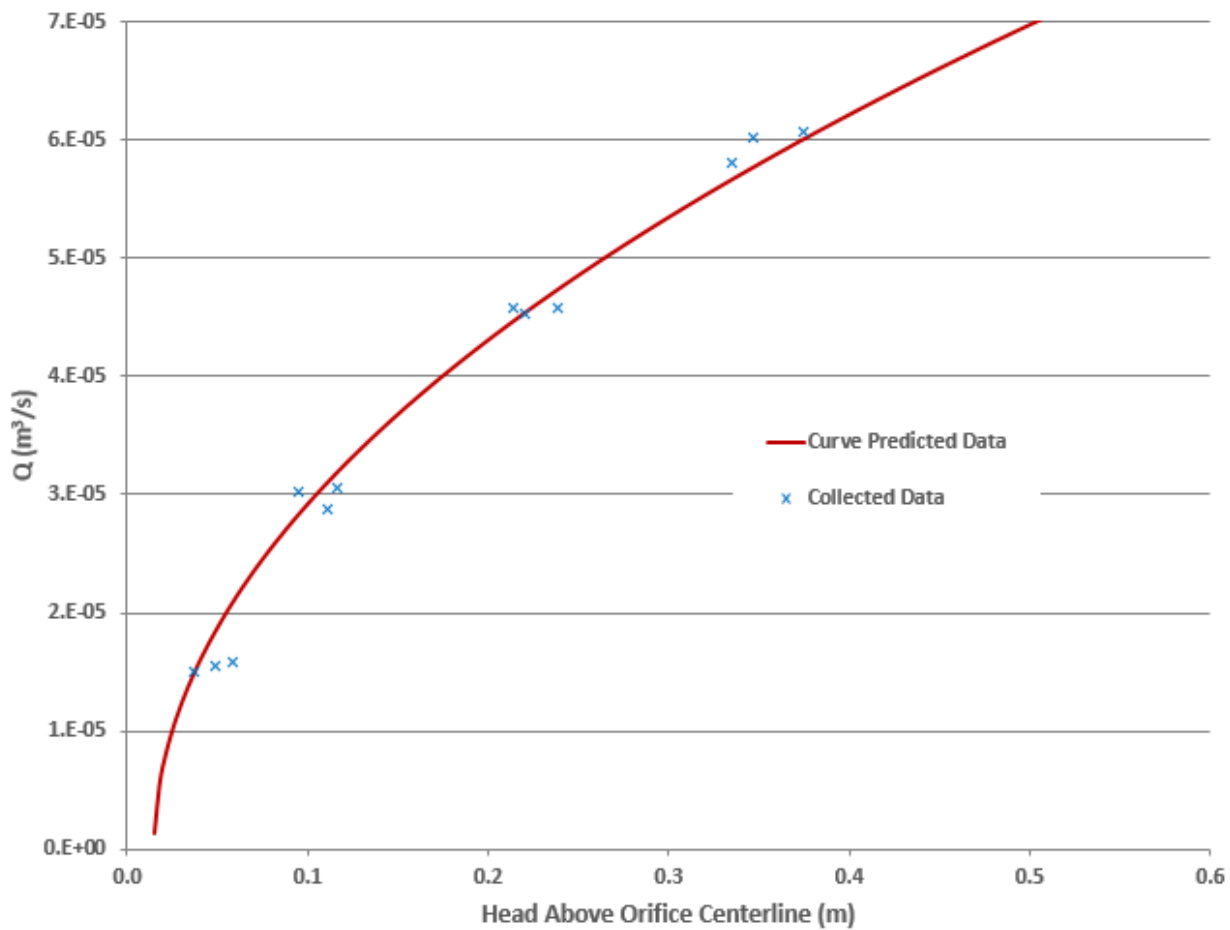
Figure 3.24 Calibration curve found from laboratory testing

3.1.2.4 Rain Gage

A 20 cm American Sigma tipping bucket rain gage on the roof of the Center for Engineering Education and Research (CEER) building was used to determine rainfall at the site. The rain gage measured rainfall at 5 minute intervals, and was calibrated once per year. Bird wire was installed on the rain gage to prevent birds from landing on the rain gage and creating inaccurate data. Figure 3.25 displays the American Sigma rain gage used for the Fedigan Rain Gardens. The rain gage tips after 0.0254 cm of rainfall. It is calibrated by placing around 473 mL of water in a container and letting it drop through a very small hole into the rain gage. The water should empty through the container into the rain gage in a time period longer than 45 minutes. After the water

empties into the rain gage, the collected should indicate that 1.45 cm ± 0.05 cm of water fell into the rain gage. If this fails, the tipping screws are adjusted in increase or decrease the number of tips necessary.

Figure 3.25 American Sigma rain gage (Hach Flow 2016)

3.1.2.5 Data Logger and Communications

Both rain gardens at Fedigan Hall have a Campbell Scientific CR1000 data logger box. All instrumentation for each rain garden is hardwired to the CR1000 dedicated to that particular rain garden. Figure 3.26 depicts the Campbell Scientific CR1000 data logger. The data logger at the FRGR is connected to the internet, while the rain garden at the FRGI uses a radio to connect wirelessly to the internet. The data logger box at the FRGI uses a Campbell Scientific RF401 900 MHz spread-spectrum radio, which is shown in Figure 3.27. This radio is attached to an antenna located on Fedigan Hall, which transmits data from the FRGI. The data is then collected with

Campbell Scientific software. The data logger box must be kept dry. A sealed bag of desiccant, which is changed regularly, was used inside the box to keep moisture levels low. Indicator paper was used to monitor ambient moisture within the box, which noted when the desiccant bag needed to be replaced. A tube of desiccant is attached to each pressure transducer wire and changed color when it indicates saturation. Putty seals, which were used to keep the box dry, were checked periodically. Higher ambient moisture or insects within the box indicated the need for new putty seals.

Figure 3.26 Campbell Scientific CR1000 data logger (Campbell Scientific 2016)

Figure 3.27 Campbell Scientific RF401 spread-spectrum radio (Campbell Scientific 2016)

3.2 Pavilion Traffic Island

3.2.1   Rain Garden Design and Construction

The Pavilion Traffic Island (PTI) was constructed in 2007 and planting was completed in 2008.

The site is located behind The Pavilion, which is a multi-purpose arena at Villanova University.

Figure 3.28 and Figure 3.29 depict the construction of the PTI, and Figure 3.30 shows the PTI

after planting.

Figure 3.28 Construction of the PTI (photograph courtesy of Villanova Urban Stormwater Partnership)

Figure 3.29 Placement of engineered media during construction of the PTI (photograph courtesy of Villanova Urban Stormwater Partnership)
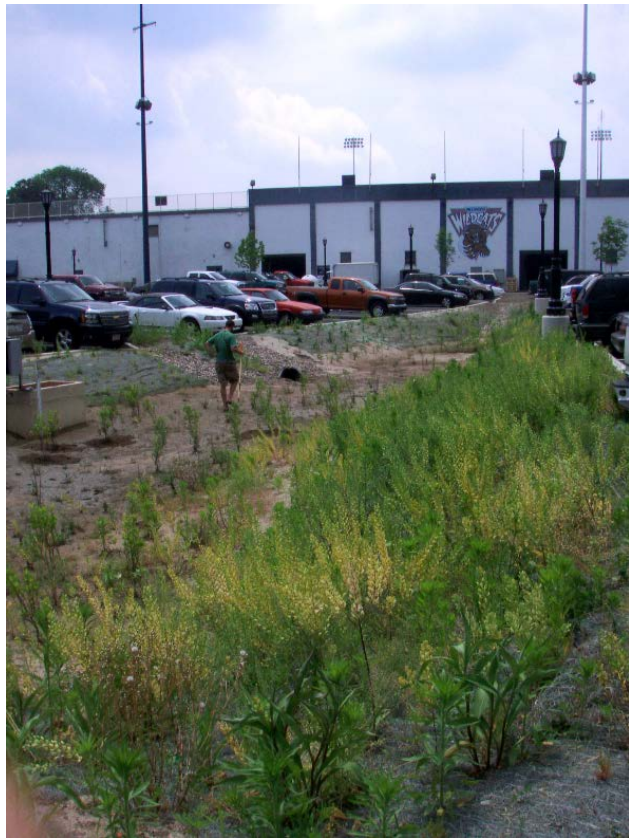
Figure 3.30 The planted PTI in May of 2008 (photograph courtesy of Villanova Urban Stormwater Partnership)

The PTI has an approximate surface area of 469 m^2 and an approximate surface storage volume of 275 m^3. A portion of stormwater runoff from the parking lot at the Pavilion on Villanova University's campus enters the PTI via curb cuts. The rain garden impervious drainage area is 3469 m^2 and the total drainage area (impervious and pervious) is 4384 m^2. Figure 3.31 displays a plan view of the PTI.
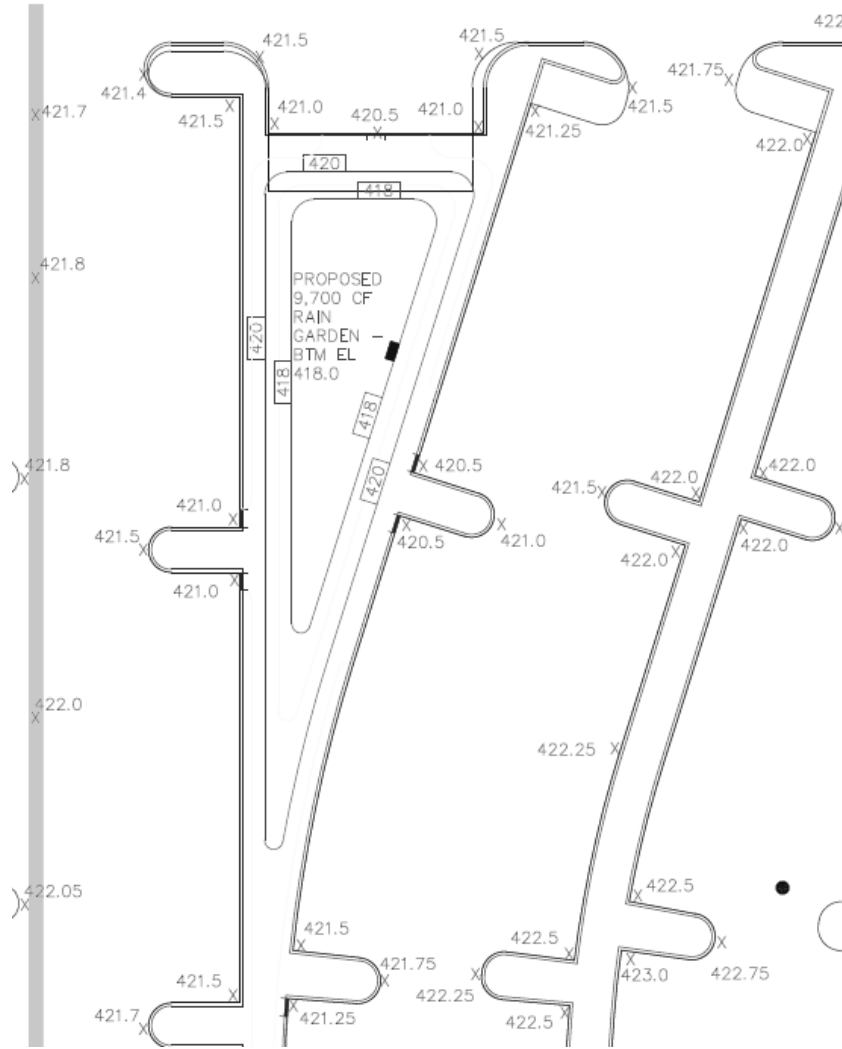
Figure 3.31 Plan view schematic of the PTI (drawing courtesy of SmithGoup, Inc.)

The PTI contains a concrete box that is 0.83 m in height with a 0.38 m diameter discharge pipe at the bottom of the box. This box was used for overflow, as any water that ponds to this height would exit through the discharge pipe. The bottom floor of the box is about 0.61 m below the ground surface of the PTI. The engineered media depth is approximately 1.22 m. Figure 3.32 shows a design schematic for the PTI. The top of the box is where overflow occurs, which is 0.83 m above the bottom of the pond. The dashed blue lines indicate a perched water table that is present within the PTI. The lower blue line specifies the lowest recorded perched water table in

69

this study, and the upper dashed blue line specifies the highest recorded perched water table recorded after a storm event. The slopes at the PTI are 3:1 (H:V).
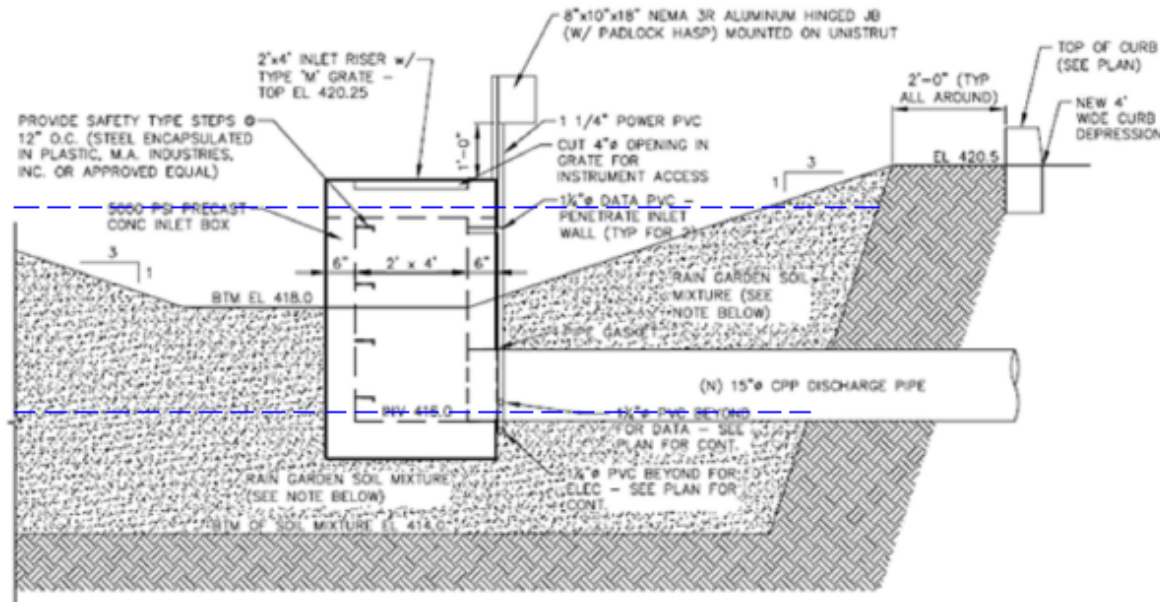
Figure 3.32 Detail design schematic of the PTI (drawing modified from SmithGroup, Inc.)

A volumetric weir that was present at the discharge pipe at the PTI was found to be washed away prior to site instrumentation. A new weir was designed, fabricated, and installed in the concrete box at the PTI. The weir, as demonstrated in Figure 3.33, is a 60° sharp crested V-notch weir used to measure outflow. Prior to weir installation, it was found that water was leaking from the PTI pond into the inlet box. Additionally, the ground surface of the box was not level during inspection. Concrete was used to level the bottom of the box, and concrete and rebar was used to rebuild part one of the walls of the box which was found to be the cause of major leakage. The weir was installed with the bottom of the weir at the same elevation as the bottom of the discharge pipe. Treated wood was used to create frame for the new weir, and concrete sealant and flashing were used to plug any remaining leakage areas within the box or in the weir frame. Additionally, a piece of treated wood was placed over the top of the weir to prevent water from

directly falling behind the weir. Figure 3.34 depicts the repairs made and completed weir and frame in the PTI concrete box.
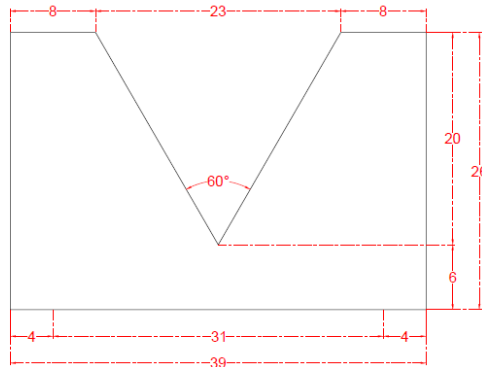
Pavillion Traffic Island Weir Design #1
(units in inches)

Figure 3.33 Design schematic of the new 60° V-notch weir at the PTI

Figure 3.34 Concrete box repairs and new 60° V-notch weir at the PTI

The PTI engineered media was initially designed to contain 85% sand, 10% fines (silts and clays), and 5% organics. However, field observation and sieve analyses provided different results. The soil appeared much sandier than other 85% sand mixtures, which prompted multiple sieve analyses. After six sieve analyses (ASTM D422) were performed, it was validated that the PTI contained 95% sand and 5% fines. Dry bulk density values obtained from core samples ranged from 1.06 g/cm^3 to 1.46 g/cm^3, with an average value of 1.31 g/cm^3. Soil data obtained from the PTI are presented in Appendix A.

The native soil beneath the engineered media is believed to have been compacted prior to or during construction of the rain garden. Some compaction can be witnessed in Figure 3.28, which shows that there are some areas of ruts in the native soil. Figure 3.35 indicates that compaction of the native soil layer is an issue because water from a storm is seen ponded in the system prior to complete placement of the engineered media.

Figure 3.35 The PTI ponded during construction (photograph courtesy of Villanova Urban Stormwater Partnership)

A stagnant perched water table has been observed within the rain garden, and was first encountered during soil core collection. During core collection, it was determined that the native soil interface was much stiffer than the native soil beneath, and the native soil beneath was much drier than the engineered media and interface above it. To determine how this perched water table reacted to storm events and how it influenced other rain garden performance parameters, a monitoring well was installed within the pond and instrumented with a pressure transducer. The monitoring well is 10 cm in diameter, screened with slotted PVC from the ground surface to the bottom of the engineered media layer, and rises 45 cm above the ground surface of the rain

garden. Figure 3.36 demonstrates the monitoring well installation. Due to the sandy material collapsing during the auguring process, a 0.30 m diameter PVC pipe was driven into the material first. After this, the material inside the 0.30 m PVC pipe was augured, and the monitoring well was placed into the media. The area around the well was backfilled with sand and bentonite. Figure 3.37 depicts the completed monitoring well in the PTI pond. From data collected, it was determined that around 0.6 m of the media can be above the water table within the PTI during a dry period.

Figure 3.36 Monitoring well installation at the PTI

Figure 3.37 The monitoring well in the pond at the PTI

During an investigation of two wells in the vicinity of the PTI, it was found that the water table within the PTI is independent of the groundwater table in the area. Two monitoring wells were gaged to determine the groundwater elevation outside of the PTI. Figure 3.38 shows the location of the monitoring well within the PTI, as well as the monitoring wells MW-1 and MW-2. The monitoring wells MW-3 and MW-4 were not used during this study because they were found to be unmaintained during the investigation. As presented in Table 3.3, the groundwater elevation outside of the PTI was found to be around 2.5 m below the perched water table within the PTI, which is a big enough difference to feasibly believe an independent perched water table within the PTI exists.
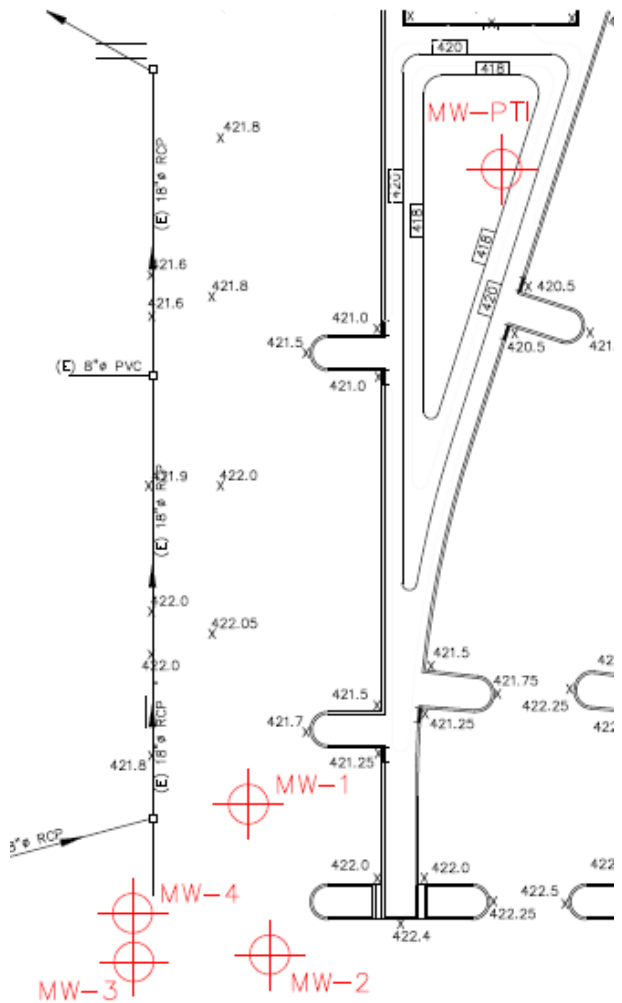
Figure 3.38 Locations of monitoring wells used in the PTI water level investigation (drawing modified from SmithGroup, Inc.)

Table 3.3. PTI well data from the investigation on 07/17/15

PTI Ground Elevation Prior to Construction (m)	128.17
Top of Native Layer Elevation in PTI (m)	126.19
Top of Engineered Media Elevation in PTI (m)	127.41
Water Elevation in PTI (m)	127.83
Ground Elevation at MW-1 (m)	128.60
Groundwater Elevation at MW-1 (m)	125.23
Ground Elevation at MW-2 (m)	128.70
Groundwater Elevation at MW-2 (m)	125.32

Other visual aspects of the PTI show that the perched water table exists and hinders rain garden performance, showing that the PTI is not behaving as designed. Long ponding periods occur after storm events, and the vegetation currently in the rain garden are typical wetland plants. Figure 3.39 shows the PTI with current vegetation in 2015, and Figure 3.40 demonstrates a ponding event at the PTI.

Figure 3.39 Vegetation present at the PTI

Figure 3.40 Ponding at the PTI after a rain event (photograph courtesy of Villanova Urban Stormwater Partnership)

Four constant-head single-ring infiltration tests were conducted in 2007 found that the hydraulic conductivity of the native soil beneath the engineered media was between 1.6×10^{-3} cm/s and 2.7×10^{-3} cm/s, with an average value of 2.1×10^{-3} cm/s. The test technicians noted that prior to the infiltration tests, around 2.5 cm to 5.0 cm of soil was removed. This demonstrates that the native soil, when it was not compacted, had a suitable hydraulic conductivity. Figure 3.41 depicts an infiltration test being performed at the PTI.

Figure 3.41 Single-ring infiltration test being performed at the PTI (photograph courtesy of Villanova Urban Stormwater Partnership)

The residual volumetric water content varies based on depth within the engineered media. During a dry period, the soil moisture sensor closest to the surface at 10 cm read a residual volumetric water content of around 0.005 (0.5%) while the sensor located at 35 cm read a residual volumetric water content of around 0.020 (2.0%). The saturated volumetric water content of the sensors was found to vary from 0.325 (32.5%) to 0.350 (35.0%). The residual water content is likely not less than 0.020 (2.0%), so the 10 cm sensor reading of 0.005 (0.5%) is not considered accurate. However, a residual water content of 0.020 (2.0%) is plausible for a sandy material. The soil moisture sensor at 66 cm consistently recorded a volumetric water content higher than 0.300 (30.0%), implying that the water level within the rain garden did not drop below 66 cm, even during a very dry period. The varying water contents are likely due to

macropores present in the engineered media, which is much sandier and prone to higher void spaces because particle sizes do not vary as much as within other rain gardens.

Using the soil mix depth of 1.22 m and Equation 3.1, the maximum potential soil storage was found to be around 188.82 m^3 if no perched water table is present. These calculations are presented in Table 3.4. However, the perched water table level was found to be 0.66 m above the native soil layer during a dry period, meaning that the maximum depth of dry engineered media is only around 0.56 m. Considering this as the maximum potential soil available for storage, the maximum potential soil storage is actually only 102.15 m^3. The values for these calculations are provided in Table 3.5. The storage volume within the soil is depended on the perched water table, which varies based on time between storms and seasonal effects such as temperature. If ponded due to cold temperatures or a recent storm, the PTI soil storage volume could be zero. Therefore, the soil storage volume lost due to the perched water table ranges between 102.15 m^3 and 188.82 m^3, or around 54% to 100%. The runoff volume of rainfall volume that falls directly into the rain garden is calculated in the same way as the FRG.

Table 3.4. PTI ideal maximum soil storage and runoff volume calculation values

Rain Garden Surface Area (m²)	Depth of Engineered Media (m)	Impervious Surface Area (m²)	Retained Water Content	Saturated Water Content	Maximum Available Void Space	Maximum Soil Storage (m³)
469	1.22	3469	0.020	0.350	0.330	188.82

Table 3.5. PTI actual maximum soil storage and runoff volume calculation values

Rain Garden Surface Area (m²)	Maximum Depth of Engineered Media Above Water Table (m)	Retained Water Content	Saturated Water Content	Maximum Available Void Space	Actual Maximum Soil Storage (m³)
469	0.56	0.020	0.350	0.330	86.67

The PTI was inspected periodically to make visual observations of ponding after rain events, as well as to ensure major leakage from the pond into the box was not occurring. The PTI was inspected on a more frequent basis than the Fedigan Rain Gardens because it was of interest to determine how a "failed" rain garden behaved both during and after rain events.

3.2.2 Site Instrumentation

The estimated instrumentation cost for the PTI was around $10,000. The site did not contain any instrumentation to collect samples for water quality testing. All instrumentation data was collected continuously.

3.2.2.1 Pressure Transducers

A Campbell Scientific CS451 pressure transducer was installed in the pond in a PVC pipe with holes to allow water to enter. This PVC pipe was installed against the concrete box to prevent movement and inaccurate ponding measurements. A Campbell Scientific CS451 pressure transducer was also installed in the concrete box to measure outflow with the V-notch weir. The pressure transducers were calibrated similarly to the pressure transducers used at the Fedigan Rain Gardens. The equation used to measure outflow is provided in Appendix B; outflow occurs when the box level reaches 0.15 m. Pressure transducer calibration data are provided in Appendix B.

3.2.2.2 Soil Moisture Sensors

Stevens HydraProbe II soil moisture sensors were installed within the engineered media at the PTI to measure volumetric water content, conductivity, and temperature at specified points. HydraProbe II sensors were installed at depths of 10 cm, 35 cm, and 66 cm. Figure 3.42 displays a Stevens HydraProbe II. These sensors were calibrated in the same manner as the Decagon 5TE soil moisture sensors. However, a different equation was used in the calibration, which is

outlined in Appendix B. This is because the sensors were calibrated on the loam setting and compared to the sand calibration setting for the Stevens HydraProbe II. Additionally, this equation was used because it allowed for temperature-corrected dielectric permittivity (ε_R). The equation to calculate temperature-corrected permittivity using permittivity and temperature is provided in Appendix B. The calibration data for the Stevens HydraProbe II soil moisture sensors installed at PTI are provided in Appendix B.

Figure 3.42 Stevens HydraProbe II (Stevens Water Monitoring Systems 2016)

Additionally, a duplicate sensor was installed at 35 cm and a sensor was installed at 114 cm, which was the native soil interface in the location where Stevens HydraProbe II sensors were installed. However, the duplicate sensor at 35 cm and the sensor installed at 114 cm malfunctioned and had to be removed and sent back to the manufacturer. These two sensors were not used in this study.

3.2.2.3 Well Transducer

A Schlumberger (now Van Essen) CTD-Diver was installed in the monitoring well in the PTI pond. The CTD-Diver has the capability of recording water level, conductivity, and temperature. An SDI-12 DCX interface unit was necessary to use a Campbell Scientific SDI-12 data logger with the CTD-Diver. A CTD-Diver is depicted in Figure 3.43 and Figure 3.44 displays the DCX interface unit. The CTD-Diver was calibrated by Stevens Water Monitoring Systems, Inc., prior to installation. The calibration of the CTD-Diver was checked every 6 months. This was done by putting the sensor in three known conductivities and determining what conductivity the sensor reads. If the sensor was reading accurately, the same procedure was done with three known water depths to determine if the water level was working properly. Finally, the sensor was placed in three buckets of water with three known temperatures, and the sensor temperature readings were compared. If the sensor was reading within the accuracy for each parameter, recalibration was not deemed necessary. This was within ±1% for the conductivity measurement, ±0.18 °F for the temperature measurement, and 0.05% for the water level measurement (Stevens Water Monitoring Systems 2016). During all calibration checks that occurred during this study, it was determined that recalibration was not necessary. This calibration information is provided in Appendix B.

Figure 3.43 Van Essen CTD-Diver (Stevens Water Monitoring Systems 2016)

Figure 3.44 Diver DCX used for CTD-Diver SDI-12 communication (Stevens Water Monitoring Systems 2016)

3.2.2.4 Rain Gage

A 20 cm American Sigma tipping bucket rain gage was recalibrated and reinstalled at the PTI above the data logger box. Bird wire was installed on the rain gage to prevent birds from landing on the rain gage and creating inaccurate data. The rain gage was recalibrated yearly, and the rain

gage was calibrated similarly to the one installed on the CEER roof for the Fedigan Rain Gardens. The rain gage at the PTI collects rain data in 5 minute intervals.

3.2.2.5 Data Logger and Communications

The PTI uses a Campbell Scientific CR6 data logger box, which is depicted in Figure 3.45. All instrumentation for the rain garden is hardwired to the CR6, which is located in a box in front of and above the concrete box. To collect data remotely, a Campbell Scientific RF401A 900 MHz spread-spectrum radio is used with a 900 MHz 9 dBd Yagi antenna to communicate with a RF401 spread-spectrum radio at a site near the constructed stormwater wetlands on Villanova University's campus. This site is hardwired to the internet, which allows the PTI data to be collected using Campbell Scientific LoggerNet software. The RF401A radio is displayed in Figure 3.46, and the Yagi antenna is shown in Figure 3.47. The antenna is attached to a metal angle, which is attached the poles which hold up the metal housing which contains the CR6 data logger box. The data logger box must be kept dry. A sealed bag of desiccant, which is changed regularly, was used inside the box to keep moisture levels low. Indicator paper was used to monitor ambient moisture within the box, which noted when the desiccant bag needed to be replaced. A tube of desiccant is attached to each pressure transducer wire and changed color when it indicates saturation. Putty seals, which were used to keep the box dry, were checked periodically. Higher ambient moisture or insects within the box indicated the need for new putty seals.

Figure 3.45 Campbell Scientific CR6 data logger (Campbell Scientific 2016)

Figure 3.46 Yagi antenna used at the PTI (Campbell Scientific 2016)

Figure 3.47 Campbell Scientific RF401A spread-spectrum radio (Campbell Scientific 2016)

3.3 Bioinfiltration Traffic Island

3.3.1 Rain Garden Design and Construction

The Bioinfiltration Traffic Island (BTI) is located on west campus at Villanova University. The SCM is a retrofit unlined rain garden and is an existing traffic island. The BTI was constructed in 2001 and has been monitored continuously for water quantity data since 2003. The BTI was constructed by excavating the traffic island to a depth of 1.8 m and mixing the soil with construction sand at a 1:1 ratio to a depth of 1.2 m. The site was designed and constructed to retain and infiltrate a 2.54 cm storm event. The total construction cost was around $29,000. Figure 3.48 and Figure 3.49 show construction at the BTI in 2001, and Figure 3.50 depicts the BTI in 2010.

Figure 3.48 Construction at the BTI in 2001 (Prokop 2003)

Figure 3.49 Soil mix being placed at the BTI in 2001 (Prokop)

Figure 3.50 The BTI with vegetation in 2010 (photograph courtesy of Villanova Urban Stormwater Partnership)

Prior to mixing, native soils at the BTI were analyzed to determine the Unified Soil Classification System (USCS) and United States Department of Agriculture (USDA) soil classifications. Before mixing with construction sand, sieve analyses (ASTM D422) indicated that native soils classified as a USCS sandy silt (ML) and a USDA sandy loam with construction sand, with 41-62% sand, 26-45% silt, and 5-10% clay. After mixing, sieve analyses (ASTM D422) indicated that the soil mix classified as a USCS silty sand (SM) and USDA sandy loam consisting of 55-79% sand, 15-30% silt, and 6-15% clay. After construction, the BTI was mulched. However, the BTI has not been mulched after this because an organic layer has built up

in the system. The native soil thickness varies from 6 m to 9 m and is underlain by mica schist. The groundwater table slopes in the northwest direction at approximately 1.5% and is typically close to the top of the mica schist (Nemirovsky et al. 2015). The ground surface also slopes in the northwest direction, but at around 1% (Nemirovsky et al. 2015). Figure 3.51 depicts the area where the BTI is located with two cross-sections. Figure 3.52 shows the A-A' cross-section and Figure 3.53 demonstrates the profile produced from the B-B' cross-section.
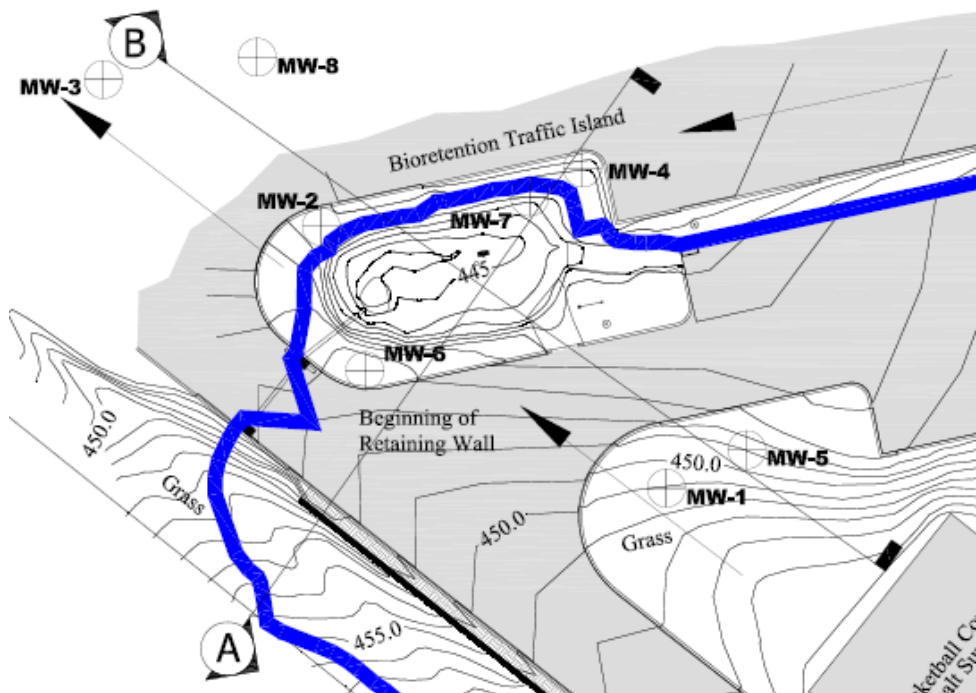
Figure 3.51 The BTI and adjacent area with cross-sections (modified from Nemirovsky et al. 2015)
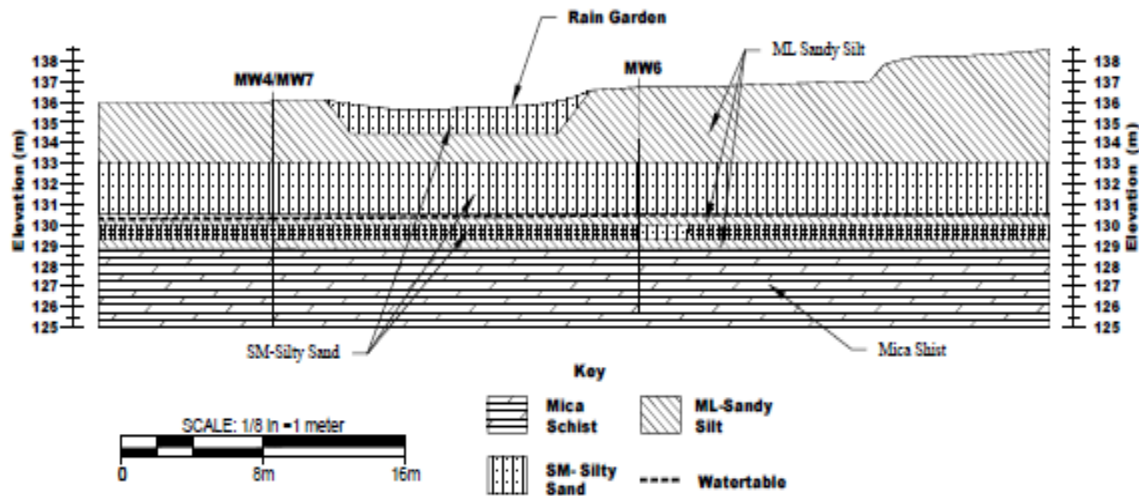
Figure 3.52 The A-A' cross-section of the BTI (reprinted from Nemirvosky et al. 2015)
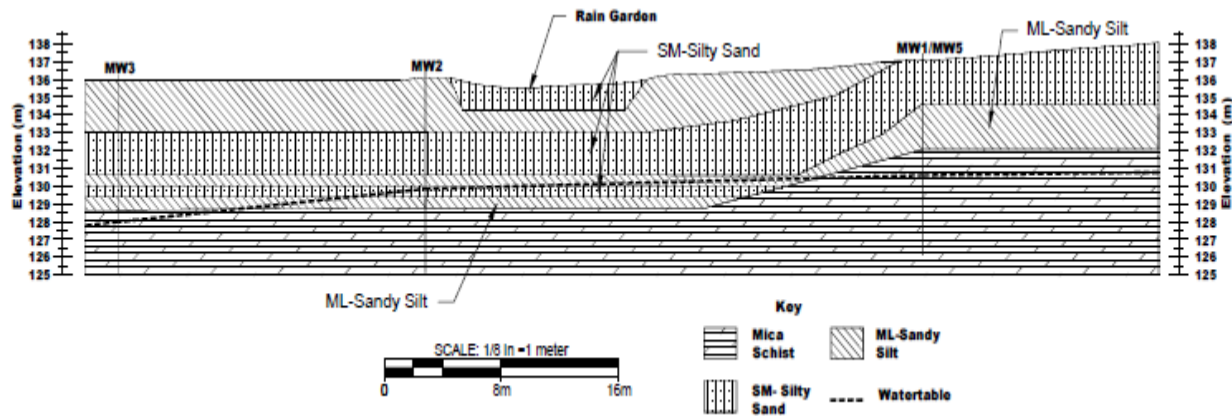
Figure 3.53 The B-B' cross-section of the BTI (reprinted from Nemirvosky et al. 2015)

During a site investigation in November 2014, two samples were collected at depths of 0 cm to 5 cm and 5 cm to 36 cm, respectively (Zukowski et al. 2016). At the sampling location, it was determined that the first 5 cm of the soil within the BTI bowl was a silt loam or loam with many fine roots, and the following 31 cm of soil was a sandy loam with little gravel (Zukowski et al. 2016). In addition to this, the soils were observed to have redoximorphic features such as small iron concentrations, which can be seen in Figure 3.54 (Zukowski et al. 2016). The upper soil

91

layer was deemed to be an organic material layer that has built up at the BTI over the course of

its 15 year life. The thickness of this layer ranged from 2.54 cm to 7.62 cm throughout the BTI

(Zukowski et al. 2016). The soil layer change can be observed in Figure 3.55.

Figure 3.54 Redoximorphic features in the BTI soil (Emerson et al. 2015)

Figure 3.55 The organic layer overlaying the BTI soil mix (Emerson et al. 2015)

Soil samples were taken to a laboratory for water content testing (ASTM D2216), sieve analyses (ASTM D422), and ash and organic content testing (ASTM D2974) (Zukowski et al. 2016). The sample collected from 0 cm to 5 cm was called S1, and the sample collected from 5 cm to 36 cm was called S2. The data collected from the site investigation can be found in Appendix A. The results of the sieve analyses indicated that the sample S1 classified as a USCS sandy silt and a USDA silt loam, and the sample S2 classified as a USCS silty sand and a USDA loamy coarse sand (Zukowski et al. 2016). These data are provided in Table 3.6 and Table 3.7. Atterberg limits testing (ASTM D4318) conducted previously at the BTI confirmed that site soils were non-plastic. Results of the water content testing (ASTM D2216) showed S1 and S2 had water contents of 99% and 19%, respectively (Zukowski et al. 2016). Results of the organic content

93

testing (ASTM D2974) indicated that the sample S1 had an organic content of 16.2% and the sample S2 had an organic content of 2.3% (Zukowski et al. 2016).

Table 3.6. BTI USCS soil classifications (modified from Zukowski et al. 2016)

Sample	USCS Classification Guidelines				
	% Gravel	% Sand	% Fines	Classification	Name
S1	0.3	37.7	62.0	ML	Sandy Silt
S2	7.5	67.0	25.5	SM	Silty Sand

Table 3.7. BTI USDA soil classifications (modified from Zukowski et al. 2016)

Sample	USDA Classification Guidelines				
	% Gravel	% Sand	% Silt	% Clay	Name
S1	3.1	38.1	49.1	9.6	Silt Loam
S2	14.	64.0	19.6	1.7	Loamy Coarse Sand

The BTI has a soil mix depth of 1.22 m, a maximum ponding depth of 0.46 m, and around 3:1 (H:V) slopes. A profile schematic of the BTI is provided in Figure 3.56. Native vegetation that has been planted sustains well throughout the year. The vegetation is cut back prior to the winter months and grows back during the spring months without additional planting. Dead vegetation is also removed in the early spring to enhance aesthetics. Prior to September 2013, inflow was controlled by two curb cuts on the north end and two inlet grates on the south end. The curb cuts were connected to the pond via channels lined with rip-rap. In September 2013, the site was modified so that flow at the north end was channelized to one transition area which consists of a sloped concrete pad leading into a rip-rap channel. Figure 3.57 shows the inlet channel in 2016. Water travels into this inlet channel and into the bowl of the BTI.
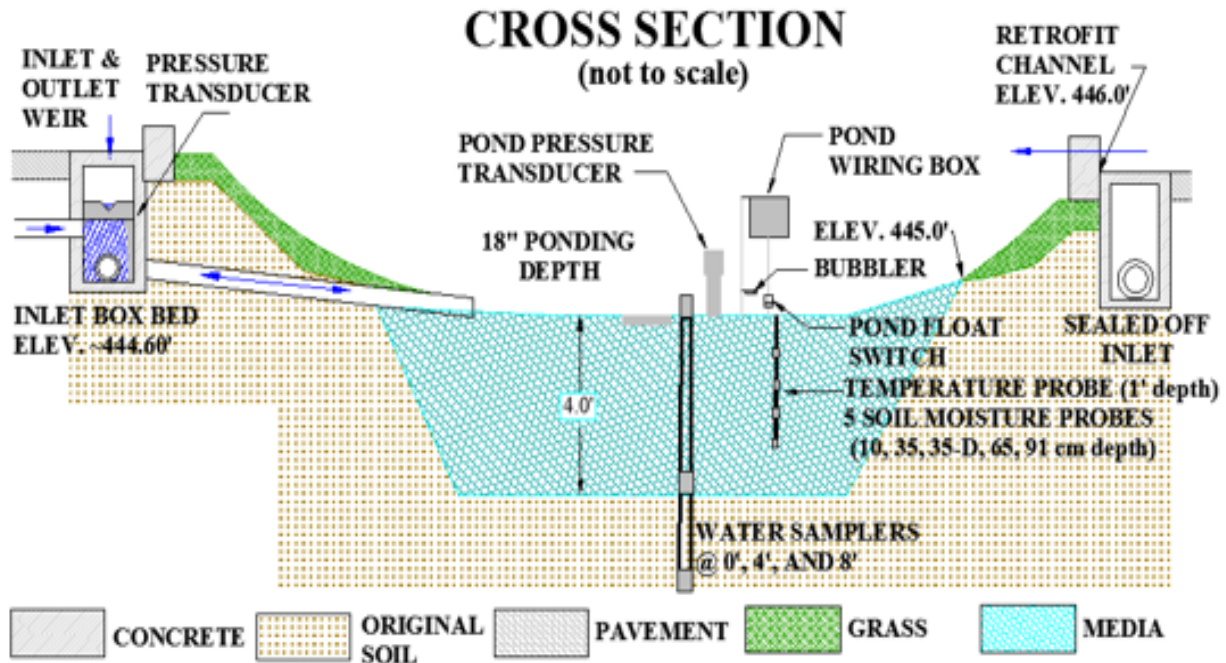
Figure 3.56 A basic profile of the BTI (Lord 2013)

Figure 3.57 The inlet channel leading into the BTI (photograph courtesy of Villanova Urban Stormwater Partnership)

An inlet/outlet box installed at the BTI was outfitted with a V-notch weir to measure outflow. The original weir was a 0.46 m square aluminum plate with a maximum head of 0.23 m and a 90° angle. The original weir was replaced in June 2014 with a larger, wider aluminum weir to provide more accurate flow measurements during larger events. The inlet/outlet box and weir are shown in Figure 3.58. The current weir at the BTI has a maximum head of 0.38 m and a 60° angle.

Figure 3.58 The outlet box and weir at the BTI (photograph courtesy of Villanova Urban Stormwater Partnership)

Every six months, general maintenance checks are done at the BTI to clean out any debris in the pond, inlet channel, and outlet box. Leaf litter in the outlet box is removed to prevent clogging or inaccurate flow measurements. Figure 3.59 demonstrates leaf build up in the outlet box. During the fall especially, leaves can build up in the outlet box and become frozen in place behind the weir during the winter months. Figure 3.60 demonstrates frozen conditions in the outlet box at

the BTI. Therefore, it is necessary to performance a maintenance check prior to freezing conditions. Sediment can build up in the inlet channel on the north end and must be removed because it can skew water quality measurements of the first flush sample and because it increase sediment loads into the BTI. It can also clog the inlet channel and reduce the performance of the BTI.

Figure 3.59 Leaves in the outlet box at the BTI (photograph courtesy of Villanova Urban Stormwater Partnership)
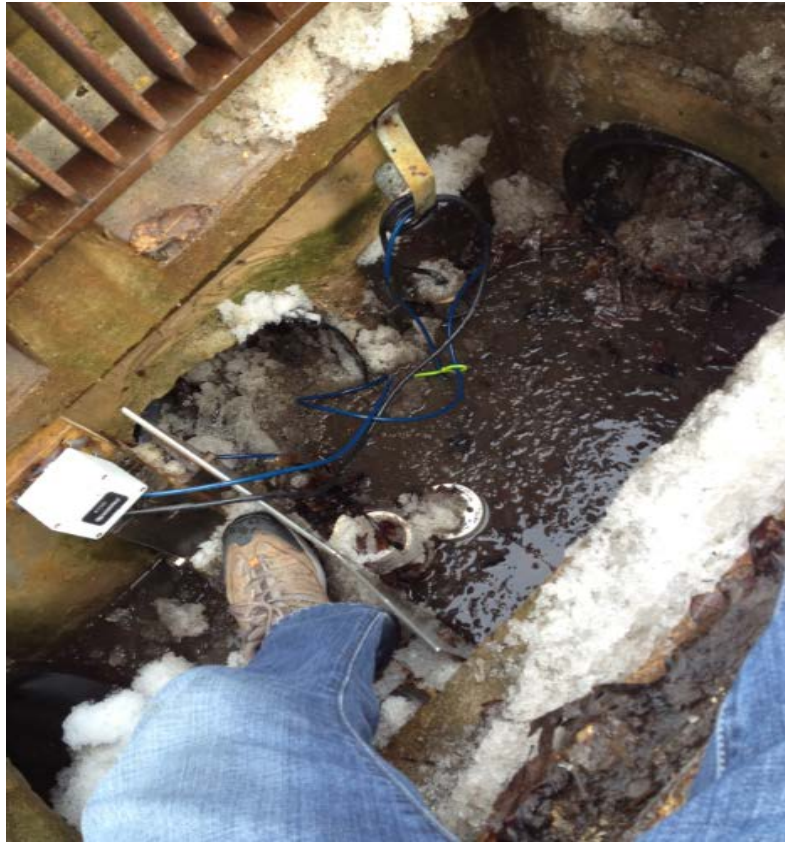
Figure 3.60 Frozen conditions in the outlet box at the BTI(photograph courtesy of Villanova Urban Stormwater Partnership)

There are 8 groundwater monitoring wells installed in the vicinity of the BTI to monitor the effects of groundwater mounding, as witnessed by Nemirovsky et al. (2015). Four of the monitoring wells were installed around the BTI, two monitoring wells were installed upstream of the BTI, and two monitoring wells were installed downstream of the BTI. Of the 8 monitoring wells, 7 have been outfitted with In-Situ AquaTroll 200 pressure transducer to measure water level and conductivity. The data collected from these monitoring wells is outside of the scope of this study, since this study focuses on the performance of rain gardens and not the effects of groundwater mounding. The monitoring well locations, which are labeled MW-1 through MW-8, are demonstrated in Figure 3.51.

Unlike the PTI and the FRG, the BTI is outfitted to measure water quality. A first-flush sampler was installed at the inlet channel to measure water quality prior to entering the BTI bowl. A grab sample is taken from the BTI bowl during a storm event after around 0.25 cm has fallen, and another grab sample is taken from the bowl after the storm event is complete. Additionally, a Sigma 900 autosampler collects a sample from the BTI bowl during storm events. A sample bottle placed behind the V-notch weir in the outlet box collects an overflow sample. Finally, there are 6 pore water samplers to collect water samples within the soil at the BTI and at a background location. The purpose of this is to compare the pore water quality at the BTI to the pore water quality of a background area. The pore water lysimeter samplers at the BTI collect water at depths of 0 m, 1.22 m, and 2.44 m. The pore water lysimeters at the background location collect pore water samples at depths of 0.30 m, 0.91 m, and 1.83 m. Figure 3.61 provides the locations of the water quality sampling equipment described. The water quality data, sampling procedures, and sampling equipment are outside of the scope of this study. The purpose of this study was to make recommendations of rain garden design based on hydrologic performance, not water quality data.
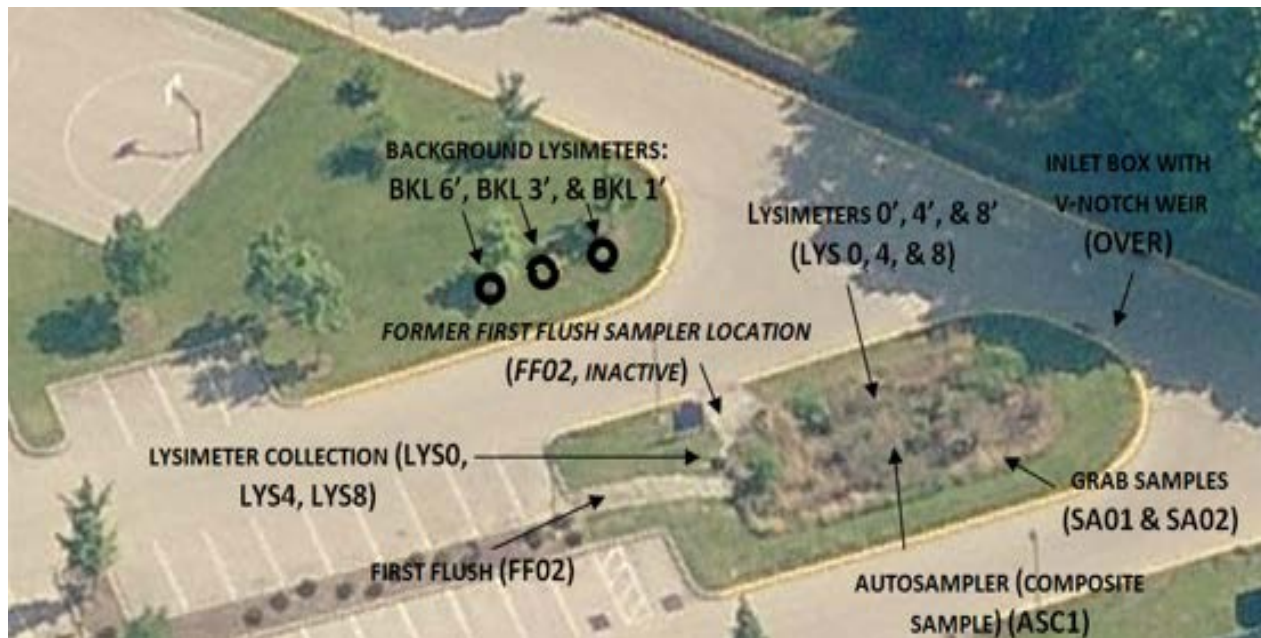
Figure 3.61 Water quality sampling locations at the BTI (Lord 2013)

The BTI has an approximate surface area of 235 m² and an impervious drainage area of 2350 m². The total drainage area (impervious and pervious) is 5261 m². The estimated residual water content present in the BTI is around 0.200 (20.0%). This is estimated by observing soil moisture sensor readings. Residual volumetric water contents at 10 cm appear to be around 0.175 (17.5%), residual volumetric water contents at 35 cm appear to be around 0.200 (20.0%), and residual volumetric water contents at 66 cm appear to be around 0.230 (23.0%). Therefore, based on the soil moisture sensors and soil type, an average residual water content of 0.200 (20.0%) is likely. Based on soil moisture sensor data during saturation and the soil type, the volumetric water content at saturation was estimated to be 0.400 (40.0%). Using the soil mix depth of 1.22 m and Equation 3.1, the maximum potential soil storage was found to be around 57.34 m³. Table 3.8 provides the necessary parameters for storage calculations at the BTI. The runoff volume of rainfall volume that falls directly into the rain garden is calculated in the same way as the FRG and PTI.

Table 3.8. BTI soil storage and runoff volume calculation values

Rain Garden Surface Area (m²)	Depth of Engineered Media (m)	Impervious Surface Area (m²)	Retained Water Content	Saturated Water Content	Maximum Available Void Space	Maximum Soil Storage (m³)
235	1.22	2350	0.200	0.400	0.200	57.34

3.3.2 Site Instrumentation

3.3.2.1 Pond Instrumentation

All instrumentation at the BTI was installed and calibrated prior to this study. The study dictated instrumenting the FRG and the PTI and using data collected from the current instrumentation at the BTI. Much of the instrumentation at the BTI is similar to the equipment used at the other sites. The BTI was instrumented with an American Sigma rain gage, which behaves and is calibrated similarly to the ones used for the FRG and the PTI. The rain gage measures rainfall at the BTI. There are also 4 Stevens HydraProbe II soil moisture sensors which operate in the same manner as the sensors used at the PTI. These soil moisture sensors are installed at depths of 10 cm, 35 cm, and 66 cm. There is also a duplicate soil moisture sensor installed at 35 cm. These soil moisture sensors measure volumetric water content, temperature, and conductivity at the BTI. Previously, Decagon GS3 soil moisture sensors were installed at depths of 23 cm and 91 cm to measure volumetric water content, temperature, and conductivity. These have since been removed.

In addition to the soil moisture sensors installed in the BTI pond, there is an Instrumentation Northwest (INW) PS9800 pressure transducer used to measure ponding levels. The INW PS9800 pressure transducer is shown in Figure 3.62. This pressure transducer behaves and is calibrated similarly to the Campbell Scientific CS451 pressure transducers used at the PTI and the FRG.

Figure 3.62 The INW PS9800 (Instrumentation Northwest USA 2016)

Additionally, an OTT CBS bubbler was installed in the pond to measure water levels. The INW PS9800 is used more as a double-checking measure with ponding measurements being recorded by the bubbler. The OTT CBS bubbler is shown in Figure 3.63. A tube that runs from the bubbler and feeds into an EPS 50 bubble chamber, which is depicted in Figure 3.64. When ponded, the pressure above the EPS 50 bubble chamber introduces bubbles which travel to the bubbler sensor device. These bubbler sensor correlates these bubbles with water depth to determine the depth of ponded water. The bubbler self-calibrates, so routine calibrations are not necessary as is the case with the pressure transducers used at the rain garden sites.

Figure 3.63 The OTT CBS bubbler sensor (OTT Hydromet 2016)

Figure 3.64 The EPS 50 bubble chamber (OTT Hydromet 2016)

An additional pond instrument used as a checking mechanism for the bubbler is the Gems LS-270 level float switch, which is illustrated in Figure 3.65. These level switches operate by

detecting water and returning a 5V reading when it is wet. This reading is simplified as a "1", which provides confirmation that ponding is occurring at the BTI. These instruments are also used to measure pressure transducer drift over time.

Figure 3.65 The Gems LS-270 level switch (Gems Sensors 2016)

Ponding has been measured with the bubbler since 09/01/2013. Prior to this, the INW PS9800 pressure transducer was used from 11/18/2011 to 09/01/2013. An ultrasonic sensor was present during this period which has since been removed. This ultrasonic sensor was used to measure water level in the pond by detecting water using non-contact ultrasonic waves. These waves are emitted from the sensor and return to the sensor. The echo is analyzed by the sensor considering the time between the emission and reception of the echo. This determines the distance between the sensor and the water. Since the height of the instrument is known, the number recorded by the ultrasonic sensor can be subtracted from the instrument height to determine the water height. The ultrasonic sensor was used at the BTI from 11/18/2011 to 09/01/2013 as a backup instrument to the pressure transducer. If the pressure transducer malfunctioned in this time

period, the ultrasonic sensor was used to determine ponding depth. From 01/01/2003 to 11/18/2011, the ultrasonic sensor was the only water level measurement device in the BTI bowl, so it was used to measure ponding. Table 3.9 provides a timeline of ponding measurement devices in the BTI.

Table 3.9. Water level measurement devices used in the pond at the BTI (modified from Zukowski et al. 2016)

Start Date	End Date	Instrument	Notes
01/01/2003	11/18/2011	Ultrasonic Sensor	None
11/18/2011	09/01/2013	Pressure Transducer	If malfunctioning, ultrasonic sensor used
09/01/2013	Current	Bubbler	Float switch and pressure transducer used as a check

A Campbell Scientific T107 temperature probe is used to measure water temperature within the bowl at the BTI. If ponding is not present, this instrument measure air temperature. The Campbell Scientific T107 temperature probe is illustrated in Figure 3.66.

Figure 3.66 The Campbell Scientific T107 temperature probe (Campbell Scientific 2016)

3.3.2.2 Outlet Box Instrumentation

A Campbell Scientific CS451 is used in the outlet box with the weir to measure overflow. This instrument operates and is calibrated in the same manner as the pressure transducers used at the PTI and the FRG. This was previously an INW PS9800 pressure transducer, similar to the one used in the pond. Similar to the pond, there is a Gems LS-270 level switch in the weir box used as a check to indicate if water is present within the box.

3.3.2.3 Data Logger and Communications

Similar to the FRGI, the BTI has a Campbell Scientific CS1000 data logger which instrumentation are connected to. This data logger collects the water quantity data and transmits it using a RF401 radio, similar to the radio used at the FRGI. The Yagi antenna used by the BTI is similar to the one used at the PTI. The CS1000 data logger collects data and transmits it to the FRGI using the RF401 radio and Yagi antenna. From this point, it is transmitted with the FRGI data and collected with Campbell Scientific LoggerNet software.

3.4 Site Design Comparison

The sites used in this study have different designs including varying loading ratios, media depths, engineered media/soil type, and ponding depth. These design components were compared in this study to make recommendations on rain garden design to increase performance and cost-effectiveness. Table 3.10 provides the design components of each site and how they compare to the PADEP (2006) guidelines. The GREEN boxes indicate that the design components that follow PADEP (2006) recommendations, and the RED boxes designate those which do not.

Table 3.10. Rain garden site designs compared to the PADEP (2006) guidelines. Red indicates that the component design does not follow PADEP (2006) recommendations and green indicates that the component does follow PADEP (2006) recommendations.

Design Component	PADEP (2006) Recommendations	FRGI	FRGR	PTI	BTI
Impervious Drainage Area-to-Infiltration Area	5:1	~0.9:1	~1:1	~7:1	10:1
Total Drainage Area-to-Infiltration Area	8:1	~0.9:1	~1:1	~9:1	~22:1
Media Depth (m)	0.45	0.35	0.66	1.22	1.22
Maximum Ponding Depth (m)	0.15	0.30	0.30	0.91	0.46
Slopes (H:V)	3:1	3:1	3:1	3:1	3:1
Organic Material (%)	5%-10%	~5	~5	<5	16.2 for organic layer, 2.3 for soil mix
Fine-Grained Material (%)	Some for water retention and pollutant removal	~10	~10	<5	62.0 for organic layer, 25.5 for soil mix
Native Vegetation?	YES	YES	YES	NO*	YES
Compacted Native Interface?	NO	NO	N/A	YES	NO

* The vegetation at the PTI is not the native vegetation planted there after construction. However, this was not intended.

As shown in Table 3.10, the highest impervious drainage area-to-infiltration area ratio is 10:1, which is present at the BTI. The PTI and BTI have loading ratios that exceed the recommended PADEP (2006) value of 5:1 for impervious drainage area-to-infiltration and 8:1 for total drainage area-to-infiltration area. The FRGI and FRGR have the lowest drainage area-to-infiltration area

ratios. The FRGI is the only rain garden with a media depth shallower than the recommended 0.45 m, and all of the rain gardens exceed the maximum ponding depth of 0.30 m. The engineered media at the PTI is sandier than the PADEP (2006) guidelines which recommend at least 5% organics and some fine-grained material for water retention. The PADEP (2006) also recommends that the organic content not exceed 10%, which is the case for both soil types found at the BTI. The BTI, FRGI, and FRGR all have original, suitable native vegetation. The native soil interface at the BTI and FRGI is not compacted, and there is no native soil interface for the FRGR. The PADEP (2006) recommends that native vegetation be planted at rain gardens and that the native soil interface is not compacted. As stated, the native soil interface at the PTI is compacted and the vegetation present at the PTI is typical wetland vegetation. While native vegetation was planted originally at the PTI, it was not able to tolerate the very sandy soil and perched water table. Since the plants at the PTI are not those it was designed to contain, it was marked in RED in Table 3.10. All of the rain gardens have 3:1 (H:V) slopes, which is what the PADEP (2006) recommends. Since these recommendations are 10 years old and were made from a limited dataset, it is necessary to analyze these sites to determine how the design components affect rain garden performance.

CHAPTER 4.   INFILTRATION TESTING METHODOLOGY

4.1 Double-Ring Infiltrometer Test

The double-ring infiltrometer can be conducted using different testing procedures. The test method can be conducted following ASTM protocol (ASTM D3385), which uses a constant water level to provide constant head with water being provided to the system by graduated cylinders or Mariotte tubes. The falling-head double-ring infiltrometer test is conducted in the same manner as the constant-head double-ring infiltrometer test (ASTM D3385) except that water is added directly to the rings after each reading. In the falling-head double-ring infiltrometer test, graduated cylinders and Mariotte tubes are not used to provide a constant-head. The water can drop during the falling-head test, but also added between readings so that each reading starts with the same head level. The double-ring infiltrometer can also be performed in the manner stated by the PADEP (2006) in the BMP Manual. Since the focus of this study was to create recommendations for the PADEP, this method was selected for the double-ring infiltrometer tests performed in this study. The method is outlined by the PADEP (2006) and briefly summarized in a previous chapter. The PADEP (2006) guidelines follow the procedures of a falling-head test, with water being added to the rings after each recording. The PADEP (2006) does not state the range of hydraulic conductivities which the double-ring infiltrometer can accurately measure. However, the ASTM D3385 states that this range is greater than 1×10^{-6} cm/s but less than 10^{-2} cm/s. For hydraulic conductivities less than 1×10^{-6} cm/s, ASTM D5093 should be used, which is the testing standard for the double-ring infiltrometer with a sealed-inner ring.

The double-ring infiltrometer utilized at Villanova has a 61 cm diameter outer ring and a 30 cm diameter inner ring. Both rings have a thickness of 0.64 cm, although ASTM D3385 states that rings should have a thickness of 0.32 cm. Figure 4.1 depicts the typical double-ring infiltrometer used in infiltration testing. Double-ring infiltrometers can be fabricated from steel or aluminum, with steel rings being more durable during installations and aluminum rings being lighter and easier to transport.

30 or 60 cm. dia.
(12 or 24 in.)

Welded butt joint

Aluminum alloy reinforcing band – minimum dimensions of 19 mm (3/4 in.) height by 3 mm (1/8 in.) thick.

50 cm (20 in.)

▽ Welded

Materials: 3 mm (1/8 in.) aluminum-alloy sheet or material of similar strength
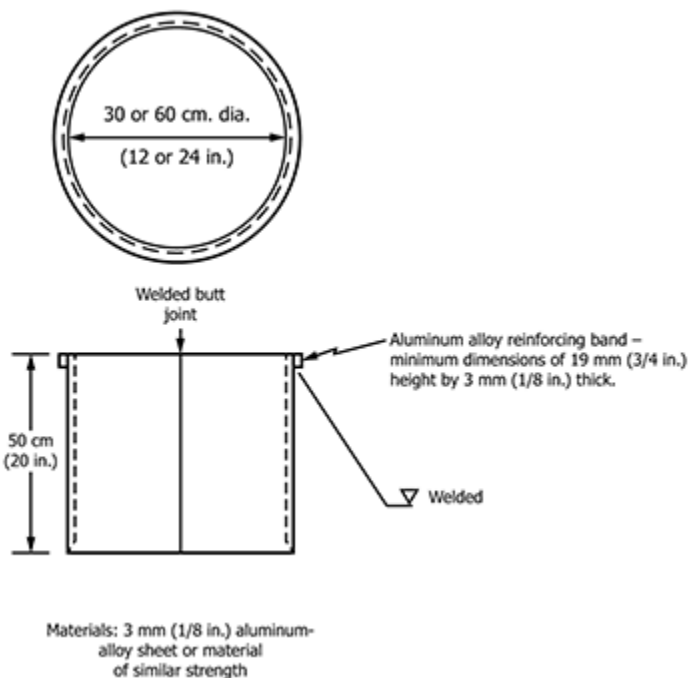
Figure 4.1 A typical double-ring infiltrometer (ASTM D3385)

The rings were driven at least around 5 cm, as per the PADEP (2006) guidelines. However, the ASTM D3385 standard states that the rings should be driven at least 15 cm and the inner ring be driven between 5 cm and 10 cm. The PADEP (2006) recommends using a flat wooden board and a rubber mallet to install the rings. The ASTM standard (ASTM D3385) states that a 1.3 mm thick hard-alloy aluminum driving plate be used with a sledge hammer to install the rings. ASTM D3385 recommends the double-ring infiltrometer be installed with a jack. In this study,

scrap wood and a steel driving plate were used to install the rings with a sledge hammer. It was difficult to install the rings using wood and a rubber mallet, so a combination of the two methods was implemented. After installation, the soil around the rings was tamped to prevent water from leaking outside of the rings. Alternatively, in some cases, bentonite was used to prevent lateral leakage of water from the rings.

As stated previously, the falling-head test recommended by the PADEP (2006) was employed instead of the constant-head test that was standardized under ASTM D3385. The PADEP (2006) do not explicitly recommend using any material within the rings to preserve the natural surficial soil when water is added. However, the ASTM D3385 standard does state the use of rubber sheets or burlap squares which are 1.5 cm thick to prevent surficial soil disturbance. In this study, foam pads were used in the rings to prevent soil disturbance, which were deemed to work well. Water was added to a height of around 10 cm, which is the minimum recommended by the PADEP (2006). The presoak and measurements were performed in the manner stated by the PADEP (2006), which was outlined in a previous chapter in this study. The PADEP (2006) recommends collected at least eight readings or four stabilized readings, whichever occurs first. The ASTM D3385 standard requires judgment of the field engineer for proper measurement procedures. ASTM D3385 states that measurements be recorded at 15-minute intervals for the first hour, 30-minute intervals for the second hour, and 60-minute intervals for the remaining 4 hours or until a constant rate is obtained. It is up to the judgment and experience of the engineer to determine when this stabilized reading is obtained. ASTM D3385 also states that the field engineer can adjust measurement readings depending on the hydrologic characteristics of the soil; however, the minimum volume of liquid flowing through the system should be at least 25 cm^3. ASTM D3385 states that in soils with very low hydraulic conductivities, measurements

could be recorded at 24-hour or longer intervals. Figure 4.2 demonstrates a double-ring infiltration test conducted at the FRGI. After the tests were installed, the steel driving plate was placed over the rings to limit evaporation of water within the double-ring infiltrometer. This recommendation is not explicitly stated in the PADEP (2006) guidelines, but is mentioned in the ASTM D3385 standard.

Figure 4.2 A double-ring infiltrometer test being conducted at the FRGI

Based on the procedures outlined by the PADEP (2006) and ASTM D3385 standard, it is apparent that the PADEP (2006) recommended testing technique is easier and faster than the ASTM D3385 standard. However, the double-ring infiltrometer testing procedure in general is difficult to perform. The rings are very large and difficult to install by hand. In test pits, this

installation can be done using the excavator to press on the driving plate or wooden boards; however, this risks damage of the rings. The double-ring infiltrometer also requires a large amount of water due to the large sizes of the rings and the duration of the test. This large amount of water may be difficult to acquire in remote sites, so water trucks may be required. Using water trucks would increase the cost of the site investigation. Considering all of this, installing and conducting a double-ring infiltrometer test can take a long duration of time. In site investigations where the number of infiltration tests conducted is limited by the time allotted, the time required to install and conduct the test becomes critical. Since the double-ring infiltrometer test requires a long duration of time, less tests can be conducted, meaning not as much of the site can be tested. This can limit the accuracy of the hydraulic conductivity values measured at the site. While the double-ring infiltrometer may ensure one-dimensional flow to determine more accurate hydraulic conductivity values, the difficulty to run the test and time required have created the need to determine if other simple, inexpensive test methods can be used to accurately measure hydraulic conductivity. The PADEP (2006) set forth these infiltration testing recommendations 10 years ago, so it is necessary to determine if new test methods designed since 2006 can be recommended for infiltration testing.

4.2 Single-Ring Infiltrometer Test

The single-ring infiltrometer used in this study was created by Princeton Hydro, LLC. The goal of the test, according to Zukowski et al. (2016), is "achieving test accuracy and repeatability, rapid testing times, and adequate precision within the range of relevant hydraulic conductivity (7.1×10^{-5} cm/s to 7.1×10^{-3} cm/s)." The single-ring infiltrometer is considered simple and inexpensive to construct and operate in the field, especially when compared to the double-ring infiltrometer. The single-ring infiltrometer is a steel ring that has a 15.2 cm diameter and is 15.2

cm long with a beveled cutting edge (Zukowski et al. 2016). The single-ring infiltrometer is marked on the outer diameter at the midpoint, which is 7.6 cm from the top of the ring. The steel ring is driven into the ground to this point, typically using a hammer and a piece of scrap wood. This means that the ring is driven 7.6 cm into the soil and 7.6 cm is left above the surface of the soil to allow for water placement within the device (Zukowski et al. 2016). The single-ring infiltrometer is shown in Figure 4.3. A filter fabric is placed in the ring prior to adding water to prevent water from causing surficial soil disturbance which can affect the infiltration rate (Zukowski et al. 2016). Water is added to the top of the ring after the filter fabric is placed, and the filter fabric is removed after the single-ring infiltrometer is filled with water (Zukowski et al. 2016). After the water drops 2.5 cm, the time is recorded with a stopwatch, and the single-ring infiltrometer is filled again. The ring is continuously filled to ensure that the head difference for readings is negligible. According to Zukowski et al. (2016), the test is run as many times as necessary until the time required for a 2.5 cm drop becomes stable. This stabilization would indicate that soils are saturated, and the infiltration rate is then correlated to the saturated hydraulic conductivity. Figure 4.4 displays a single-ring infiltration test being conducted, with the typical necessary tools also visible. In Figure 4.4, the hammer and piece of wood were used to install the ring, the red stopwatch was used to measure time required for a 2.5 cm drop, and the concrete sample container was full of water and used to add water to the ring after each 2.5 cm drop.

Figure 4.3 The single-ring infiltrometer test (photograph courtesy of Princeton Hydro, LLC)

Figure 4.4 A single-ring infiltrometer test with the typical equipment necessary to run the test

Prior to stabilization and surficial soil saturation, the infiltration is dominated by unsaturated, three dimensional water flow. Unlike the double-ring infiltrometer, there is nothing that ensures one-dimensional water flow through the soil. As the single-ring infiltrometer test is being performed and water is added between readings, the infiltration rate recorded approaches the steady infiltration rate which is correlated to the saturated hydraulic conductivity (Zukowski et al. 2016). The saturated hydraulic conductivity can be determined using the steady infiltration rate, single-ring infiltrometer geometry and the water head during the test, among other parameters (Zukowski et al. 2016). For the single-ring infiltrometer test, the VS2D (Healy and Ronan 1996) variably saturated groundwater model was modified to the single-ring infiltrometer test conditions so that the final stabilized infiltration rate and saturated hydraulic conductivity can be correlated within the model (Zukowski et al. 2016). The V2SD model uses a van Genuchten model to determine unsaturated soil properties (Healy and Ronan 1996). The model assumes homogenous and isotropic conditions because the volume of soil test is small, and it is run many times with appropriate boundary conditions to develop the correlation between the final infiltration rate and saturated hydraulic conductivity (Zukowski et al. 2016).

Since the viscosity of water is dependent on water temperature, a hydraulic conductivity correction is necessary when using the single-ring infiltrometer (Hopmans and Dane 1985; Hopmans and Dane 1986). This correction is performed using Equation 4.1 (Hopmans and Dane 1985; Hopmans and Dane 1986),

$$K_{\circ C} = K_T \left(\frac{\mu_T}{\mu_{\circ C}} \right) \qquad (4.1)$$

where $K_{\circ C}$ is the hydraulic conductivity corrected to the desired temperature, K_T is the measured hydraulic conductivity, $\mu_{\circ C}$ is the viscosity of water at the desired corrected temperature, and μ_T

is the viscosity of water at the measured temperature (Hopmans and Dane 1985; Hopmans and Dane 1986).

4.3 Pond Recession Rate Analysis

As stated, the BTI has been instrumented to measure ponding relatively continuously since 2003. The various instrumentation and devices that have been used to measure ponding at the BTI were detailed in the previous chapter. Despite the varying instrumentation, datum were checked by periodic surveying to ensure that changing instrumentation did not drastically change the accuracy of the water measurements (Zukowski et al. 2016). Between July 20, 2008 and November 21, 2011, pond recession raters were not recorded due to malfunctioning equipment within the pond (Zukowski et al. 2016). Recession rates in this time period were measured using the pressure transducer in the outlet box. The recession rate is calculated by using the falling or recession limb of the pond hydrograph when ponding is analyzed after a storm event (Zukowski et al. 2016). In this study, the recession rates of the BTI were calculated for all storms dating back to the beginning of instrumentation. The recession rates were determined using the methodology described by Emerson (2008).

The recession rate of an SCM can be considered an estimate of an area-averaged hydraulic conductivity (Zukowski et al. 2016). Emerson (2008) conducted single-ring infiltrometer tests and determined that infiltration is not constant within an SCM. Therefore, to account for the heterogeneity of soil within an SCM, the recession rate can be considered an accurate prediction of the hydraulic conductivity of the entire SCM. The as-built performance of a rain garden is affected by the soil likely heterogeneous, anisotropic, and affected by entrapped air and macroporosity (Zukowski et al. 2016). Therefore, since the recession rate after a storm acting as a large-scale infiltration tests can determine what would be considered the actual hydraulic

conductivity of a rain garden. Figure 4.5 shows a ponding event occurring at the BTI, which acts as a large-scale infiltration test. Single spot infiltrometer testing will vary across the pond due to the changing soil parameters; however, the entire area with all of these soil differences is included in the recession rate. The recession rate is assumed to follow the physics of steady ponded infiltration which includes insignificant effects of soil suction and infiltration effected by gravimetric forces and saturated hydraulic conductivity of the soil (Zukowski et al. 2016). With these valid assumptions, it is possible to then assume that the recession rate is a effective approximation of the hydraulic conductivity at the SCM (Emerson 2008).

Figure 4.5 A ponding event occurring at the BTI where the recession rate can be determined (photograph courtesy of Villanova Urban Stormwater Partnership)

4.4 Modified Philip-Dunne Infiltrometer Test

The Modified Philip-Dunne infiltrometer (Munoz-Carpena et al. 2002) uses a 10 cm diameter tub with a steel or aluminum driving ring. The driving ring has a beveled edge and can be unscrewed

from the tube itself. This is beneficial to the infiltrometer because if the infiltrometer has difficulty being installed in tough soils, the ring can be hammered in by itself and the tube can be screwed back in afterwards. This prevents hammering directly onto the tube, which can damage the infiltrometer. The infiltrometer ring is installed to a minimum depth of around 5 cm, and the tube has a height of around 61 cm. Figure 4.6 shows the Modified Philip-Dunne infiltrometer used at Villanova University. The range of hydraulic conductivities calculable with the Modified Philip-Dunne is around 1×10^{-6} cm/s to 1×10^{-2} cm/s.

Figure 4.6 A Modified Philip-Dunne infiltrometer with a steel driving ring

After the infiltrometer is installed, bentonite is applied around the cylinder to prevent lateral leakage. A silicon seal or thread seal tape is used to prevent leakage at the driving cylinder-tube interface. The current iteration of the Modified Philip-Dunne infiltrometer built at Villanova uses

an Arduino Uno Rev3 with a standard eTape made by Milone Technologies to record water depths every second. The data is stored and analyzed later to determine the hydraulic conductivity. This means that once the system is installed and the Arduino is turned on, the field engineer only needs to ensure leakage is not occurring. The field engineer does not need to be present during the infiltration test. The field engineer can move on to record other observations relevant to site design or investigation. This can help save time and cost during site investigations. An Adafruit Ultimate GPS MTK 3339 chipset is used to record the location of the infiltrometer during each test. This can help the engineer get exact locations of tests and helps create site investigation maps by providing electronic data for the location of each test.

The Modified Philip-Dunne infiltration test assumes that the water plume from the infiltrometer is spherical and uses falling-head infiltration techniques (Munoz-Carpena et al. 2002). The hydraulic conductivity is measured using by first determining the dimensionless parametric value τ_{max}, which is calculated using Equation 4.2 (Gulliver et al. 2010),

$$\tau_{max} = 0.73\left(\frac{t_{max}}{t_{med}}\right) - 1.1258; \text{ where } \frac{t_{max}}{t_{med}} < 5.4 \qquad (4.2)$$

where t_{max} is the time required for the water to completely infiltrate from the tube and t_{med} is the time required for the half of the water column to infiltrate (Gulliver et al. 2010). If the value of t_{max}/t_{med} is greater than 5.4, the resultant is invalid and the hydraulic conductivity value calculated with this τ_{max} value is not accurate. After this, the saturated hydraulic conductivity is calculated using Equation 4.3 (Gulliver et al. 2010) as shown,

$$K_s = \frac{\pi^2 \times r \times \tau_{max}}{16 \times t_{max}} \qquad (4.3)$$

where r is the radius of the infiltrometer tube (5 cm), τ_{max} is the parametric value describe previously, t_{max} is the time required for the water to completely infiltrate from the tube in

seconds, and K_s is the saturated hydraulic conductivity in cm/s (Gulliver et al. 2010). This value of K_s is the estimated hydraulic conductivity value of the soil at that specific point. Similarly to the single-ring infiltrometer, the hydraulic conductivity determined by the Modified Philip-Dunne infiltrometer can be temperature corrected using Equation 4.1 (Hopmans and Dane 1985; Hopmans and Dane 1986).

The Modified Philip-Dunne infiltrometer is easily constructible, easily and quickly installed, and the test is easier to conduct and requires less water than the double-ring infiltrometer. Since this is the case, more Modified Philip-Dunne infiltrometer tests can be conducted than double-ring infiltrometer tests given the same amount of time and water. Like the single-ring infiltrometer, the Modified Philip-Dunne infiltrometer does not have an outer ring to ensure one-dimensional flow. Rather, the unsaturated flow which occurs before saturated flow is accounted for using Equation 4.2 and Equation 4.3. However, it is much easier to conduct and can save on site investigation costs. Furthermore, Modified Philip-Dunne infiltrometer at Villanova University allows the field engineer conducting the test to let the water depth be recorded electronically, giving the engineer more freedom for additional site investigation. Presoaking is recommended because it allows the test to be conducted faster and can provide more accurate hydraulic conductivity calculations. Presoaking is recommended in the case of sandy soils because the water infiltrating may not create a spherical bulb. Since the hydraulic conductivity is faster in sandy soils, water can move through in the form of a bell shape. In a clayey soil, water infiltrating may create a flat, lens shape. Finally, a cap with a small hole can be placed onto the tube to prevent water from evaporating in the infiltrometer.

4.5 UMS KSAT

The UMS KSAT measures the hydraulic conductivity of a 250 cm^3 soil sample within a measureable range of is around 1×10^{-7} cm/s to 6×10^{-3} cm/s (UMS 2013). The UMS KSAT is a laboratory hydraulic conductivity testing technique. The other methods described previously (the double-ring infiltrometer, the single-ring infiltrometer, and the Modified Philip-Dunne infiltrometer) are field hydraulic conductivity testing techniques. The soil sample cylinder used in the UMS KSAT device has a height of 0.5 cm and a diameter of 0.8 cm (UMS 2013). The UMS KSAT determines hydraulic conductivity based on the German standards DIN 19683-9 and DIN 18130-1, as well as Darcy's Law of water flow through soil (UMS 2013). This calculation is shown in Equation 4.4 and is provided by Darcy (1856),

$$K_S = \frac{-L \times V}{H \times A \times t} \tag{4.4}$$

where K_s is the saturated hydraulic conductivity, L is the length of the sample, V is the volume of water which infiltrated into the sample, H is the head provided by the column of water, A is the area of the sample, and t is the time required to infiltrate the volume of water through the sample (Darcy 1856). A UMS KSAT test is shown in Figure 4.7.

Figure 4.7 A UMS KSAT test (Decagon Devices 2016)

The UMS sampler with a beveled edge is used to extract an undisturbed soil sample. To ensure

soil disturbance does not occur, the soil sample is extracted by digging around and underneath

the UMS sampler. When the sampler is extracted, the excess soil is scraped off and a lid is

placed on the sampler (UMS 2013). The sample is then cleaned and attached to a porous plate,

which is then placed into a tub of deionized water that is has a depth of around 2 cm (UMS

2013). Water in the tub is then raised to the height of the sample with water flowing into the soil

vertically downward. Rather, water moves upwards from the porous plate into the soil, which

reduces entrapped air within the soil (UMS 2013). Saturating the samples in this way ensure that

the saturated hydraulic conductivity is measured by the KSAT. This procedure to saturate the

KSAT samples is illustrated in Figure 4.8.
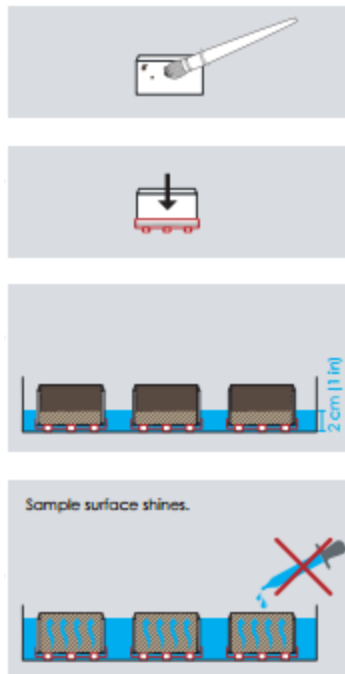
Figure 4.8 The procedure for saturating UMS KSAT samples (UMS 2013)

Before the sample is place in the apparatus, the burette is filled with deionized water by opening the fill device which is attached to a water tank containing deionized water. The burette is then opened, allowing deionized water to fill the measuring device (UMS 2013).The soil sample in the UMS sampler is placed into the measuring device and the crown is placed onto the sample (UMS 2013). The screw cap is placed onto the sample and the burette is opened until water is observed to be draining from the system through the discharge hose into the discharge tank (UMS 2013). This indicates water is moving through the system and the soil. To prevent evaporation during tests that take a long time to complete, the screw cap can be covered with a film hood (UMS 2013). This procedure to set up the KSAT apparatus is illustrated in Figure 4.9.
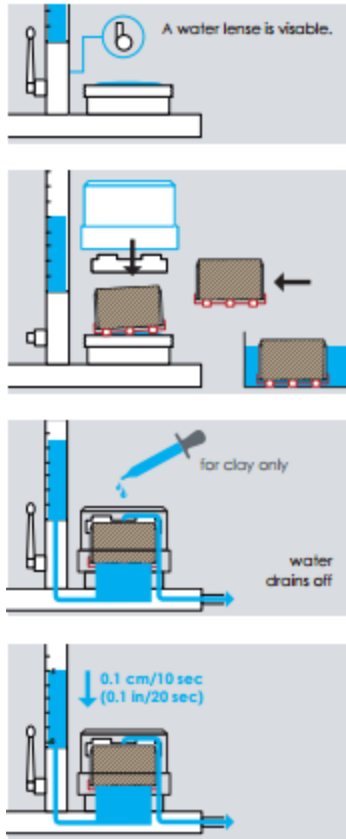
Figure 4.9 The procedure for setting up the UMS KSAT apparatus (UMS 2013)

The UMS KSAT can measure falling-head and constant-head hydraulic conductivity. The falling-head hydraulic conductivity test is performed by filling the burette up to 5 cm after the apparatus is set, and allowing water to move through the soil sample (UMS 2013). The software KSAT VIEW records the pressure head over time, and the saturated hydraulic conductivity is automatically calculated after the test is complete using Equation 4.5 provided by UMS (2013),

$$K_S = \frac{A_{Bur}}{A_{Sample}} \times L \times b \qquad (4.5)$$

where K_s is the saturated hydraulic conductivity, A_{Bur} is the area of the burette, A_{Sample} is the area of the soil sample, L is the length of the soil sample, and b is a coefficient of the fitted

125

exponential function (UMS 2013). A sample of the typical data provided by the KSAT VIEW software is depicted in Figure 4.10.
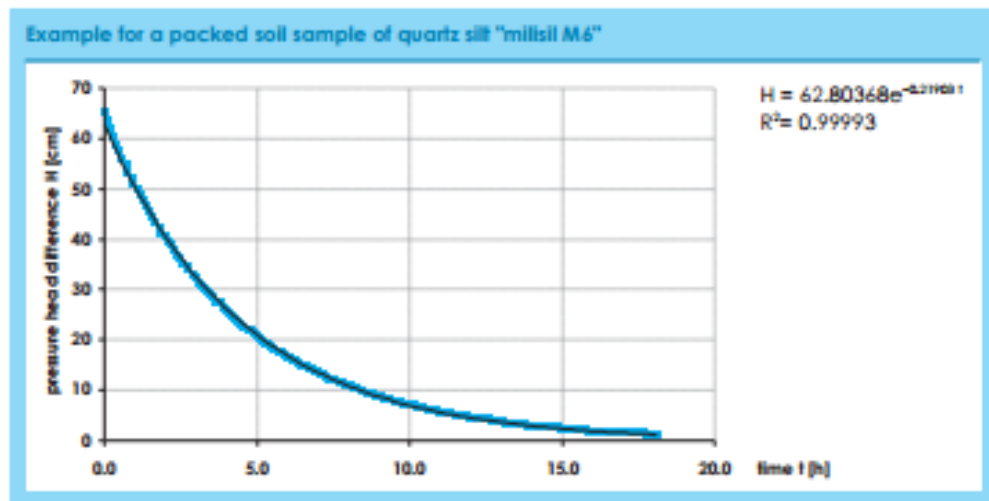
Figure 4.10 A sample output of the KSAT VIEW software (UMS 2013)

The constant-head hydraulic conductivity test is conducted in nearly the same manner as the falling-head test except that a pipe and sealing cap are placed on the burette to create a Mariotte tube (UMS 2013). In this test, the user selects particular water levels in the burette and indicates to the KSAT VIEW software when these water levels are reached (UMS 2013). The water change in the burette can be used to determine the cumulative volumetric flow of water through the soil sample (UMS 2013). The constant-head hydraulic conductivity is calculated automatically in the KSAT VIEW software using Equation 4.6 provided by UMS (2013):,

$$K_S = \frac{Q}{A_{Sample}} \times \frac{L}{H} \quad (4.6)$$

where K_s is the saturated hydraulic conductivity, A_{Sample} is the area of the sample, L is the length of the sample, H is the hydraulic head difference between the inlet and the outlet, and Q is the steady-state flow rate from the Mariotte tube (UMS 2013).

In this study, the deionized water used for the UMS KSAT was 10°C. The hydraulic conductivities measured were the falling-head hydraulic conductivity values. When UMS KSAT samples were taken in the same location as the Modified Philip-Dunne infiltrometer, they were taken after the infiltration test was completed. When the infiltrometer was removed, the soil which was tested was extracted with the UMS sampler. During this process, the removal of the Modified Philip-Dunne infiltrometer and UMS sampler was done gently to ensure disturbance of soil samples did not occur. This disturbance could cause increased porosity which would increase the hydraulic conductivity of the soil above its in-situ value.

CHAPTER 5.   STORM DATA COLLECTED

5.1 STORMS MONITORED

Two storms were compared to determine how the three sites compared during events of different sizes. The first storm occurred on 09/10/2015 after a very dry period, and the second storm occurred on 09/29/2015. The first storm was a ~2.29 cm event, which is representative of the Villanova area since 80% to 90% of the annual precipitation by volume occurs in the form of events with precipitation less than 2.54 cm (Philadelphia Water Department 2009). The rain gage used for the FRG rain gardens indicated 2.21 cm of rain, the PTI rain gage indicated 2.36 cm of rainfall, and the BTI's rain gage registered 2.06 cm of rainfall. The second storm was a ~5.72 cm event, which is closer to the PADEP 2-year, 24-hour design storm of 8.31 cm (Pennsylvania Department of Environmental Protection 2006). The rain gage used for the FRG rain gardens recorded 5.66 cm of rain, the PTI rain gage recorded 5.82 cm of rain, and the BTI rain gage recorded 5.36 cm of rain. These events were compared to observe how water moved through each system. During the first event, rainfall lasted around 25 hours with no long breaks in the storm. During the second storm, rainfall lasted around 17 hours. However, there was a nearly 6 hour break after the first 30 minutes of rainfall. If there is a 6 hour break, the storms are analyzed as separate events. However, since the break during the 09/29/2015 storm was slightly shorter than 6 hours, this was treated as one event.

In addition to this, two other storms were considered for comparison. These storms were similar in amount of precipitation, but had different characteristics. A ~1.78 cm storm event occurred on 11/10/2015 that was compared to the ~2.29 cm storm event on 9/10/2015. For this event, the rain gage used for the FRG rain gardens recorded 1.68 cm, the rain gage at the PTI registered 2.29

cm, and the rain gage at the BTI recorded 1.65 cm. The 11/10/2015 storm was different from the 9/10/2015 storm because the 11/10/2015 did not have a dry period prior to the event. This ~30-hour event looked similar for all three rain gages and lasted slightly longer than the 9/10/2015 event. A ~4.45 cm event on 10/28/2015 was compared to the 9/29/2015 storm event. For this event, the rain gage used for the FRG rain gardens recorded 4.41 cm, the rain gage at the PTI registered 4.93 cm, and the rain gage at the BTI recorded 4.01 cm. The 10/28/2015 event lasted longer than the 9/29/2015 event, and did not have the relatively significant break in rainfall that is seen in the 9/29/2015 storm event.

5.2 9/10/2015 Storm

5.2.1   Fedigan Rain Gardens

During this storm event, the Fedigan Rain Gardens performed similarly. The FRGI was observed to have minimal ponding which did not last throughout the event. Figure 5.1 shows the change in ponding over time with rainfall on the secondary axis. While some outflow was observed, it was likely due to pipe leaks and precipitation directly into the overflow riser because ponding was not high enough for overflow to occur. Additionally, soil moisture changes at the native soil interface were negligible. This is likely due to the fact that the soil was very dry from the previous dry period. This confirms that the FRGI system is designed appropriately for a typical storm in the Villanova area. Figure 5.2 displays the observed change in soil moisture over time with rainfall. Using the surface area to the rain garden and the amount of runoff into the rain garden was 1.77 m^3. This can be added to the amount of rainfall which fell into the rain garden, which was found to be 2.03 m^3. The total amount of water traveling into the rain garden was therefore found to be 3.80 m^3. Using the estimated void space of the rain garden and the known storage volume, the amount of void space available for runoff was found to be 6.44 m^3. Using

this estimation, the ratio of volume of rainfall to storage space was found to be 0.6. Using these estimations, the rain garden engineered media had available storage for the 2.29 cm rain event. During this rain event, water moved quickly through the pond and into the soil. The soil above the soil moisture sensor had enough storage for the entire rain event, meaning water did not travel deeper in the system. It is important to note that the loading ratio for the FRGI and FRGR is quite low compared to the other rain gardens researched in this study.
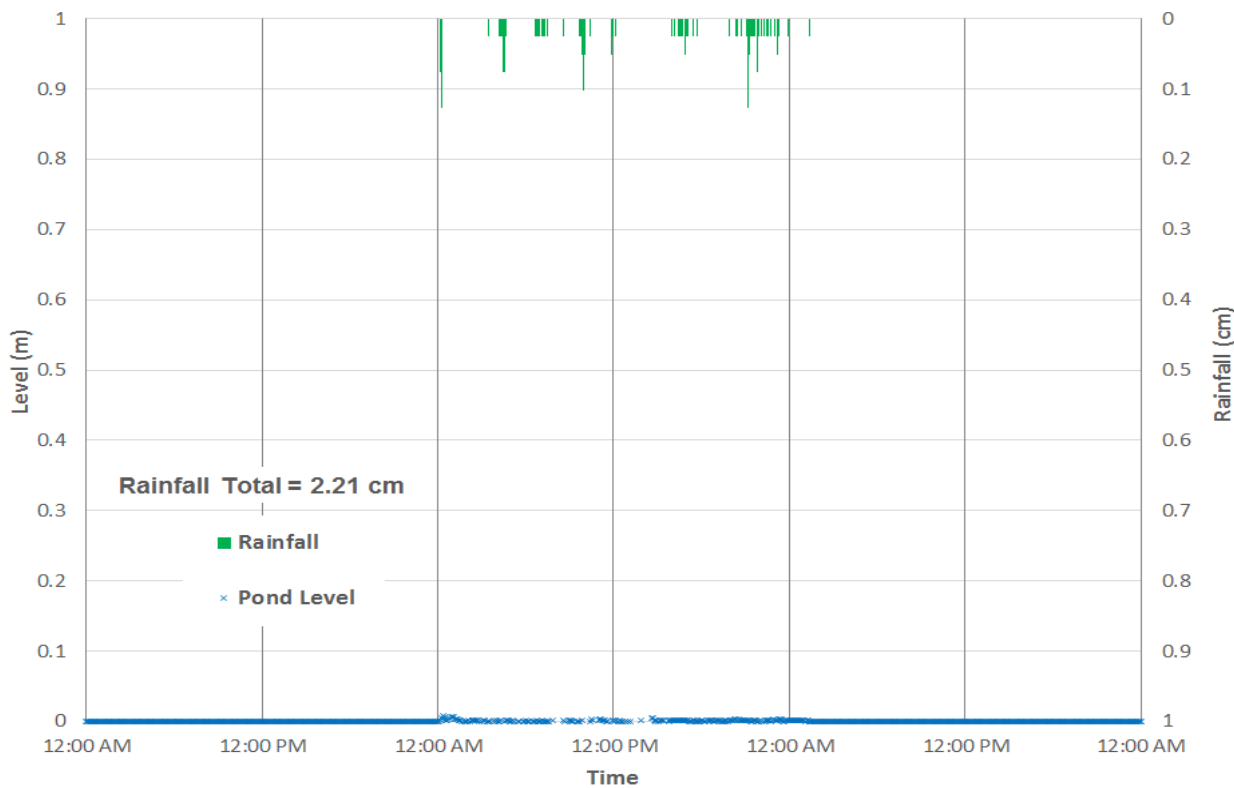
Figure 5.1 FRGI ponding data from the 09/10/2015 event
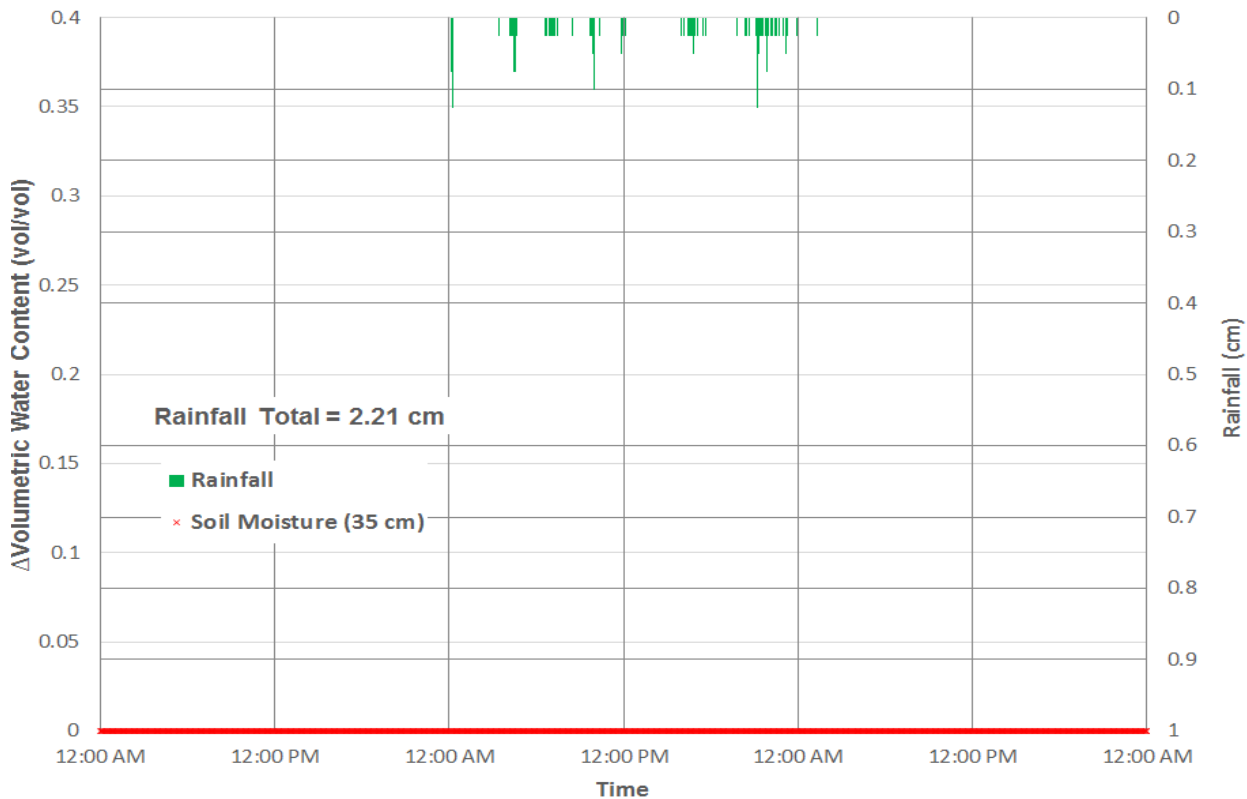
Figure 5.2 FRGI soil moisture data from the 09/10/2015 event

The bioretention rain garden (FRGR) was observed to have no ponding; however, the soil moisture changes directly above the liner were significant. The volumetric water content increased 0.039 (3.9%) with significant increases after about 8 hours of the event. The soil moisture sensor located at 66 cm demonstrates that the soil volumetric water content was 0.35 (35%) before the rainfall began. This indicates that the bioretention rain garden retains soil moisture close to saturation above the liner, even during extremely dry periods. When the 25-hour event was finished, the soil moisture began to slowly decrease. The underdrain flow peaked at 8×10^{-6} m^3/s after about 24 hours of rainfall occurred. While the peak underdrain flow occurs around the same time as the peak soil moisture, it does not begin to register any flow until about 14 hours after the soil volumetric water content begins to rise above 0.35 (35%). This implies

131

that it takes about this long before the rainfall reaches the liner of the system. The outflow begins

shortly before the underdrain flow begins, and has a peak value around the same time as the

underdrain flow. This confirms that the underdrain releases water into the overflow riser, which

then releases water through the volumetric weir. However, it was shown that the rain caused only

minor underdrain flows and outflows. As shown in Figure 5.3, the underdrain pressure

transducer and overflow riser pressure transducer begin to read increases around the same time.

The underdrain pressure transducer indicates a maximum of 0.077 m above the pressure

transducer. This corresponds to roughly 8 cm above the bottom of the underdrain, which means

the underdrain was not completely full during the rain event. Also, it is interesting to note that as

the underdrain releases water, it follows a curve similar to recession rates in rain garden ponds.

Figure 5.4 shows the flow data recorded during the rain event. The second peak in the outflow is

likely due to rainfall directly entering the overflow riser or leakage into the riser.
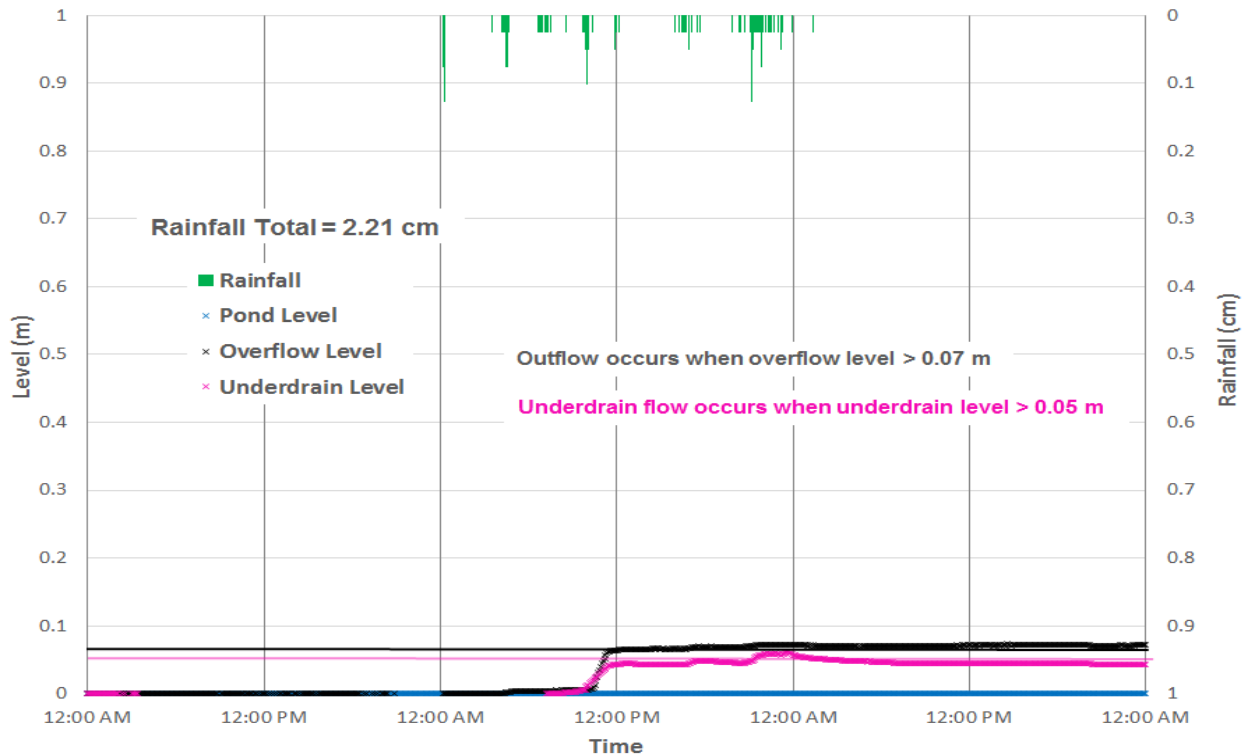
Figure 5.3 FRGR pressure transducer data from the 09/10/2015 event
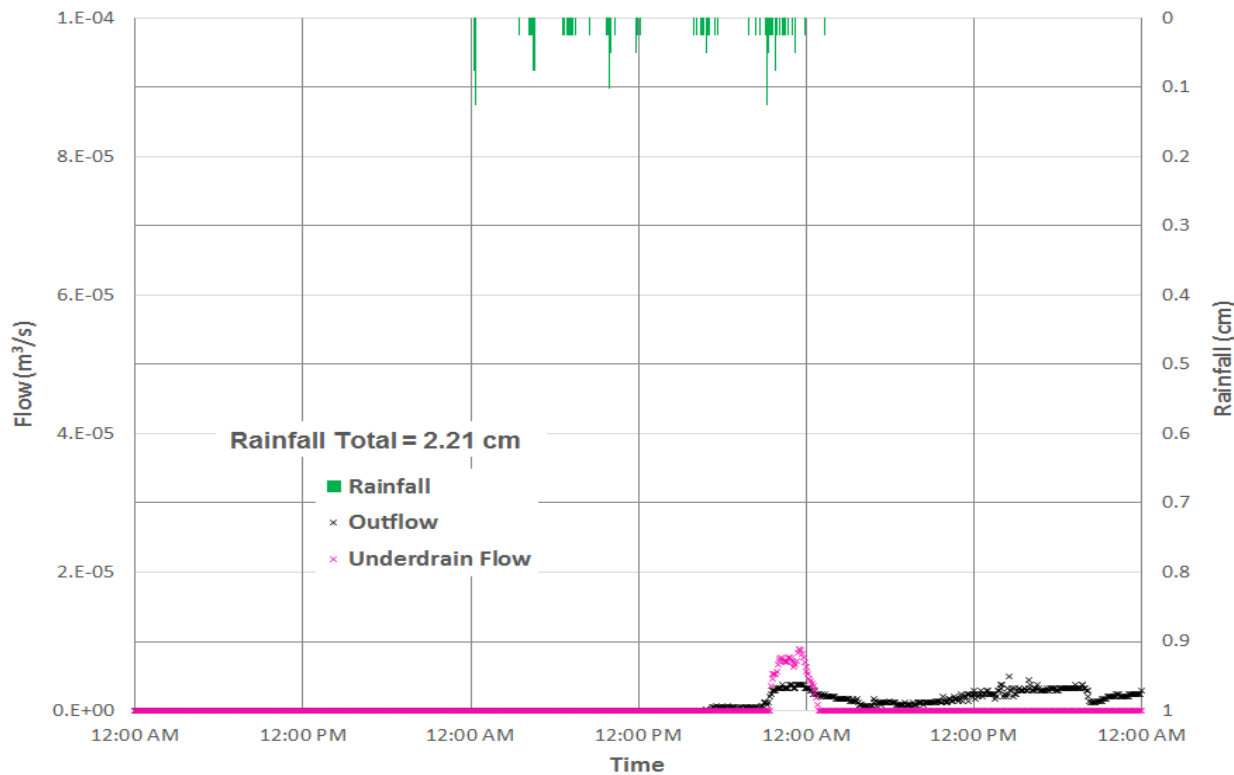
Figure 5.4 FRGR flow data from the 09/10/2015 event

Figure 5.5 shows the change in soil moisture directly above the FRGR liner, and Figure 5.6 shows the change in soil moisture plotted with the underdrain flow and outflow. Finally, Figure 5.7 displays the soil moisture change with respect to the increases in underdrain and overflow riser levels. The increase in soil moisture occurs close to the same time, displaying that water moves through the system rather quickly. This is expected with the engineered media containing high amounts of sand. Despite water moving through quickly, the system releases slowly because the orifice begins to control the outflow of the system. Since the underdrain flow is expectedly slow, the flow through the system at FRGR is dictated by the orifice at the underdrain. However, as displayed from the FRGI data, an underdrain was not needed for this event because it had available void space in the engineered media. Also, as indicated in the soil moisture sensor plots below, the volumetric water content started at a high value close to

133

saturation, which shows that the liner and underdrain system retains water as designed. After the event, the soil moisture begins to slowly decrease, but does not decrease below 0.35 (35%). While the outflow from the underdrain is treated and delayed, it is still not necessary during a typical Villanova storm event, since FRGI was able to infiltrate all of the water.
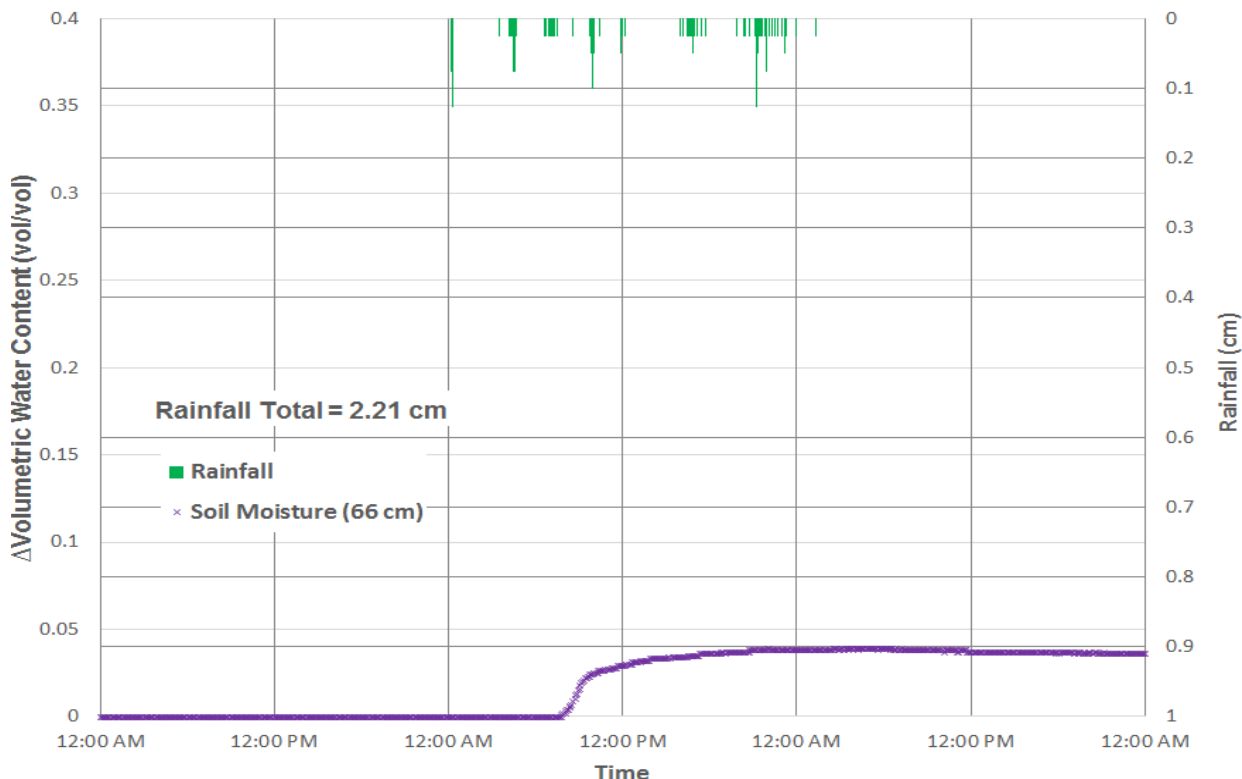
Figure 5.5 FRGR soil moisture data from the 09/10/2015 event
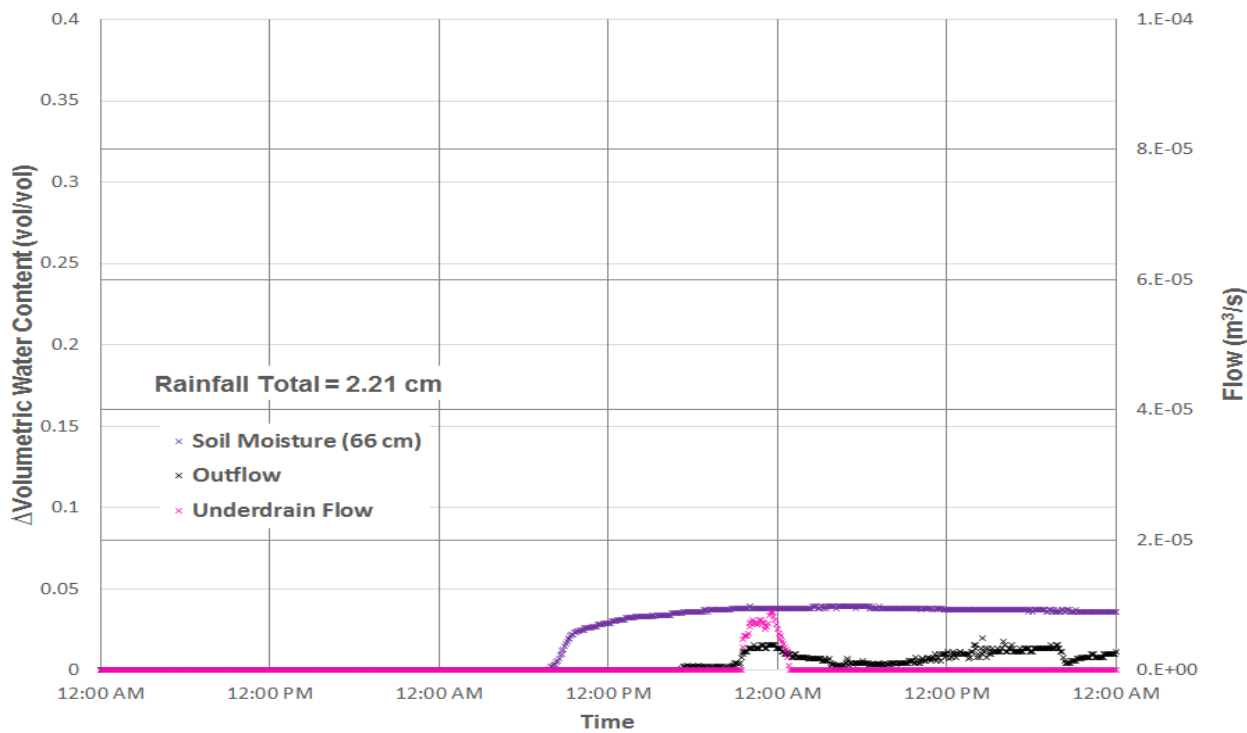
Figure 5.6 FRGR soil moisture and flow data from the 09/10/2015 event
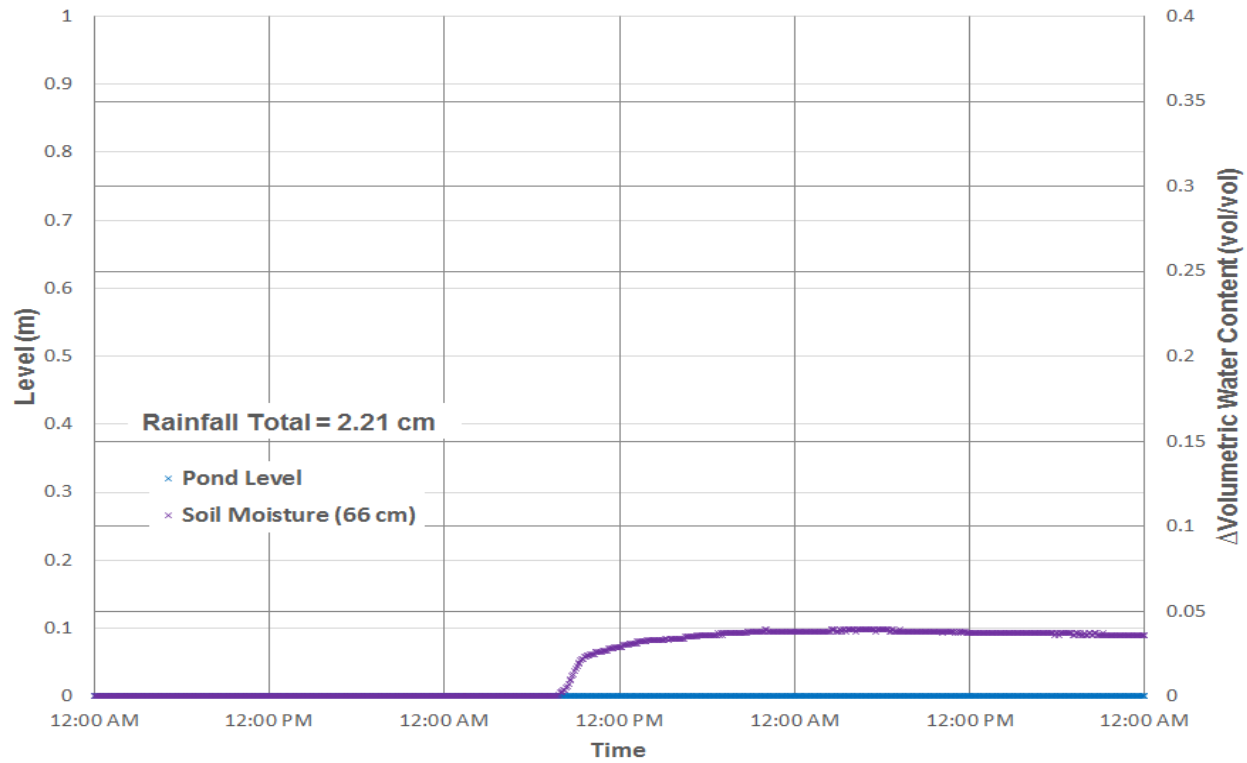
Figure 5.7 FRGR pressure transducer and soil moisture data from the 09/10/2015 event

5.2.2 Pavilion Traffic Island

During the 2.29 cm event at the PTI, ponding did not occur. This validates that the event occurred during a very dry period, since the PTI is prone to high, long-lasting ponding due to the compacted layer beneath the system. Since ponding and overflow did not occur, the well pressure transducer was used to verify water level within the system. This instrument read that the water level rose from 0.66 m to 1.07 m within the media. The water level must reach 1.22 m before ponding occurs within the system. The well transducer data are shown in Figure 5.8.
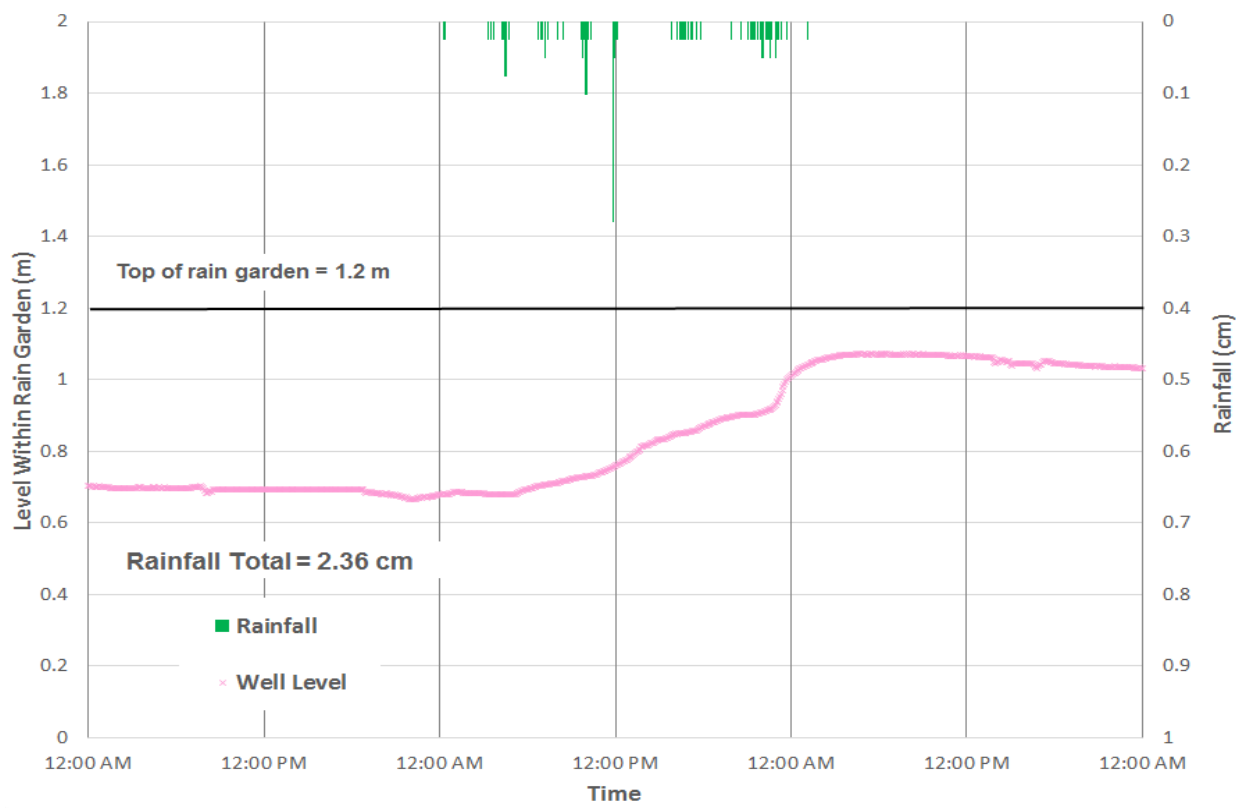
Figure 5.8 PTI well pressure transducer data from the 09/10/2015 event

The soil moisture data revealed that the sensor at 66 cm was constantly saturated during the event. This makes sense, since the well level read that the water level within the system did not drop below this depth. The soil sensor at 10 cm indicated that the volumetric water content did increase, but not up to saturation. The soil moisture sensor at 35 cm recorded a volumetric water

content increase up to saturation, and this increase began after the increase at the 10 cm soil moisture sensor ended. This indicates that macropores and high sand content allowed the water to move through the system extremely quickly, infiltrating after the soil at 10 cm became wetted close to the residual water content of the sensor at 35 cm. The volumetric water content at 10 cm began to increase after 12 hours, and the volumetric water content at 35 cm began to increase after 23 hours. This delay is likely due to the dryness of the soil. These data are shown in Figure 5.9. The perched water table in the system began to increase before the soil at 35 cm began to signify an increase in volumetric water content. However, this is likely due to preferential flow paths from macropores within the system. At the time that the soil moisture sensor at 35 cm begins to read increases in volumetric water content, the well transducer level increases much quicker.
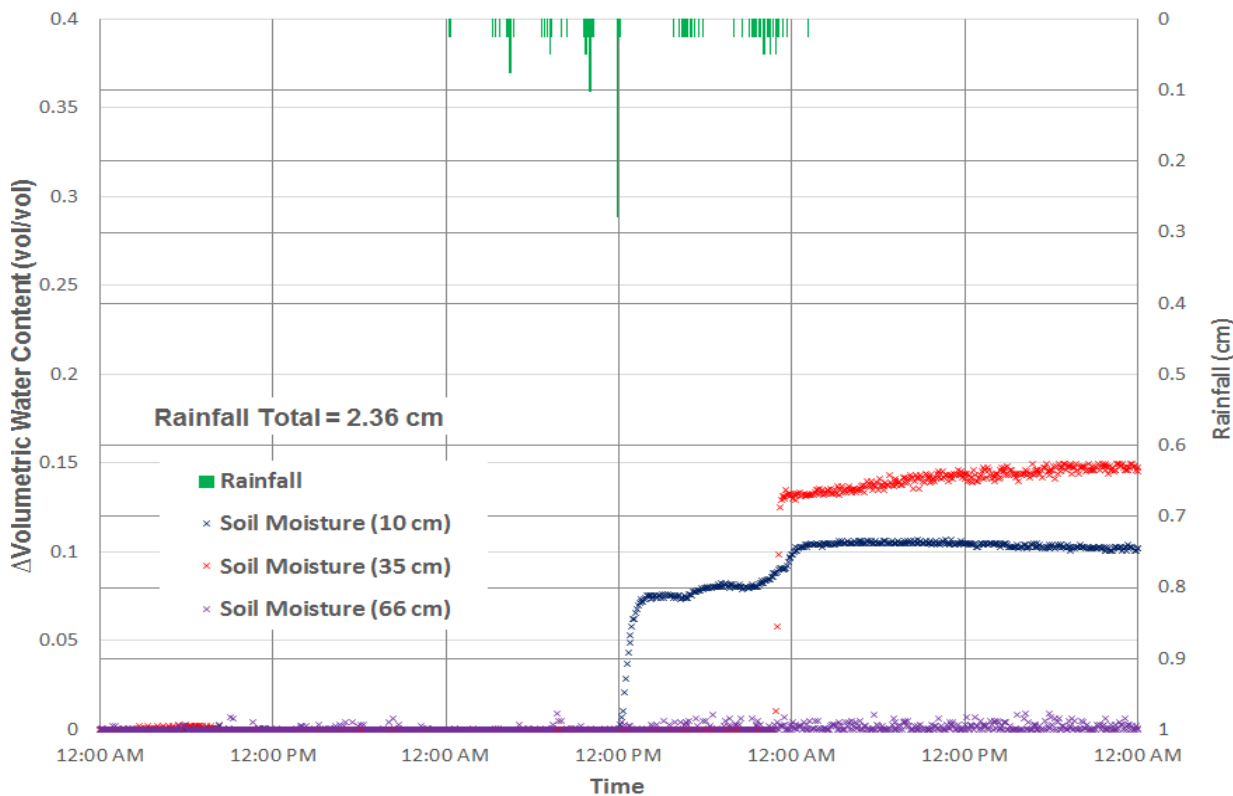
Figure 5.9 PTI soil moisture data from the 09/10/2015 event

Using an estimated void space of 0.330 (32.5%) for the 0.56 m of dry soil height above the water level and the 469 m^2 surface area of the rain garden, it was found the rain garden had an available storage of about 86.67 m^3. The runoff volume was found to be 83 m^3, and the amount of rainfall directly into the rain garden was approximated to be 11 m^3. The amount of water entering the rain garden was therefore around 94 m^3. From this estimation, it appears that all of the void space in the rain garden was filled, since the ratio of volume of rainfall to storage space was found to be about 1.1. This coincides with the data presented; since the well level did confirm that the water level within the system did approach the ground surface within the PTI. Since no ponding occurred and the well pressure transducer data presented validate water did not reach the ground surface, the rough approximation of rainfall volume to storage volume appears accurate. The discrepancy could be from differences in soil moisture and conservative calculations. This confirms that the PTI can completely store a rain event of this size during a relatively dry period.

From this analysis, it is validated that the extremely sandy material allows for the creation of macropores. High coarse-grained soil mixtures can be more prone to macropores because there is a lack of fine-grained particles to fill voids. Water moves through the system very quickly, and begins to fill the system at the native soil interface. This indicates that the sandy material does allow for quick infiltration as expected, but the compacted native soil layer hinders deep infiltration. From these storm data, it is also shown that the PTI was able to handle the event quite well despite being burdened with a perched water table. The rain garden system was able to handle the event without any ponding, demonstrating that the rain garden may not have "failed" despite the possibly compacted interface. During a typical storm event of the area, the PTI had the available storage. However, it should be noted that this is during a very dry period. The plant

growth at the PTI at this time were also typical wetland plants, stipulating that regular vegetation could struggle to grow in the very sandy soil and high water table.

5.2.3   Bioinfiltration Traffic Island

The BTI did not experience any overflow during this event. From data analyses, generally, a 2.54 cm storm event is needed for the BTI to overflow. However, ponding did occur up to 0.13 m. This occurred 24 hours into the 25-hour event. The ponding level increased during periods of rain and decreased during the storm. The BTI pond was empty 13.5 hours after the event ended. This indicates that the BTI empties within the standard time of 72 hours. However, this could be due to the very dry period in which the event occurred. This may also explain why the water ponded, was able to infiltrate, then ponded again during the event. The BTI may have been dry enough for water to infiltrate quickly once it made it through the organic layer which has built up in the BTI over time. Figure 5.10 shows the ponding plot for the 09/10/2015 event at the BTI. Figure 5.11 confirms that infiltration did move into the media during the storm, since the ponding level rose and fell during the event.
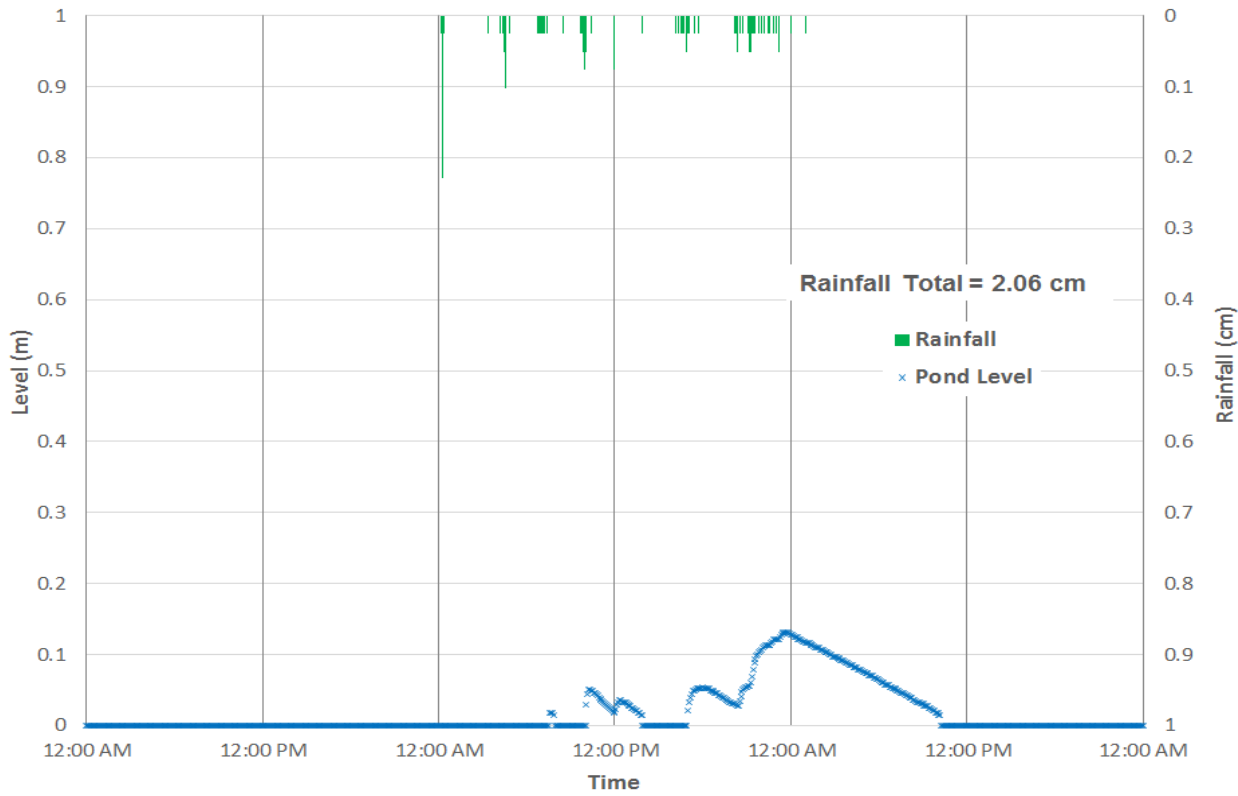
Figure 5.10 BTI pond pressure transducer data from the 09/10/2015 event

The soil moisture sensors at the BTI increased around the same time, with the 35 cm duplicate and 10 cm increasing before the others. This could be due to preferential flow paths cause by macropores. Since the BTI has sustained vegetated grow for 15 years, roots and wormholes could have caused preferential flow in the system to certain soil moisture sensors (Weiler 2005). However, all of the sensors begin to read increases in volumetric water content at around 18 hours into the event. This suggests that water moves through the system to deeper depths very rapidly. The sensors read an increase until around 24 hours into the event, at which point the soil volumetric water content levels off. The sensors begin to indicate decreases in soil moisture around 23 hours after the event ends. This is shown in Figure 5.11. The sensors confirm increases in soil volumetric water content at the same time the ponding begins to increase to maximum level. At around the time the pond begins to empty, the soil volumetric water contents

140

begin to level off. This verifies that the system is working well and water is moving through the system at a sufficient pace.
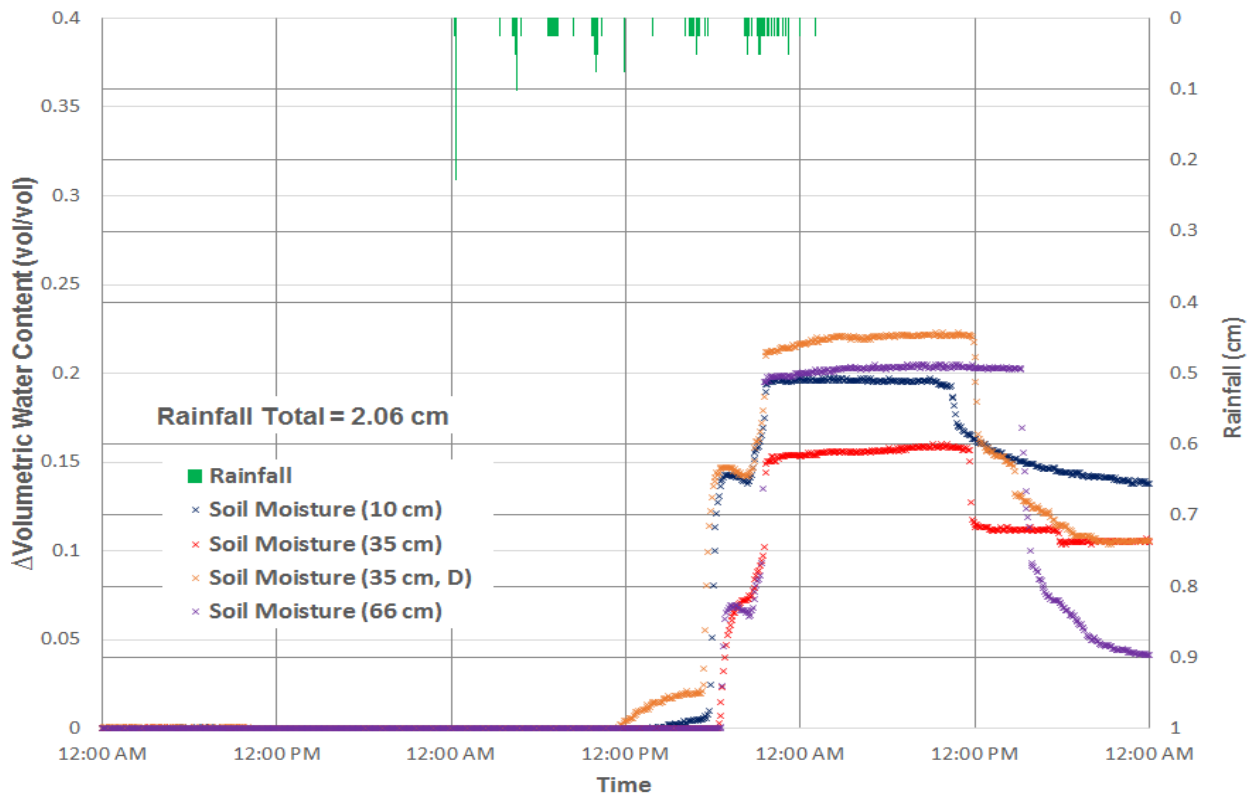
Figure 5.11 BTI soil moisture sensor data from the 09/10/2015 event

The approximate runoff volume was estimated by assuming the 56% of pervious area would not affect the runoff volume, since the storm occurred during a dry period. The runoff volume was found to be 48 m^3, and the rainfall falling directly into the BTI was calculated to be approximately 5 m^3. Therefore, the amount of rainfall entering the BTI is roughly 53 m^3. Comparing this to the 57.34 m^3 void space estimate stated in a previous section, the ratio of volume of rainfall to storage space was found to be about 0.9. The 1 m^3 discrepancy could be from differences in soil moisture and conservative calculations. The data presented indicate that this storm was stored within the BTI, even though some ponding was present. The ponding that

141

did occur (which infiltrated during the event) is likely due to the time it takes water to move through the limiting soil layer, which is the organic layer built up within the system.

These BTI data validate that despite age and a buildup of an organic layer above the engineered media, the rain garden is still working well. In fact, soil volumetric water content increases occurred at similar times as the PTI, justifying that the highly sandy engineered media which does not favor vegetation may not be necessary for rain gardens. The BTI, which has the largest drainage area to SCM area ratio of the three storms and the highest fine-grained content, performed very well in a typical storm in the Villanova area.

5.3 9/29/2015 Storm

5.3.1   Fedigan Rain Gardens

The FRGI indicated ponding occurring with two peaks which closely correspond with rainfall, as shown in Figure 5.12. The first peak occurred simultaneously with the rainfall, and then the FRGI began to empty until the rainfall started again around 6 hours later. At this time, the FRGI shows the highest point of ponding, which was 0.10 m after about 14.5 hours. The pond then slowly began to empty around 3 hours after the rainfall ended. No overflow occurred during this rain event, as 0.15 m of ponding is required before overflow occurs. Therefore, water entering the overflow device must be from leakage or rainfall falling directly into the overflow riser.
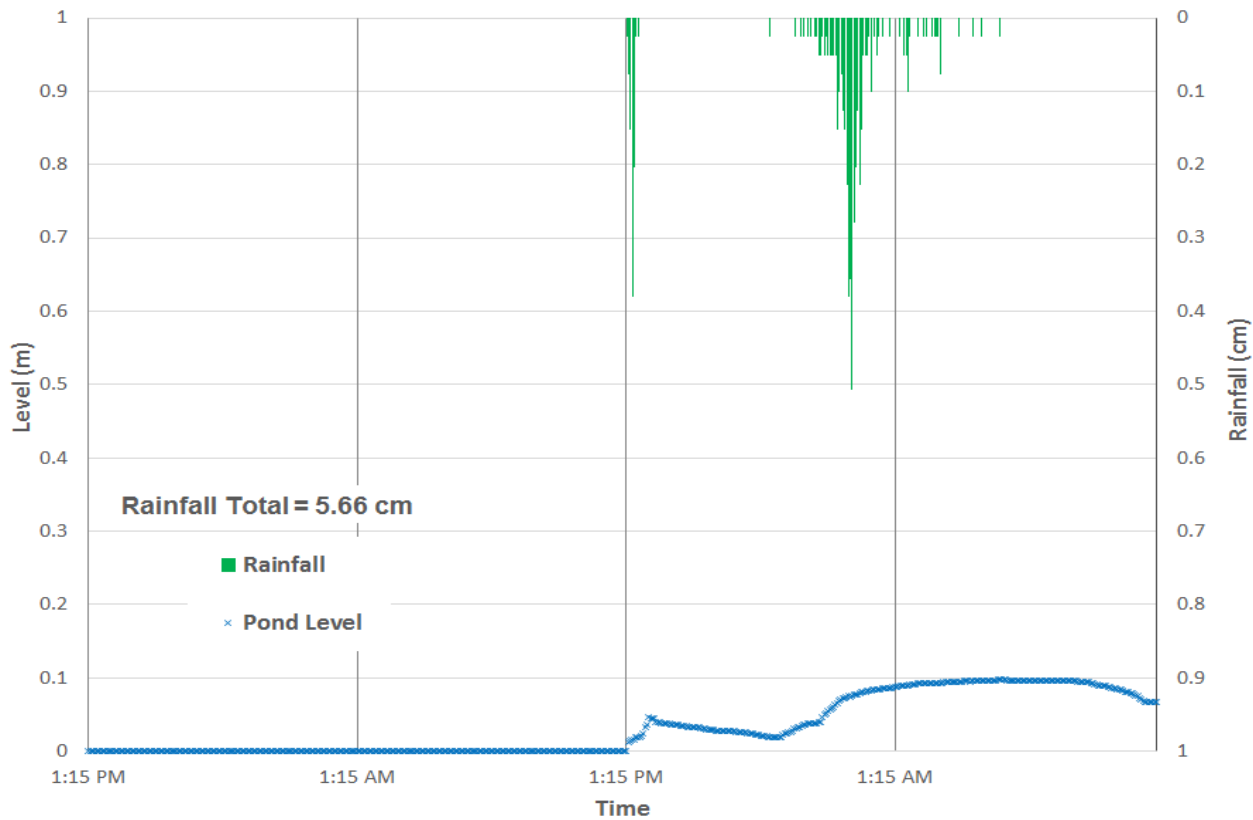
Figure 5.12 FRGI pond pressure transducer data from the 09/29/2015 event

Figure 5.13 shows the soil volumetric water content change at 35 cm during the 09/29/2015 storm. As displayed, the volumetric water content does not change during the first 0.5 hour rainfall. After the 6 hour break and rainfall began to occur again, the soil moisture sensor indicated a rapid increase in volumetric water content. The volumetric water content rose very quickly by 0.137 (13.7%). After the most intense duration of the rain event, the volumetric water content slowly by another 0.007 (0.7%). This suggests that water moved through the soil quickly, then slowly after ponding began to occur. This is demonstrated by Figure 5.14, which shows the pond level and the soil volumetric water content plotted together. The second peak of the pressure transducer occurs around the same time as the soil volumetric water content rapid

increase. As the pressure transducer demonstrates the pond is emptying, the soil volumetric

water content begins to increase again, but not as rapidly as during the rain event.
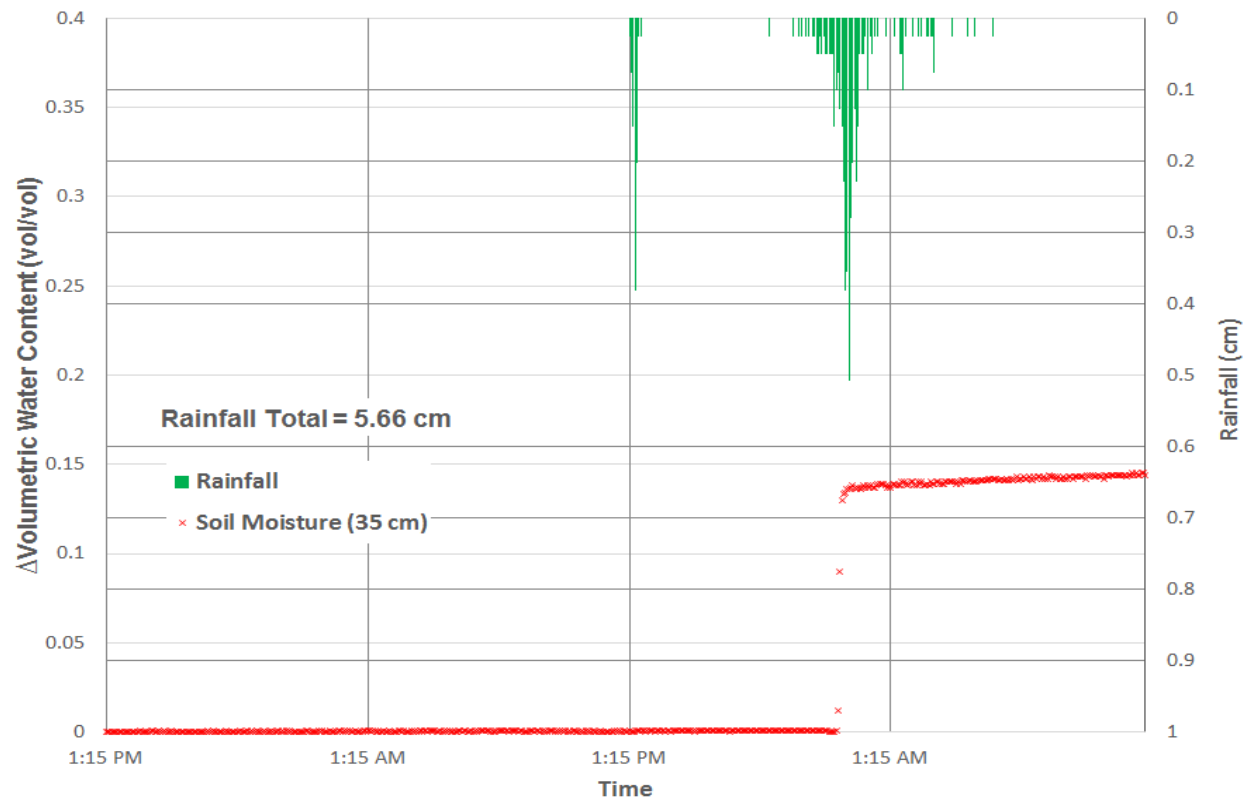
Figure 5.13 FRGI soil moisture sensor data from the 09/29/2015 event.
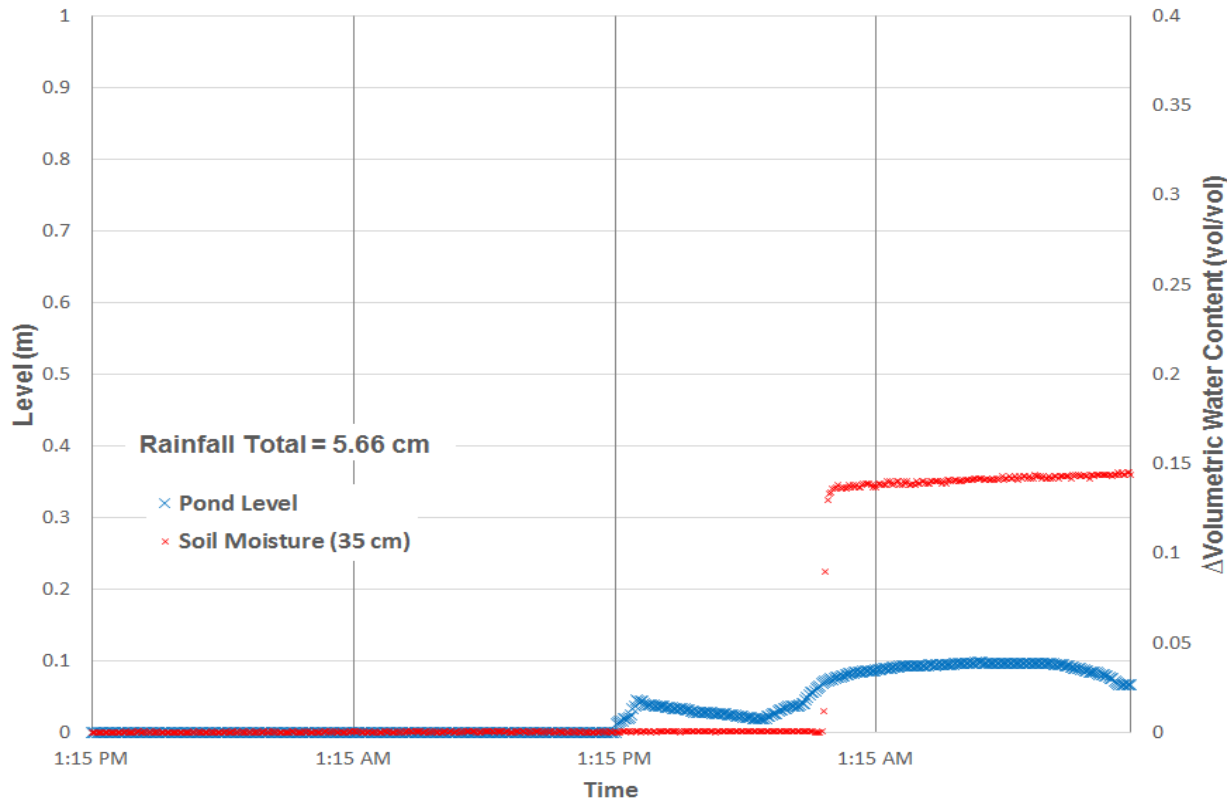
Figure 5.14 FRGI soil moisture sensor and pond pressure transducer data from the 09/29/2015 event

The FRGR performed differently than the FRGI during this storm event. Pond pressure transducer readings show that the FRGR ponded 0.06 m, which is 0.03 m less than the FRGI. As shown in Figure 5.15, the underdrain level occurred around the same time as the overflow riser level. The first pond level peak also occurs shortly before the underdrain level and overflow riser level increase. After the first 0.5 hour of rainfall, the height of water in the underdrain leveled at around 5.72 cm, and the height of water in the overflow riser and pond also leveled. When the rainfall begins again, the underdrain level rises significantly. Based on the pressure transducer reading, the underdrain was completely full and around 5 cm of pressure was applied above the underdrain, meaning there was a significant amount of water 5 cm above the underdrain. The overflow riser level and pressure transducer also increase to their maximum heights during this

second part of the storm. Based on how quickly the underdrain level and overflow riser pressure transducer read increases, it can be implied that water moves through the system very quickly. After the storm ended, the pond level began to recede. The underdrain level also began to fall at a rate similar to recession rates seen during studies at the BTI (Emerson 2008). Before the event, the overflow riser pressure transducer implied that the water level was decreasing. This could be due to evaporation or water moving back through the underdrain.
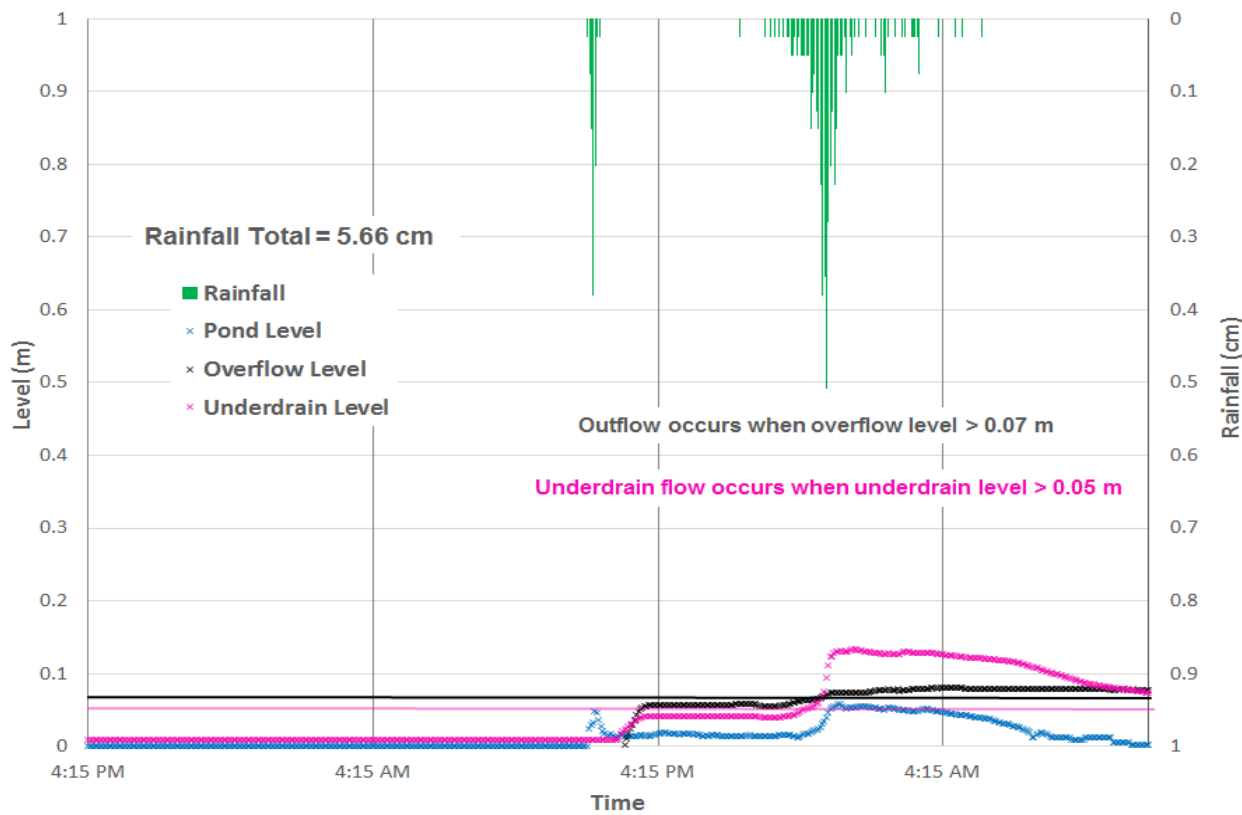
Figure 5.15 FRGR pressure transducer data from the 09/29/2015 event

From Figure 5.16, it is shown that the underdrain flow began shortly before the outflow began. With this and the information that the FRGR overflows after 0.15 m of ponding, it confirms that all outflow is treated outflow from the underdrain. These flows began during the second part of the rain event, which started 6 hours after the first 0.5 hours of rain. Figure 5.17 shows that the underdrain flow and outflow began at the same time the ponding began to increase to its highest

146

point. This implies that water moves through the system very quickly to the underdrain, where it begins to leave the system. Since there was an additional 5 cm of water above the underdrain, water is slowly exiting the system slowly as it infiltrates to the underdrain. The maximum underdrain flow rate was around 2.83×10^{-5} m^3/s and the maximum outflow rate was around 3.96×10^{-5} m^3/s.
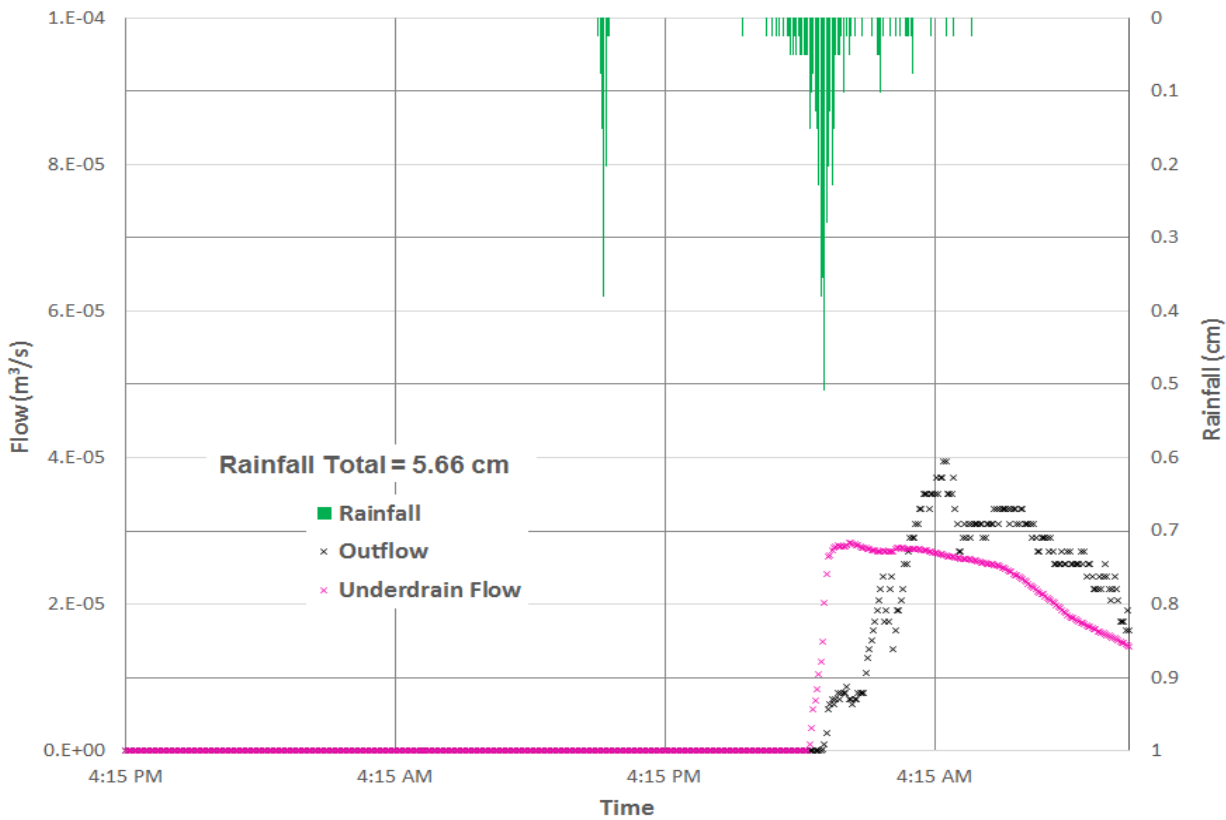
Figure 5.16 FRGR flow data from the 09/29/2015 event
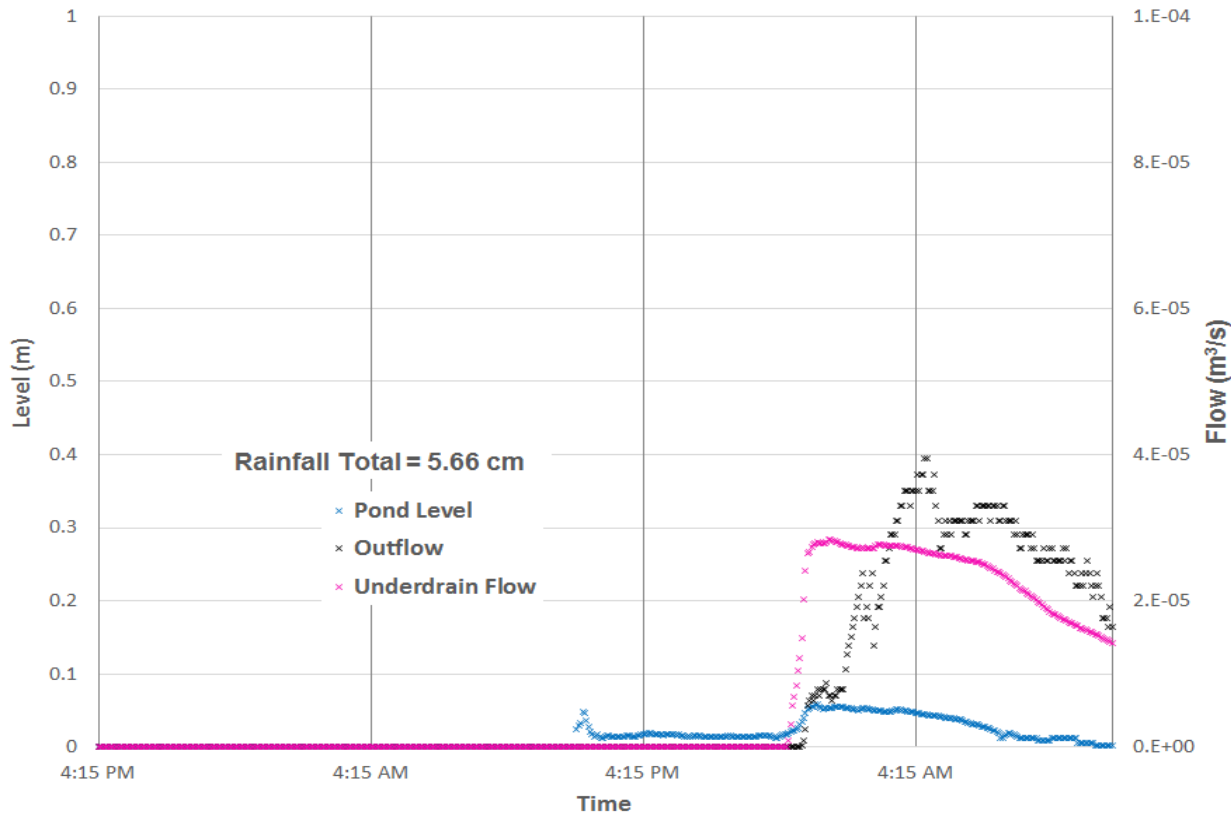
Figure 5.17 FRGR ponding data and flow data from the 09/29/2015 event

Figure 5.18 shows the change in soil moisture at 66 cm, which is directly above the liner. The soil moisture read an initial volumetric water content of 0.361 (36.1%), suggesting that the soil at this depth is close to saturation before the rain event. The soil volumetric water content increased 0.037 (3.7%) during the event. The highest soil volumetric water content was 0.398 (39.8%), which is very close to laboratory saturation. It is interesting to see that the volumetric water content increased quickly during the first 0.5 hours of rainfall, which further reinforces the idea that water moves through the system quickly. The soil moisture sensor indicate that the volumetric water content levels off after an increase of 0.017 (1.7%) after the first 0.5 hours of rainfall. This increase began around 1 hour of the rain began. The second increase began around 2 hours after the rain started again. The soil volumetric water content still increased 2 hours after

148

the event ended, and then began to decrease. Figure 5.19 displays the soil moisture sensor data plotted with the pressure transducer levels. From this plot, it can be shown that all pressure transducers and soil moisture sensors read an initial increase during the first 0.5 hours and no increases during the 6 hour break in the storm. All instruments imply additional increases during the second portion of the rain event. The pond level and soil moisture sensor increases occur at almost the same time, suggesting that water moves through the engineered media quickly. Figure 5.20 depicts the soil moisture sensor plotted with the flow data. As shown, flow does not stop increasing until the flows begin decreasing.
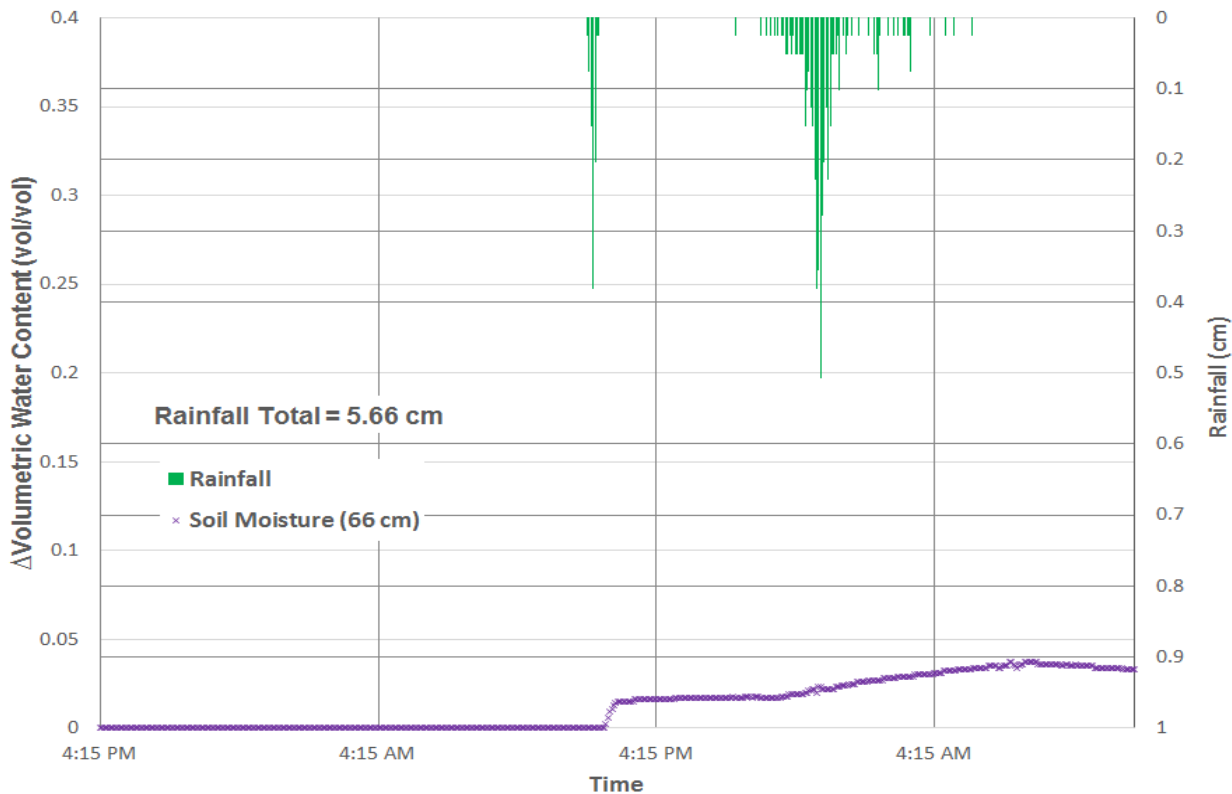
Figure 5.18 FRGR soil moisture data from the 09/29/2015 event
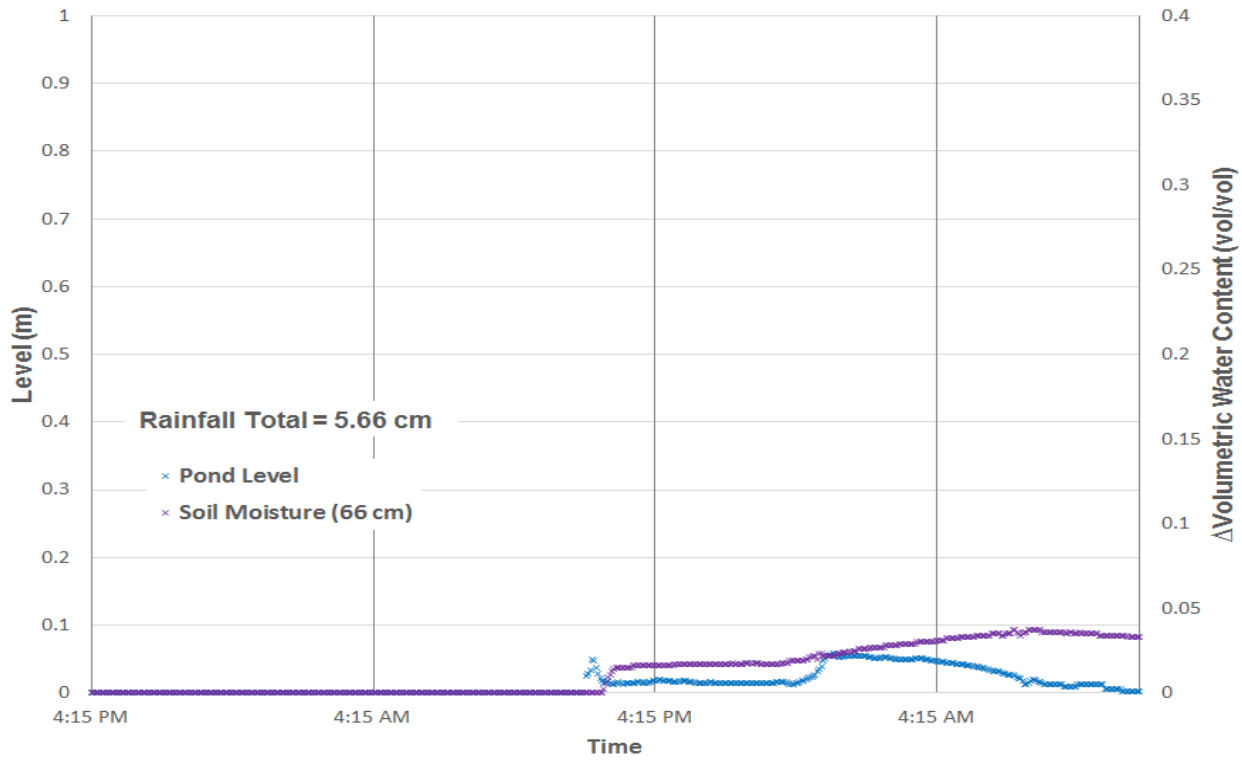
Figure 5.19 FRGR pressure transducer data and soil moisture data from the 09/29/2015 event
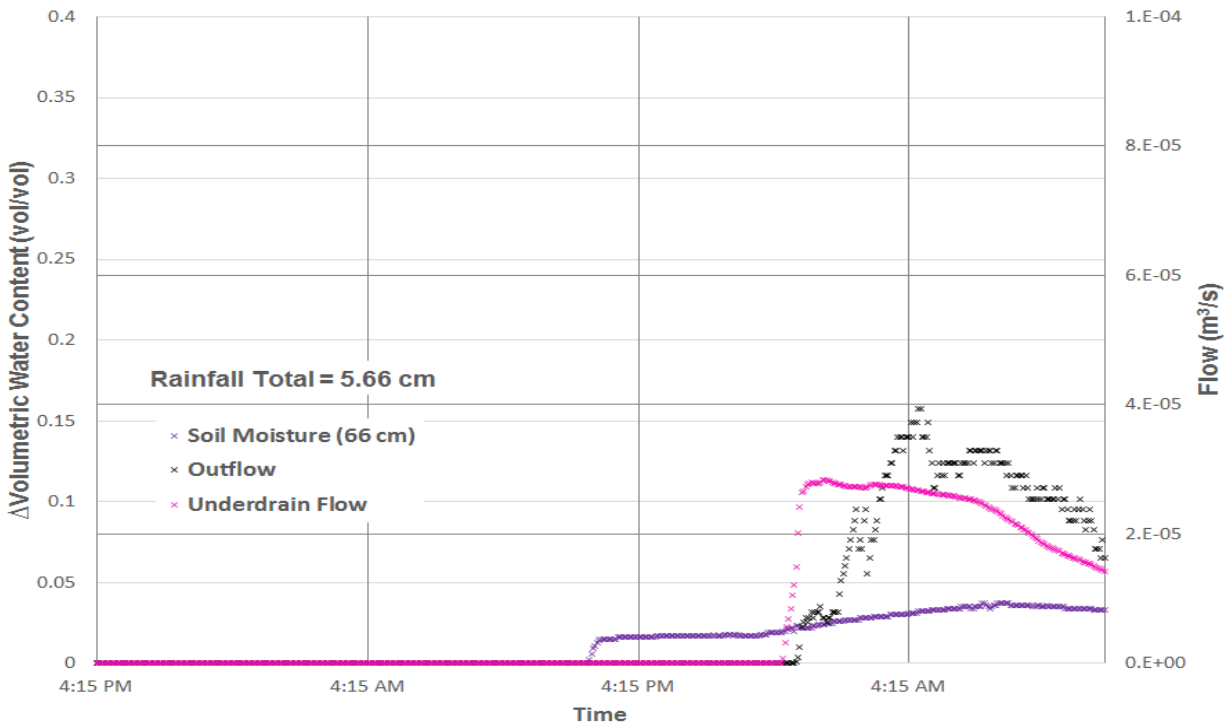
Figure 5.20 FRGR soil moisture and flow data from the 09/2/2015 event

Since overflow did not occur and all outflow was treated from the underdrain, the underdrain and liner system were not necessary for this event. The FRGI, despite having slightly higher ponding, was able to infiltrate all of the runoff from the roof of Fedigan Hall. Ponding did not exceed the recommended time of 72 hours for the FRGI during the event. For this storm event, the engineered media with native soil interface performed much better than the system with a liner and underdrain because it did not create any outflow. However, it is important to note that while this was a larger storm, the impervious drainage area-to-infiltration area is very small. It is especially small compared to the BTI and PTI. Therefore, overflow and long ponding periods are not as likely at the FRGI or FRGR.

5.3.2   Pavilion Traffic Island

During the event, the PTI did not experience any overflow. As shown in Figure 5.21, the ponding only reached a maximum of 0.62 m, and ponding would need to reach a maximum of 0.83 m before overflow would occur. The rain gage at the PTI did not indicate a 6 hour break in rain as the other rain gages did. It is unclear why this is; however, it could be due to the location of the PTI. The PTI is located on another area of campus than the other sites, so natural rainfall scatter could have caused this difference. Perhaps on this area of campus, small amounts of rainfall continued while it did not on the other side of campus. Ponding began to increase rapidly after around 2 hours, and was above 0.61 m after 4 hours of rainfall. After this, the ponding experienced only slight increases and decreases until 10 minutes after the event. At only 10 minutes after the event, the pond began to empty. However, it is important to note that this decrease is not very rapid.
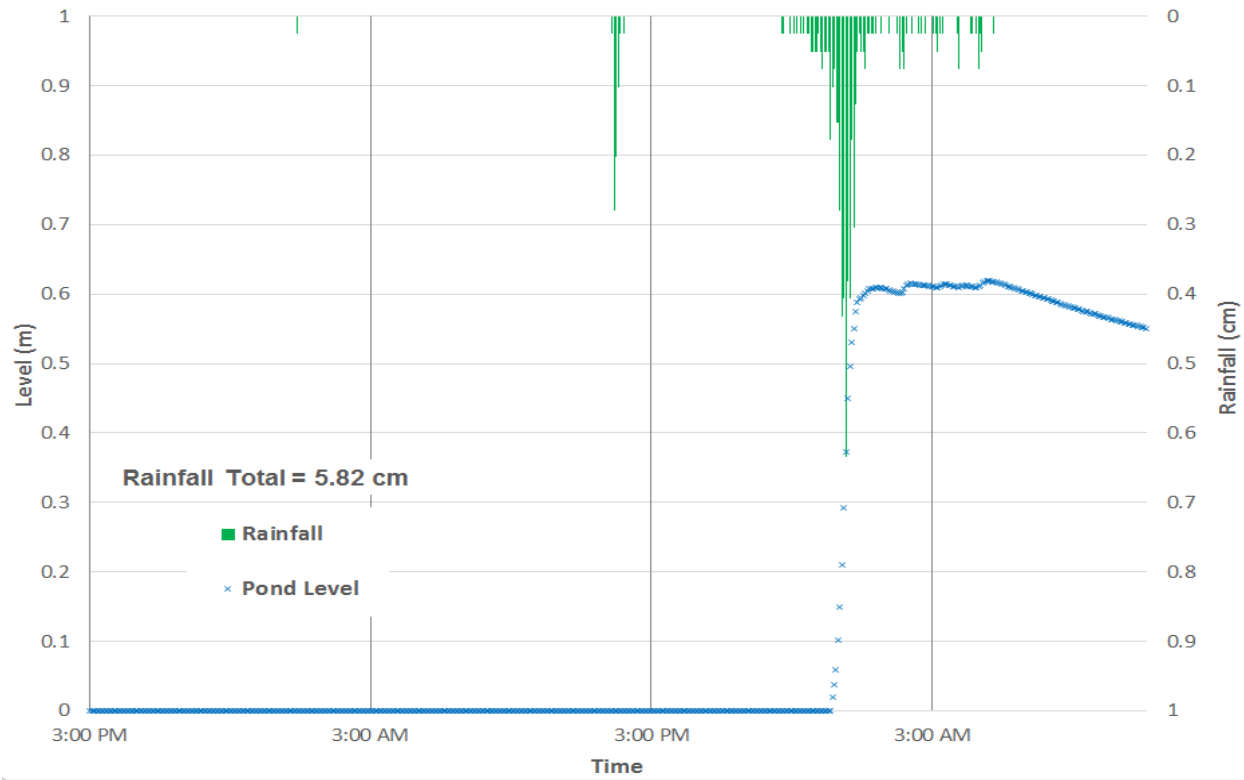
Figure 5.21 PTI ponding data from the 09/29/2015 event

The well pressure transducer indicated that the water level in the pond was around 0.49 m before the event began. The water level increased only slightly up to 0.57 m during the first 3 hours of the event. After the first 3 hours the water increased rapidly up to 1.40 m, which is demonstrated in Figure 5.22. As shown in Figure 5.23, the water level in the pond began to decrease around the same time as the water level in the pond. However, the water level in the PTI did not decrease at a rate as fast as the water in the pond. The pressure transducer in the well did not suggest that water was up to the point read by the pond pressure transducer. However, this may be because screened PVC was not used high above the height of the engineered media. This was because it was expected that the pressure transducer in the pond would be able to accurately measure this level above the engineered media. The two water levels increase at almost the same time, confirming that water infiltrated through the PTI to the well quickly.

152
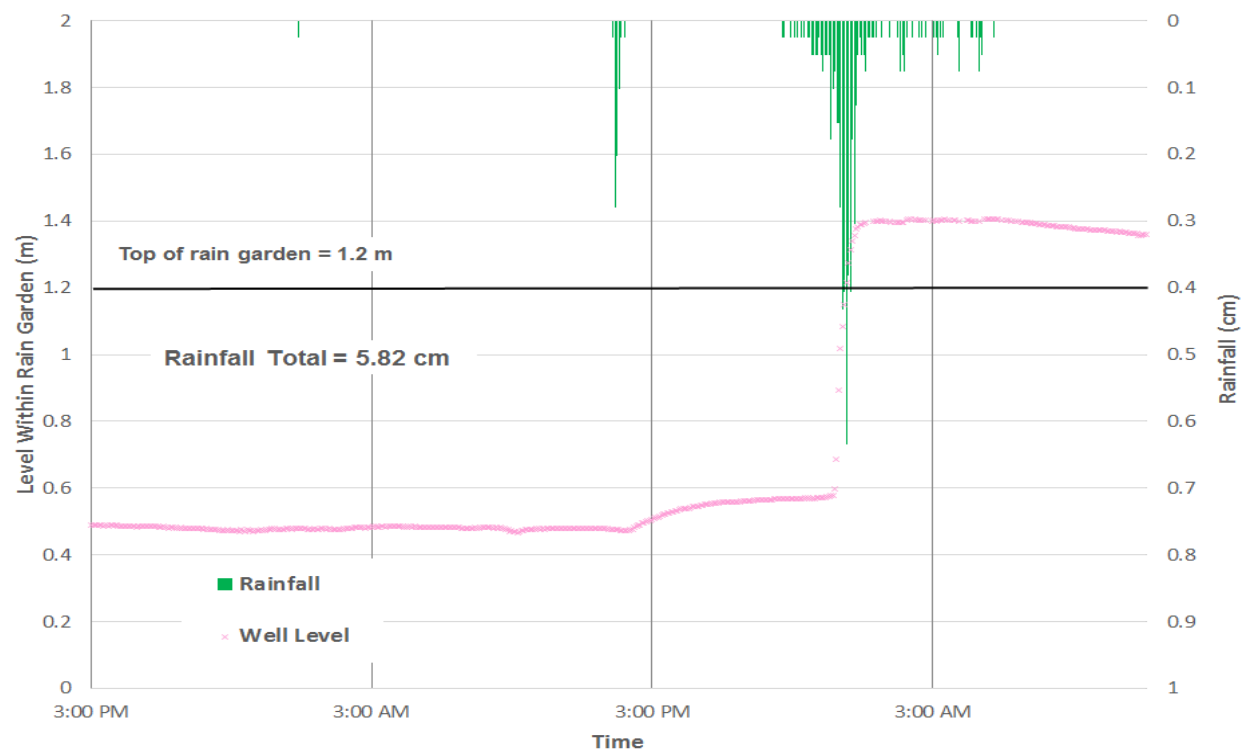
Figure 5.22 PTI well transducer data from the 09/29/2015 event
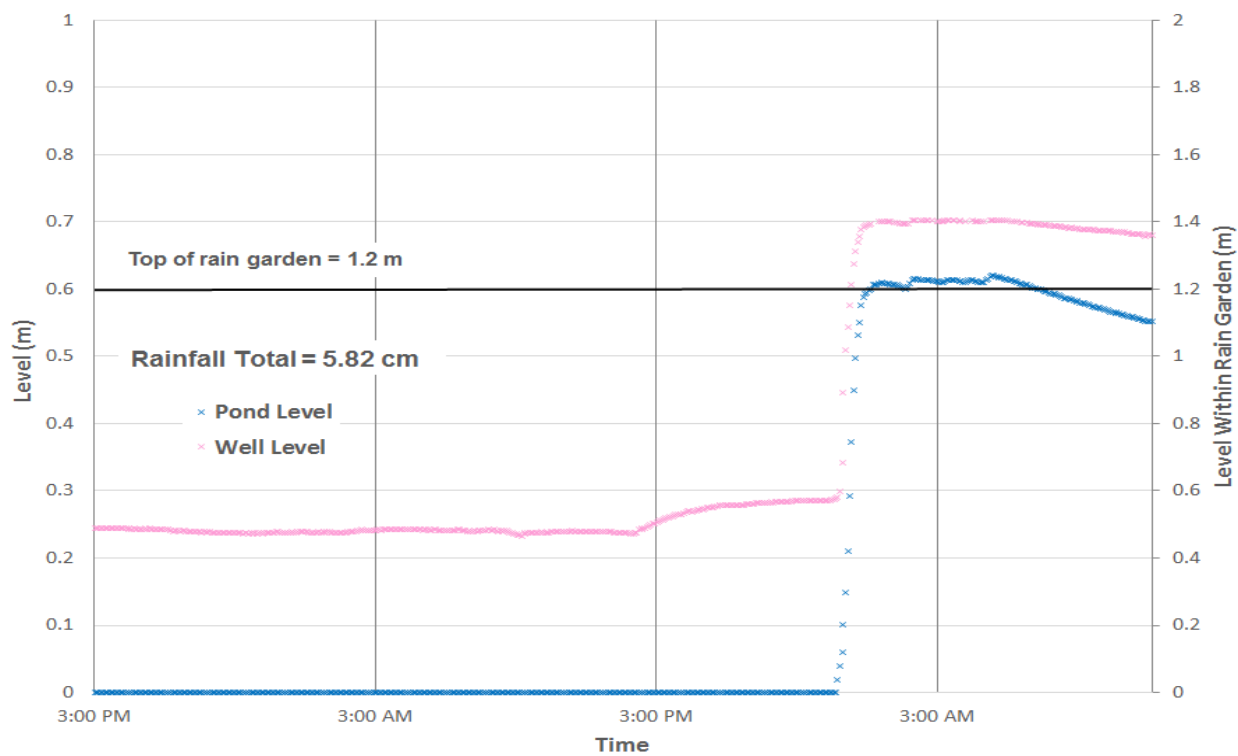
Figure 5.23 PTI ponding data and well transducer data from the 09/29/2015 event

The soil volumetric water contents are displayed in Figure 5.24. The plot shows that the soil moisture sensor at 10 cm and 35 cm increased at almost the same time. The soil moisture sensor at 10 cm reads an increase of 0.297 (29.7%) after around 3 hours of rainfall. This quick increase is followed by a small increase of 0.012 (1.2%), which continues approximately 7 hours after the event ends. The sensor similarly had a rapid increase at the same time; however, it only increased 0.165 (16.5%). This is likely because the soil moisture sensor at 10 cm was reading lower volumetric water contents before the event began. After approximately 7 hours after the event ended, the soil moisture sensor at 35 cm increased an additional 0.013 (1.3%). The soil moisture sensor at 66 cm indicated only a slight increase of around 0.022 (2.2%) after 3 hours of rainfall. This is likely because the soil in that area was very close to saturation, as demonstrated by the well transducer. These data confirm that water moves through the system very fast and fills the engineered media from the bottom up. This is likely because of the compacted native layer beneath the engineered media. These data also imply that water infiltrates slowly after the rain event ends and ponding has occurred. This is because the soil in the engineered media is at saturation or near saturation already, and the infiltration of the native soil layer begins to control the system. Figure 5.25 shows the soil moisture sensor data plotted with the well transducer data. This demonstrates that the well transducer did start to read a slight increase before the soil moisture sensors indicated an increase in volumetric water content. This is likely due to macroporosity or water entering the slotted polyvinyl chloride (PVC) pipe before it moves down through the system. However, the rapid increases occur around the same time, which validates the system fills very quickly and cannot move into the native soil layer beneath the rain garden. Figure 5.26, which shows the soil moisture sensor data plotted with the ponding data, demonstrates this as well. Figure 5.26 also shows that the slight increases in volumetric water

content begin around the same time as the ponding reaches its maximum level. This confirms that the slight increases in volumetric water content are water infiltrating from the pond. The decrease in ponding displayed in this plot is likely related to this as well.
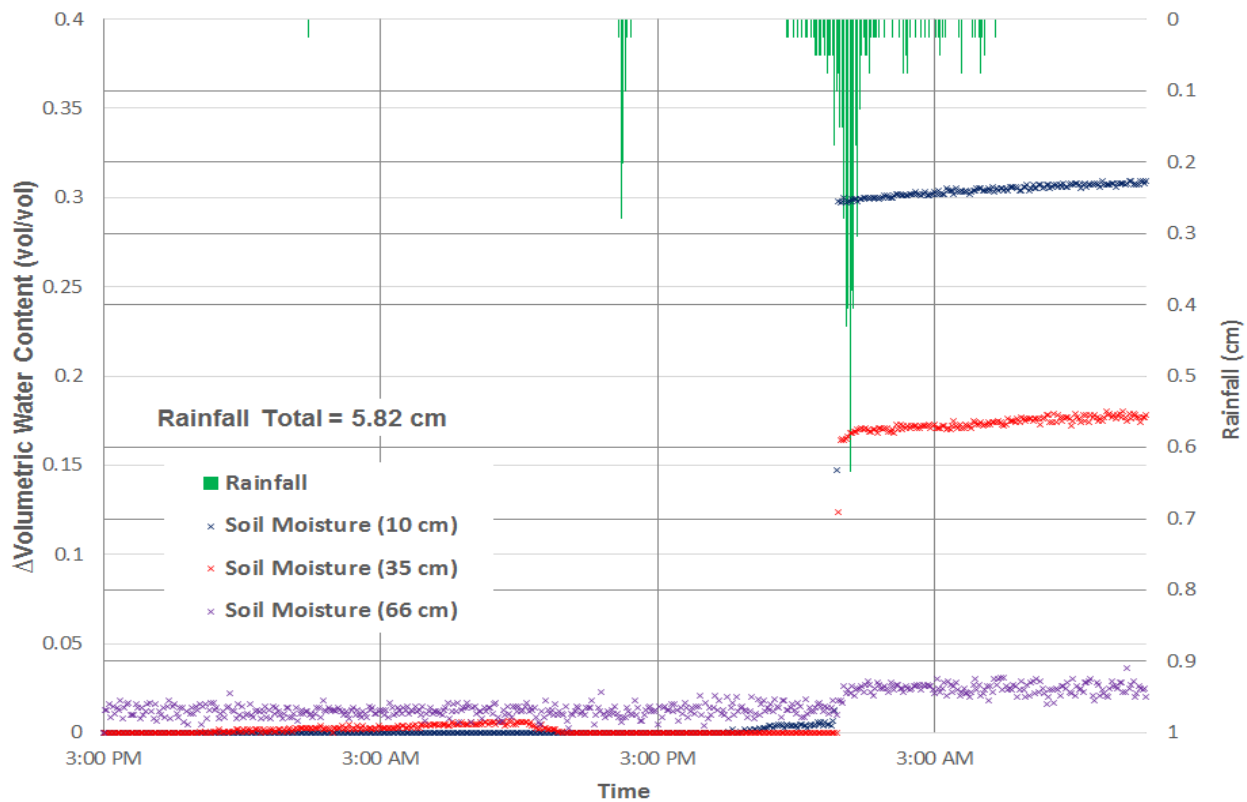
Figure 5.24 PTI soil moisture sensor data from the 09/29/2015 event

155
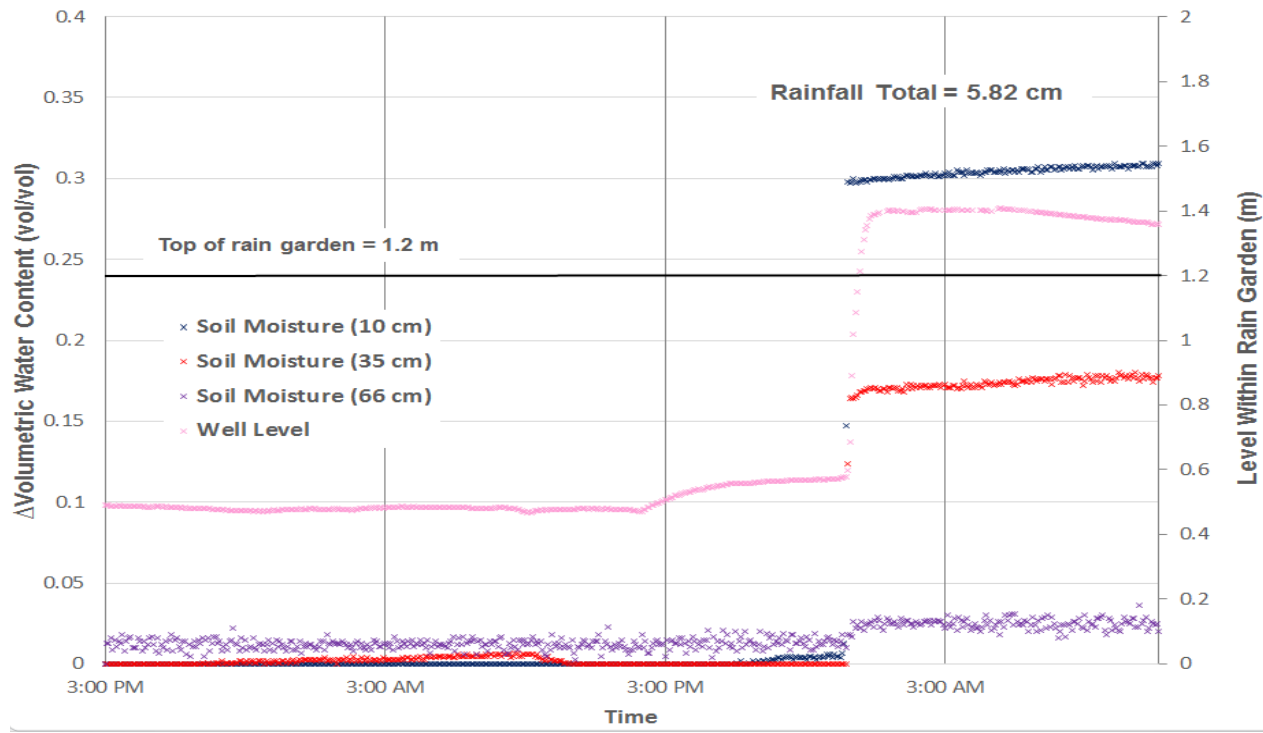
Figure 5.25 PTI soil moisture sensor data and well transducer data from the 09/29/2015 event
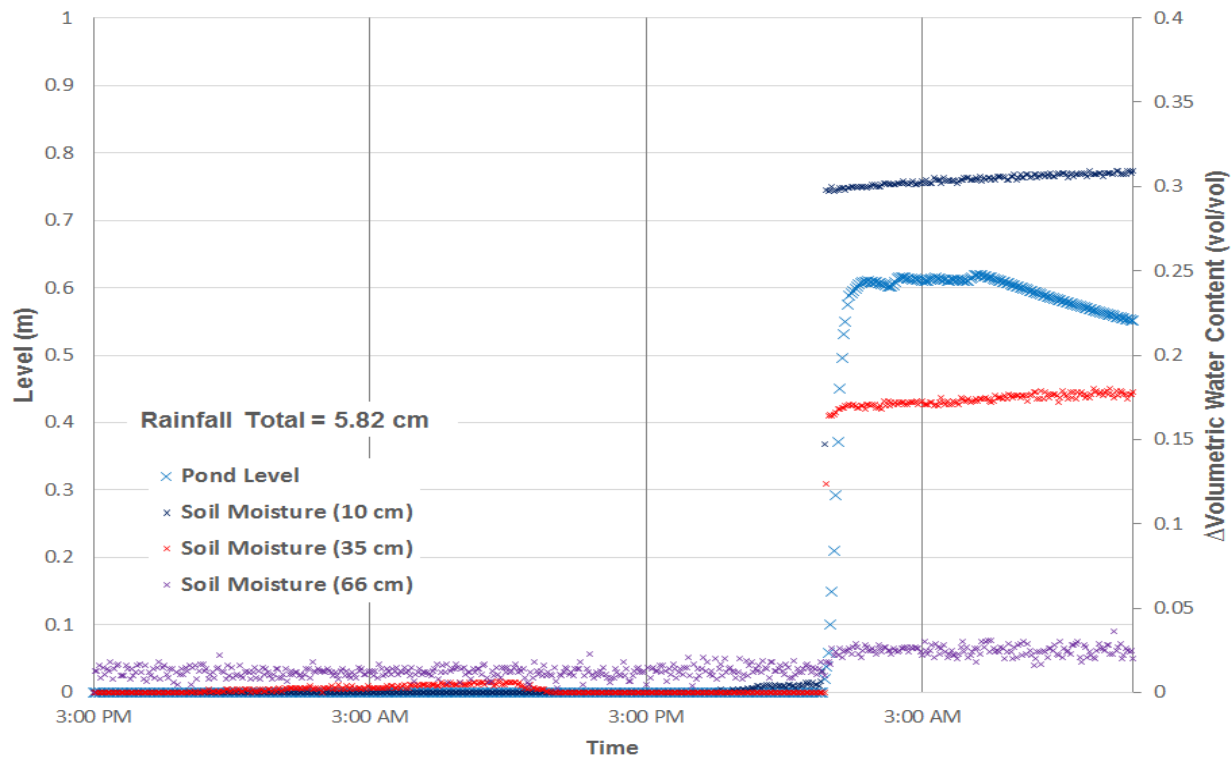
Figure 5.26 PTI soil moisture sensor data and ponding data from the 09/29/2015 event

156

Data from this storm validate that the PTI is large enough to handle the storm without overflow. However, this is likely because of the large bowl depth of 0.83 m. The large bowl depth may be necessary due to the high drainage area and potentially compacted native soil layer. The sandy material allows water to infiltrate very fast; however, the potentially compacted native soil interface begins to control infiltration when the engineered media is saturated. This event also causes ponding lasting longer than 72 hours, which is not comparable to rain garden criteria. These data are not displayed, since a smaller rain event shortly after the 09/29/2015 (but not within the 6 hour storm constraint). The drainage area and size of the PTI are appropriate for this event. Despite ponding issues and being considered a "failed" rain garden, the system did not experience any overflow during a rain event that is a little closer to the PADEP design requirements than the 09/10/2015 storm.

5.3.3 Bioinfiltration Traffic Island

From Figure 5.27, the pressure transducers demonstrate two peaks in both the weir and pond, which is similar to the FRG rain gardens. The BTI rain gage read that there was a 6 hour break in the storm, similar to the rain gage used for the FRG rain gardens. During the break, the pond level fell from 0.19 m to 0.01 m, showing that water does infiltrate quickly after ponding occurs. The pond level reaches a maximum of 0.63 m 10.5 hours after the event begins. Since the BTI has a bowl depth of around 0.5 m, this confirms that overflow did occur within the system. Also, since the rain event caused over 1 inch of rain, overflow was expected. The pressure transducers experience similar recession curves after 10.5 hours of rain, which is when the most intense portion of the event occurs. This implies that water infiltrates quickly when soils are not saturated.
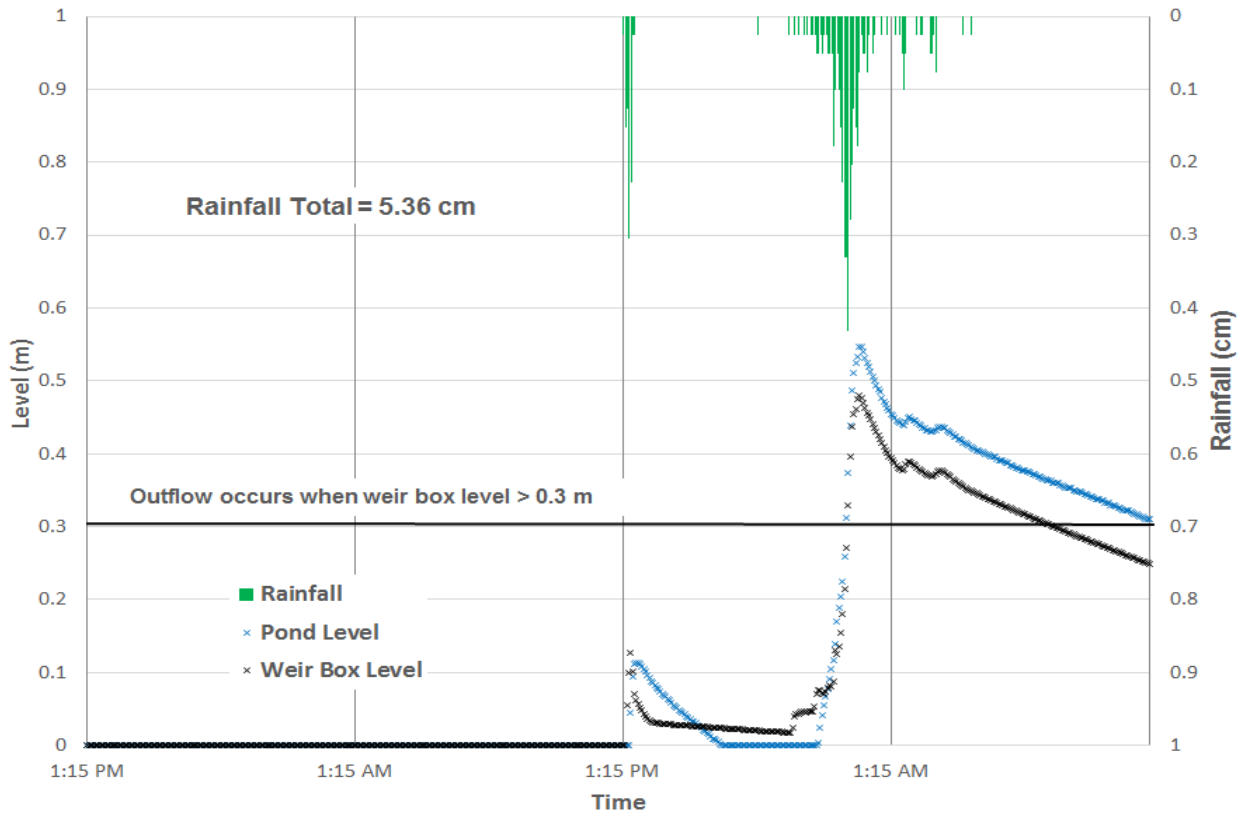
Figure 5.27 BTI pressure transducer data from the 09/29/2015 event

Figure 5.28 shows the overflow that occurred at the BTI during the 09/29/2015 event, and Figure 5.29 shows the ponding that occurred during overflow. As displayed, the overflow the maximum value is $1.06{\times}10^{-2}$ m³/s and occurs when the ponding is maximum at 0.63 m. After soils become saturated, ponding occurs rapidly. This proves that overflow occurs at the BTI as expected.
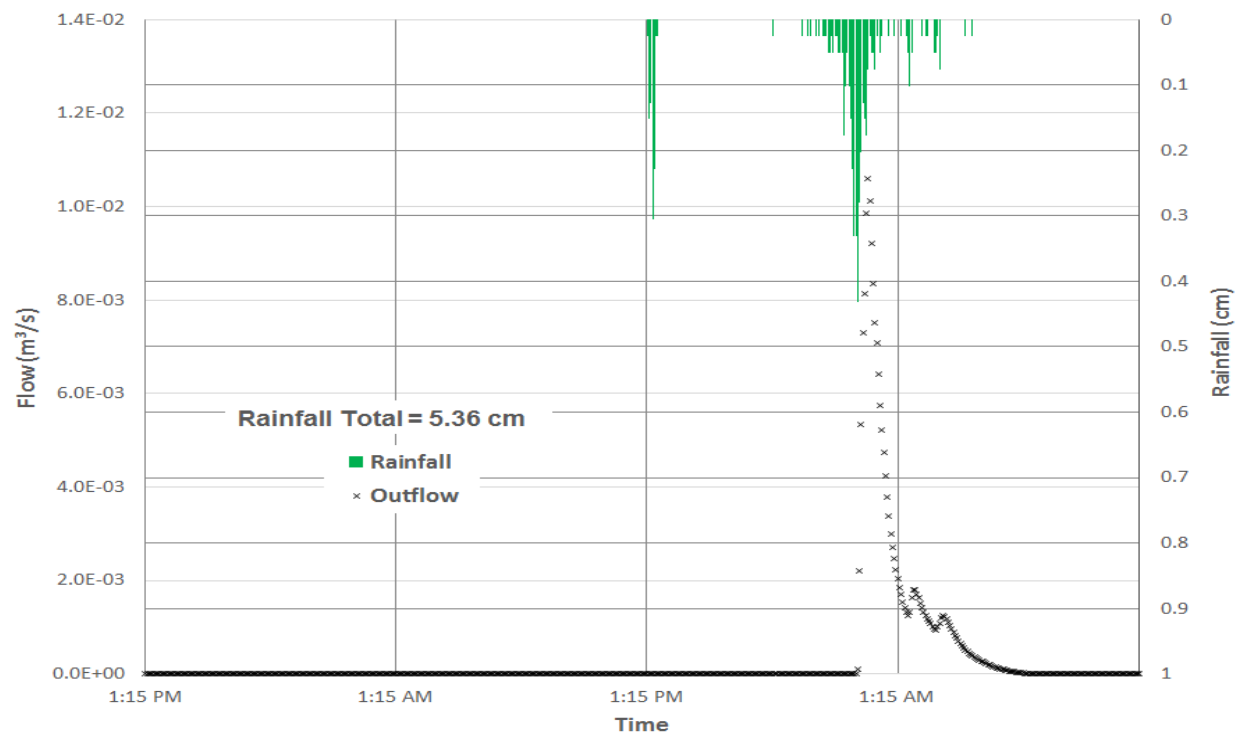
Figure 5.28 BTI overflow data from the 09/29/2015 event
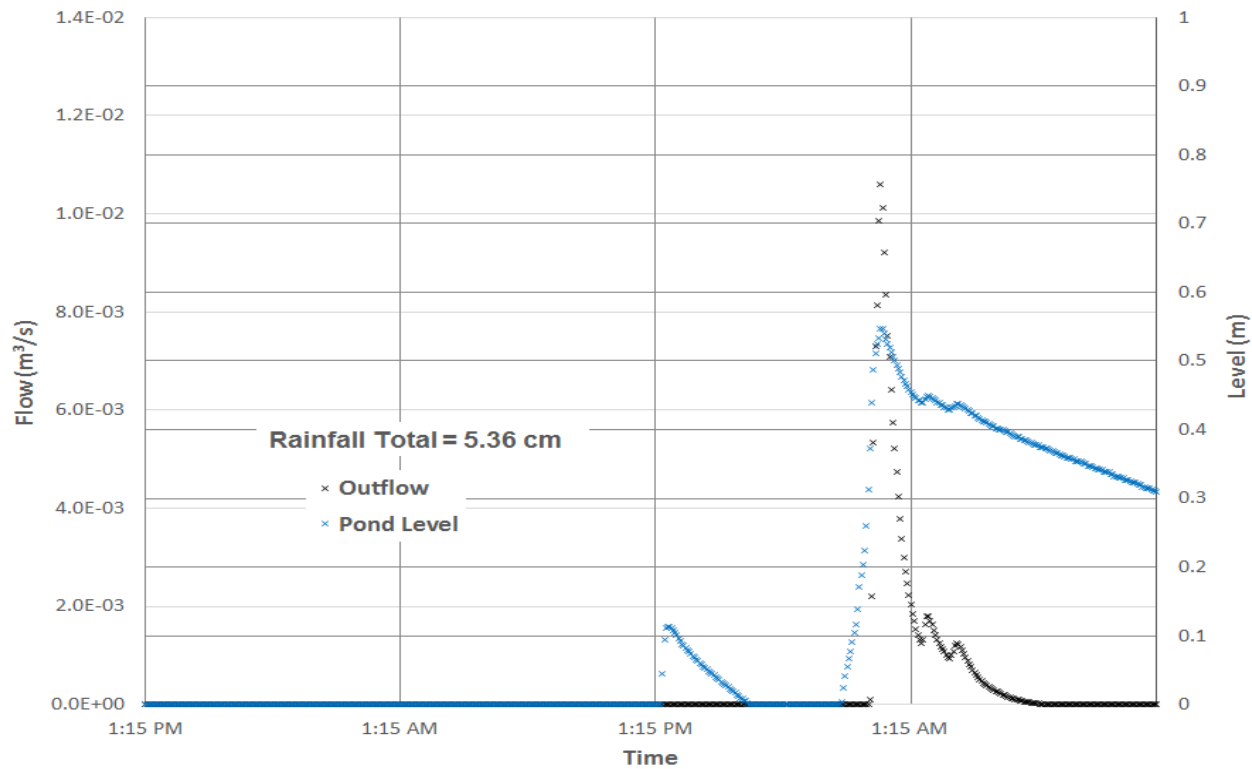
Figure 5.29 BTI overflow data and ponding data from the 09/29/2015 event

159

The soil moisture sensors at the BTI indicated rapid increases in volumetric water content until the 6 hour break. At the break, the soil volumetric water content began to drop until the rain began again. When the rain started again (10.5 hours after the event began) the soil volumetric water contents increased back to saturation. During the event, the soil moisture sensors showed very different increases in volumetric water content, as shown in Figure 5.30. This could be due to macroporosity within the system. Since the increases occurred around the same time, it suggests that water moves through the system very quickly. Since the volumetric water content decreased rapidly throughout the system during the break in the storm, it implies that the soil mix drains quickly. Figure 5.31 shows the soil volumetric water content increases plotted with the pressure transducer data. The increases in volumetric water content occur at nearly the same time as the pond begins to fill during the first ponding spike. The second ponding spike does not occur until after the soil moisture sensors spike for the second time. This validates that water was able to continue to infiltrate during the storm after the break in rainfall because water had moved through the soil quickly during the break. As the pond began to empty, the soil moisture sensors read small increases in volumetric water content. This likely suggests infiltration of the water in the pond into the engineered soil mix.
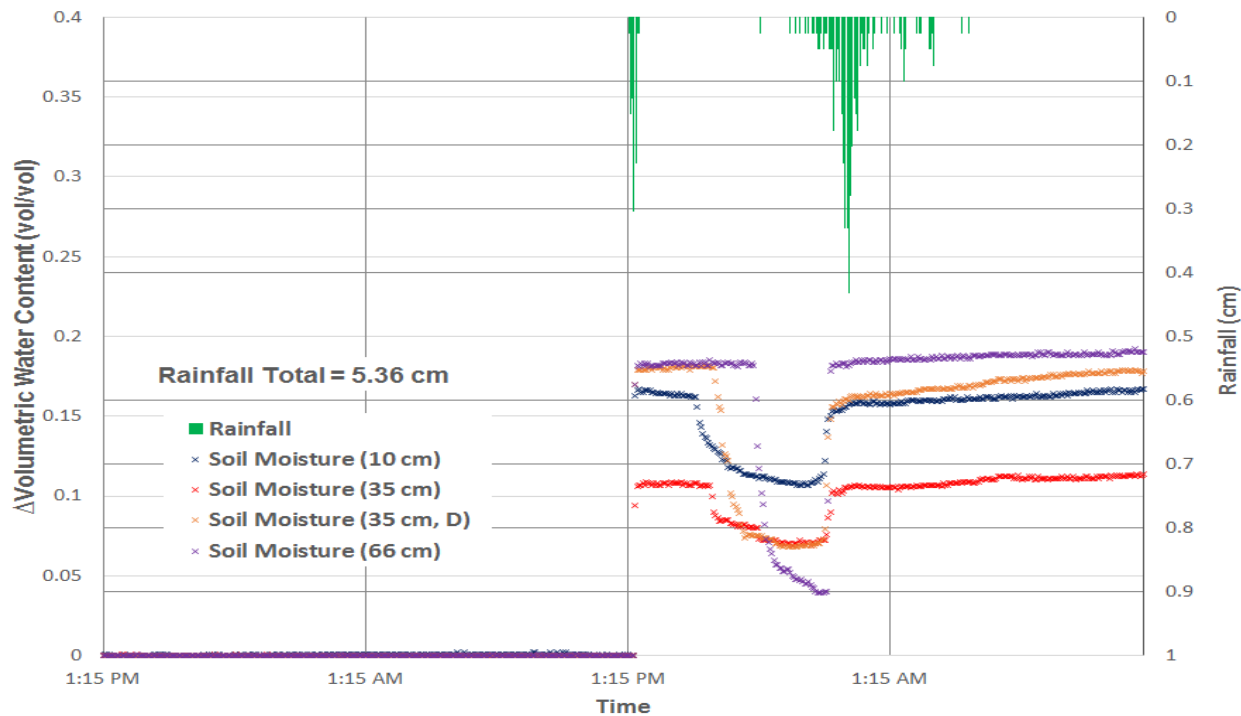
Figure 5.30 BTI soil moisture sensor data from the 09/29/2015 event
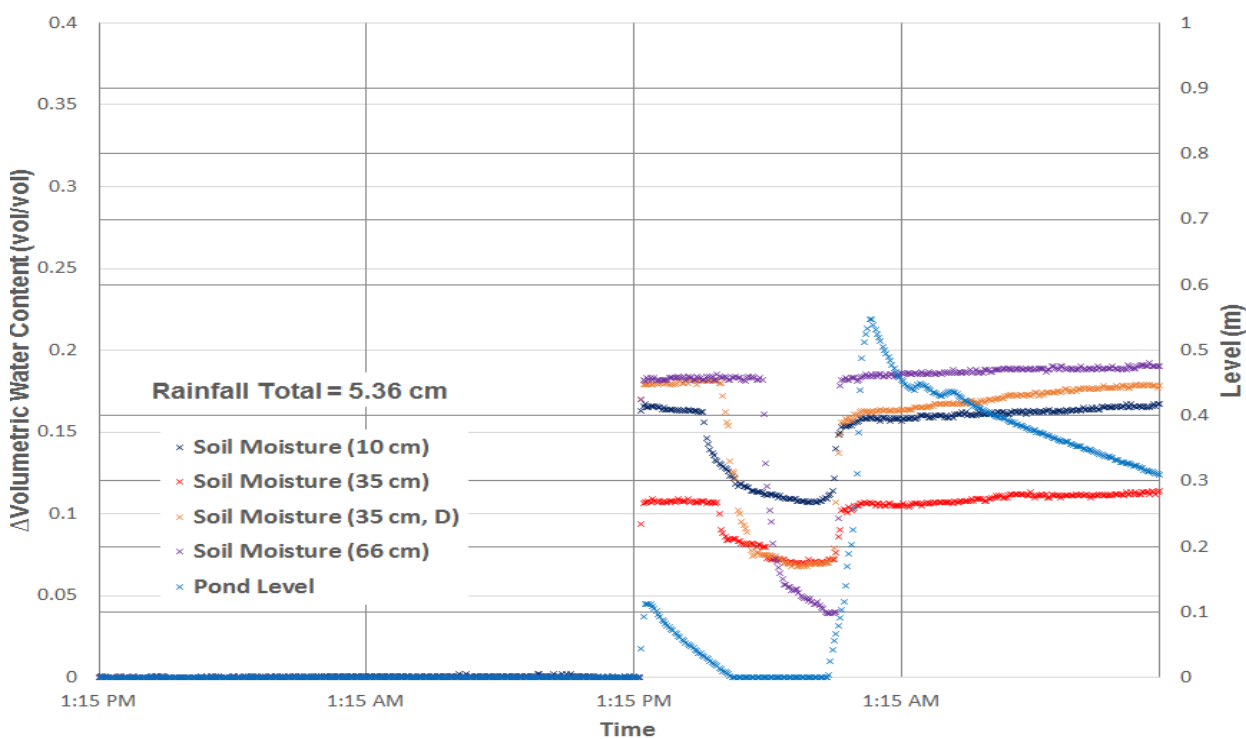
Figure 5.31 BTI soil moisture sensor data and pressure transducer data from the 09/29/2015 event

Data from the BTI imply that the system drains quickly after water infiltrates through the organic layer, similarly to the 09/10/2015 storm. The information confirms that the BTI does produce overflow in larger events, which is likely due to the high loading ratio. The BTI quickly infiltrates water into the engineered soil mix and does not pond for more than 72 hours. This validates that the BTI does perform well during these events, despite overflow. The BTI does have the highest loading ratio of all three sites, so overflow can be expected. With a larger bowl depth (such as the bowl depth at the PTI), overflow can be reduced. The soil type seems appropriate for this rain garden, despite having the highest amount of fines when compared to the other sites.

5.4 11/10/2015 Storm Comparison

5.4.1 Fedigan Rain Gardens

During the 11/10/2015 storm, the pressure transducer at the FRGI indicated that some ponding occurred after about 7.5 hours of rainfall. However, this ponding level was only around 0.02 m, which is much smaller than the 0.15 m necessary for overflow to occur. This is slightly higher than the ponding level that occurred during the 9/10/2015 storm, which was only around 0.01 m. These data are plotted in Figure 5.32. From this comparison, it is suggested that ponding does not occur often in the FRGI during a storm smaller than 2.54 cm, which is the typical Villanova storm event. This is proven from the dry period storm (9/10/2015) and the 11/10/2015 storm.
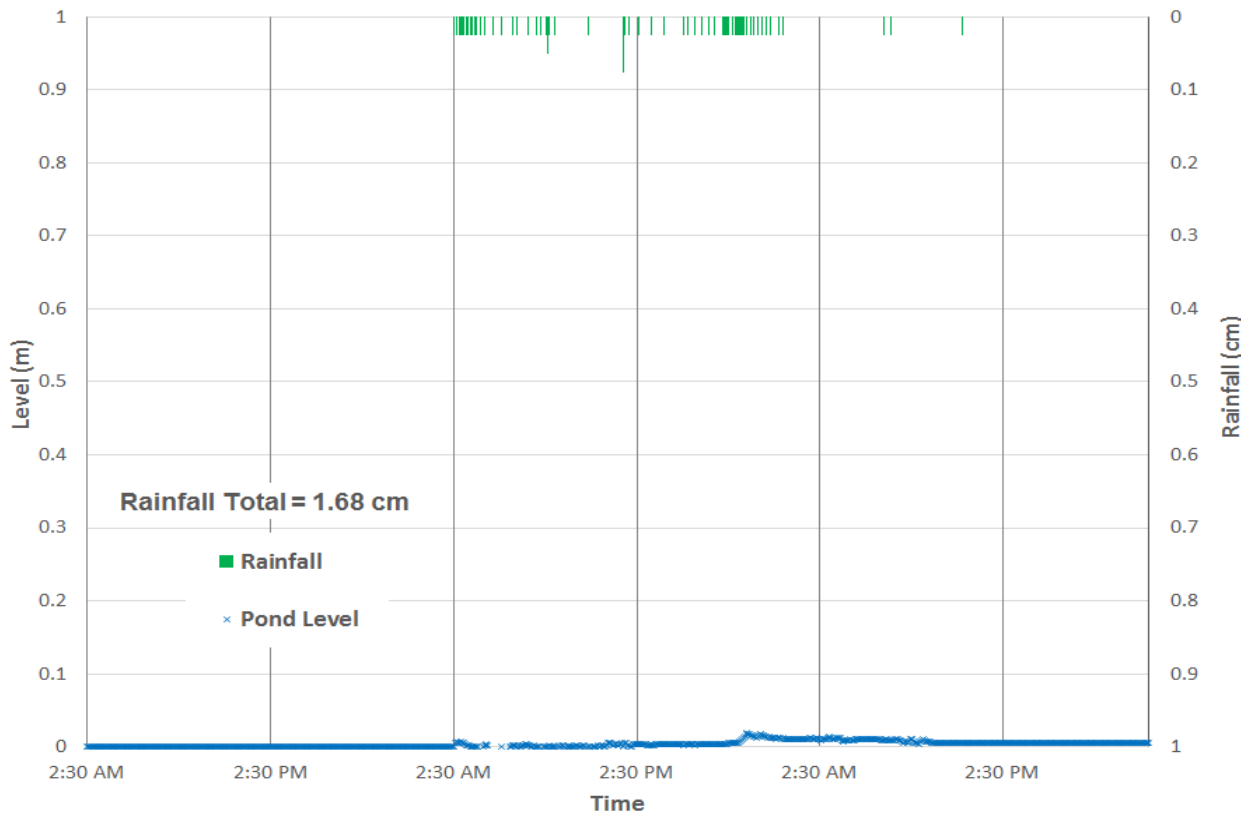
Figure 5.32 FRGI pond pressure transducer data from the 09/29/2015 event

The volumetric water content at 35 cm increased about 0.06 (6%) during the 11/10/2015 storm. In comparison, the soil moisture sensor at 35 cm did not record any change in volumetric water content during the 9/10/2015 storm. The volumetric water content data from the 11/10/2015 event are displayed in Figure 5.33. The volumetric water content at 35 cm was found to be around 0.300 (30.0%) before the 11/10/2015 storm event, and about 0.222 (22.2%) before the 9/10/2015 storm event. This comparison shows that water can infiltrate to the native soil interface if the soils above are not significantly dry.
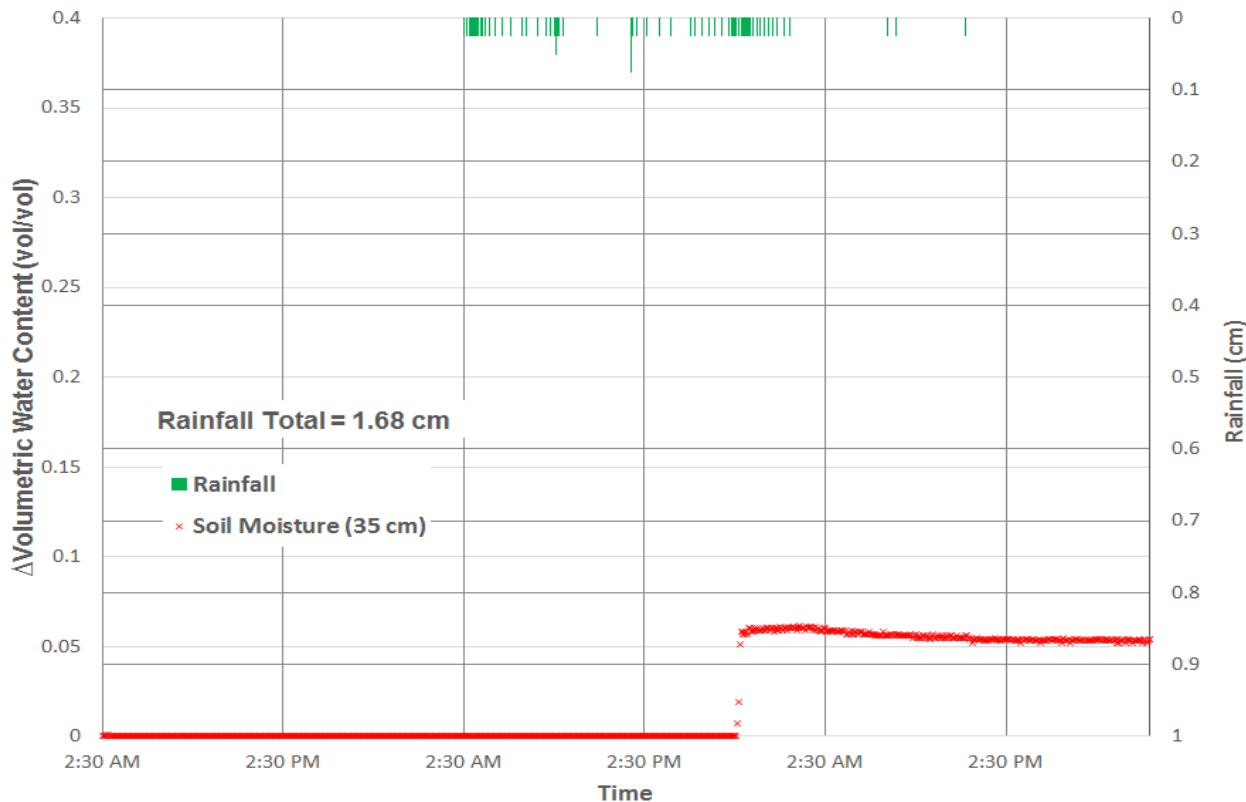
Figure 5.33 FRGI soil moisture sensor data from the 11/10/2015 event

During the 11/10/2015 storm event, ponding was almost negligible at the FRGR with the maximum pond level recorded as 0.01 m. This is similar to data presented for the 9/10/2015 event, which indicated no ponding occurred. The slight increase in ponding during the 11/10/2015 event is followed by an increase in the underdrain level, which is then followed by the overflow riser. This shows that the water infiltrated through the system quickly, entered the underdrain, and flowed through to the overflow riser. The underdrain level and overflow riser level begin rising faster during 11/10/2015 storm than during the 9/10/2015 event. This could be due to small breaks in rainfall during the 9/10/2015 rain event. Also, the overflow riser and underdrain pressure transducer suggest that water may be moving back from the overflow riser through the underdrain. This is demonstrated before the storm, where noticeable decreases in

underdrain level and overflow riser level can be observed. The data collected from the FRGR pressure transducer are displayed in Figure 5.34.
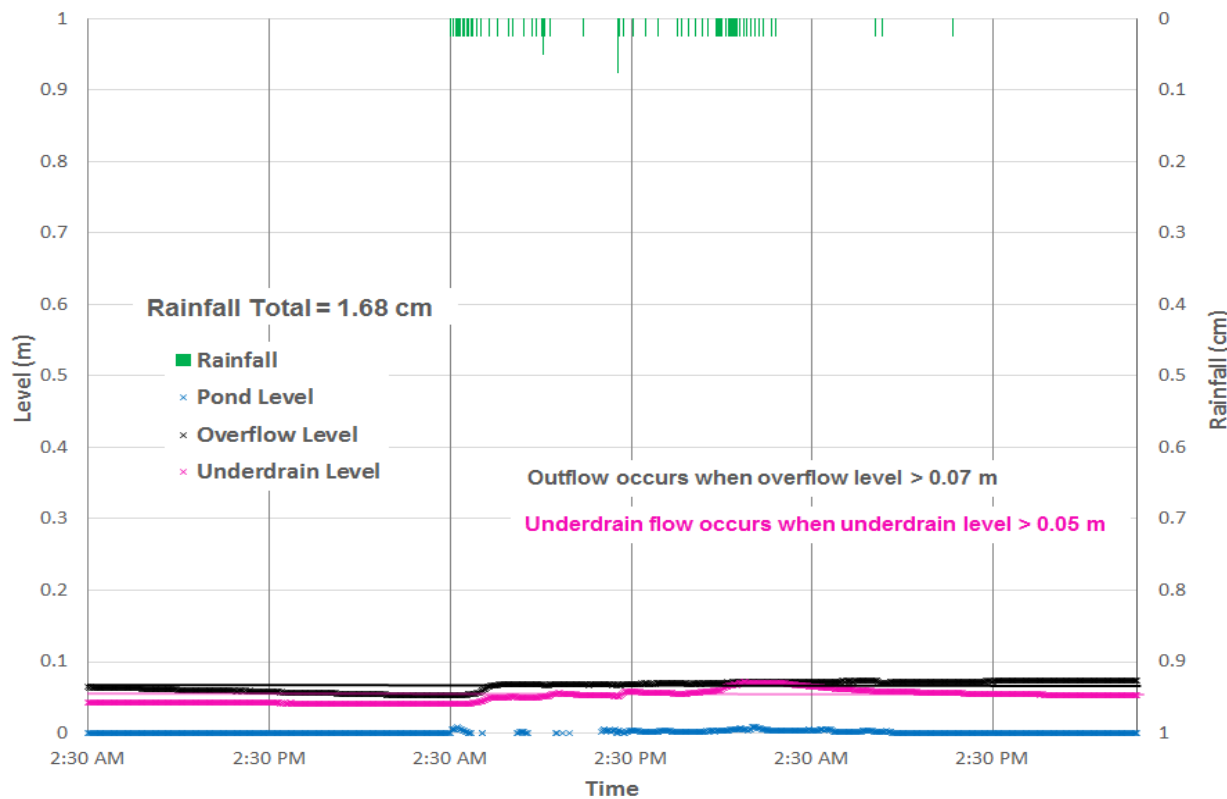
Figure 5.34 FRGR pressure transducer data from the 11/10/2015 event

The underdrain flow and outflow at the FRGR during the 11/10/2015 storm was not similar to the flow data collected during the 9/10/2015 storm. Higher underdrain flows and outflows were observed during the 11/10/2015 than during the 9/10/2015 storm. This is likely due to higher volumetric water contents above the underdrain and liner system during the 11/10/2015 storm. During the 11/10/2015 storm, it is probable that less infiltrated water was retained as soil moisture. Some of the increases in underdrain flow are followed closely by increases in outflow. These flow data collected from the 11/10/2015 storm at FRGR are plotted in Figure 5.35. From Figure 5.36, it is suggested that the small increases in ponding do not correlate with increases in flow rates during the 11/10/2015 event.

165
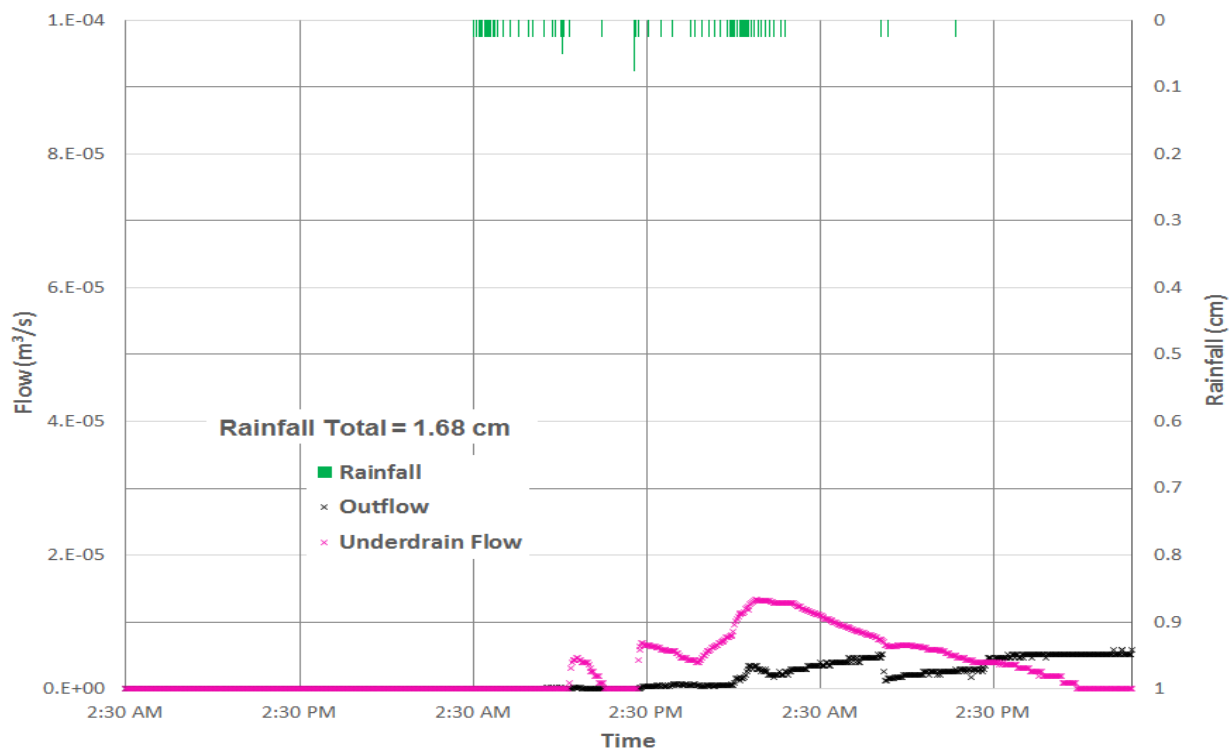
Figure 5.35 FRGR flow data from the 10/28/2015 event
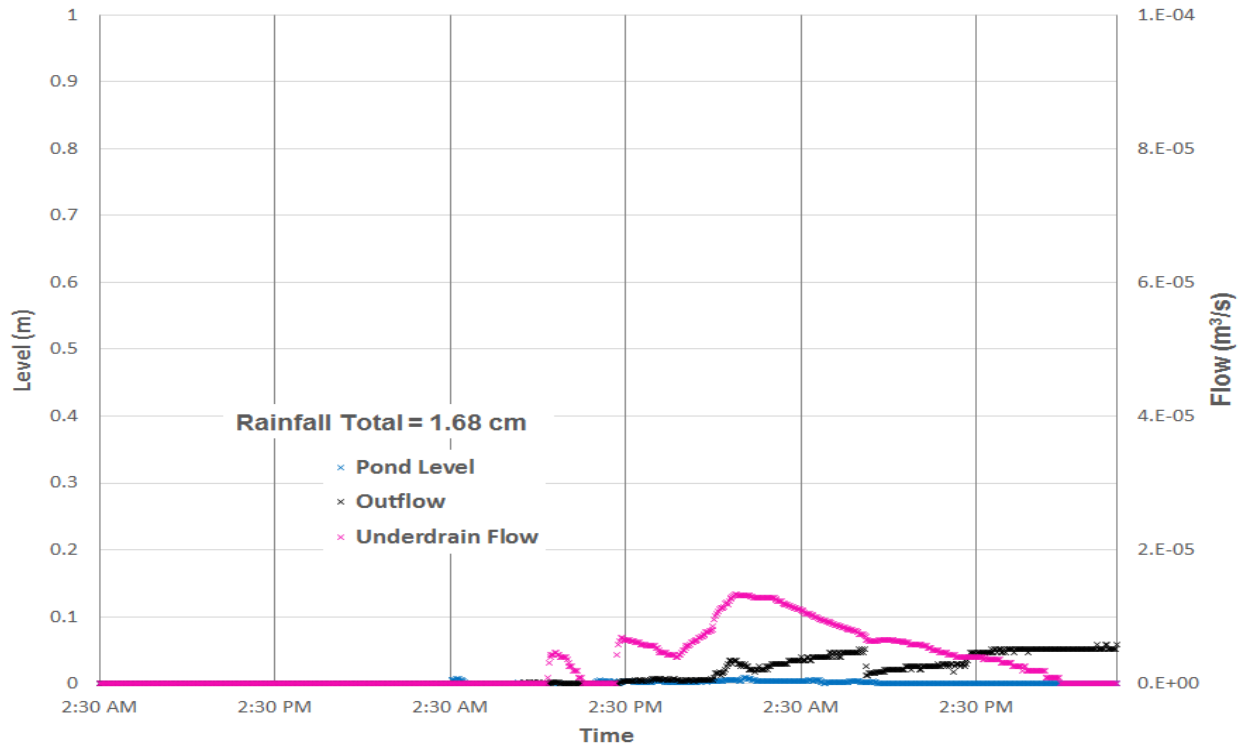
Figure 5.36 FRGR ponding data and flow data from the 10/28/2015 event

166

The rainfall from the 11/10/2015 storm did not cause any increase in volumetric water content at 66 cm at the FRGR. This differs from the 9/10/2015 storm, which caused an increase of 0.039 (3.9%) of volumetric water content at this depth. However, the soil moisture sensor at 66 cm deep indicated that the volumetric water content was 0.384 (38.4%) prior to the start of the 11/10/2015 storm. This is 0.034 (3.4%) higher than the volumetric water content observed at this depth prior to the 9/10/2015 event. It is likely that the soil media at this depth was at saturation or very close to saturation prior to the 11/10/2015 storm, so an increase in volumetric water content did not occur. The soil moisture data from the 11/10/2015 storm collected from the FRGR can be found in Figure 5.37.
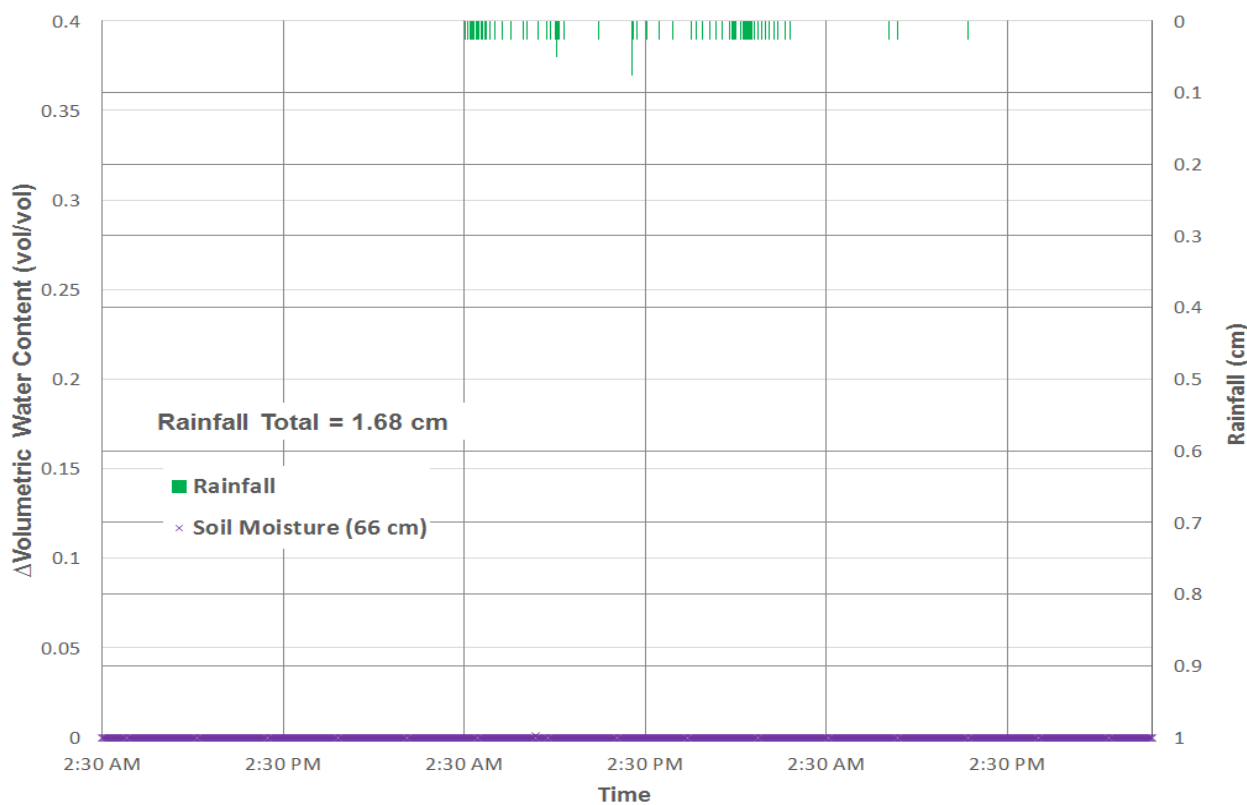
Figure 5.37 FRGR soil moisture data from the 10/28/2015 event

From the data collected for the 11/10/2015 storm and 9/10/2015 storm, both rain gardens perform well during the typical Villanova storm. Neither rain garden displayed overflow or

produced ponding lasting longer than 72 hours. Water infiltrates quickly in both systems; however, the volumetric water content directly above the underdrain and liner system at the FRGR does remain high after rain events. In one case, the soil was even saturated prior to the event, causing more underdrain flow and subsequent treated outflow. The volumetric water content at the native soil interface at the FRGI does suggest increases in volumetric water content during the 11/10/2015 storm. This sensor did not record an increase in volumetric water because the soil media above retained the water. This shows that the storage for these rain gardens is adequate for the typical Villanova rain event, so an underdrain and liner is not necessary. The soil media, which is sandier than the BTI but less sandy than the PTI, is performing well in both systems.

5.4.2 Pavilion Traffic Island

During the 11/10/2015 storm event, the PTI did experience ponding up to 0.16 m after 24 hours of rainfall. Approximately 24 hours after the rainfall event, the ponding dropped to about 0.11 m. After 72 hours had passed since rainfall had ended, the PTI pond was empty. This confirms that the PTI can adequately remove water from a typical Villanova rain event within the 72 hour constraint. This ponding scenario is different from the event that occurred during the dry period (9/10/2015), which observed no ponding during. The ponding data from the 11/10/2015 is plotted in Figure 5.38.
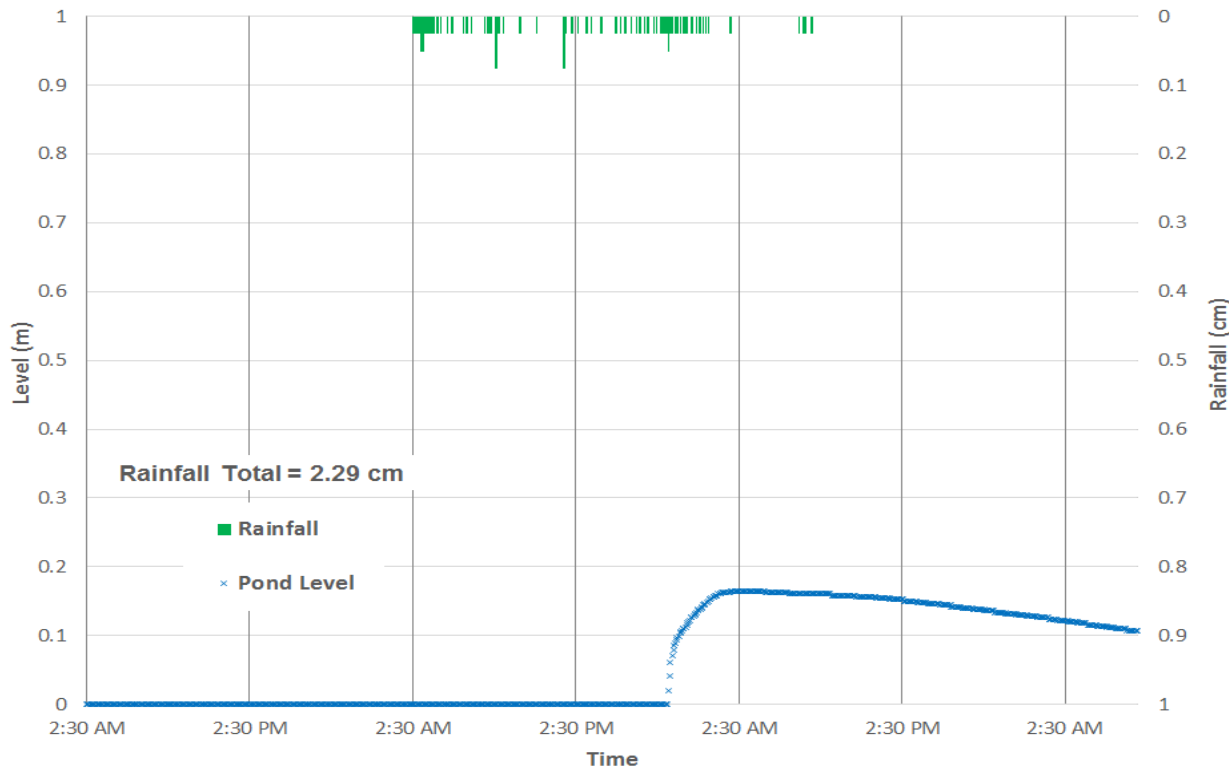
Figure 5.38 PTI ponding data from the 11/10/2015 event

During the 11/10/2015 storm event, the well transducer indicated that the perched water table in the PTI rose from 1.01 m to 1.48 m during the rainfall event. The overall rise in water table was higher during the 9/10/2015 storm (which displayed a rise from 0.70 m to 1.07 m). However, the water table was much deeper within the PTI during the 9/10/2015 storm due to lack of rain beforehand. The water level in the PTI did not reach the ground surface of the bowl during the 9/10/2015 storm. In contrast, the PTI completely filled with water after 14 hours of rainfall during the 11/10/2015 storm. The PTI well transducer data are displayed in Figure 5.39. The well transducer indicated that the water began filling the media before ponding occurred. The pressure transducer in the pond demonstrated that ponding began to occur 5 hours after the PTI completely filled with water. While this does not seem accurate, this may be due to the fact that the well could be influenced by macroporosity around the PVC. This macroporosity could have

been created during the well installation. This would cause the water in the well to fill before the rest of the PTI. These data are shown in Figure 5.40.

Figure 5.39 PTI well transducer data from the 11/10/2015 event
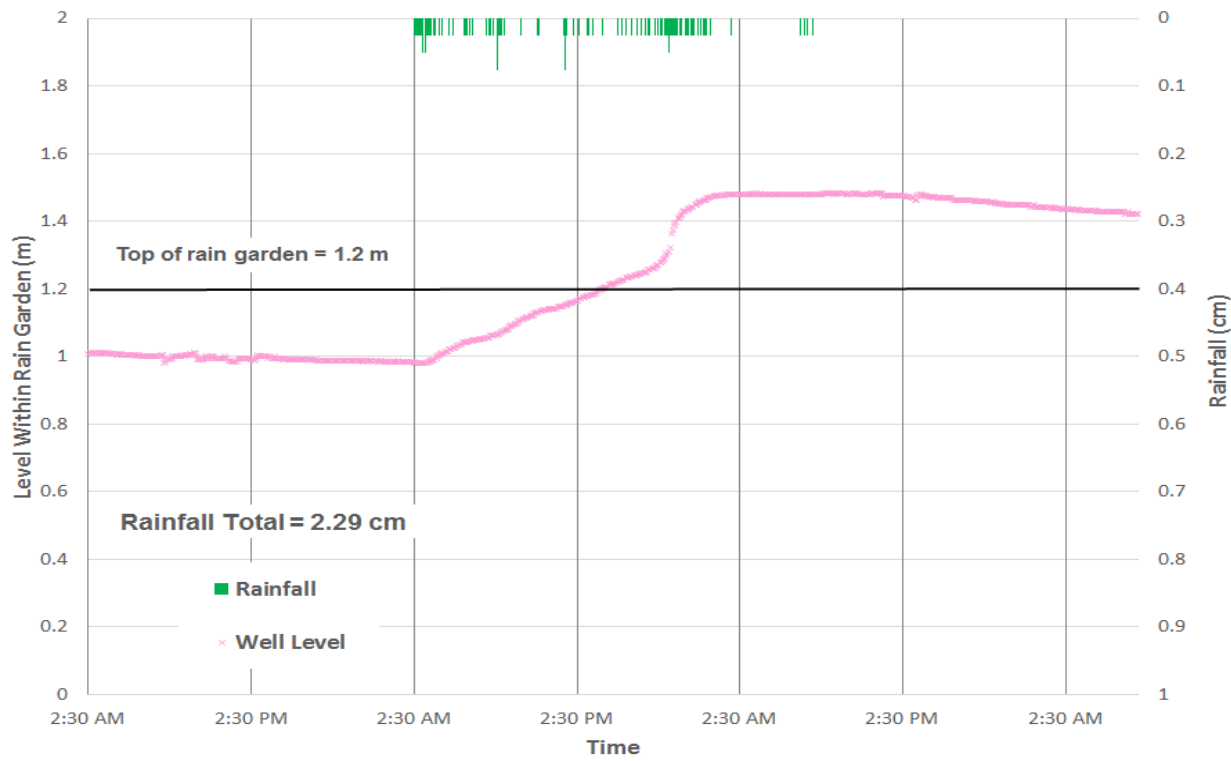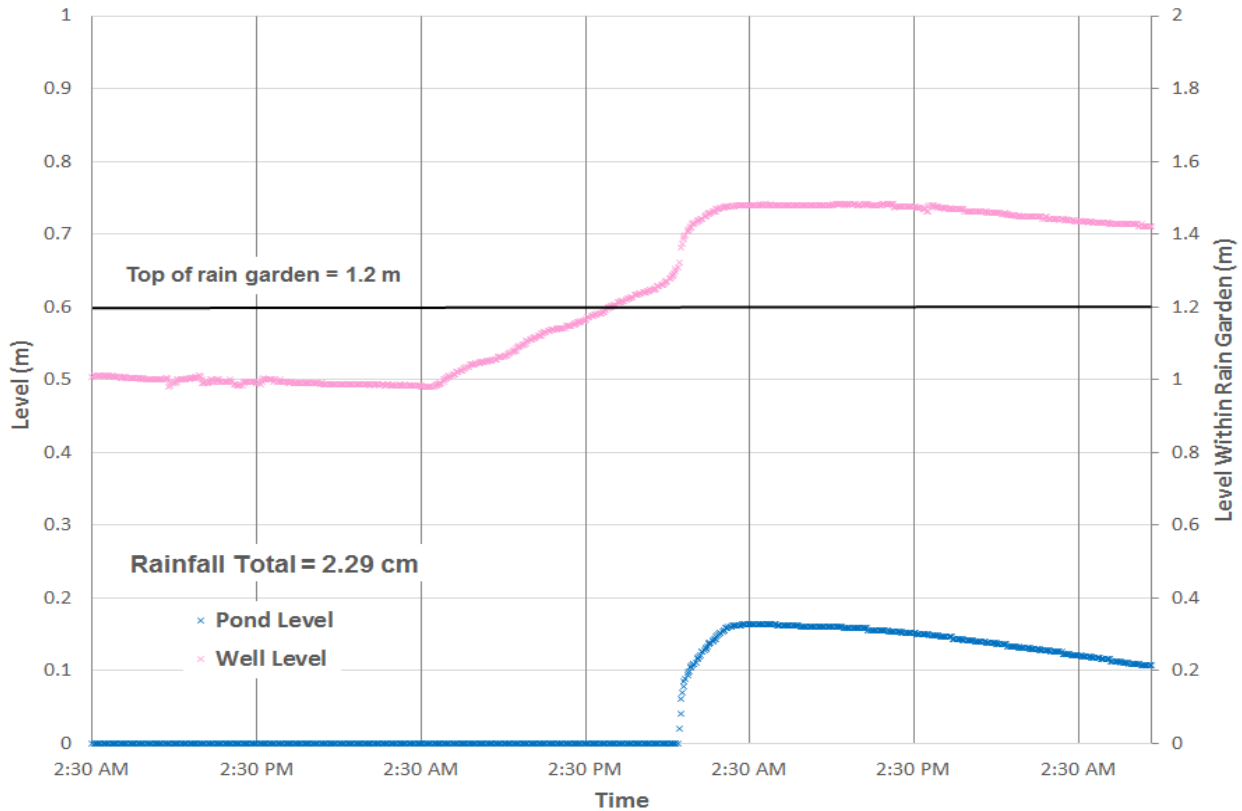
Figure 5.40 PTI ponding data and well transducer data from the 11/10/2015 event

During the 11/10/2015 storm, the volumetric water content at 35 cm deep and 66 cm deep did not change. This is because the media at this depth was already completely saturated before the event took place, since the well transducer read the perched water was located only 0.2 m below the ground surface of the bowl. In contrast, the volumetric water content at 35 cm deep was not at saturation during the 9/10/2015 event, so an increase did occur for that event. The volumetric water content at 10 cm deep increased around 0.099 (9.9%) during the storm event, and the rise in volumetric water content began around 12 hours after the event started. This is very similar to the 9/10/2015 storm event, which showed that the volumetric water content at 10 cm deep increased around 0.106 (10.6%). Similarly, the increase in volumetric water content at 10 cm deep during the 9/10/2015 storm began 12 hours after the rain event began. This shows that water moves through the first 10 cm very similarly during any type of typical Villanova storm

171

event. The shape of the increase in volumetric water content at 10 cm deep is staged and more rapid during the 9/10/2015; however, this could be due to the dryness of the soil. The soil may have been so dry during the 9/10/2015 event that the suction could have changed how the soil became wetted. The 10 cm soil moisture sensor demonstrated an expected curve during the 11/10/2015 sensor; however, it began with a water content 0.269 (26.9%) higher than during the 9/10/2015 storm, so it could have followed a different wetting pattern. During the 11/10/2015 storm, the volumetric water content at 10 cm deep stopped increasing in about 6 hours, which was much faster than the 12 hours required during the 9/10/2015 storm. This was expected due to the dryness of the media during the 9/10/2015 storm. The soil moisture data for the 11/10/2015 storm are demonstrated in Figure 5.41.
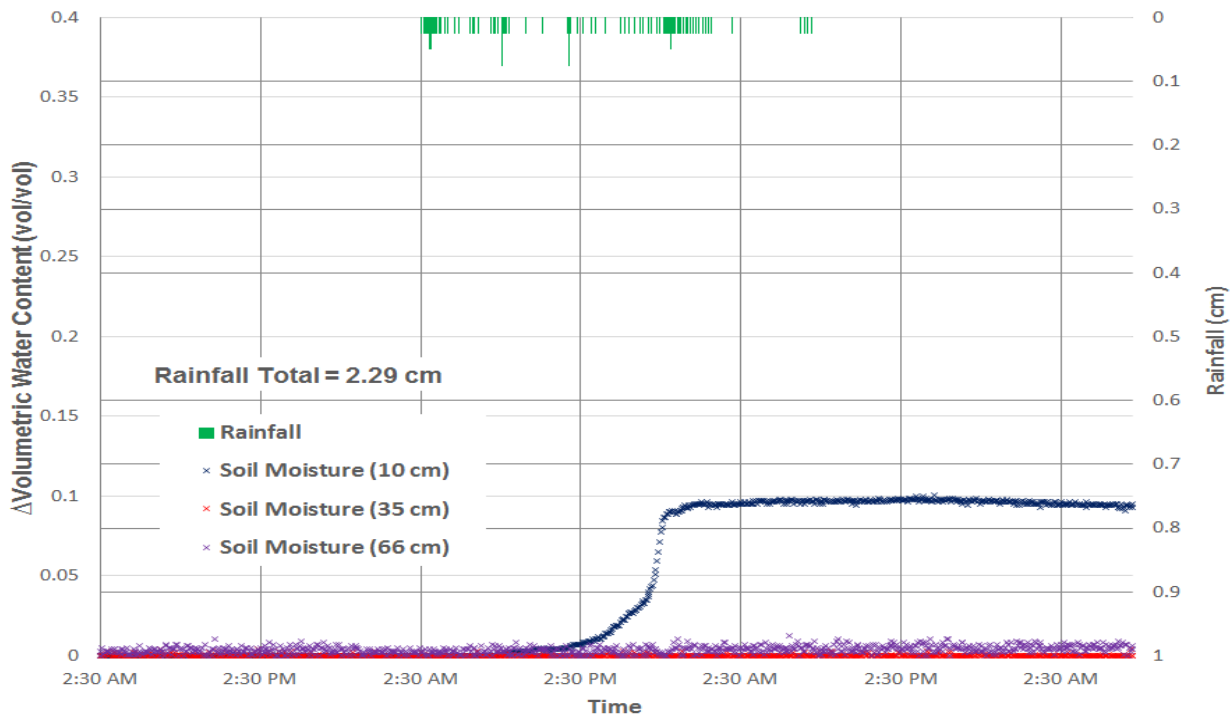
Figure 5.41 PTI soil moisture sensor data from the 11/10/2015 event

Similarly to the 9/10/2015 storm, the volumetric water content increase at 10 cm deep occurred after the well transducer indicated the PTI perched water table was rising. Also, in both storm

events, the volumetric water content stopped increasing before the well transducer level stopped

rising. This could be due to macroporosity and quick infiltration rates of the sandy material. The

well transducer data and soil moisture sensor data are shown in Figure 5.42. As expected from

the high infiltration rates of the sandy material, the volumetric water content 10 cm deep began

increasing before ponding occurred during the 11/10/2015 storm. These data are plotted together

in Figure 5.43.
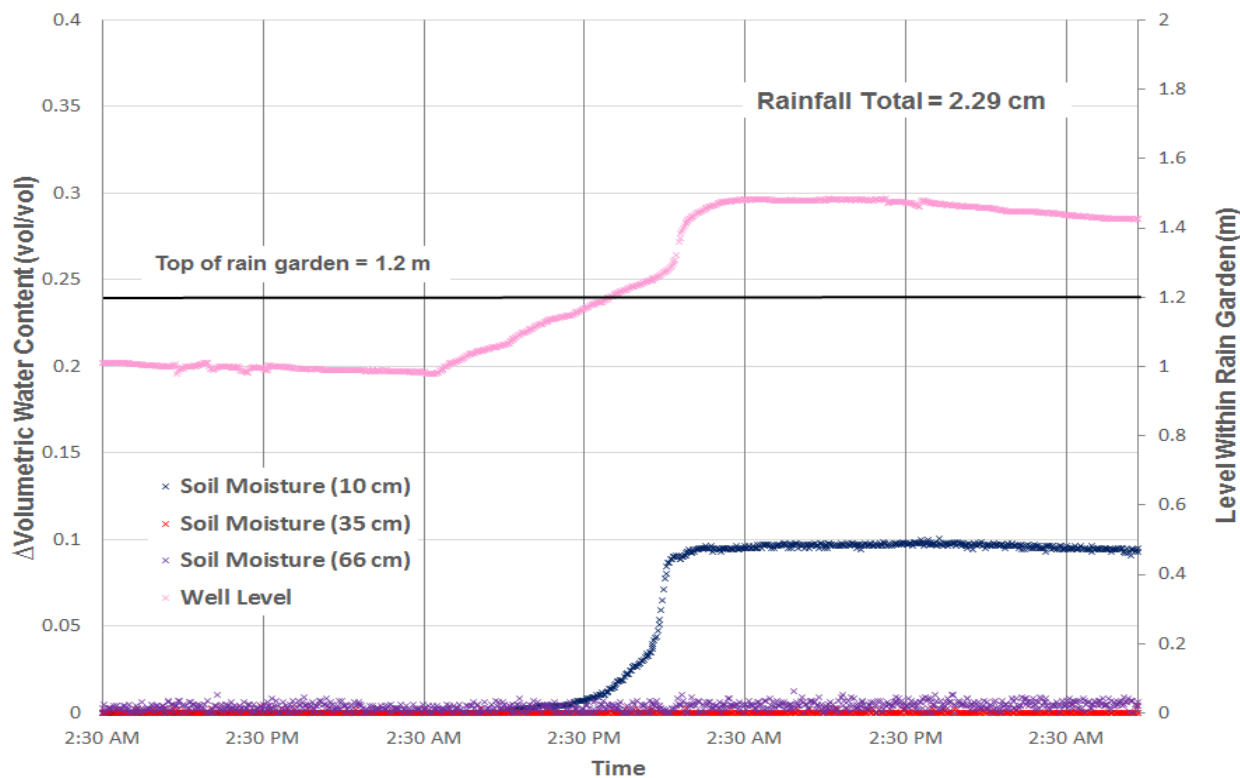
Figure 5.42 PTI soil moisture sensor data and well transducer data from the 11/10/2015 event
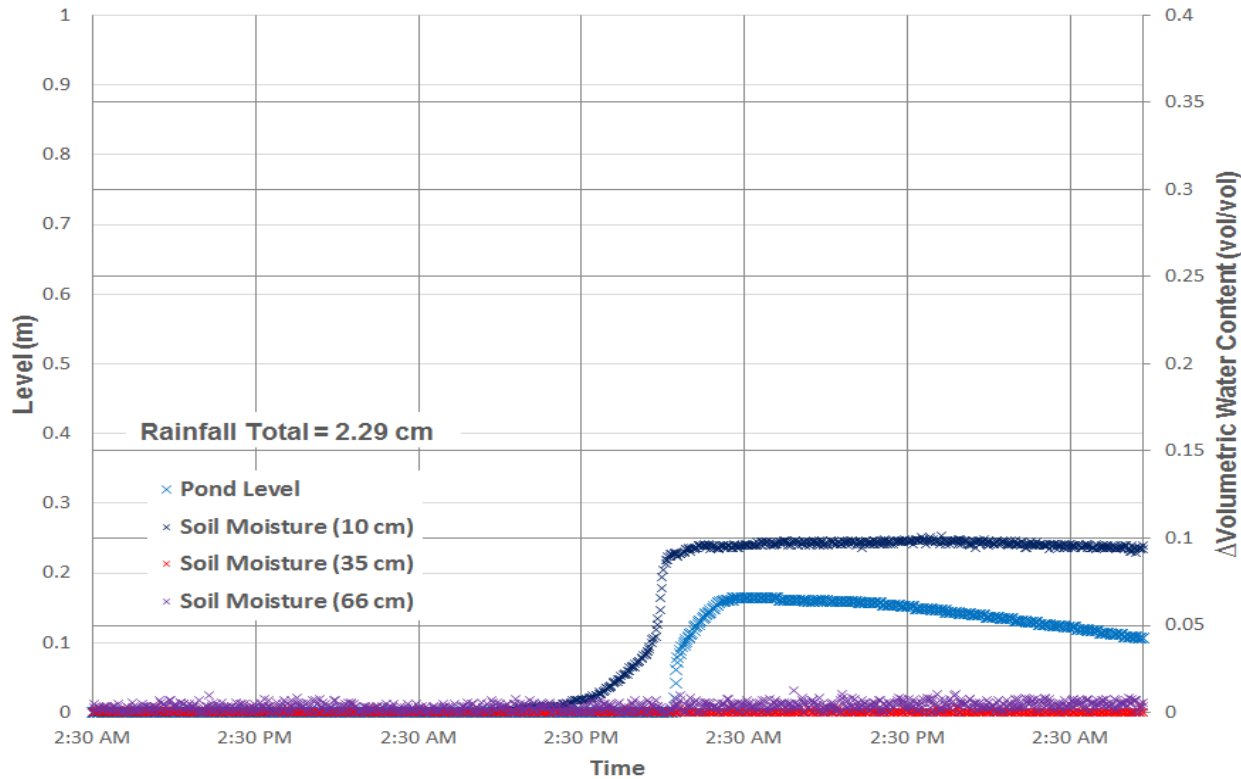
Figure 5.43 PTI soil moisture sensor data and ponding data from the 11/10/2015 event

From these data, it is shown that the PTI performs well in both storm events which closely coincide with the typical Villanova storm event. These data imply that the rain garden, despite being considered a "failed" rain garden, does not incur long ponding periods during these types of events. The PTI did not indicate any ponding during a rainfall event which occurred during a dry period. The data collected in this study suggests that the PTI works adequately for 80% to 90% of the storms in a typical year at Villanova.

5.4.3   Bioinfiltration Traffic Island

During the 11/10/2015, the BTI did not experience overflow. This is expected, since the rainfall did not exceed 2.54 cm. Similarly, the BTI did not display overflow during the 9/10/2015 event. Ponding at the BTI was only slightly higher during the 11/10/2015 storm than the 9/10/2015 storm. However, the pond pressure transducer did not indicate significant infiltration was

occurring during the 11/10/2015 storm event as it did during the 9/10/2015 storm event. During the 11/10/2015 event, some minor increase and decreases in ponding were observed during breaks in rain; however, these were not as significant as during the 9/10/2015 storm event. This could be due to longer breaks in rainfall dryness of the soil during the 9/10/2015 storm. The ponding data from the 11/10/2015 storm are demonstrated in Figure 5.44.
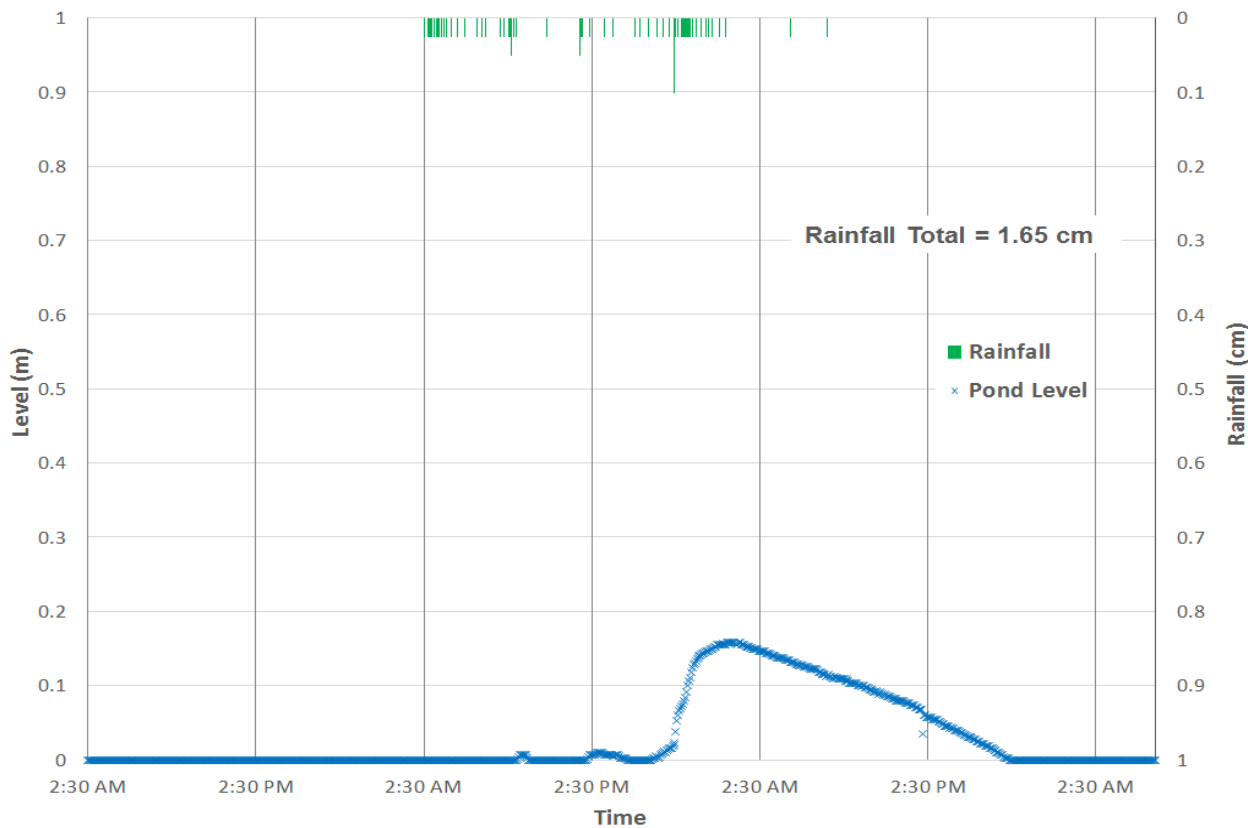
Figure 5.44 BTI pressure transducer data from the 11/10/2015 event

During the 11/10/2015 storm event, the volumetric water content at 10 cm deep begins to increase before the other sensors indicate increases in water content. This is in contrast to the 9/10/2015 storm in which the volumetric water content at the 35 cm deep duplicate sensor began to imply an increase first. The sensors imply increases in volumetric water content faster during the 11/10/2015 storm than during the 9/10/2015 storm. This could be due to soil above the

sensors being extremely dry during the 9/10/2015 storm, or the vegetation requiring more water at that time and not allowing water to infiltrate to the sensors during the 9/10/2015 storm. Before the 11/10/2015 storm, the volumetric water content at all soil moisture sensors was higher than during the 9/10/2015 storm. However, the soil moisture sensor at 66 cm deep only indicated a volumetric water content 0.009 (0.9%) higher before the 9/10/2015 event. The soil moisture sensor at 66 cm deep increased around 0.205 (20.5%) during both the 11/10/2015 event and 9/10/2015 event. After the 9/10/2015 event, the volumetric water content at 66 cm decreased rapidly after around 14 hours. This was rapid decrease did not occur during the 11/10/2015 event, and it could be related to the dryness of the native soil beneath the engineered soil mix. However, the other soil moisture sensors suggested lower increases in volumetric water content during the 11/10/2015 storm because the soil media was wetter before the event began. Similarly to the 9/10/2015 storm event, there is a different in volumetric water content increases in the 35 cm soil moisture sensor and the 35 cm duplicate soil moisture sensor. This could be due to macroporosity and natural heterogeneity of soil, allowing more water to enter the duplicate sensor area. The soil moisture data for the 11/10/2015 event are shown in Figure 5.45. The higher increase in the soil moisture sensor at 66 cm deep compared to the other soil moisture sensors during the 11/10/2015 storm is likely because the soil at that depth was drier than the other depths before the storm began. The duplicate soil moisture sensor at 35 cm deep indicated a volumetric water content increase about 0.043 (4.3%) more than the soil moisture sensor at 35 cm deep during the 11/10/2015 storm. The soil moisture sensor at 35 cm deep had a lower volumetric content than the duplicate sensor at 35 cm deep by about 0.009 (0.9%). This could have caused a higher increase in volumetric water content at the duplicate sensor. Heterogeneity

of soil and macroporosity may have also allowed for more water storage available at the duplicate sensor.
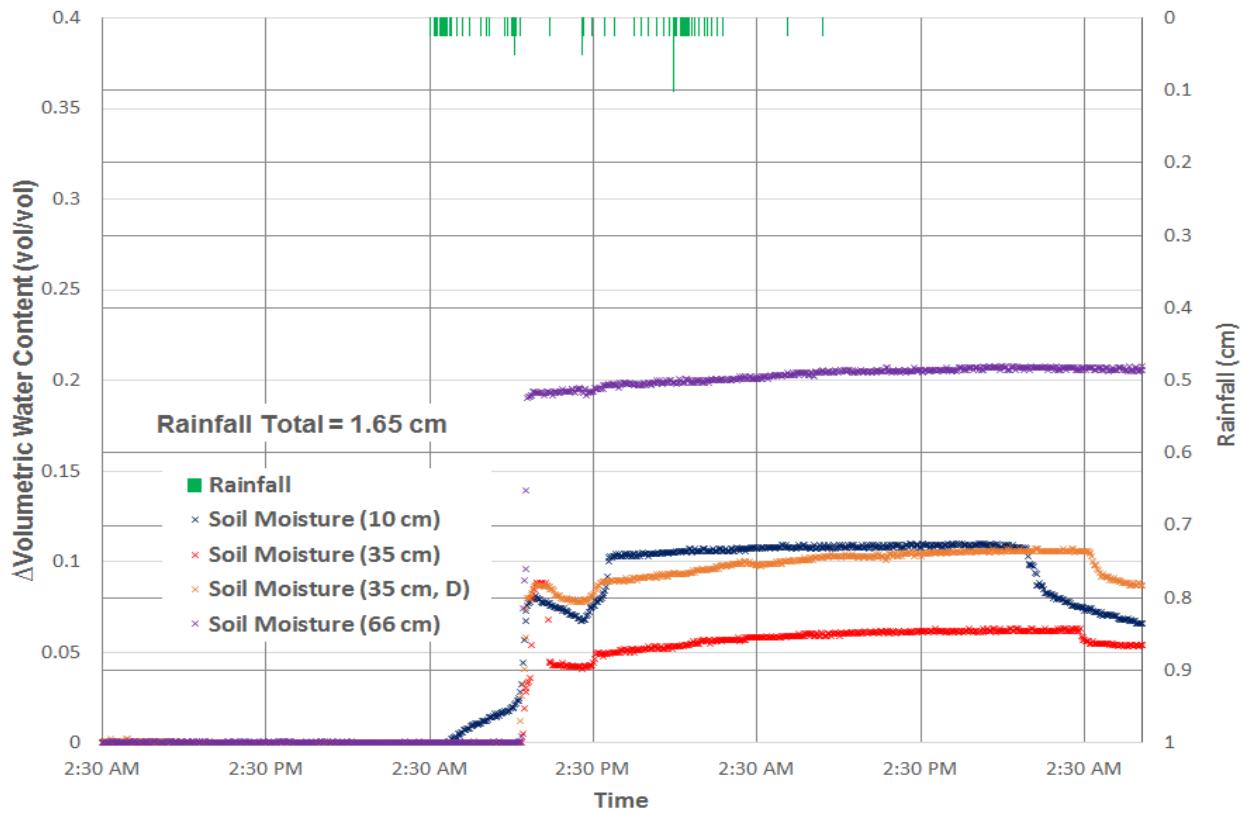
Figure 5.45 BTI soil moisture sensor data from the 11/10/2015 event

From Figure 5.46, it is implied that ponding does not occur until after the volumetric water content at all depths incur their greatest increase during the 11/10/2015 storm. This is expected, since the 1:1 sand-soil mix should allow for a quick infiltration rate. Additionally, the presence of macropores can create faster infiltration. When ponding reached its maximum level, the soil moisture sensors were reading minor increases in volumetric water content. This is due to infiltration from the pond. When ponding ended, the volumetric water content began to drop at 4 cm deep after 2 hours. Approximately 6 hours after ponding ended, the volumetric water content at both 35 cm deep sensors began to drop. This shows that water from the pond infiltrates quickly past these sensors during the 11/10/2015. The water from the pond seemed to infiltrate

177

much quicker during the 9/10/2015 based on the soil moisture sensor plots. This is likely due to the dryness of the soil.
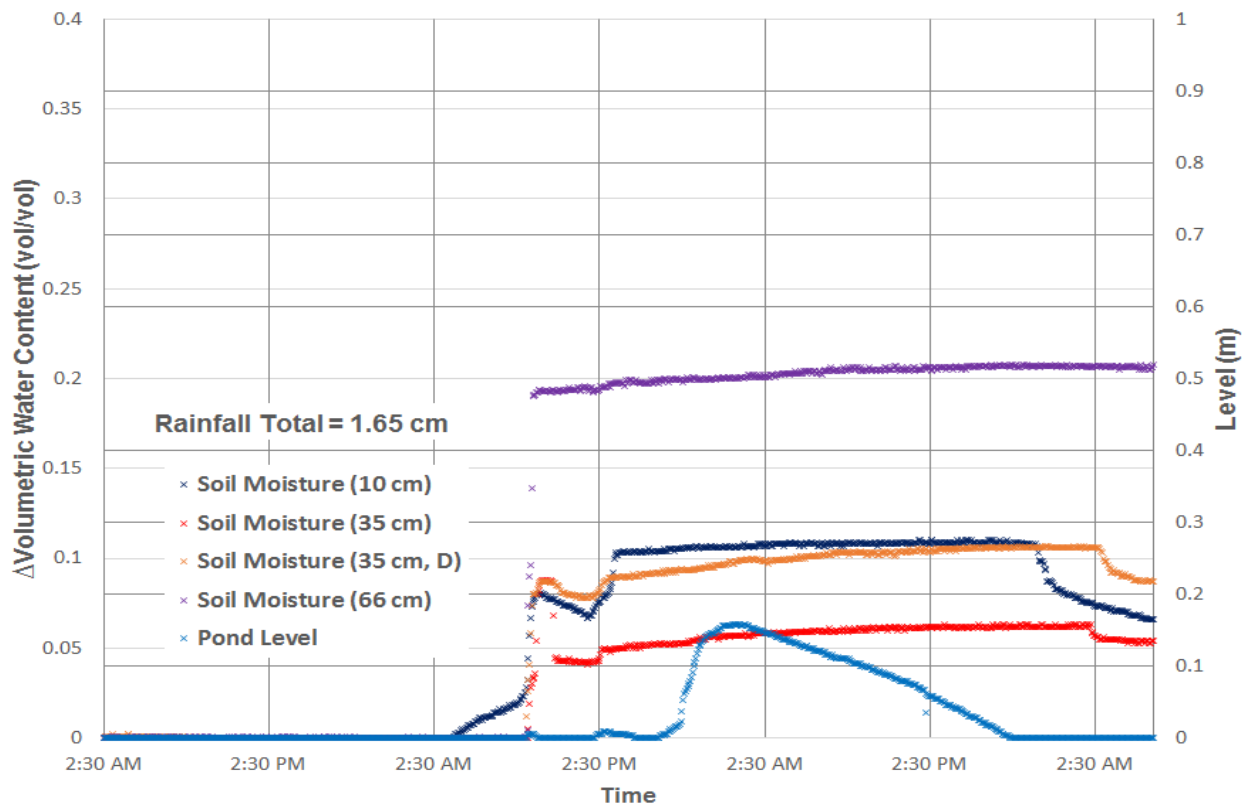
Figure 5.46 BTI soil moisture sensor data and pressure transducer data from the 11/10/2015 event

The data from both storms implies that the BTI is performing well after 15 years of operation on Villanova's campus. Ponding longer than 72 hours and overflow is not observed in either storm. The presence of an organic layer may influence infiltration during a rain event; however, the BTI is able to handle the amount of rainfall from a typical Villanova rain event.

5.5 10/28/2015 Storm Comparison

5.5.1   Fedigan Rain Gardens

During the 10/28/2015 storm, multiple peaks in ponding were observed at the FRGI. However, the highest level of ponding observed was only 0.04 m, so overflow did not occur at the FRGI.

178

The ponding at the FRGI was significantly smaller during the 10/28/2015 storm than the 9/29/2015 storm, which showed ponding up to around 0.1 m. Ponding did not last more than 72 hours, and the pond emptied much faster during the 10/28/2015 storm than the 9/29/2015 storm. The reason for the difference in ponding between the two events is unclear. It could be that the intensity of some points of the 9/29/2015 storm was much higher than those during the 10/28/2015 storm. This could have been too fast for all of the water to infiltrate. It is unlikely that temperature differences could have caused this, since the temperature during the two events was about the same with the temperature during the 10/28/2015 being a bit colder at times. The volumetric water content at 35 cm deep was 0.050 (5.0%) higher during the 10/28/2015 storm, so it is unlikely the soil was dryer during the 9/29/2015. Regardless, the data confirm that the FRGI does not pond for longer than 72 hours during these types of events. This data is displayed in Figure 5.47.
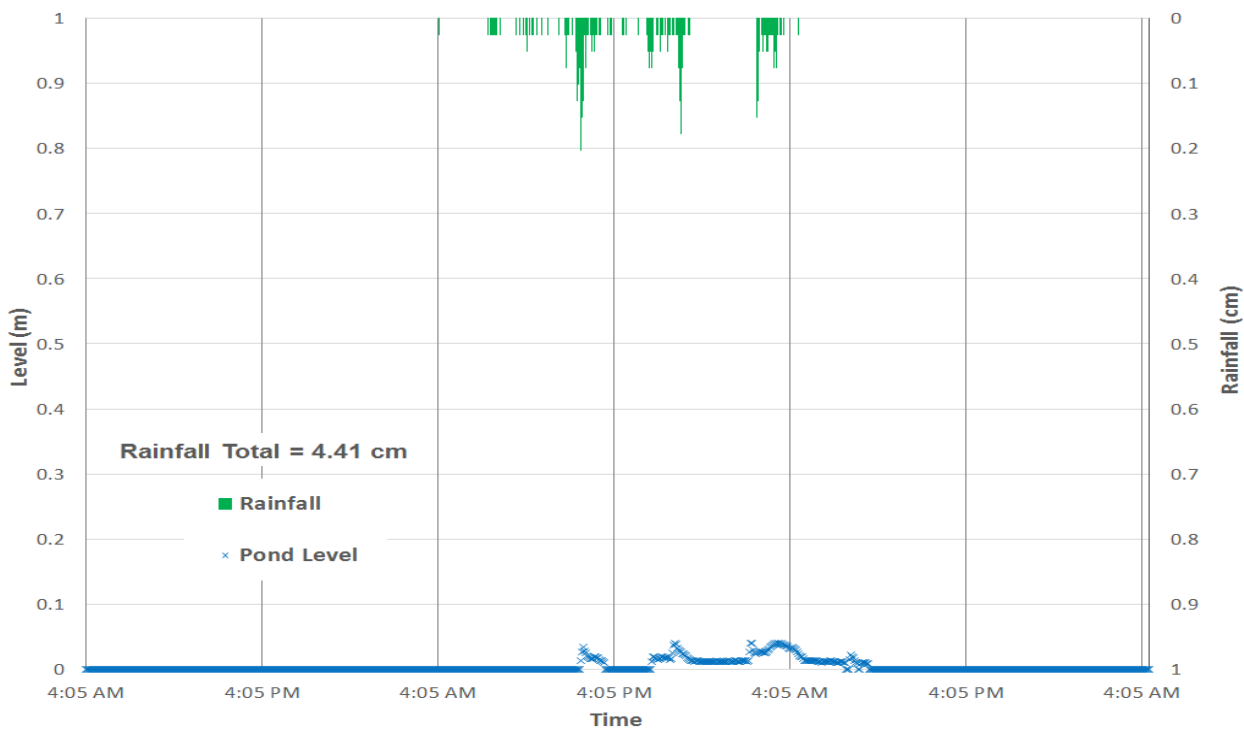
Figure 5.47 BTI soil moisture sensor data and pressure transducer data from the 11/10/2015 event

The volumetric water content at 35 cm rose about 0.111 (11.1%) during the 10/28/2015 storm event, which is about 0.033 (3.3%) less than that observed during the 9/29/2015 storm. This could have been due to more water in the pond during the 9/29/2015 storm. This is likely due to the fact that the soil at this depth was 0.050 (5.0%) dryer during the 10/28/2015 storm. The soil at 35 cm during the 9/29/2015 event would have needed more water to reach saturation. The soil moisture sensor data collected during the 10/28/2015 event is shown in Figure 5.48. During the 10/28/2015 storm, the volumetric water content at 35 cm deep began increasing during the first peak in ponding, as demonstrated in Figure 5.49. This differs from the 9/29/2015 storm in that the volumetric water content at 35 cm did not increase until the second peak in ponding. This could be due to dryer soil above the 35 cm soil moisture sensor causing water from the first peak to stay above the native soil interface.
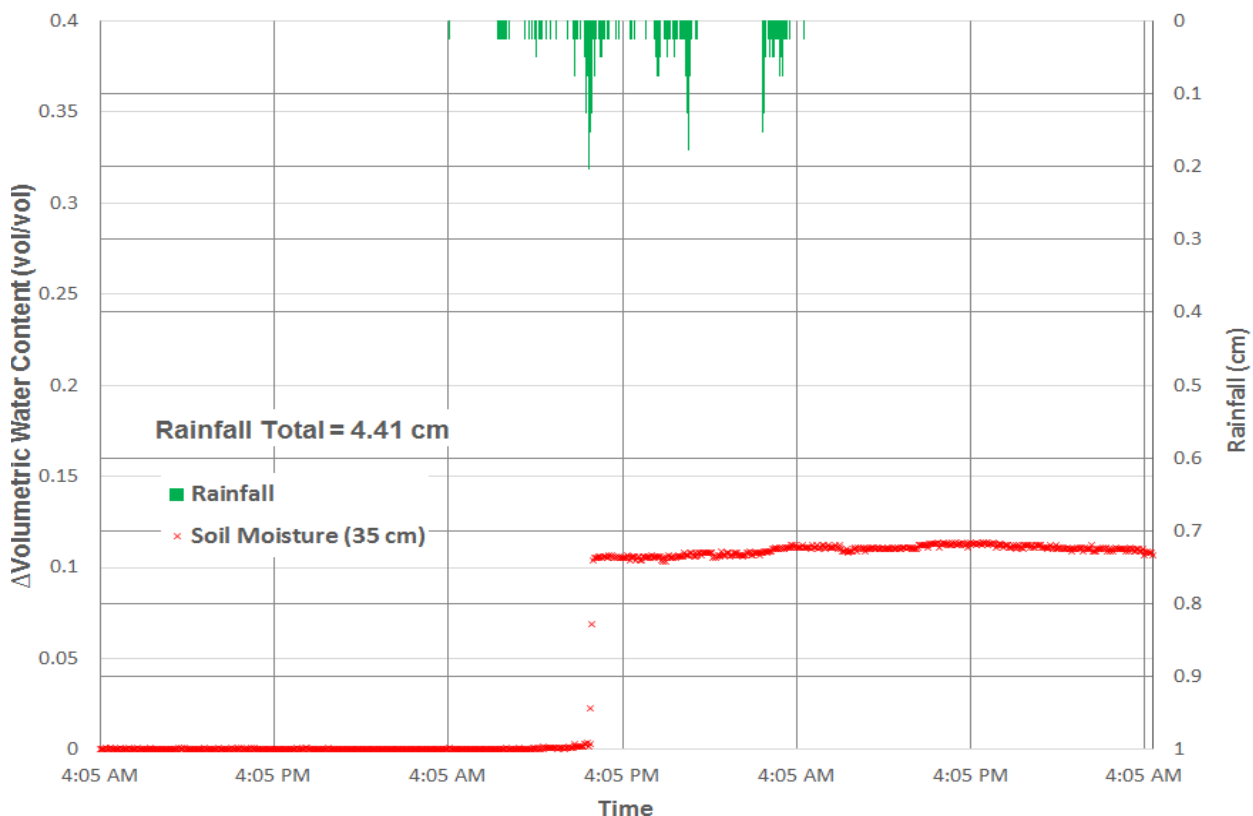
Figure 5.48 FRGI soil moisture sensor data from the 10/28/2015 event

180
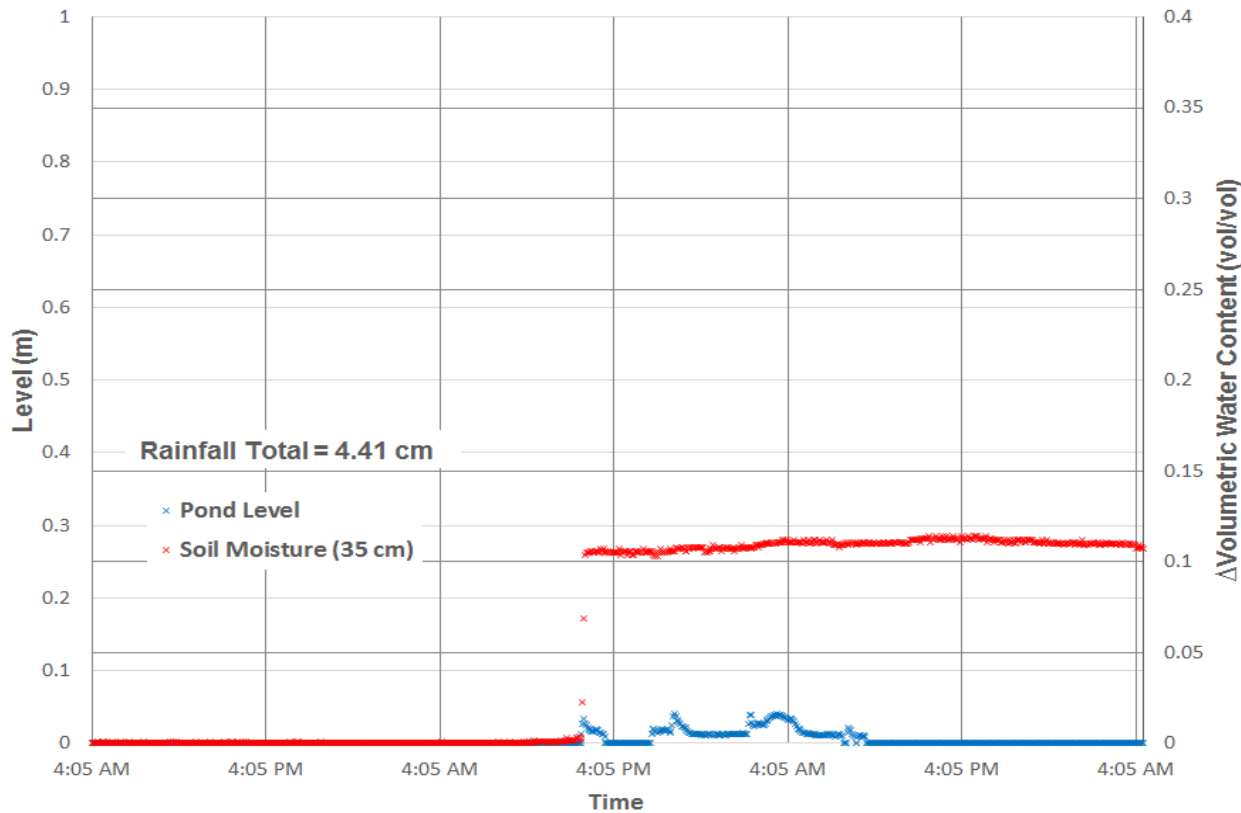
Figure 5.49 FRGI soil moisture sensor and pond pressure transducer data from the 10/28/2015 event

During the 10/28/2015 storm event, the maximum ponding level at the FRGR was around 0.045 m. This confirms that overflow did not occur at the FRGR during this event, which is also the case for the 9/29/2015 event. This ponding level was slightly smaller than the ponding observed during the 09/29/2015 storm. However, this may be due to more rainfall occurring during the 9/29/2015 storm. Similar to the 9/29/2015 event, some infiltration is observed during a break in rainfall during the 10/28/2015 storm. The underdrain level began rising first during the 10/28/2015 storm event, followed closely by the overflow riser level. This is different from the 9/29/2015 storm event, which indicated ponding occurring before a rise in underdrain level or overflow riser level. This may be due to a more intense period of rain which occurred early during the 9/29/2015 storm. However, this shows that water infiltrated through the system faster

181

than ponding could occur during the 10/28/2015 storm. Similar to the 9/29/2015 rain event, the underdrain level rises and falls at similar times as the pond level. This could indicate that water is infiltrating through the media quickly to the underdrain as it ponds at the surface. The FRGR pressure transducer data for the 10/28/2015 event are plotted in Figure 5.50. The slowly decreasing overflow riser water level suggests that water is evaporating and possibly moving back through the underdrain.
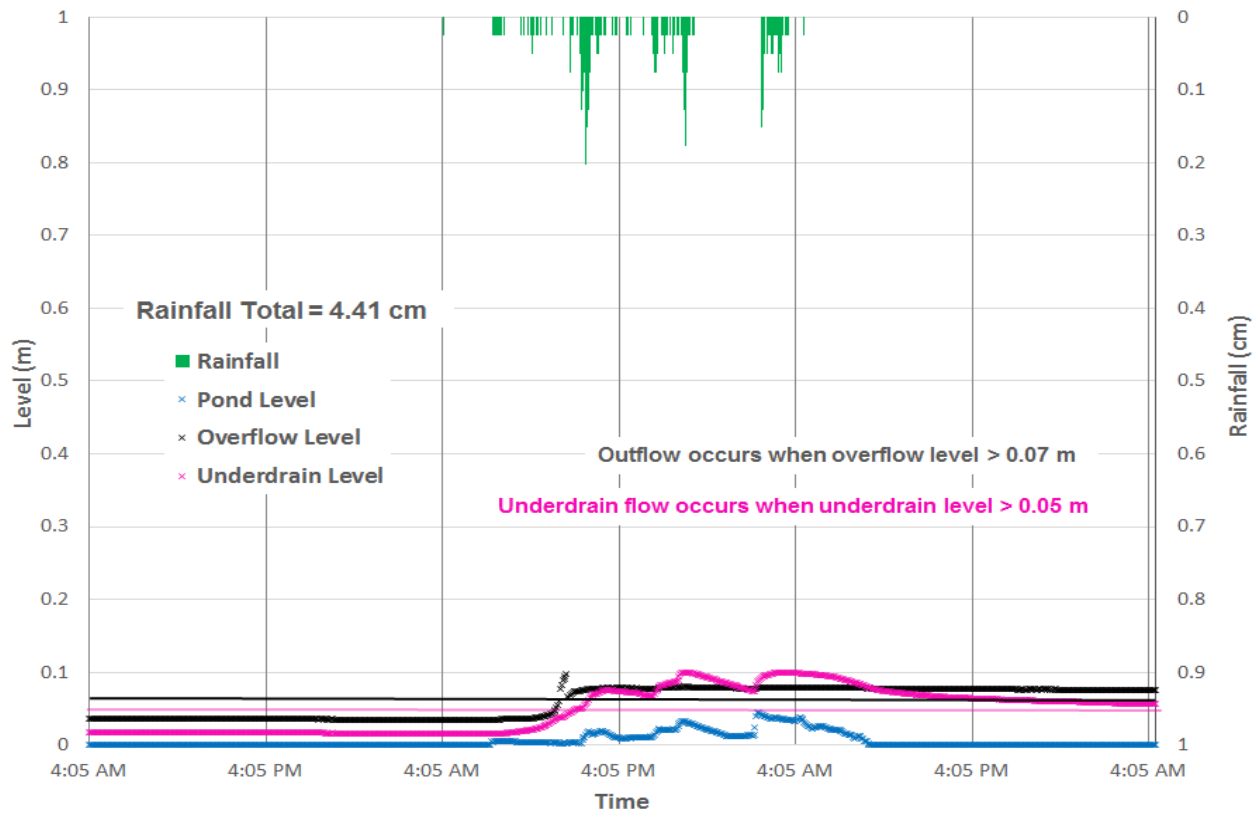
Figure 5.50 FRGR pressure transducer data from the 10/28/2015 event

During the 10/28/2015 storm, outflow and underdrain flow at the FRGR were slightly smaller than that observed during the 9/29/2015 storm. This could have been due to less rainfall providing less water to move through the system. However, the flow shapes are dramatically different for each event. During the 9/29/2015 event, underdrain flow did not occur until after the break in rainfall. Outflow began shortly after underdrain flow began during the 9/29/2015 storm,

182

and the shapes of the two flow rate plots were not very similar. There was also no drop and subsequent increase in underdrain flow during the 9/29/2015 event. During the 10/28/2015 storm event, the underdrain level and overflow level followed a similar shape, with decreases during smaller amounts of rainfall and breaks. During increases of rainfall, both flow rates rose again. Also, outflow began shortly before underdrain flow; however, this may have just been rain falling directly into the overflow causing outflow to begin before underdrain flow. The difference in flows could be from the lack of intense rain periods observed during the 9/29/2015 storm event. The flow data collected during the 10/28/2015 storm is plotted in Figure 5.51. Figure 5.52 shows the ponding data plotted with the flow data collected during the 10/28/2015 rain event. Increases in outflow and underdrain flow occurred shortly after peaks in ponding, which suggests that water infiltrates quickly through the pond and exits through the underdrain. This phenomenon was also observed during the 9/29/2015 storm; however, there was one peak in ponding during the 9/29/2015 storm where flow did not occur. This water may have not infiltrated through the entire media depth if soil was drier at this time.
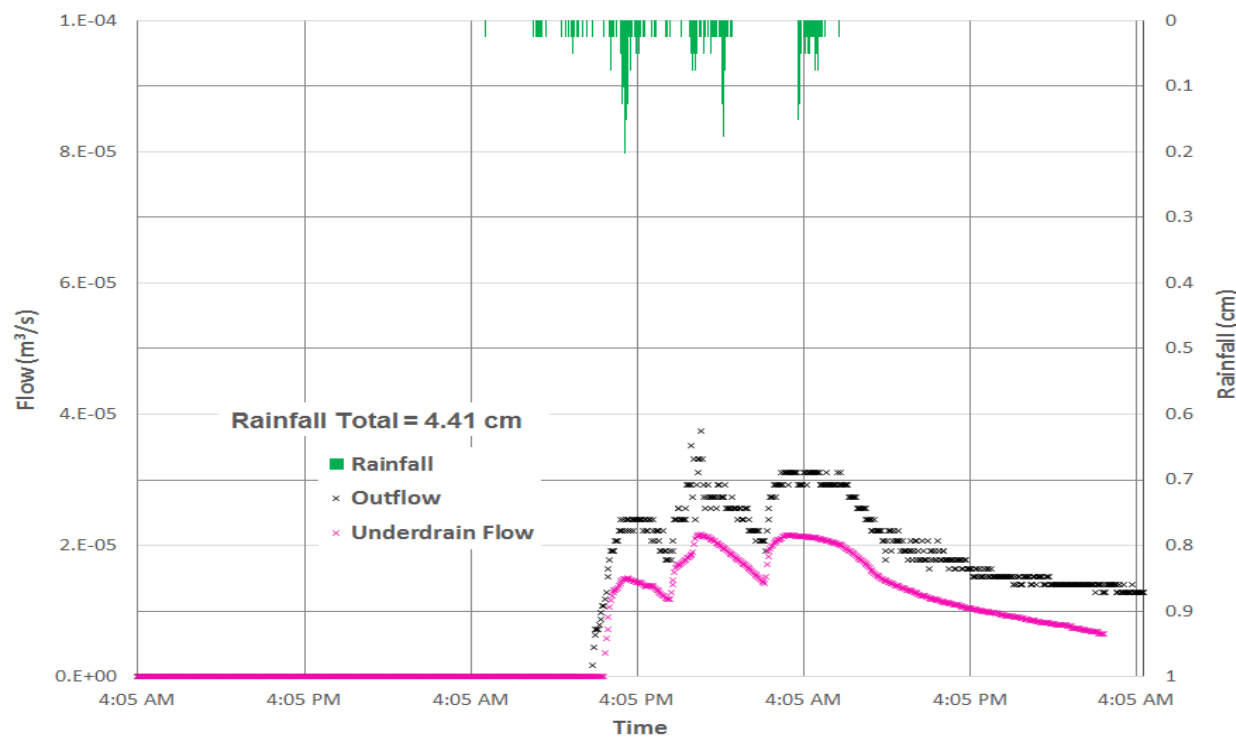
Figure 5.51 FRGR flow data from the 10/28/2015 event
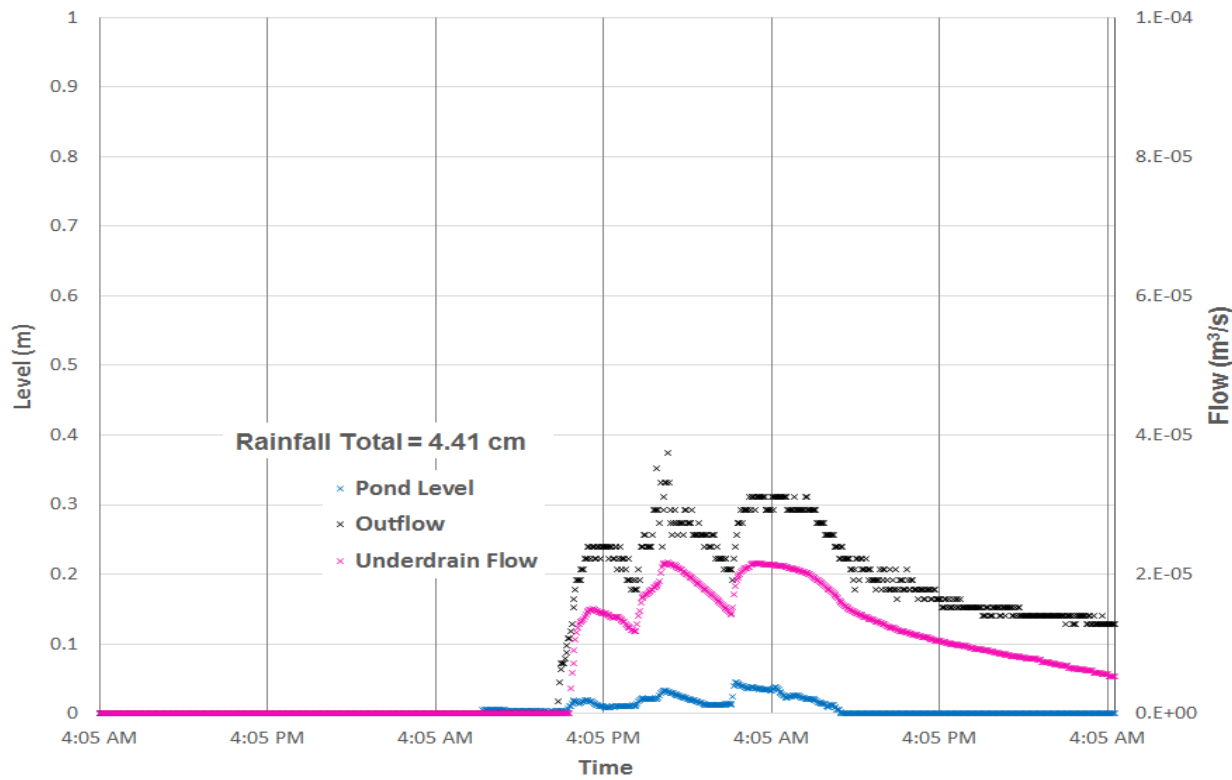
Figure 5.52 FRGR ponding data and flow data from the 10/28/2015 event

The soil moisture sensor at 66 cm deep at the FRGR did not begin to indicate an increase in volumetric water content until 11 hours after the 10/28/2015 event began. In contrast, the volumetric water content began to increase almost immediately after rainfall began during the 9/29/2015 storm. This could be due to a very intense period of rainfall observed almost immediately during the 9/29/2015 storm. During the 10/28/2015 storm, the volumetric water content at 66 cm deep at the FRGR rose 0.023 (2.3%). This is smaller than the increase observed during the 9/29/2105 event; however, the volumetric water content before the 10/28/2015 storm was 0.016 (1.6%) higher than before the 9/29/2015 storm. The soil moisture sensor data for the FRGR collected from the 10/28/2015 storm is displayed in Figure 5.53. As depicted in Figure 5.54, volumetric water content at 66 cm increased shortly after ponding levels began to decrease during the 10/28/2015 event at the FRGR. The volumetric water content at 66 cm stopped increasing around the time when the ponding level was zero, and began decreasing shortly after. This is somewhat similar to the data observed during the 9/29/2015 storm at the FRGR. However, volumetric water contents began to decrease before the pond was empty at the FRGR during the 9/29/2015 storm, and the volumetric water content did increase before the pond level at particular point during the storm. However, this could be expected if the soil media was drier prior to the 9/29/2015 storm. As plotted in Figure 5.55, volumetric water content after the 10/28/2015 storm stopped increasing when the underdrain flow and outflow began decreasing. This scenario also occurred during the 9/29/2015 storm at the FRGR.
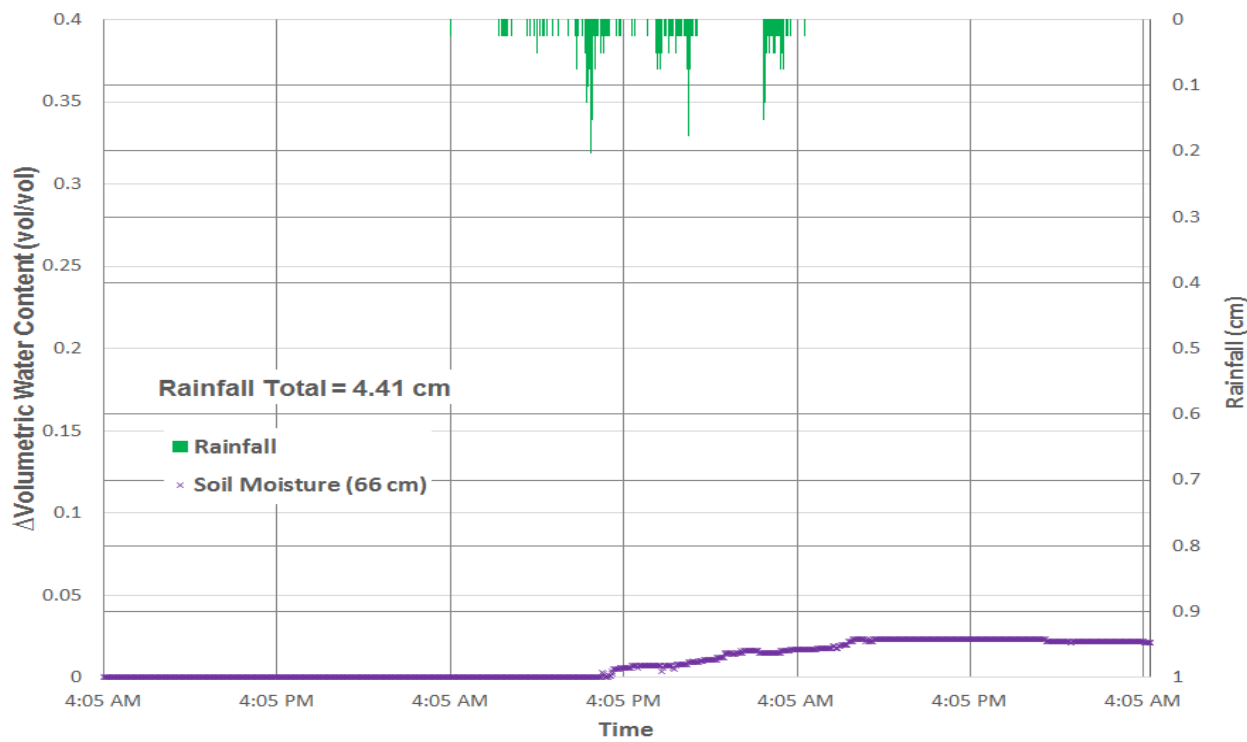
Figure 5.53 FRGR soil moisture data from the 10/28/2015 event
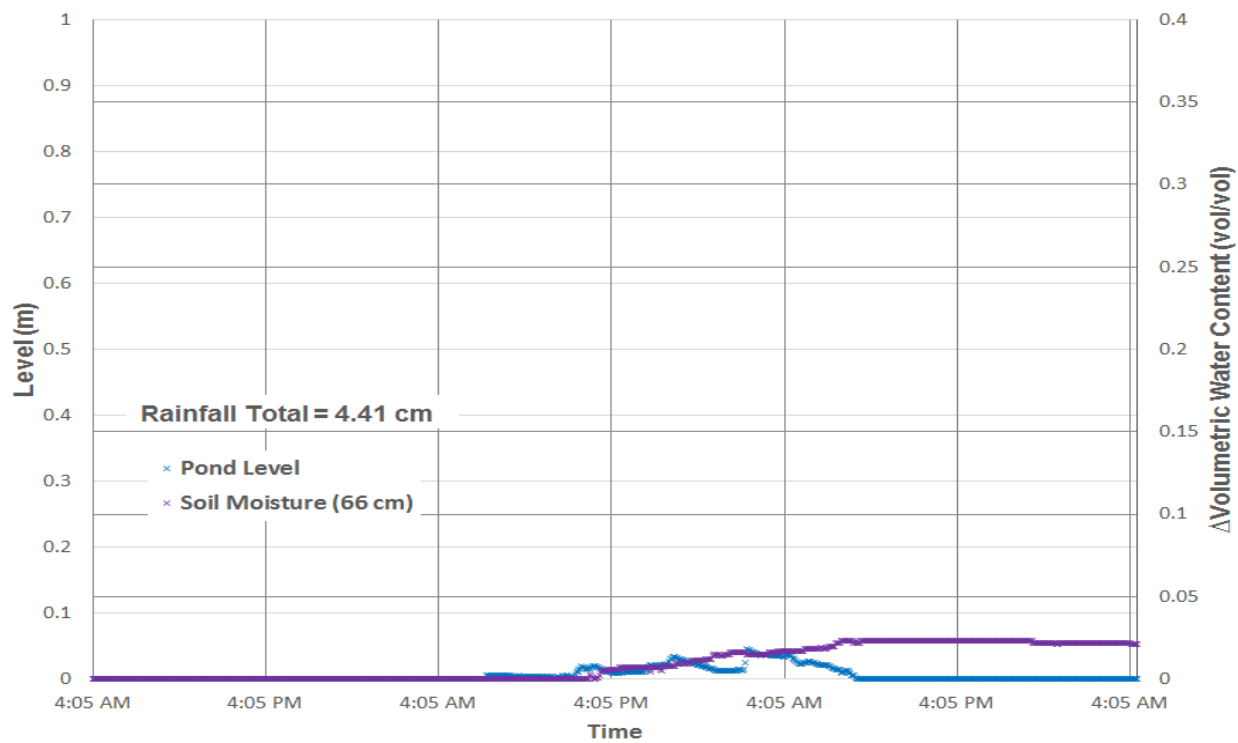
Figure 5.54 FRGR pressure transducer data and soil moisture data from the 10/28/2015 event
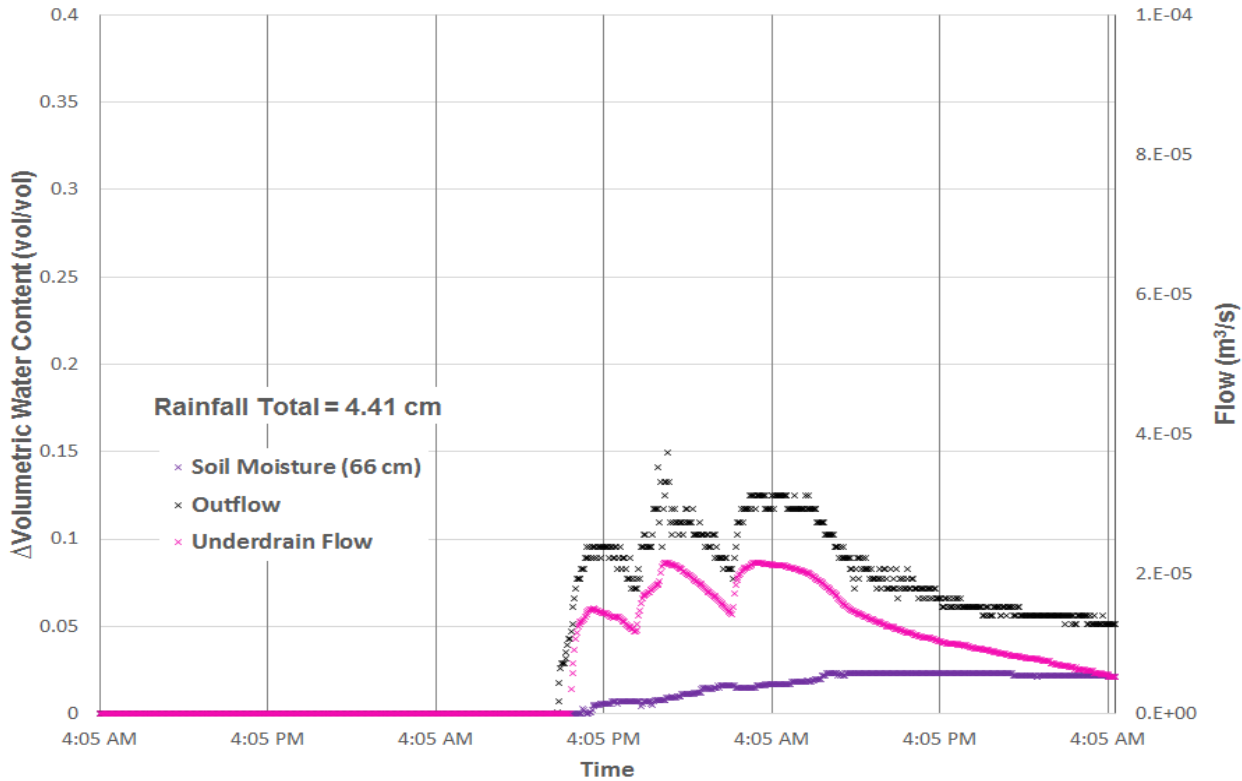
Figure 5.55 FRGR soil moisture and flow data from the 10/28/2015 event

Since overflow did occur during the 10/28/2015 storm event and the FRGI and FRGR were able to infiltrate water well during the event, it appears an underdrain and liner system was not necessary. Similar to the 9/29/2015 storm, the data shows that the FRGI performed well enough without treated outflow leaving the system. The engineered media at the rain gardens infiltrates water quickly and allows for enough storage space for storms of this size.

5.5.2 Pavilion Traffic Island

During the 10/28/2015 storm event, the PTI pond level was found to reach a maximum of 0.49 m. During periods of little or no rain, the pond pressure transducer did indicate that the pond level was decreasing. This is likely infiltration occurring during the storm event. This differs from the 9/29/2015 storm, in which the maximum pond level was observed to be around 0.62 m. During the 9/29/2015 storm, the initial part of the storm before the break did not cause any

observable ponding. After 10 hours of rainfall, the PTI pond level began to increase during the 10/28/2015 storm. The pond level was 0.05 m approximately 72 hours after the 10/28/2015 storm. The ponding data for the 10/28/2015 storm are provided in Figure 5.56.
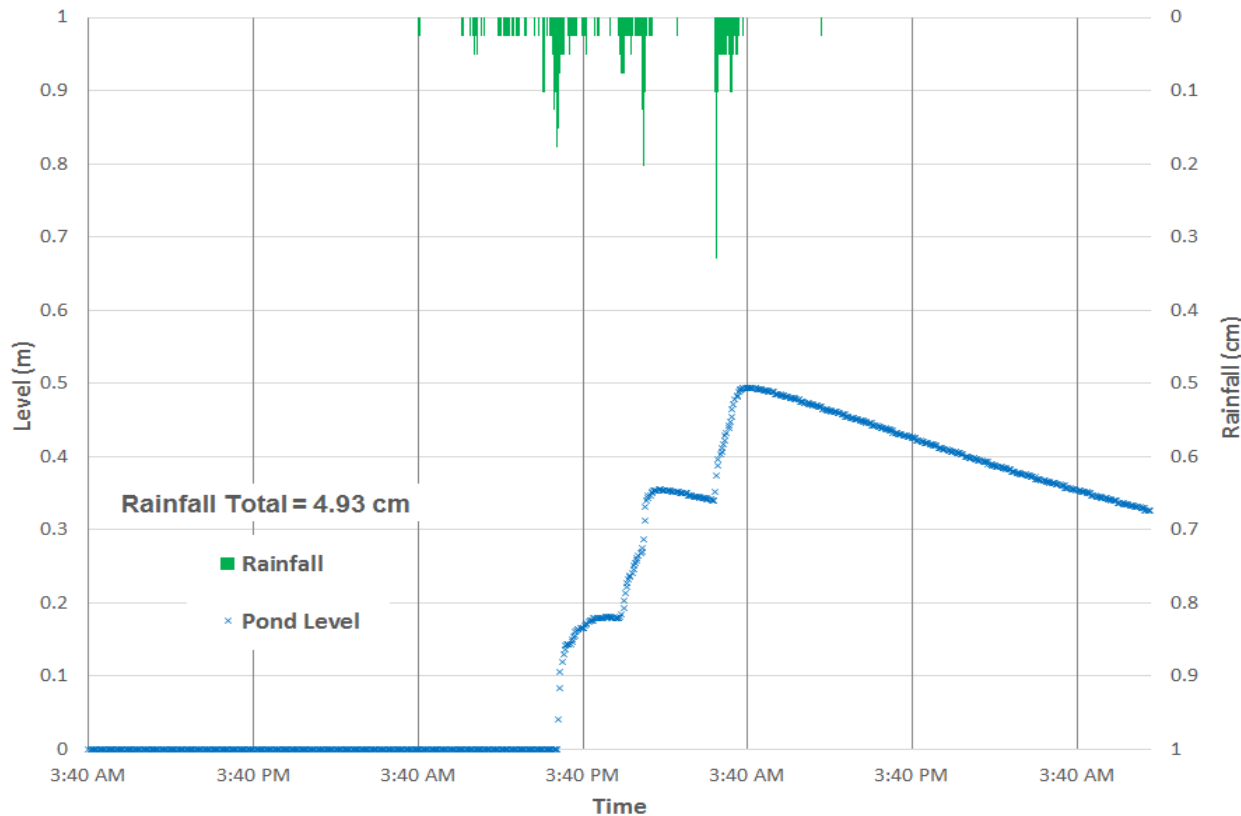
Figure 5.56 PTI pond pressure transducer data from the 10/28/2015 event

The well transducer indicated that the perched water table in the PTI began at around 0.82 m before the 10/28/2015 storm began. The perched water table began to rise after approximately 7.5 hours of rainfall during the 10/28/2015 event. During the 9/29/2015 event, rainfall that occurred before the extended break caused the water table to rise. Before the 9/29/2015 storm, the well transducer suggested a deeper water table. However, both events confirm that the sandy material at the PTI allows the water table rises quickly during storm events. Figure 5.57 validates this observation. Figure 5.58 shows the pond pressure transducer data plotted with the well

transducer data. This figure confirms that the staged increased in the pond level closely match those demonstrated by the well transducer when the water is above the ground surface of the PTI. This reaffirms that the well transducer and pond pressure transducer are working well in tandem at the PTI.
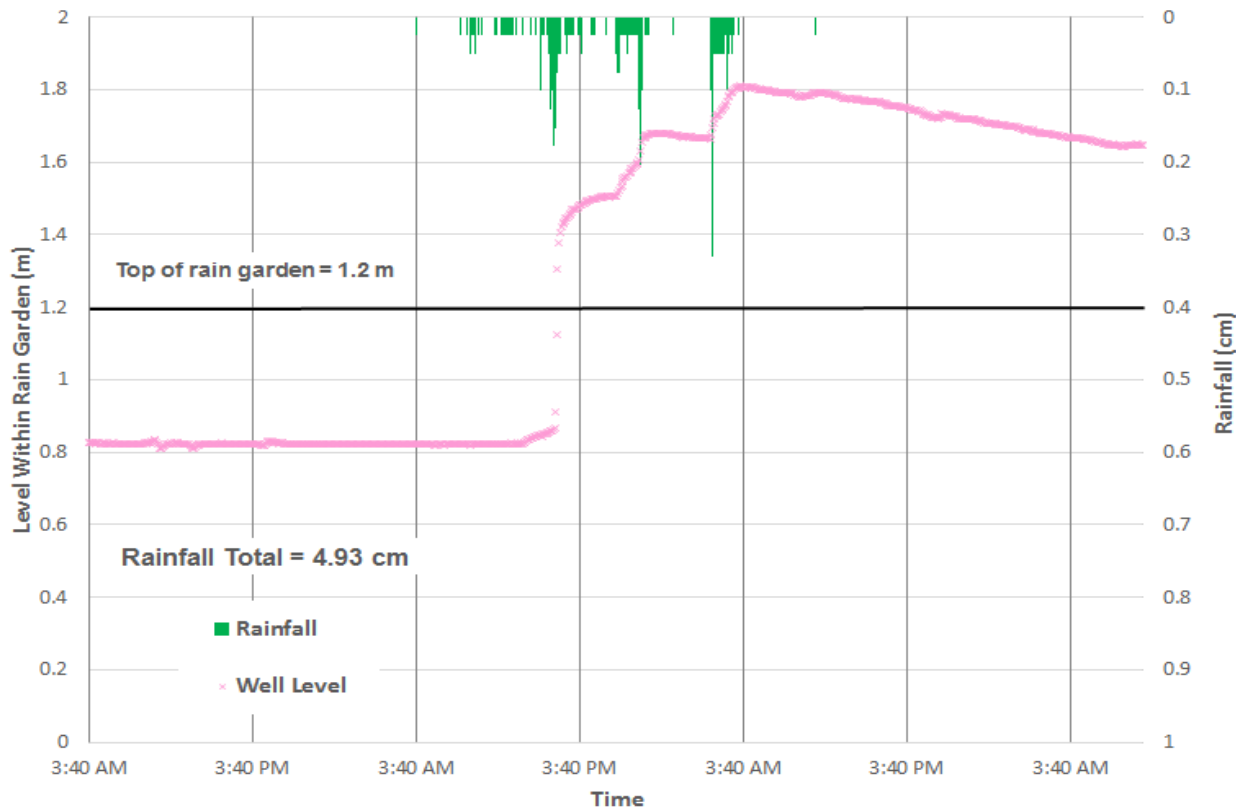
Figure 5.57 PTI well transducer data from the 10/28/2015 event
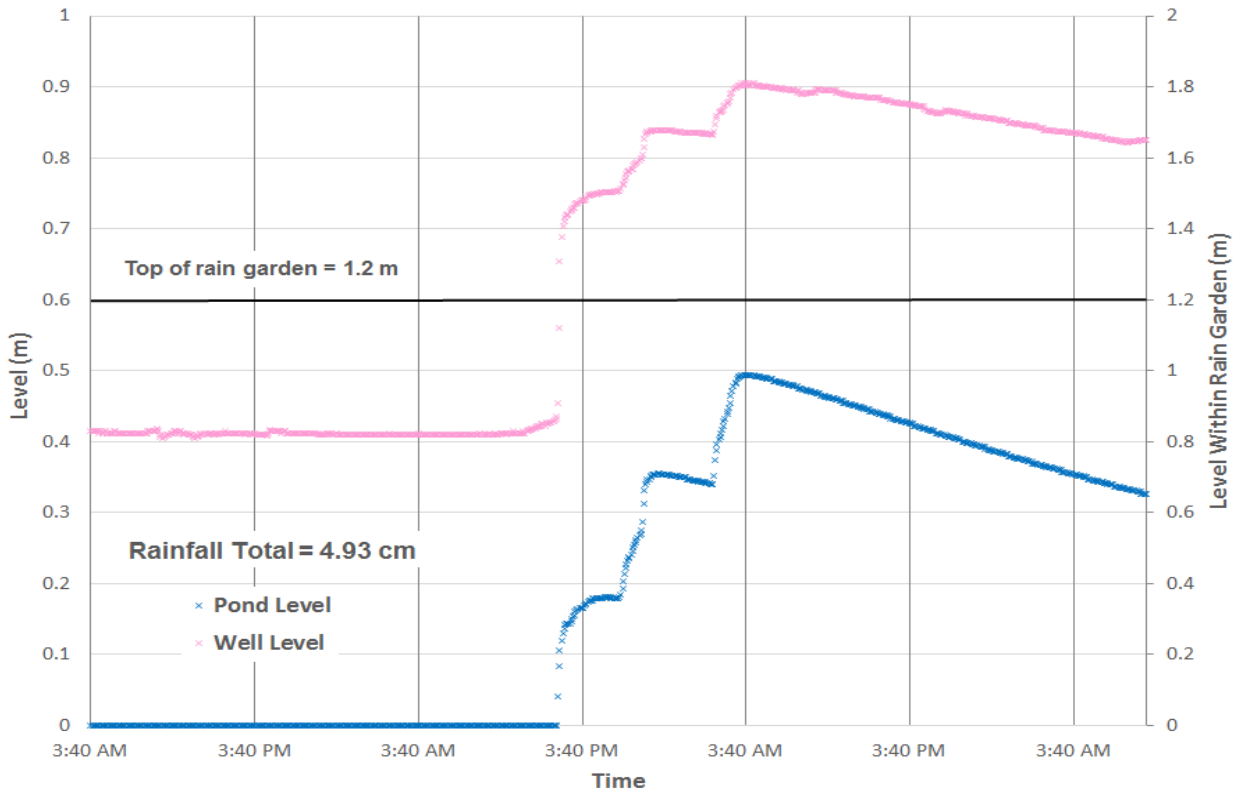
Figure 5.58 PTI ponding data and well transducer data from the 10/28/2015 event

The soil moisture sensor at 10 cm indicated a volumetric water content rise of 0.225 (22.5%) during the 10/28/2015 storm, which was smaller than increase found during the 9/29/2015 storm event. The volumetric water content at 35 cm increased by 0.068 (6.8%), which is much smaller than the increase shown during the 9/29/2015 storm. As validated by the well transducer data, the water level was very close to the soil moisture sensor located 35 cm deep. The volumetric water content at 66 cm scattered around zero, indicating that the soil at this depth was saturated prior to the storm event. The soil moisture sensor at 66 cm deep did actually imply a rise in volumetric water content during the 9/29/2015 storm. The volumetric water content at all analyzed depths was larger prior to the 10/28/2015 event, which confirms that the soil could store more water and allow for larger volumetric water content increases during the 9/29/2015 rain event. During the 10/28/2015 storm, the soil moisture sensor at 10 cm deep suggested an

190

increase before the 35 cm deep sensor, but this did not occur during the 9/29/2015 storm. This could be due to the drier soil media during the 9/29/2015 event. Furthermore, the rainfall that occurred before the break during the 9/29/2015 storm did not cause any increase in volumetric water content. This could be due to the drier soil media above the 10 cm soil moisture sensor. The soil moisture sensor data collected during the 10/28/2015 event are plotted in Figure 5.59.
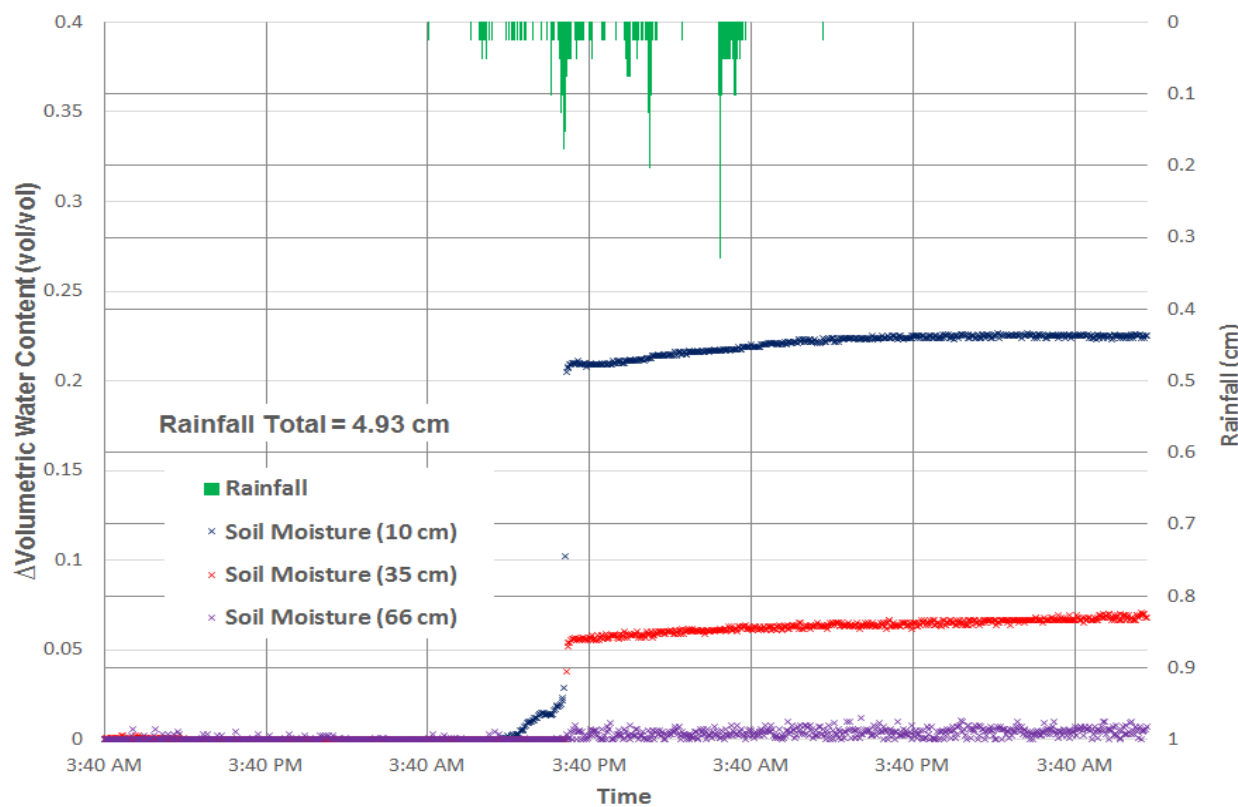
Figure 5.59 PTI soil moisture data from the 10/28/2015 event

As indicated in Figure 5.60, the well transducer implies a rising perched water table at approximately the same time the soil moisture sensors suggest increased in volumetric water content. This confirms that water moves through the media very quickly and begins to fill the PTI during the storm event. This scenario also occurred during the 9/29/2015 storm. As suggested by Figure 5.61, the pond level began increasing a little later than the increase in

volumetric water content at the analyzed depths during the 10/28/2015 event. This could be due to macroporosity and fast infiltration rates. This same phenomenon is also observed during the 9/29/2015 storm.
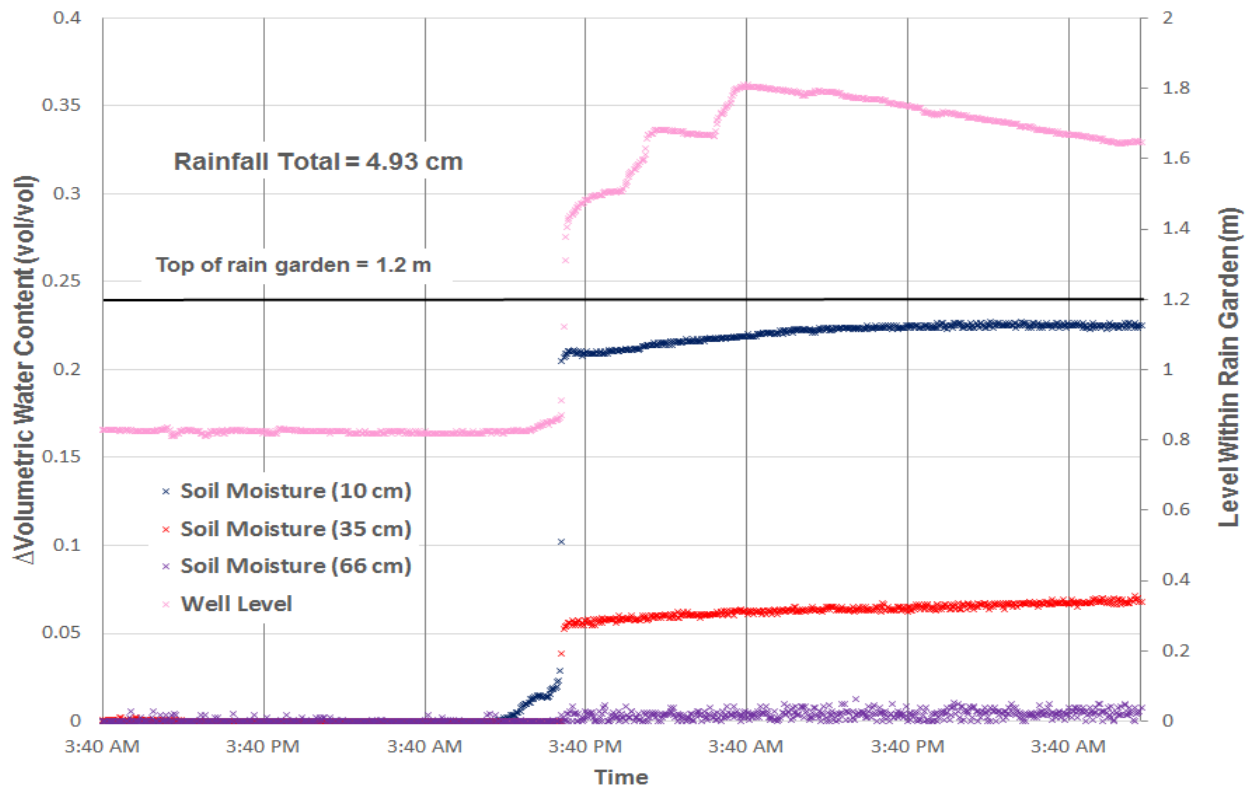
Figure 5.60 PTI soil moisture sensor data and well transducer data from the 11/10/2015 event
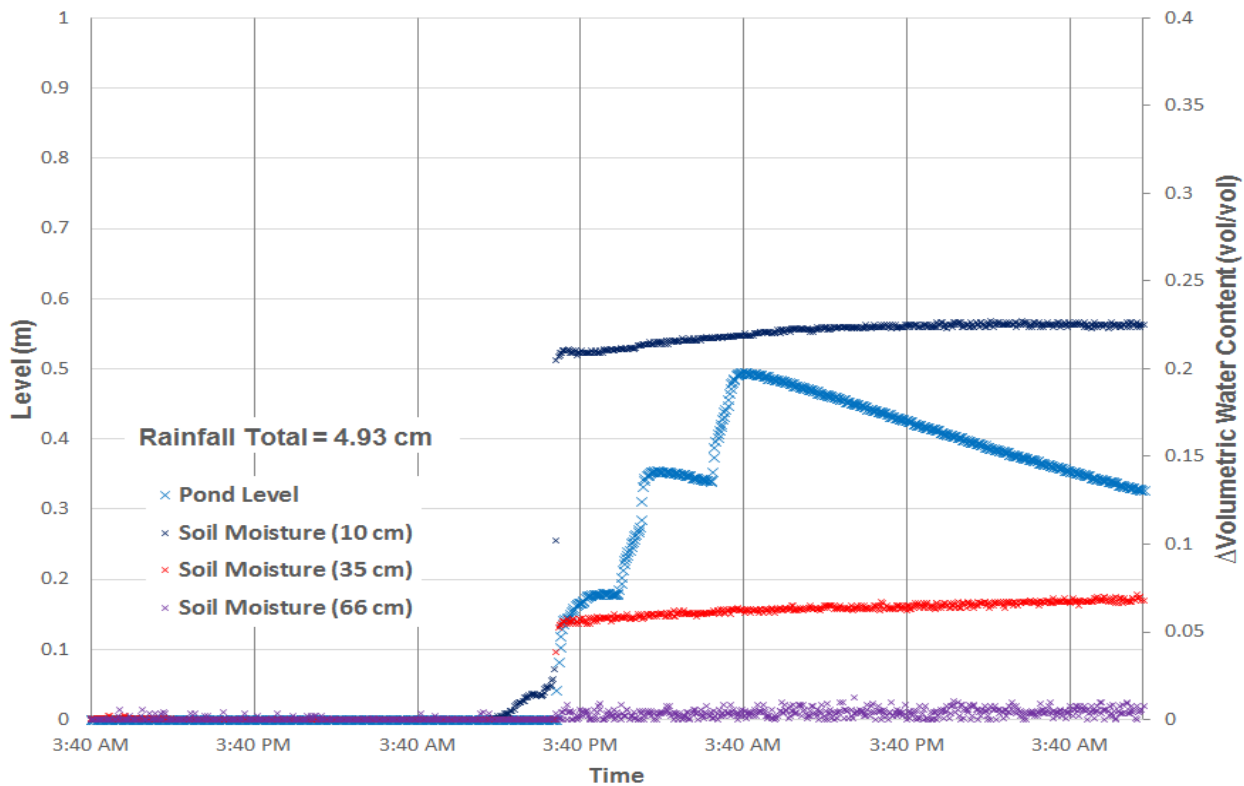
Figure 5.61 PTI soil moisture sensor data and ponding data from the 10/28/2015 event

The PTI behaves similarly during both the 10/28/2015 storm and 9/29/2015 storm. Prior to the 9/29/2015 storm, the soil media had lower volumetric water contents, which caused some changes in soil moisture data. During the 10/28/2015 storm event, it is also implied that infiltration occurred during the event, since there were some noticeable pond level decreases. However, since the soil moisture sensors had reached near saturation and the well transducer indicated the PTI perched water table was above ground surface, this infiltration cannot be observed in the other instrumentation. The data from both storms implies that the "failed" PTI cannot adequately perform during a storm larger than the typical Villanova storm. This is due to the ponding present after 72 hours. The data does indicate that the media allows for quick infiltration; however, the sandy material does not allow for natural vegetation to be sustained within the PTI. Furthermore, the high infiltration rates and sandy media may not be necessary

193

since the other rain gardens with lower sand contents have shown competent performance during all events.

5.5.3 Bioinfiltration Traffic Island

During the 10/28/2015 storm, overflow was observed at the BTI. This is also the case for the 9/29/2015 storm event. Similar to the PTI, the pond pressure transducer at the BTI indicated infiltration during the storm event. This is observed in the staged ponding increased and decreases. This was also implied during the 9/29/2015 storm event before the break in rainfall. Similar to the 9/29/2015 storm, the weir pressure transducer level closely followed the pond pressure transducer during the 10/28/2015 storm. The maximum pond level observed during the 10/28/2015 storm was around 0.42 m, which is smaller than that observed during the 9/29/2015 event. However, this could be due to more rainfall occurring during the 9/29/2015 event. The pressure transducer data for the 10/28/2015 storm is displayed in Figure 5.62.
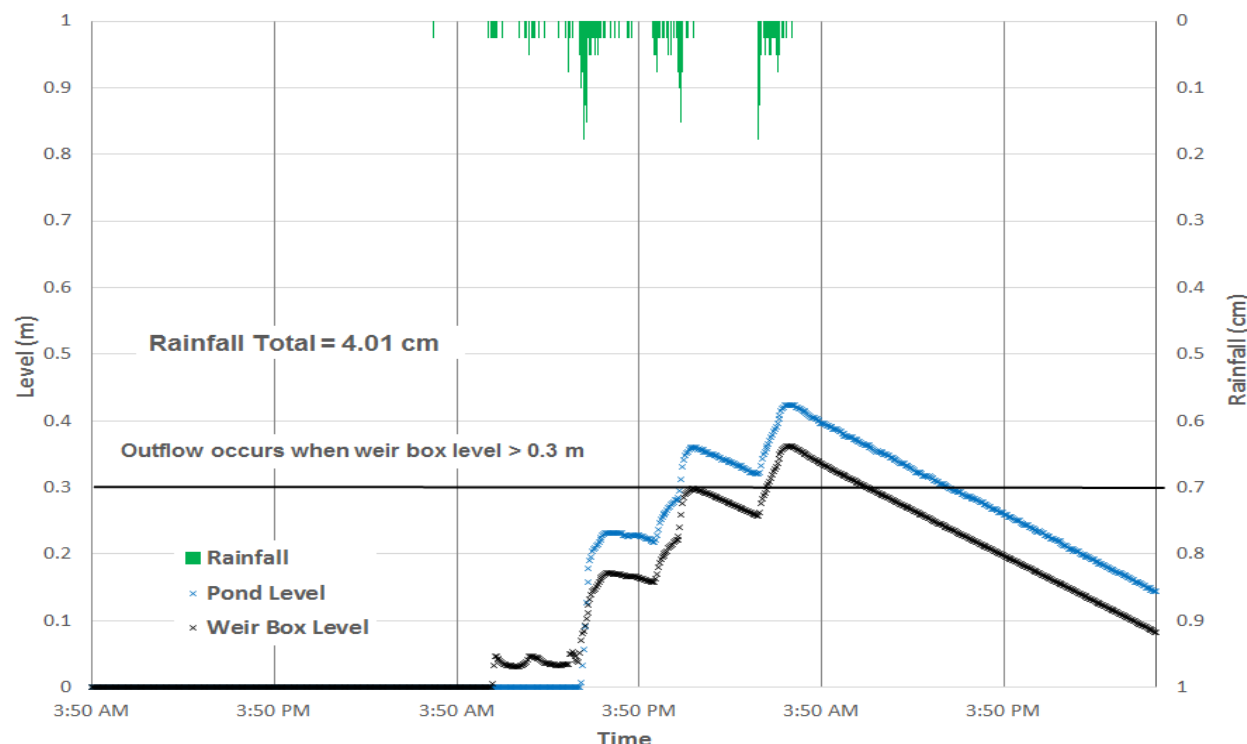
Figure 5.62 BTI pressure transducer data from the 10/28/2015 event

Significantly less overflow was observed during the 10/28/2015 storm than the 9/29/2015 storm, as can be indicated in Figure 5.63. This is confirmed by the water level in the weir box being lower during the 10/28/2015 storm than the 9/29/2015 storm. This is likely due to less rainfall occurring during the 10/28/2015 storm. As displayed in Figure 5.64, the maximum overflow occurs at approximately the same time as the maximum ponding level. This scenario also occurs in the 9/29/2015 storm.
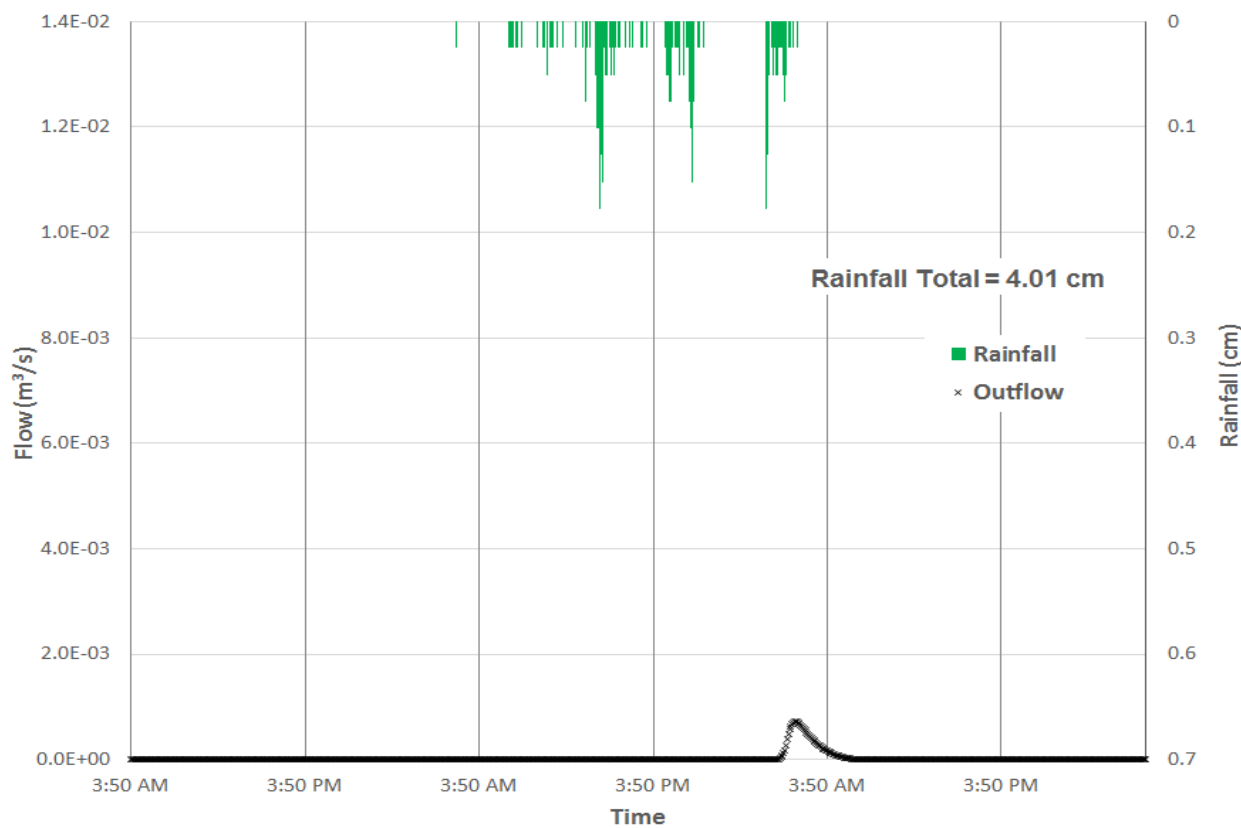
Figure 5.63 BTI overflow data from the 10/28/2015 event
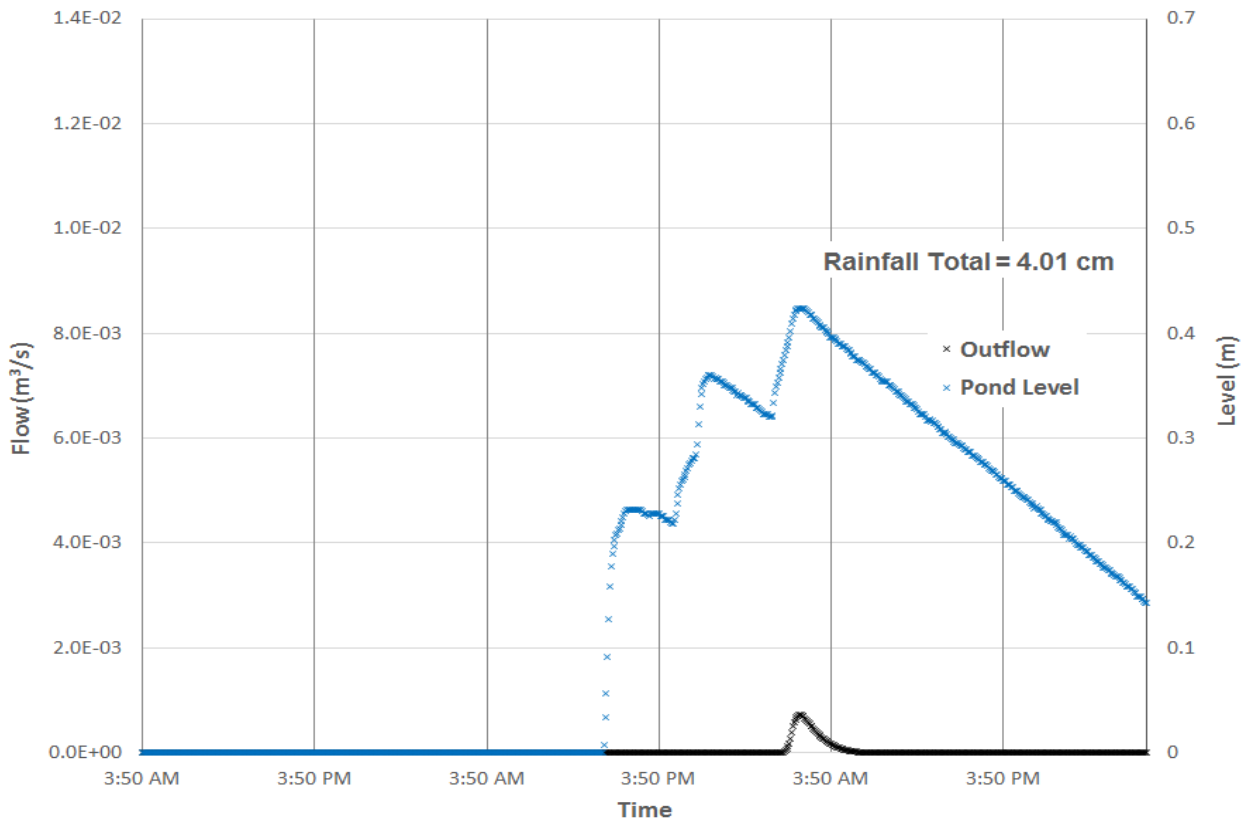
Figure 5.64 BTI overflow data and ponding data from the 10/28/2015 event

The volumetric water contents at 10 cm, 35 cm, the duplicate 35 cm sensor, and 66 cm indicated higher increases during the 9/29/2015 storm than the 10/28/2015 storm. This is similar to the PTI, and is likely due to the same reason: drier initial volumetric water contents. During the 10/28/2015 event, the soil moisture sensor at 10 cm observed a slight increase before the other sensors. However, the major increases in volumetric water content occurred at around the same time for all analyzed sensors. This shows quick infiltration during the storm event. The soil moisture sensor at 35 cm deep indicated a slight drop in volumetric water content at 11 hours after the 10/28/2015 event began. It is unclear what could have caused this; however, the duplicate sensor provided the same drop. This drop is not seen during the 9/29/2015 storm event. This could be water moving past the 35 cm depth during a period of less rainfall. Another major

difference in soil moisture sensor data for the two events is the presence of a decrease in volumetric water content during the 9/29/2015 rain event. This occurred during the break, implying that water moved through the system quickly when no rain was occurring. Since there was no break during the 10/28/2015 event, this infiltration was not observed. The soil moisture sensor data for the 10/28/2015 event is plotted in Figure 5.65.
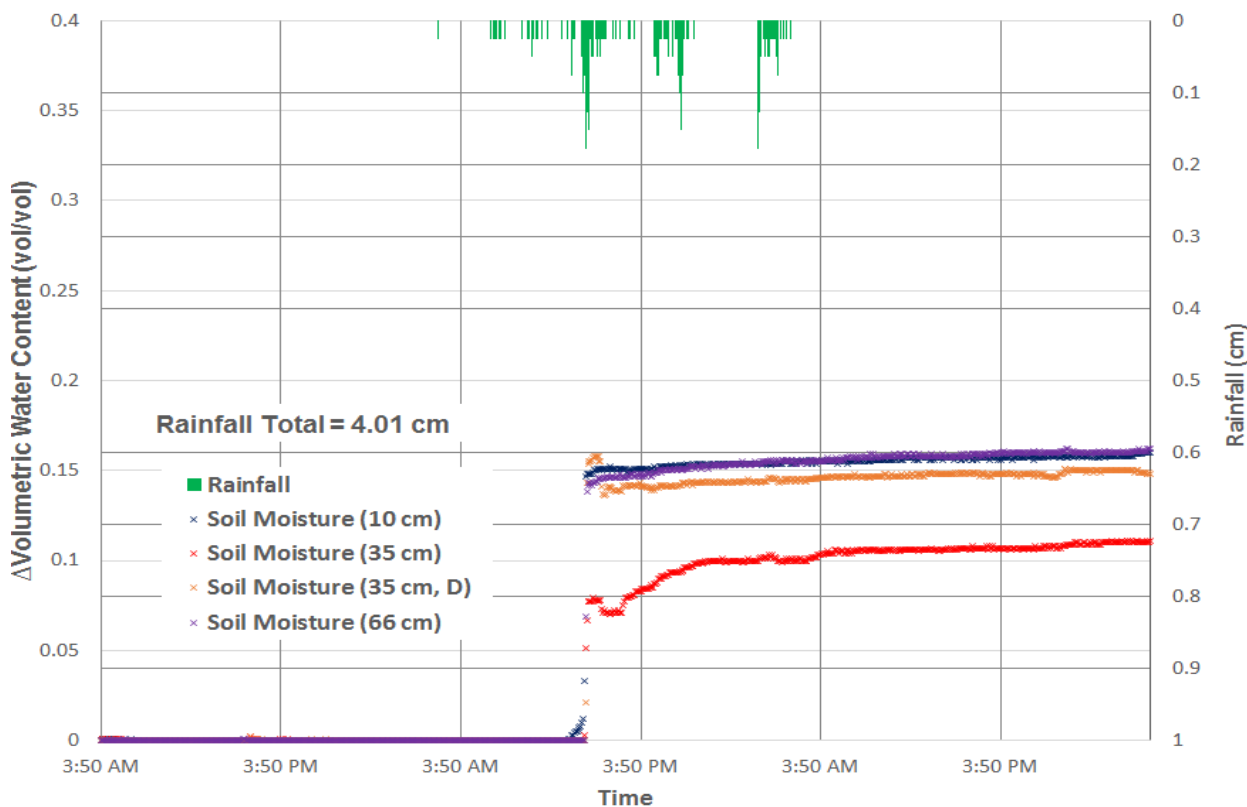
Figure 5.65 BTI soil moisture sensor data from the 10/28/2015 event

The level in the pond began rising shortly after the soil moisture sensor at 10 cm indicated an increase in volumetric water content during the 10/28/2015 storm. However, the pond level increase and soil volumetric water content increases occur at approximately the same time, as demonstrated in Figure 5.66. This also occurs during the 9/29/2015 event, implying that water infiltrates quickly during a storm of this size. The soil moisture sensors at 35 cm read a drop in volumetric water content at the first pond peak, and begin increasing again when the pond water

begins infiltration. This could show that water moved quickly past the 35 cm depth, then began to infiltrate to the 35 cm depth shortly after. The 9/29/2015 event shows two peaks in volumetric water content and ponding level, while the 10/28/2015 event shows only one peak in volumetric water content and three smaller peaks in ponding level. This is due to the break in the storm and the larger amount of water infiltrated during the break.
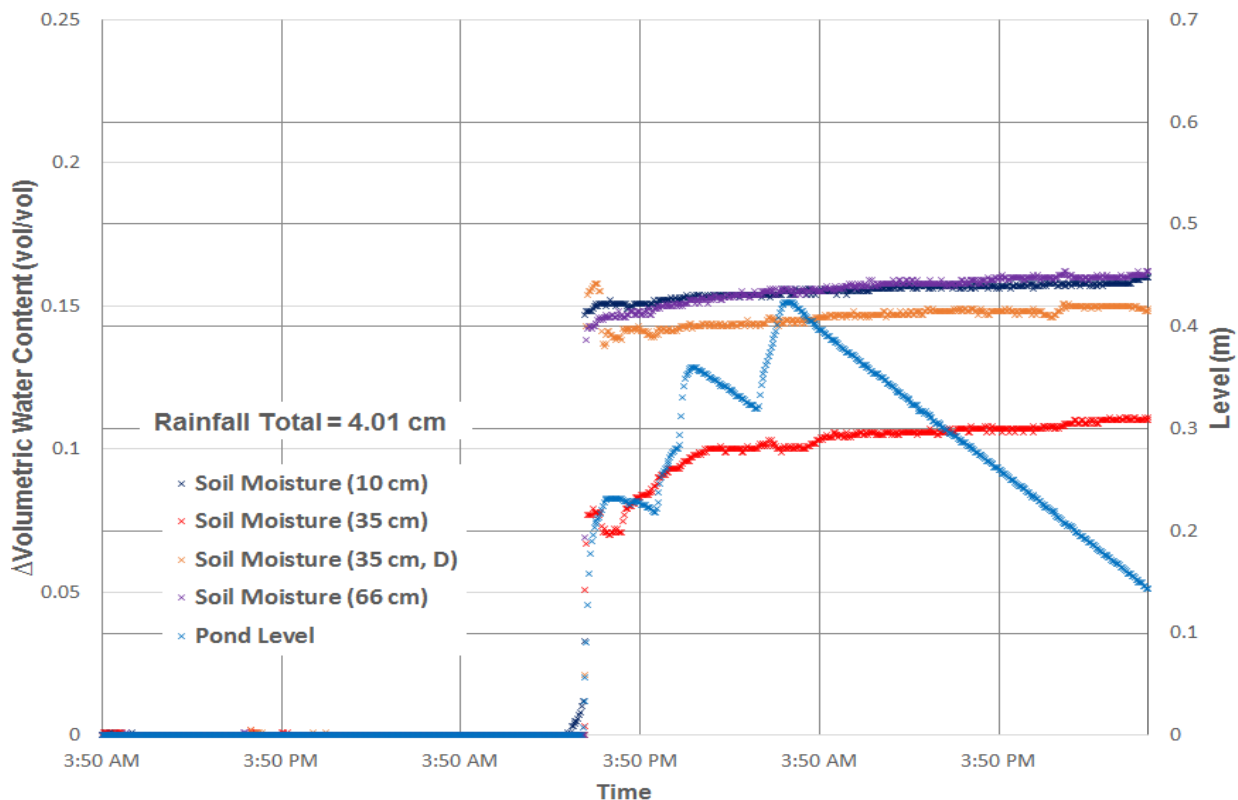
Figure 5.66 BTI soil moisture sensor and pond pressure transducer data from the 10/28/2015 event

The BTI performed well during both events. Ponded water did not remain 72 hours after either the 9/29/2015 or 10/28/2015 event. The BTI was also able to infiltrate water quickly through the system, despite the presence of an organic layer above the sand-soil mix. This shows that the high loading ratio and sand-soil mix are can perform well in the Villanova area. In fact, the ponding behaved similarly to the PTI, which has a much higher coarse-grained component.

These data show that it may not be necessary to have a higher sand content which creates a more difficult situation for vegetation growth. These data also show that after 15 years and an organic buildup, the BTI can still function well.

CHAPTER 6.   INFILTRATION DATA COLLECTED

6.1 Single-Ring Infiltrometer Comparison Data

6.1.1   Single-Ring Infiltrometer Data Collected

During the fall of 2014, seven single-ring infiltrometer tests were performed at the BTI in the locations provided in Figure 6.1. These tests were performed by Zukowski et al. (2016) as part of a study to compare the single-ring infiltration testing method with the long-term average recession rate of the BTI. A single-ring infiltrometer test conducted at the BTI is depicted in Figure 6.2. During the initial field investigation, the soil at the BTI was saturated from a previous storm but ponding was not present within the SCM. The water temperature, hydraulic conductivity, and depth of the organic silt loam layer were recorded for each of the seven tests.
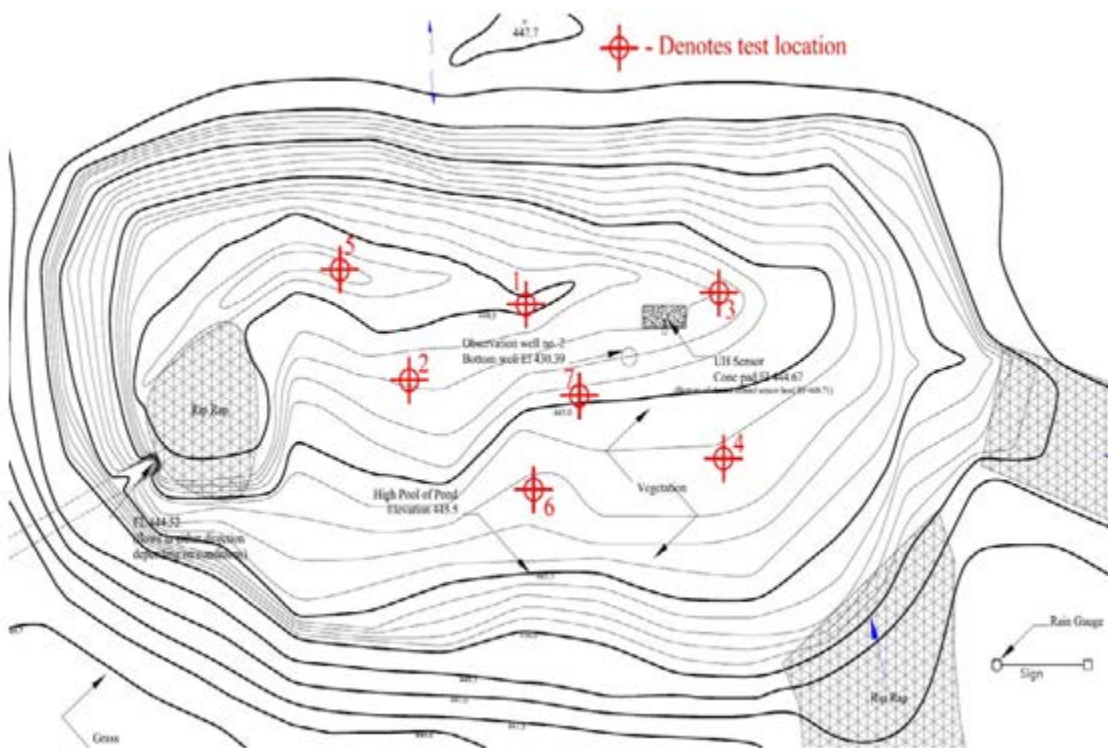
Figure 6.1 Single-ring infiltrometer test locations at the BTI (reprinted from Zukowski et al. 2016)

Figure 6.2 A single-ring infiltration test at the BTI (Emerson et al. 2015)

All temperatures were corrected to 12°C using Equation 4.6. While the usual temperature used for correction is 20°C, 12°C was used because it is the average temperature of the water in the BTI. The dynamic viscosity of water at 12°C is 0.00128 kg/m-s according to calculations provided by Touloukian et al. (1975).

Table 6.1 provides the data collected during the single-ring infiltrometer study. The study found that the temperature-corrected hydraulic conductivity varied from $7.1{\times}10^{-6}$ cm/s to $1.8{\times}10^{-3}$ cm/s, with the geometric mean being $2.7{\times}10^{-4}$ cm/s. The silt loam organic layer varied from 2.5 cm to 7.6 cm, which was measured using a shovel and a measuring tape (Zukowski et al. 2016).

Table 6.1. Single-ring infiltrometer data collected during the field investigation (modified from Zukowski et al. 2016)

Test No.	Temperature of Water (°C)	Depth of Organic Silt Loam (cm)	Hydraulic Conductivity (cm/s)	Temperature Corrected Hydraulic Conductivity (cm/s)
1	16.5	7.6	$<7.1\times10^{-6}$	$<7.1\times10^{-6}$
2	16.5	6.4	1.4×10^{-4}	1.1×10^{-4}
3	16.3	2.5	1.7×10^{-3}	1.6×10^{-3}
4	16.9	2.5	1.9×10^{-3}	1.8×10^{-3}
5	15.9	5.1	2.1×10^{-4}	2.2×10^{-4}
6	16.9	3.8	1.4×10^{-4}	1.5×10^{-4}
7	15.7	6.4	8.5×10^{-4}	1.3×10^{-3}

6.1.2 Recession Rate Data Collected

The BTI maintains separation from the groundwater table and does not contain a perched groundwater table within the system (Nemirovsky et al. 2015). Temperature fluctuations throughout the year cause viscosity changes, which result in variation of the hydraulic conductivity (Emerson and Traver 2008). The recession rates were determined using the methodology set forth by Emerson (2008). Using data collected since 2003, the average recession rate was found to be 1.9×10^{-4} cm/s, with an average temperature of 12°C, with seasonal variation on the order of a factor of two (Zukowski et al. 2016). Figure 6.3 provides the recession rate data from the BTI collected during storms between 2003 and early 2015 (Zukowski et al. 2016).
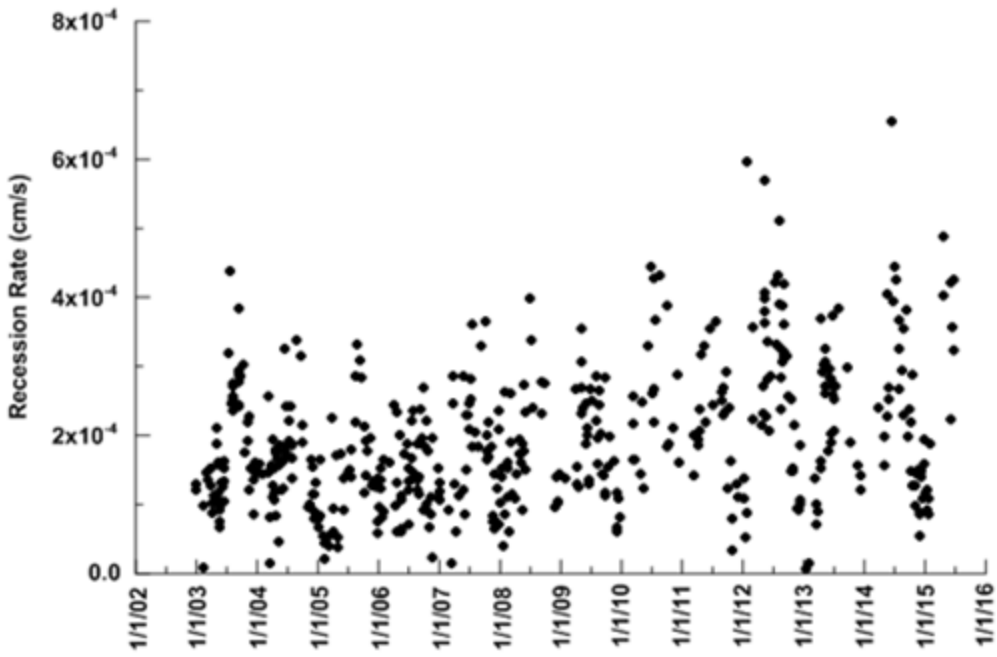
Figure 6.3 Recession rate data collected from the BTI (modified by Zukowski et al. 2016)

6.2 Modified Philip-Dunne Infiltrometer Comparison Data

6.2.1   Fedigan Rain Garden Infiltration Testing

During the summer of 2014, three double-ring infiltrometer tests were conducted at the FRGI. During the summer of 2015 and early fall of 2015, four Modified Philip-Dunne tests were conducted at the FRG, with two being performed at the FRGI and two being performed at the FRGR. Two of these tests were conducted in the same area as the double-ring infiltrometer tests to compare the methods. Finally, two KSAT laboratory tests were conducted at the FRG, with one being performed at the FRGI and the other being performed at the FRGR. One sample used in KSAT analysis was extracted from an area near a double-ring infiltrometer test, and the other was taken from an area near a Modified Philip-Dunne test. This was done to compare the KSAT laboratory hydraulic conductivity testing method with the field methods. To compare the methods, the hydraulic conductivity values obtained from the double-ring infiltrometer and

203

Modified Philip-Dunne infiltrometer were normalized to 10°C using Equation 4.1. The dynamic viscosity of water at 12°C is 0.00131 kg/m-s according to calculations provided by Touloukian et al. (1975). Figure 6.4 shows a double-ring infiltrometer test being installed at the FRGI, and Figure 6.5 show a double-ring infiltrometer test being conducted at the FRGI. The locations of the tests performed are shown in Figure 6.6, and the data collected from the FRG are provided in Table 6.2.

Figure 6.4 FRGI-02 being installed at the FRGI

Figure 6.5 FRGI-02 being performed at the FRGI

Figure 6.6 Infiltration test locations at the FRG

Table 6.2. Infiltration testing data collected at the FRG

Sample No.	Modified Philip-Dunne (cm/s)	Double-Ring (cm/s)	KSAT (cm/s)
FRGI-01	4.3×10^{-4}	6.8×10^{-4}	-
FRGI-02	1.5×10^{-4}	4.2×10^{-4}	-
FRGI-03	-	1.3×10^{-3}	1.4×10^{-3}
FRGR-01	1.7×10^{-4}	-	8.1×10^{-5}
FRGR-02	1.4×10^{-3}	-	-

6.2.2 Bioinfiltration Traffic Island Infiltration Testing

During the summer of 2015, two Modified Philip-Dunne infiltrometer tests were conducted at the BTI. Additionally, samples were taken at these locations for the UMS KSAT laboratory hydraulic conductivity testing method. These locations were chosen because they are in the vicinity of two of the single-ring tests performed, which were test number 1 and test number 6 from the previous section of this chapter. This provided the necessary information to compare the Modified Philip-Dunne infiltrometer test method, the KSAT test method, and single-ring infiltrometer test method. As was the case with the infiltration test data collected from the FRG, the Modified Philip-Dunne infiltrometer and single-ring infiltrometer data were normalized to 10°C for comparison with the KSAT. The locations of the tests performed are shown in Figure 6.7, and the data collected from the BTI are provided in Table 6.3. The KSAT samples taken from the BTI failed during the testing procedure, so the KSAT data are not provided.

Figure 6.7 Infiltration test locations at the BTI

Table 6.3. Infiltration testing data collected at the BTI

Sample No.	Modified Philip-Dunne (cm/s)	Single-Ring (cm/s)
BTI-01	3.5×10^{-6}	5.8×10^{-6}
BTI-02	1.8×10^{-4}	1.2×10^{-4}

6.2.3   Upper Moreland Site Infiltration Testing

During the fall of 2015, a test pit investigation was undertaken for the design of an SCM at the Upper Moreland Middle School. This site was not on Villanova University's campus where the previously mentioned rain garden sites are located. This site was included in this study because it is different from the other rain garden sites mentioned. It has native soils which had a high fine-grained content, so it provided a unique opportunity to test the Modified Philip-Dunne infiltrometer in a different soil type, as well as compare properties of fine-grained materials to hydraulic conductivity values. Furthermore, it provided an opportunity to determine how the

Modified Philip-Dunne infiltrometer could be used to determine hydraulic conductivity values in test pits during site investigations for SCM design. The goal of the investigation was to determine the underlying soils at the site, as well as conduct necessary infiltration testing to determine what kind of SCM would be best suited for the site and properly design the selected SCM. A total of 15 test pits were dug with an excavator and infiltration testing was conducted within the test pits, which ranged between 1.2 and 1.5 m in depth. In each test pit, a private consultant conducted a falling-head infiltrometer test method with a PVC pipe. For this comparison study, these test results were ignored because they do not account for the head of water within the pipe and unsaturated flow beneath the PVC pipe. Two double-ring infiltrometer tests were conducted and three Modified Philip-Dunne infiltrometer tests were conducted to compare the methods in native soil. Additionally, six soil samples were taken for gradation size distribution testing using the sieve and hydrometer analysis methods (ASTM D422) and Atterberg limits testing (ASTM D4318). The sampler used also allowed for quick determination of the dry unit weight of the soil samples. The goal was to classify the soil at the Upper Moreland site and determine if Atterberg limits parameters correlated to hydraulic conductivity values found. Six samples were also taken for KSAT laboratory analysis for the comparison study. Figure 6.8 depicts the test pits dug at the Upper Moreland site, and Figure 6.9 and Figure 6.10 show all of the infiltrometer tests being conducted in test pits.

Figure 6.8 Test pits dug at the Upper Moreland site

Figure 6.9 Infiltration testing being conducted in a test pit at the Upper Moreland site

Figure 6.10 Infiltration testing being conducted in a test pit at the Upper Moreland site

The goal of this study was to compare data from the double-ring infiltrometer test method, the Modified Philip-Dunne infiltrometer test method, the UMS KSAT laboratory hydraulic conductivity test method, and the plasticity index determined by the Atterberg limits testing. The double-ring infiltrometer tests, which were conducted at TP 14 and TP 5, did not indicate any change in water level during the test, which validated infiltration was too slow to measure at these locations. As was the case with the infiltration test data collected from the FRG and BTI, the Modified Philip-Dunne infiltrometer data were normalized to 10°C for comparison with the KSAT. The locations of the tests performed are shown in Figure 6.11, and the data collected from the Upper Moreland site are provided in Table 6.4. In Table 6.4, the term BDL was used to indicate that the hydraulic conductivity could not be determined because the value was "below the detection limit".

Figure 6.11 Test pit locations and infiltration tests conducted at the Upper Moreland site

Table 6.4. Infiltration testing data collected at the Upper Moreland site

Sample No.	Modified Philip-Dunne (cm/s)	KSAT (cm/s)
TP 14	BDL	BDL
TP 13	1.4×10^{-5}	1.3×10^{-3}
TP 12	-	1.2×10^{-5}
TP 10	-	4.6×10^{-6}
TP 7	3.0×10^{-5}	8.1×10^{-6}
TP 5	-	BDL

Figure 6.12 shows soil laboratory samples being prepared for sieve, hydrometer, and Atterberg limits testing. These data and the dry unit weight data are provided in Appendix A. From the laboratory testing, it was determined that all soil samples except TP 13 were classified as USCS silt and USDA silt loam. TP 13 was classified as a USCS sand and a USDA sand. **Figure 6.13** depicts where the soil samples plotted on the USDA soil triangle. These classifications are represented in Table 6.5.

Figure 6.12 Samples TP 12 and TP 13 being prepared for laboratory testing
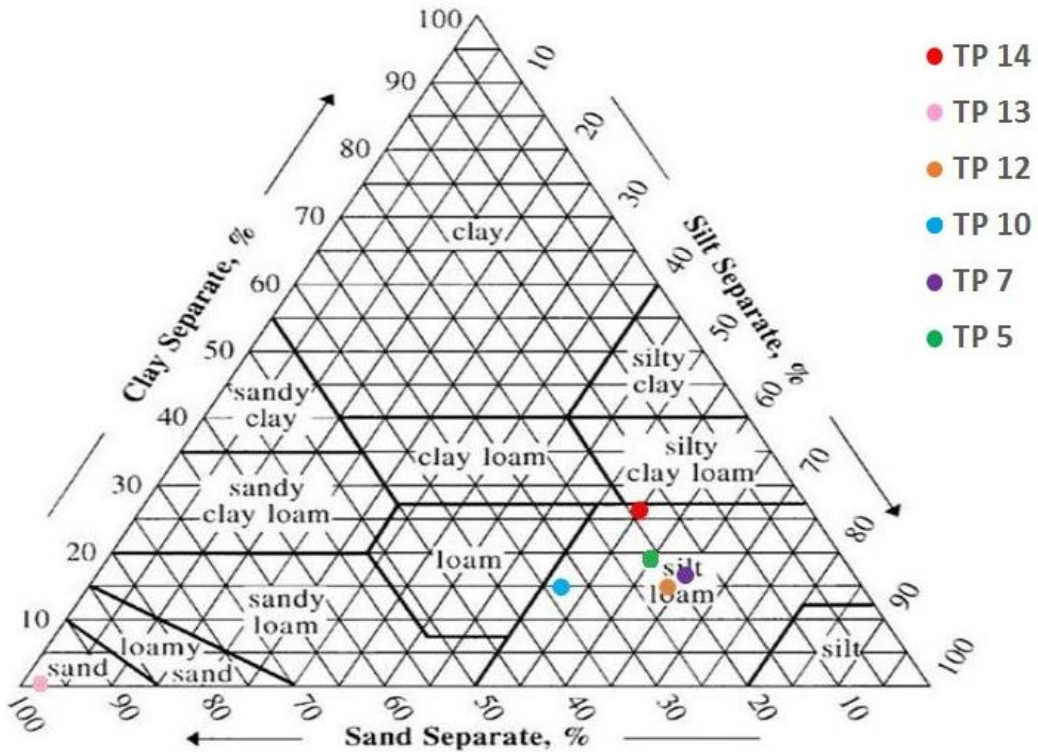
Figure 6.13 Upper Moreland soil samples plotted on the USDA soil triangle

Table 6.5. Soil classifications at the Upper Moreland site

Sample No.	USCS Classification	USCS Description	USDA Classification
TP 14	ML	Silt	Silt Loam
TP 13	SP	Poorly-graded Sand	Sand
TP 12	ML	Silt	Silt Loam
TP 10	ML	Silt with sand	Silt Loam
TP 7	ML	Silt	Silt Loam
TP 5	ML	Silt	Silt Loam

Figure 6.14 illustrates where the soils plotted on the plasticity chart from the results found during

Atterberg limits testing. Figure 6.14 confirms that the soil samples plotted close to the silty clay

and low-plasticity clay portions of the chart, indicating that these samples classify as silt material

but may behave closely to typical clay material. Samples TP 14 and TP 5 plotted almost directly

on the line that divides the low-plasticity silt and low-plasticity clay ranges.
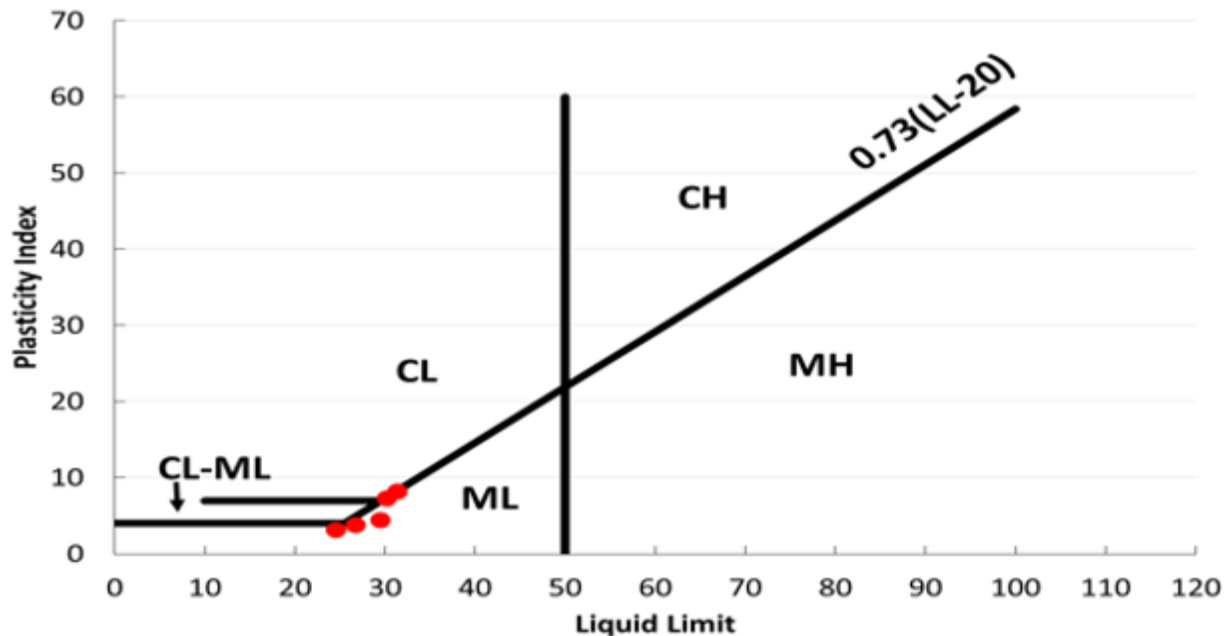
Figure 6.14 Plasticity data collected from soil samples at the Upper Moreland site

CHAPTER 7. INFILTRATION DATA DISCUSSION

7.1 Single-Ring Infiltrometer Data Discussion

From the data provided in the previous chapter, the recession rate data verify that the single-ring infiltrometer produces an accurate hydraulic conductivity value. Both test methods produced hydraulic conductivity values that were within the same order of magnitude (Zukowski et al. 2016). This validates the use of the single-ring infiltrometer test method as a means of determining hydraulic conductivity in the field at an SCM. This can be used to determine SCM performance post-construction. The value of hydraulic conductivity that falls within the same order of magnitude, which is considered an accurate prediction, is the geometric mean of the seven single-ring infiltrometer tests. This validates that multiple single-ring infiltrometer tests are necessary to correctly to determine the hydraulic conductivity due to heterogeneity of soils and variations in macroporosity and compaction. The seven tests performed at the BTI covered 0.13 m^2, which is <0.1% of the SCM surface area, with the tests being spread out over the surface area of the BTI (Zukowski et al. 2016). Since the single-ring tests were able to be installed and conducted more quickly and used less water than the double-ring infiltrometer tests, multiple tests could be performed encompassing various areas of the BTI to accurately determine the hydraulic conductivity of the entire SCM. As validated with the data collected, the geometric mean of the hydraulic conductivity of the tests more accurately predicted the hydraulic conductivity than any single test alone (Zukowski et al. 2016). This confirms that infiltration testing techniques such as the single-ring infiltrometer can be used instead of the double-ring infiltrometer which is recommended by the PADEP (2006).

The hydraulic conductivity and depth of organic silt loam layer were compared to determine if a relationship between the two existed. During the field investigation, it was hypothesized that the hydraulic conductivity would decrease with increasing depth of organic layer because the silt loam had more fine material than the underlying rain garden soil mix. As observed in Figure 7.1, there is a decline in hydraulic conductivity when the depth of the organic silt loam layer is greater than 3.81 cm with the exception of test number 7 (Zukowski et al. 2016). This validates that the depth of the organic layer does have some effect on the hydraulic conductivity. As previously stated, the organic layer likely formed over time from sedimentation and vegetation in the SCM. However, this appears to have little effect on the overall hydraulic conductivity as the average value has not changed greatly since construction of the BTI in 2001 (Zukowski et al. 2016).
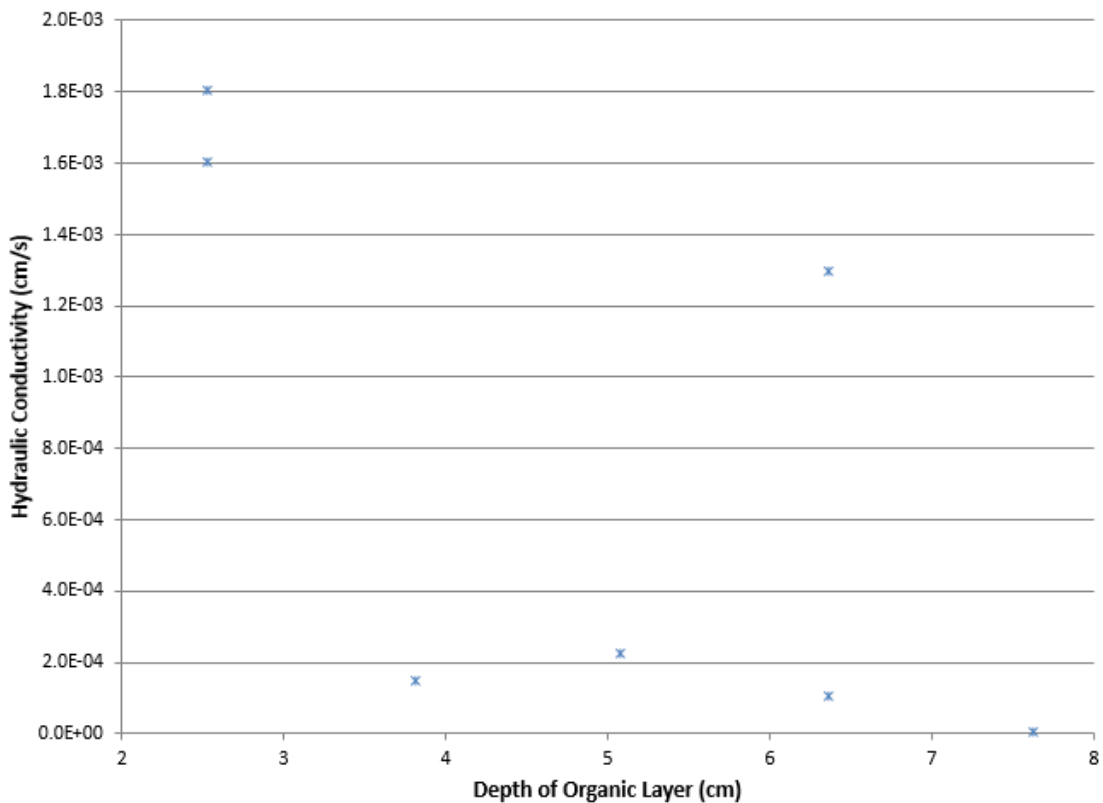
Figure 7.1 Hydraulic conductivity values obtained and the depth or the organic silt loam layer for each test

To determine if fewer infiltration tests were needed to accurately predict the hydraulic conductivity of the BTI assuming that the recession rate is an accurate estimate of hydraulic conductivity, Figure 7.2 was made comparing the number of tests and the geometric mean hydraulic conductivity. This was done by combining all possible tests to determine the hydraulic conductivity range that could have been achieved. For seven infiltration tests, all seven points were plotted. For six infiltration tests, all possible combinations of the results of six tests were used to determine the range. For example, the geometric mean of the first two tests was determined, then test one and test three, then test one and test four, and so on. For five infiltration tests, all possible combinations of the results of the five tests were plotted. This procedure was repeated until the geometric hydraulic conductivity determined from all seven tests was plotted. In Figure 7.2, it was found that the spread of hydraulic conductivity values determined shrinks as more tests are conducted. Figure 7.2 verifies the notion that it is the geometric mean hydraulic conductivity of the seven tests which represents the most accurate hydraulic conductivity measurement. Seven infiltration tests appear to provide a fairly accurate estimate based on these data. However, it is still of interest to determine how many tests would be needed to accurately measure hydraulic conductivity per square area of an SCM. This could save time and cost during site investigations.
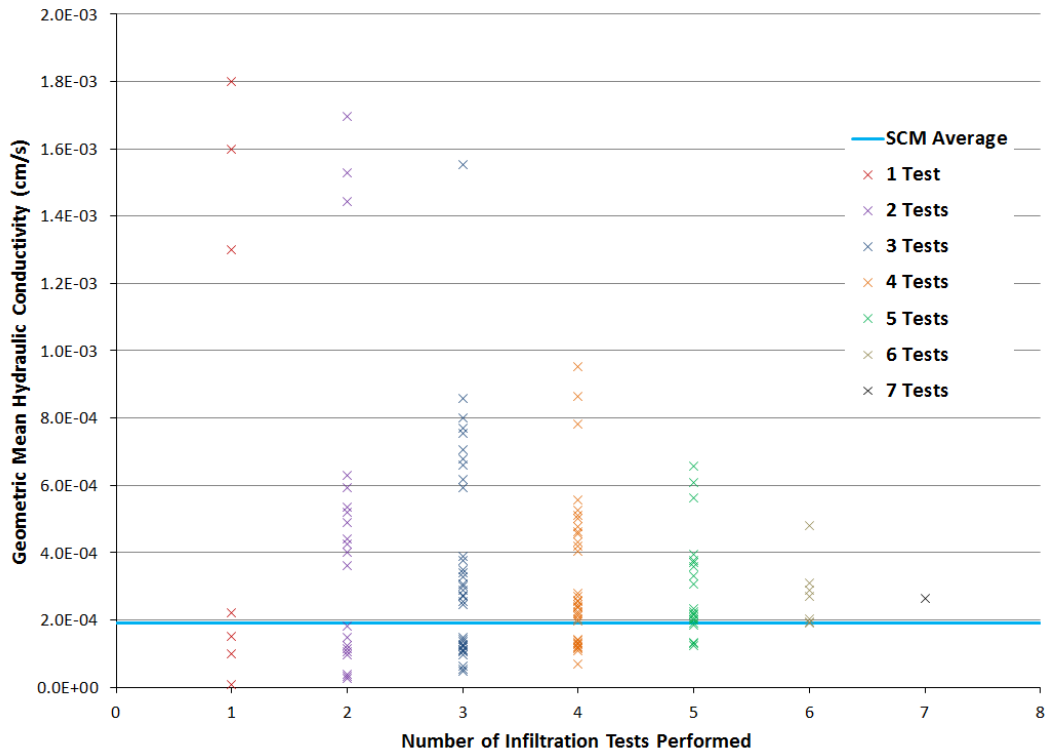
Figure 7.2 Geometric mean hydraulic conductivity of tests given the number of tests performed

7.2 Modified Philip-Dunne Infiltrometer Data Discussion

Comparing the preliminary data collected, the Modified Philip-Dunne infiltrometer constructed at Villanova compares favorably with the UMS KSAT, the double-ring infiltrometer, and the single-ring infiltrometer. The Modified Philip-Dunne infiltrometer produces values in the same order of magnitude as the double-ring infiltrometer and KSAT laboratory measurement at the FRG. The double-ring infiltrometer produced a hydraulic conductivity that is approximately one order of magnitude larger than the hydraulic conductivity produced by the KSAT.

At the BTI, the Modified Philip-Dunne infiltrometer produced hydraulic conductivities within the same order of magnitude as the hydraulic conductivities produced by the single-ring infiltrometer. Based on data collected from the study comparing the single-ring infiltrometer to the recession rate at the BTI, it was safe to assume that the results provided by the single-ring

were accurate. While it would be desirable to have KSAT hydraulic conductivity values from the BTI for comparison, the failed tests did not allow for this comparison.

At the Upper Moreland site, the Modified Philip-Dunne infiltrometer hydraulic conductivity at TP 13 was approximately two orders of magnitude slower than the hydraulic conductivity found by the UMS KSAT. This could be due to placement of the Modified Philip-Dunne infiltrometer in the test pit. The KSAT sample was taken in a location that was not exactly same spot as the Modified Philip-Dunne infiltrometer. This was because bentonite used to seal the infiltrometer in place during the testing procedure, and this bentonite could have entered the sample and affected the laboratory hydraulic conductivity value. Heterogeneity of the native soils may have caused this hydraulic conductivity difference. The Modified Philip-Dunne infiltrometer hydraulic conductivity at TP 7 was approximately one order of magnitude faster than the hydraulic conductivity found by the KSAT laboratory method. Additionally, the Modified Philip-Dunne, double-ring infiltrometer, and KSAT could not provide a hydraulic conductivity at TP 14 because the value was too small. Thus all three methods provided similar results. At TP 5, the KSAT and double-ring infiltrometer both indicated that the hydraulic conductivity was too small to be determined. While the KSAT, double-ring infiltrometer, and Modified Philip-Dunne infiltrometer could not predict the hydraulic conductivity at some locations due to the rate being too slow, it still shows that all devices produced similar results.

As confirmed by the data obtained, the Modified Philip-Dunne infiltrometer accurately predicts the hydraulic conductivity of native soil and engineered media, comparing well with the KSAT laboratory method. In general, the Modified Philip-Dunne infiltrometer is able to predict the hydraulic conductivity within one order of magnitude, with exceptions likely coming from heterogeneity of soils. The placement of the test and sample (if it was slightly different from the

placement of the test) could have caused a difference in hydraulic conductivity, especially in native soils with increase heterogeneity. Human error in soil sampling could have caused increased porosity or compaction. Changing these two soil properties would result in a different hydraulic conductivity than what would be found in-situ. Another factor creating differences in hydraulic conductivity could have been the different assumptions within the hydraulic conductivity determination for each infiltrometer. It is also important to note that the UMS KSAT sample is a single-point test. The hydraulic conductivity determined from this test only considers the 250 cm^3 of soil tested. Water infiltration from the Modified Philip-Dunne infiltrometer could have an area of influence greater than 250 cm^3 depending on the type of soil. Especially in the case of native soils with higher heterogeneity, the hydraulic conductivity at a Modified Philip-Dunne infiltrometer could be affected by the soil around the test area. The UMS KSAT hydraulic conductivity value would not be able to consider in-situ heterogeneity which is not present within the soil sample.

The Modified Philip-Dunne infiltrometer data compared well with the double-ring infiltrometer and single-ring infiltrometer as well, producing hydraulic conductivity values within the same order of magnitude as the ring infiltrometers. This validates the use of the Modified Philip-Dunne infiltrometer as a means of infiltration testing. The Modified Philip-Dunne infiltrometer, like the single-ring infiltrometer, requires less water and is easier to install than the double-ring infiltrometer. As a result, more Modified Philip-Dunne tests can be performed in the same amount of time. This suggests that the Modified Philip-Dunne infiltrometer can be used instead of the double-ring infiltrometer which is recommended by the PADEP (2006). Different testing methods yield varied results due to different assumptions and equations. As electronic components become cheaper and better, they will likely be used more often in infiltration testing

methods because they can provide more accurate measurements and create easier field scenarios for engineers.

The hydraulic conductivity data were plotted with the plasticity indices to determine if a relationship exists between plasticity and hydraulic conductivity. The hydraulic conductivity from the KSAT generally decreases with increasing plasticity with the exception of TP 10 as confirmed by Figure 7.3. This could be due to TP 10 have a higher dry unit weight than TP 7, which also affects hydraulic conductivity. Additionally, the plasticity index difference is only 0.61 and the Atterberg limits testing could have a human error that resulted in a small difference in plasticity index when one really did not exist. Furthermore, TP 7 and TP 10 had hydraulic conductivities in the same order of magnitude, which is also often considered close enough that the difference between the two values is negligible. TP 14 and TP 5 had the highest plasticity indices with values of 8.28 and 7.35, respectively. These two samples also had the lowest hydraulic conductivity values, which were below the detection limit of the KSAT. The hydraulic conductivity used for these samples to plot on Figure 7.3 was the KSAT detection limit, which was 1.2×10^{-6} cm/s. This was done to visualize the relationship and compare the data to from these samples to the other fine-grained samples. The two samples with the highest plasticity indices had the lowest hydraulic conductivity produced by the KSAT and the sample with the lowest plasticity index had the highest hydraulic conductivity, showing the relationship between these soil parameters.
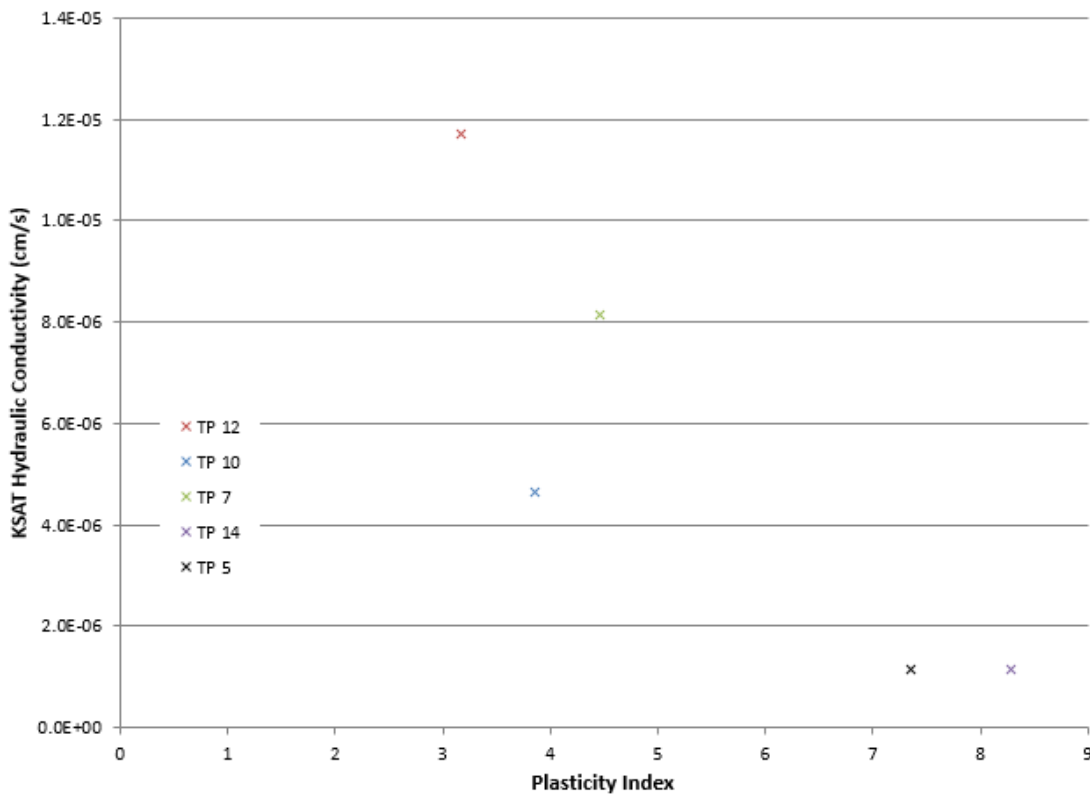
Figure 7.3 Plasticity index and KSAT hydraulic conductivity data from the Upper Moreland site

The hydraulic conductivity data from the KSAT were plotted with the dry unit weight data in Figure 7.4 to determine if a relationship exists between those soil parameters. There is an apparent relationship between these two soil parameters, with the three samples with the lowest dry unit weights have the highest hydraulic conductivities; however, these data do not create a trend. This could be due to very small differences in dry unit weight that could have been due to laboratory or human error. TP 10 had a dry unit weight smaller than TP 12 by only 0.04 g/cm^3 and larger than TP 7 by only 0.02 g/cm^3. This is difference is almost negligible. Furthermore, TP 7 and TP 10 had hydraulic conductivities in the same order of magnitude, which is also often considered close enough that the difference between the two values is negligible. TP 14 and TP 5 had the highest dry unit weights with values of 1.74 g/cm^3 and 1.80 g/cm^3, respectively. These two samples also had the lowest hydraulic conductivity values, which were below the detection

limit of the KSAT. The hydraulic conductivity used for these samples to plot on Figure 7.4 was the KSAT detection limit, which was 1.2×10^{-6} cm/s. This was done to visualize the relationship and compare the data to from these samples to the other fine-grained samples. Since these values that had relatively higher dry unit weights had relatively lower hydraulic conductivity, a relationship between these two soil parameters is validated.
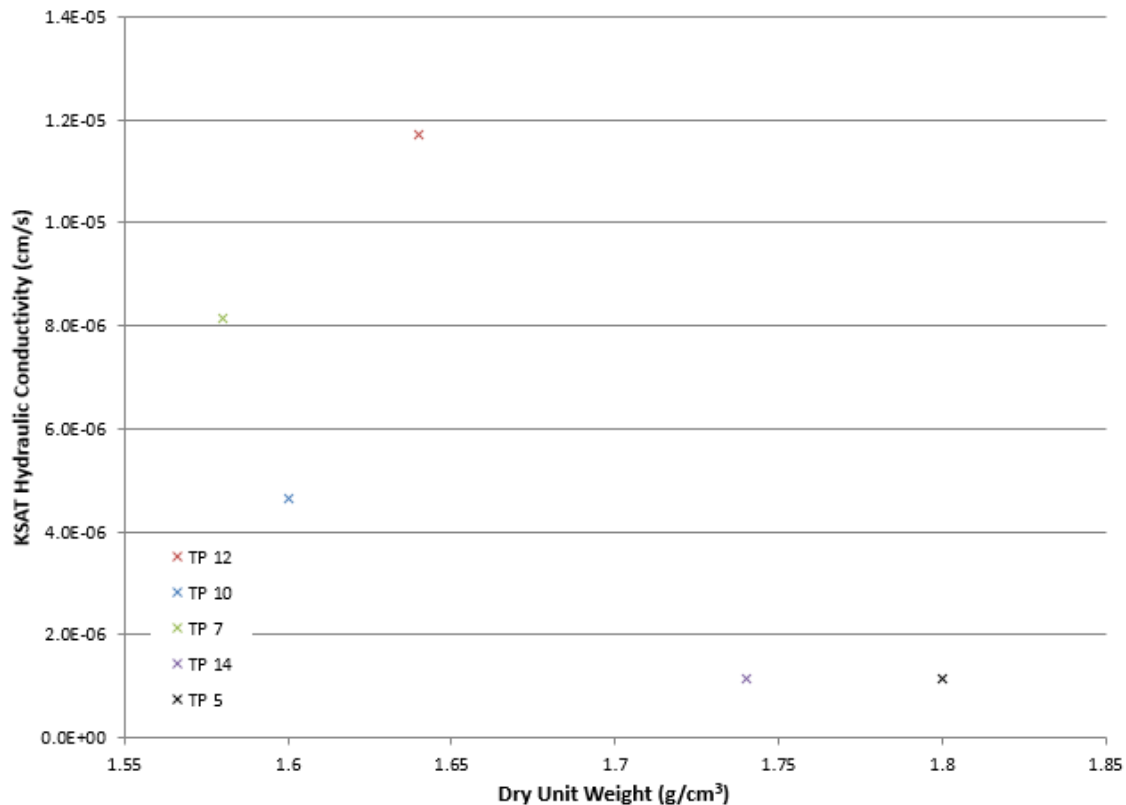
Figure 7.4 Dry unit weight and KSAT hydraulic conductivity data from the Upper Moreland site

Due to heterogeneity of site soils, especially native soils, it is necessary to conduct a proper site investigation prior to designing and SCM and after the construction of an SCM to measure performance. The soils data validates the need to classify soils by the USCS method and USDA method, as there is an observed relationship between hydraulic conductivity and plasticity. Since SCM surficial soils do change over time, as observed at the BTI, it is necessary to re-evaluate

and re-test soils in the laboratory when conducting infiltration testing, even if they have been done in the past. Additionally, it is necessary to determine in-situ density as this will also affect infiltration at an SCM or in native soils beneath an SCM.

CHAPTER 8.   SITE DATA DISCUSSION AND RECOMMENDATIONS

8.1 Fedigan Rain Gardens

During the typical Villanova storms and the larger storms, the data collected indicate that the FRGI and the FRGR are performing well. Data showed that the rain gardens were able to infiltrate water during rain events and quickly after rain events, with no storms showing ponding periods lasting longer than 72 hours. During a dry period, the FRGI was able to completely capture the runoff from a typical Villanova storm of around 2.54 cm (Philadelphia Water Department 2009) within the soil storage. This was validated by observing no change in soil volumetric water content below the native soil interface. During larger events, neither the FRGI nor the FRGR indicated overflow or ponding periods lasting longer than 72 hours. From the storm data collected, both rain gardens are able to quickly infiltrate water during and after storm events. While the retained water content is higher than expected, this could be due to heterogeneity of the soil and the placement of the soil moisture sensors. Infiltration tests also validated that the systems have adequate hydraulic conductivity. Observing all of the storm data and infiltration testing data, it is confirmed that the FRGI and the FRGR are performing well.

Both rain gardens are able to sustain native vegetation, and soil cores at the native soil interface at the FRGI validated that substantial compaction was not present. The FRGI was able to sustain native vegetation with the liner retaining water. Therefore, water retention was high enough in the engineered media. Sieve analyses confirmed that the engineered media follows the design and the PADEP BMP Manual (2006) recommendations for soil media composition. The impervious drainage area-to-infiltration area and total drainage area-to-infiltration area also follow the PADEP BMP Manual (2006) recommendations. However, the FRGI media depth is

below the recommended value of 0.45 m and both rain gardens have larger potential ponding depths than the recommended 0.15 m. However, ponding in all four events analyzed did not reach a maximum value of 0.15 during this period. This could be due to the lower loading ratios and high sand content allowing the water to infiltrate more quickly. Though water retention was high, the sand content was also high. This could be due to the slight heterogeneity of soil and the placement of the soil moisture sensor which was recording the volumetric water content. However, based on the data collected, it appears that the PADEP (2006) recommendations for engineered media depth and ponding depth can be adjusted or left to the judgment of the engineer. The shallower media depths at the FRG do not hinder performance because of the smaller drainage area ratio. The added ponding depth does not appear to have compacted the surficial. Lower media depths and higher potential ponding levels are acceptable based on the type of engineered media and the amount of stormwater runoff that the site will receive during a typical storm.

Furthermore, as mentioned previously in this study, it is confirmed that the underdrain and liner are not necessary to control storm events in Pennsylvania. The typical Villanova storm and even the larger storms (closer to the 2-year design storm of around 8.31 cm, according to PADEP (2006)) did not produce overflow at either the FRGI or the FRGR. Furthermore, the FRGI was able to sustain native vegetation without the liner retaining water. The FRGR produced treated outflow through the underdrain which the FRGI indicated could have been either retained in the rain garden or infiltrated through the native soil interface or been evapotranspirated. This indication is made by comparing the two systems during each storm event and determining that the FRGI did not produce overflow. The soil moisture sensor at the liner indicated volumetric water contents at saturation or near saturation, indicating that the system retained water that was

not necessary. Water moved quickly to reach the liner; however, in some instances, the soil was already saturated at liner. With a low loading ratio and a higher coarse-grained engineered media, the liner and underdrain are not necessary at the FRGR.

The major recommendation from the FRG is that the underdrain and liner are not necessary in Pennsylvania given the typical storms that occur throughout the year. The water movement through the system is fast enough that overflow does not occur. It is recognized that underdrains and liners may be necessary in some specific situations such as karst areas, near slopes or mines, or areas impacted by environmental contamination. However, these should be considered separate research topics since these scenarios did not exist at any of the rain gardens compared in this study. Additionally, the engineered media at the FRG should be considered for rain gardens in Pennsylvania because it had adequate organics and fine-grained material to support vegetation, and the sand component was able to infiltrate water quickly. With this engineered media, a shallower media depth and a higher maximum ponding depth can be recommended. It is important to note that the loading ratio at FRG is very low compared to most retrofit rain gardens. Therefore, while this lower loading ratio did improve performance, it is difficult to consider the impervious drainage area-to-infiltration area at FRG as a practical recommendation. Since the engineered media has a higher coarse-grained component, it is also possible it could receive more stormwater runoff. This is verified by the storage volume calculations, since the FRGI had additional storage volume after the 09/10/2015 event. The slopes of the FRG, which follow the PADEP (2006) recommendations, are also considered reasonable as they do not appear to inhibit rain garden performance.

8.2 Pavilion Traffic Island

The PTI was able to infiltrate water quickly during storm events because of the very sandy engineered media. However, the perched water table hindered performance in almost all four of the analyzed storms. During a dry period, the PTI had ample soil storage for the stormwater runoff volume of a typical Villanova storm. However, all other storms had ponding periods lasting longer than 72 hours due to the inability to infiltrate water past the compacted native soil layer. The soil media containing little organic content and little fine-grained material, combined with the perched water table, did not allow for the planted vegetation to survive. Thus, wetland vegetation became more prevalent at the PTI. Despite the perched water table, the high maximum ponding depth allowed the system to avoid overflow for all four storm events. Within a 72 hour period, we would not expect any events occurring that would overflow the system.

The PTI performed well during the 09/10/2015 event; however, longer ponding periods were present after the other three events. This is because the 09/10/2015 event occurred during a dry period and the perched water table had fallen to the lowest point recorded in the PTI. If the native soil interface was not compacted, the sandier soil at the PTI was able to move water faster through the system, thus giving it the ability to take more runoff volume from impervious area. However, the perched water table prevents the system from infiltrating water quickly enough. The larger ponding depth, although outside of PADEP BMP Manual (2006) recommendations, is useful at the PTI because the larger head from ponding helps move water through the system more quickly. Therefore, while many aspects of the PTI design seem appropriate, the compacted native soil interface prevents it from performing well.

While some design parameters from the PTI can be recommended, it is difficult to measure performance of individual components because the perched water table inhibits water from

moving well through the system. The main recommendation from storm studies at the PTI is that the native soil interface of a rain garden must not be compacted during construction. Fixing the native soil interface compaction at the PTI can increase performance. Measures should be taken to ensure that the native soil interface experiences no traffic. The native soil should be tilled before the placement of the engineered media, and the placement of the engineered media should also occur in small amounts initially. If the engineered media is placed onto the native soil first, compaction could occur from the weight of the placed media. A loading ratio higher than that specified by the PADEP (2006) may be acceptable with an engineered media containing a high amount of sand, since it would be able to infiltrate water faster. However, the engineered media should contain some organic and fine-grained material to support vegetation and allow for pollutant removal. The combination of a lack of this type of soil in the engineered media and the perched water table likely created the scenario where the wetland vegetation grew at the PTI. Therefore, it is recommended that the engineered media of a rain garden contain higher organic material and fine-grained material than the engineered media at the PTI. The media depth and slopes at the PTI are acceptable

The ponding depth at the PTI is much larger than the PADEP (2006) recommendation of 0.15 m. The larger ponding depth was not the reason why ponding persisted after 72 hours; therefore, higher ponding depths than specified by the PADEP (2006) can be considered in rain garden design. Despite the compacted native soil interface, no water was left in the pond before the start of any of the storms recorded. In fact, the higher ponding depth may even help infiltrate water through the PTI faster because it increases the head. The higher ponding depth did not appear to significantly compact the engineered media from visual observations and soil moisture sensor measurements. Higher ponding depths can allow the rain garden to receive more runoff volume

and help push water through the system. To verify these recommendations, future research at the PTI could include fixing the compaction issue and collecting storm data. After this, the PTI performance can be compared before and after the compaction issue was remediated.

8.3 Bioinfiltration Traffic Island

The BTI was constructed in 2001, which was well before the PADEP (2006) recommendations were put in place. The BTI performed well during all four storm events with no ponding evident after 72 hours. Despite its age and the highest loading ratio of all of the rain gardens analyzed, the BTI is able to handle both the typical Villanova storm events and larger storm events. The organic layer that has built up at the BTI over time does seem to affect single-point infiltration tests, but not the performance of the BTI as a whole. The special variability of the infiltration at the BTI can be linked to this organic layer, since it varies in depth across the BTI and the soil mix is likely more homogenous than the organic silt loam layer. The organic layer may limit infiltration slightly during rain events, as shown with the periods of increased ponding followed by immediate infiltration. This can be water backing up at the organic layer, then being pushed through. The larger ponding depths can increase head, which can help push water through the hydraulically limiting organic layer. The BTI infiltrates water quickly during and after storm events, which is somewhat surprising considering the higher fine-grained content than the other rain gardens. Although infiltration through the system is not as fast as the other systems, this should be expected since the other systems use a high coarse-grained engineered media. During a dry period, the BTI had ample soil storage for the entire runoff volume of a typical Villanova storm. The fine-grained soils at the BTI do not reduce performance during storm events. The fine-grained material and organic content also helps the native vegetation, which is growing so well that it does not need to be re-planted every season. Instead, it is cut away in the late

fall/early winter season and grows back in the spring. The roots of the system are better sustained in fine-grained material and in soil media with deeper depths. The presence of roots improves ET and increases macroporosity, both of which help water move through the system faster.

The organic layer and soil mix at the BTI do not follow PADEP (2006) recommendations; however, this is not inhibiting performance. This organic layer has built up since construction. Significant compaction of the organic layer or soil mix was not found during site investigations; however, the depth of the organic silt loam layer did vary throughout the system. The organic silt loam layer especially has a higher organic content and fine-grained material content. The maximum ponding depth is also higher than that recommended by the PADEP (2006). However, this is not an issue because water does not remain ponded after 72 hours. Additionally, as stated in the case of the PTI, the larger ponding depth may allow for a larger head which can push the water through the system faster. With the higher ponding depth, the higher loading ratio than recommended by the PADEP (2006) can be implemented. Overflow occurred for the two larger events (09/29/2015 and 10/28/2015). The overflow occurring did not seem significant, especially during the 10/28/2015 storm. This is outside of the PADEP (2006) requirements since overflow occurred in a storm providing less runoff than the 2-year, 24-hour storm. However, this retrofit rain garden design was found to have ample soil storage for the typical Villanova storm of less than or equal to around 2.54 cm (Philadelphia Water Department 2009).

The age of the BTI does not impact its performance, so the main recommendation at the BTI is that mulching does not need to be done after the rain garden is constructed and the soil does not need to be restored up to at least 15 years after construction of the rain garden, assuming that the rain garden is designed and constructed appropriately. The organic layer that has built up does not cause performance issues of the BTI as an entire system; however, it can impact spot

infiltration tests. Therefore, its removal is not necessary for the BTI to continue to behave normally. If clogging occurs in the future, the organic layer may be reduced or removed. It is also recommended that the soil mix comprising higher fine-grained material may be considered in rain garden design. This can save money by requiring less imported media. Since some native soils contain a high coarse-grained content, native soils should be considered if infiltration testing and soil laboratory testing deems hydrologic properties feasible. This concept should be considered for future research, since it could save construction costs for rain gardens and other green infrastructure. The 3:1 horizontal-to-vertical slopes at the BTI, as well as the other rain gardens, seems appropriate based on visual appearance and data collected from this study. Finally, the higher loading ratio is acceptable if the hydrologic properties of the soil can infiltrate water quickly and if the maximum ponding depth is higher than the PADEP (2006) recommendations. If the soils at the rain garden can infiltrate water quickly and after a rain event, and the rain garden system can hold more water, a higher loading ratio should be considered acceptable in design.

8.4 Overall Comparisons and Recommendations

From all of the data collected in this study, as well as the site observations, recommendations can be made for rain garden design. For field investigations, it was found that the single-ring and Modified Philip-Dunne infiltrometer can be used in place of the double-ring infiltrometer. These methods are simple, inexpensive, require less water, and can be conducted faster than the double-ring infiltrometer. Therefore, more of these tests can be conducted, so more of the area can be analyzed. These infiltrometers provide similar results as the double-ring infiltrometer, particularly at SCMs. Based on the UMS KSAT data, the PADEP (2006) recommendation of laboratory techniques should be considered reasonable. The UMS KSAT data did provide results

outside of the order of magnitude of other methods, and this is likely because it is only a point measurement and not the result of infiltration for the entire area. Additionally, it is recommended that soils be classified based on USCS and USDA methods. This is because soil grain size and Atterberg limits can affect infiltration. Although limited to only five samples, the data provided in this study indicates that plasticity does have an effect on the hydraulic conductivity of a soil. Finally, the PADEP (2006) recommendation of conducting bulk density testing should be considered. This study shows that the dry bulk density does have an impact on the hydraulic conductivity of a soil, and this also directly affects rain garden performance.

During construction, it is recommended to ensure compaction of the native soil interface and placed engineered media is kept to a minimum. Data from the PTI confirm that a compacted native soil interface can cause the rain garden to not behave as designed. In the case of the PTI, it caused ponding to exist after 72 hours. PADEP (2006) guidelines should be followed closely to ensure the native soil interface is not compacted. Data from this study confirms that rain gardens without a compacted native interface, such as present at the FRGI and BTI, perform well. The BTI and FRGI, which contain native soil interfaces that are not compacted, were able to infiltrate water well.

Comparing the vegetation at each site, it was found that the native vegetation was best sustained at the BTI. This is because of the higher fine-grained material present in the soil mix. The native vegetation is cut and removed during the winter grows back well in the spring. This shows that native vegetation performs well in rain gardens with a higher fine-grained content and requires little maintenance. The native vegetation originally planted at the PTI was not able to tolerate the conditions of the rain garden. This is due to the perched water table; however, the higher sand content in the engineered media may have also played a role. Instead, wetland vegetation has

sustained at the PTI. The vegetation at the FRGI and FRGR was able to tolerate the conditions for most of the year. During some dry periods, vegetation did struggle at these rain gardens. This is likely due to the higher sand content not able to retain water as was the case at the BTI.

For this study, it is of interest to compare the four rain gardens based on the conditions at the bottom of each rain garden. As stated, the FRGI and BTI infiltrate water into native soil much better than the PTI due to native interface compaction at the PTI. The three rain gardens that have native interfaces do not overflow during the typical Villanova storms. Additionally, the FRGI, FRGR, and PTI did not overflow during the typical Villanova storm or larger storm. As previously stated, the vegetation was sustained at the FRGI without the use of a liner to increase water retention. With this knowledge and since overflow did not occur at the FRGR or FRGI during any of the four storm events, the liner and underdrain system is not necessary for rain gardens Pennsylvania which are not in risk areas such as karst topography, in close proximity to mines, or at the toe of a slope. The FRGR created treated outflow during all four storm events and did not act to promote rain garden performance above that seen at the FRGI.

Comparing all four soil media types, it was found that the PTI was able to infiltrate water the fastest during storm events. The FRGI and FRGR also quickly infiltrated water during storm events, and the infiltration tests indicate that the engineered media has sufficient hydraulic conductivity. The soil at the BTI also quickly infiltrated water during storm events, which could be due to macroporosity created overtime due to the root systems within the rain garden. For this reason, it was determined that native soils or soils containing more fine-grained material should be used in rain gardens. If these soils have sufficient hydraulic conductivity values, using native soils or soils with a higher fine-grained content can save on cost without drastically inhibiting rain garden performance. Additionally, as stated previously, this type of soil can promote the

growth and sustainability of native vegetation, which can save on maintenance costs. Keeping maintenance within the rain garden to a minimum can help mitigate the potential surficial soil compaction as well. As validated by the BTI, older rain gardens can behave normally without vigorous maintenance. The organic layer present does not inhibit performance of the whole system during or after rain events. Native vegetation growth can also promote the growth of macropores due to root growth, which can promote rain garden performance.

The rain gardens in this study have different soil types, soil media depths, ponding depths, and loading ratios. The performance of the rain gardens is effect by all of the components acting together in the system. Based on information and data gathered in this study, recommendations for rain garden design should not be component-specific. Instead, rain gardens should be designed as an entire system with all components being designed together. This study found that the mechanisms of a rain garden are effected by all of the components acting together as a whole rather than single design parameters. Engineers should consider rain gardens whole systems with the inter-workings effecting the entire performance of the system. For example, the impervious drainage area-to-infiltration area works together with the type of engineered media to effect rain garden performance. If the engineered media has a higher sand content that can infiltrate water quickly, a higher loading ratio can be used, as witnessed at the BTI. Another example is the effect of the media depth necessary based on the loading ratio. If the loading ratio is small, a shallow engineered media depth may not hinder performance. Finally, if the engineered media depth has a high sand content which can infiltrate water quickly, higher ponding depths can be used. Using all of this information, it is recommended that rain gardens be designed as whole systems without major recommendations on each of these components (loading ratios, engineered media type, engineered media depth, ponding depth). Since all of these components

effect one another and all work together to effect rain garden performance, all of the design considerations should be made with the other design components in mind. This can promote the design and construction of cost-effective, robust rain gardens. Future research into the design components of rain gardens can include analyzing erosion at rain gardens based on slopes.

The guidelines for which recommendations were made apply mainly to the PADEP BMP Manual (2006). However, the recommendations made from this study also apply to the Chesapeake Bay Total Maximum Daily Loading (TMDL) (2010), the Municipal Separate Storm Sewer System (MS4) TMDL (2013), the Environmental Protection Agency (EPA) National Management Measure for Nonpoint Source Pollution (2006). From the storm data collected, additional hydrologic modeling of the rain gardens was not deemed necessary. The larger storms are close to the PADEP design storms (2-year, 24-hour storms), and during the time of data collection, no larger storms were collected. Since instrumentation at the FRG and the PTI was not working or non-existent at the start of the study, much of the study consisted of designing, calibrating and installing this equipment. Future research could include continued data collection to collect data from even larger storms or hydrologic modeling of the FRGI, the FRGR, the PTI, and the BTI.

CHAPTER 9.   SUMMARY

9.1 Conclusions

This study compared rain garden designs to the recommendations set forth in the Pennsylvania Department of Environmental Protection (PADEP) BMP Design Manual, which was published in 2006, using collected storm data for four storms. The PADEP (2006) guidelines are typical in most state regulations in the United States. This study was needed to update the PADEP (2006) recommendations since the knowledge of rain gardens and green infrastructure has grown greatly since its publication. The goal of this study was to use data collected to create recommendations for rain garden design in Pennsylvania or areas similar with a similar climate and regulatory requirements. The Fedigan Rain Gardens (FRG), Pavilion Traffic Island (PTI), and Bioinfiltration Traffic Island (BTI) were chosen for this study because they vary in design, loading ratios, and age. The Fedigan Rain Gardens were selected because they are identical except that one contains a liner and underdrain and the other does not. The rain garden with the liner and underdrain is called the Bioretention Fedigan Rain Garden (FRGR), and the rain garden with the native soil interface is called the Bioinfiltration Fedigan Rain Garden (FRGI). The Pavilion Traffic Island was chosen because it contains sandier engineered media and it has a perched water table due to a compacted native soil layer. The Bioinfiltration Traffic Island was chosen because it is the oldest rain garden on Villanova University's campus, has the highest loading ratio, and contains a 1:1 native soil-sand mix. Sites were instrumented with proper water quantity measuring devices. Each site was investigated and soils were tested in the laboratory and infiltration testing was conducted to verify post-construction performance. Four storms were selected in the study: two of which were close to the typical storm which occurs at Villanova and

the other two being larger storms which are closer to the PADEP (2006) design storm (2-year, 24-hour storm).

Additionally, infiltration testing recommendations set forth by the PADEP (2006) were evaluated by conducting different testing methodologies and comparing the results. The purpose was to determine if other methods other than the double-ring infiltrometer can be used to accurately measure in-situ hydraulic conductivity. Although the double-ring infiltrometer is generally recommended it has several drawbacks: it requires large volume of water, a great deal of energy to install, and takes longer to conduct than other infiltration tests. A simple, inexpensive single ring infiltrometer was used at the Bioinfiltration Traffic Island and the results were compared to the storm-measured recession rate of the rain garden. The recession rate is considered the most accurate form of hydraulic conductivity measurement at the rain garden because the infiltration rate of the entire rain garden is measured. A comparison of the methods revealed that the single-ring infiltrometer accurately predicts the hydraulic conductivity of soil within a rain garden. The results indicate that the depth of a silt loam organic layer present at the Bioinfiltration Traffic Island does have an effect on the infiltration at single spot locations. In addition to this, a Modified Philip-Dunne infiltrometer built at Villanova University was compared to the other test methods to determine if the method can be used to accurately measure hydraulic conductivity. Soil laboratory tests were also conducted to determine if correlations exist between Atterberg limits and hydraulic conductivity, as well as dry unit weight and hydraulic conductivity.

The study found that all rain gardens were performing as designed except the Pavilion Traffic Island, which was not infiltrating water into the native soil layer at the projected rate because the interface was compacted. The PTI was the only rain garden which had ponding periods lasting longer than 72 hours; however, had ample soil storage to store a typical Villanova storm during a

dry period. It was found that the sandy soils in the bowl could infiltrate water quickly; however, the perched water table was limiting deeper infiltration. The Bioinfiltration Traffic Island, with its larger loading ration, was found to be performing well 15 years after construction. During the site investigation, a silt loam organic layer was found to have built up at the surface of the rain garden. Despite this, the Bioinfiltration Traffic Island was able to infiltrate water well during and after rain events. From the data collected at the Fedigan Rain Gardens, it was determined that a liner and underdrain are not necessary. For all four storm events analyzed, overflow did not occur at either rain garden. The engineered media and native soils were able to infiltrate water quickly enough that ponding was not an issue at the site, and the typical Villanova storm was able to be completely stored within the engineered media during a dry period.

Based on the collected data, recommendations were made to the PADEP (2006) guidelines:

- Emphasis should be placed on avoiding compaction of the native soil interface. PADEP (2006) guidelines should be followed to ensure compaction and disturbance of soils is kept to a minimum. When comparing the sites with native soils, it was found that the FRGI and the BTI did not have ponding periods lasting longer than 72 hours. This is because the interface layer in these two rain gardens is not compacted. Fixing the native soil interface at the PTI can increase performance of the rain garden.

- Native soils or soils with a higher proportion of fine-grained soil better promotes native vegetation, which increases rain garden performance. The native vegetation was most sustainable at the BTI than the other sites. This is because of the finer grained material content in the soil mix. The fine-grained soil has higher water retention, which promotes growth of native vegetation. The media depth was deeper than at the FRGI and FRGR, which promotes the growth or roots. This increases ET and can encourage the creation of

macroporosity, which increases infiltration. The vegetation at the BTI requires less maintenance than at the FRGI and FRGR, which can be because of the higher sand content present in the media at the FRG. The vegetation at the FRGR was not significantly more sustainable than at the FRGI. The vegetation at the PTI was not the originally planted native vegetation. Wetland vegetation is persistent at the PTI because of the perched water table and high sand content.

- The FRGI and BTI are better at infiltrating water into the native soil than the PTI due to the compaction of the native interface at the PTI. Overflow did not occur at any of the rain gardens during the typical Villanova storm of around 2.54 cm (PADEP 2006). The BTI did overflow during the two larger events (storms greater than the typical Villanova storm of 2.54 cm); however, this overflow was not significant. Since overflow did not occur during any of the storm events and the vegetation at the FRGI grew well without higher water retention, the liner and underdrain were deemed not necessary. The engineered media at the PTI was able to infiltrate water the fastest due to the higher sand content. The FRGI and FRGR also quickly infiltrated water due to a high sand content in the engineered media at the rain gardens. The soil at the BTI did not hinder rain garden performance despite having a higher fine-grained content. Water was able to infiltrate during storm events, and the soil storage was large enough to capture the runoff volume of a typical Villanova storm. The fine-grained material at the BTI better promotes vegetation roots which can create macroporosity, increasing infiltration. Since the BTI was able to perform well during the four storm events recorded, it is recommended to use native soils or soils with higher fine-grained soils to save on construction costs and promote vegetation growth. These soils can be evaluated using the infiltration tests and

the soil tests described in this study to determine if native soils or soils with high fine-grained content are suitable to act as rain garden media.

- If designed and constructed appropriately, soil restoration and maintenance at a raid garden can be kept to a minimum. The BTI does have an organic layer that has built up over time. During infiltration tests, it was determined that this layer does effect spot hydraulic conductivity values. However, it does not affect the overall performance of the BTI. This can reduce costs and minimize rain garden disturbance or compaction, which effect rain garden performance. Using soils with a higher fine-grained content does not inhibit performance and reduces vegetation maintenance, as seen at the BTI. Therefore, these soils are recommended if deemed suitable.

- Rain gardens should be designed with all of the components in mind as these SCMs operate as a system. Overall the rain garden performance was found to be based on how the system behaves, not on single design components. It was found that the design parameters of rain gardens affect one another. For example, a larger loading ratio can be used if soils are sandier and can infiltrate water faster. Also, if the loading ratio is smaller, shallower engineered media depths can be used. Tailoring the design of the components to the contributing drainage area and treating the rain garden as a whole system rather than a single component can save construction costs and create more sustainable rain gardens.

- For smaller communities such as residential areas, simple rain gardens with standard designs may be appropriate. Rain gardens with smaller media depths without underdrains, such as FRGI, may be used because of the smaller impervious drainage area-to-infiltration area loading ratios.

- For higher impervious drainage area-to-infiltration area loading ratios, a more engineered or intensive approach may be necessary. In these areas, the space used for rain gardens is usually reduced and a retrofit design is necessary. For these rain gardens, an increased media depth could improve rain garden performance.

- Rain gardens can continue to perform even with components not behaving as designed. The PTI was able to store all of the runoff volume in the soil for a typical Villanova storm during a dry period even with the perched water table. The BTI also performed well despite the buildup of an organic layer. These two rain garden were able to overcome these potentially limiting factors, suggesting that rain gardens are robust systems.

From the infiltration testing data, the following recommendations were made:

- Simpler techniques such as the single-ring infiltrometer and Modified Philip-Dunne infiltrometer should be used to determine in-situ infiltration rates. These devices can be used with the same level of certainty as the current PADEP (2006) recommendation of the double-ring infiltrometer and are much easier to perform. Since the other test methods provide accurate predictions of hydraulic conductivity, require less water, are easier to install, and are much faster than the double-ring infiltrometer, more of these tests can be performed. For this reason, using the single-ring infiltrometer or Modified Philip-Dunne infiltrometer allows more of the rain garden to be tested, providing a more accurate result of the hydraulic conductivity. Multiple tests are needed because of heterogeneity and variation present, especially in native soils.

- Site soils should be classified using both the Unified Soil Classification System and United States Department of Agriculture classification system. This study confirmed that

soil type and Atterberg limits effect hydraulic conductivity. Classifying soils using both techniques provides relevant Atterberg limits data and gradation data which can improve rain garden design.

- Bulk density testing should be performed to quantify the compaction of site soils. It has been validated in this study that dry unit weight effects hydraulic conductivity.

9.2 Future Work

Future rain garden studies could include performing hydrologic modeling of larger storms at the Bioinfiltration Fedigan Rain Garden (FRGI), the Bioretention Fedigan Rain Garden (FRGR), the Pavilion Traffic Island (PTI), and the Bioinfiltration Traffic Island (BTI). This could be done to analyze how the rain gardens behave in these scenarios and to create additional recommendations for rain garden design and construction. Furthermore, the sites should remain instrumented to continue to analyze storm events. To further understand the behavior of the FRG, additional soil moisture sensors can be placed in the engineered media and the inlet boxes can be instrumented to measure inflow. Future research at the PTI can include remediating the native soil interface to allow for faster infiltration through this soil layer. This can allow for better analyses of the PTI including how the sandier engineered media compares to other soil types, which is difficult to do at this point because the perched water table is the limiting factor of the rain garden. This could also allow future researchers to determine if the sandier engineered media plays a major role in the limited vegetation at the site. Future research at the FRGR can include performing additional laboratory and field tests on the underdrain well cap with an orifice. This should be done to further verify the equation used to calculate flow through the orifice, as well as understand how the system behaves over time. The overflow risers can also be better equipped to calculate overflow, since the volumetric weirs can be inaccurate if water falls

over the weir or splashes over the weir at the outflow pipe. Finally, future rain garden research can include using native soils in rain gardens to determine if this cost-effective measure produces rain gardens that perform well using the recommendations provided in this study.

Future infiltration testing research could include performing many infiltration tests at a rain garden to determine the spatial variability of the engineered media. This can also be done at the BTI to perform a more in-depth analysis of spatial variability of the organic silt loam layer. Performing this type of research can help researchers better understand the heterogeneity of engineered media and further investigate the effect of organic material on hydraulic conductivity. Future research could also include using statistical analyses to determine how many infiltration tests are required per square area of a rain garden to accurately predict the hydraulic conductivity. This is important for field engineers to confirm post-construction performance of rain gardens in an appropriate amount of time. Future research could also include further comparisons of the Modified Philip-Dunne infiltrometer to other test methods. A larger scale comparison, or comparison of the testing method to the known recession rate of a rain garden such as the BTI, could further validate the use of the Modified Philip-Dunne infiltrometer in place of the double-ring infiltrometer. These studies could also include further calibration and optimization of the electronic components used on the Modified Philip-Dunne infiltrometer. The Modified Philip-Dunne infiltrometer can also be used with other field sensors, such as soil moisture sensors and tensiometers, to determine the soil matric potential and volumetric water content. These values can be used to create the SWCC, which can be used to determine the wilting point and other important parameters of rain garden soils. Future research can also investigate the influence of macroporosity and entrapped air on the effect of infiltration at a rain garden. These aspects of rain garden soil are difficult to measure, and their effect is difficult to

quantify. Finally, future research could include further comparison of hydraulic conductivity to Atterberg limits and dry unit weight. Since only five samples were used for this analysis in this study, a more in-depth comparison could find correlations between hydraulic conductivity and Atterberg limits, as well as hydraulic conductivity and dry unit weight.

REFERENCES

Ahmed, F., Gulliver, J.S, Nieber, J.L. (2014). "Determining infiltration loss of a grassed swale." *World Environmental and Water Resources Congress 2014: Water without Borders*, ASCE, Va., 8-14.

Ahmed, F., Gulliver, J.S, and Nieber, J.L. (2015). "Estimating swale performance in volume reduction." *Proceedings, World Environmental and Water Resources Congress 2015: Floods, Droughts, and Ecosystems*, ASCE, Va., 255-260.

Ahmed, F., Gulliver, and J.S, Nieber, J.L. (2015). "Field infiltration measurements in grassed swales." *Vadose Zone Journal*, 13(10), in press.

Ahmed, F., Gulliver, J.S, and Nieber, J.L. (2011). "Rapid infiltration measurement of LID best management practices." *Proceedings, World Environmental and Water Resources Congress 2011: Bearing Knowledge for Sustainability*, ASCE, Va., 4379-4388.

American Society for Testing and Materials (ASTM). (2009). "Standard test method for infiltration rate of soils in field using double-ring infiltrometer." *D3385-09*, West Conshohocken, Pa.

American Society for Testing and Materials (ASTM). (2010). "Standard test methods for laboratory determination of water (moisture) content of soil and rock by mass." *D2216-10*, West Conshohocken, Pa.

American Society for Testing and Materials (ASTM). (2010). "Standard test method for liquid limit, plastic limit, and plasticity index of soils" *D4318-10*, West Conshohocken, Pa.

American Society for Testing and Materials (ASTM). (2014). "Standard test methods for moisture, ash, and organic matter of peat and other organic soils." *D2974-14*, West Conshohocken, Pa.

American Society for Testing and Materials (ASTM). (2007). "Standard test method for particle-size analysis of soils." *D422-63(2007)e2*, West Conshohocken, Pa.

Asleson, B.C, Nestingen, R.S., Gulliver, J.S., Hozalski, J., Nieber, J.L. (2008). "Performance assessment of low impact stormwater practices." *Proceedings, World Environmental and Water Resources Congress 2008*, ASE, Va., 1-11.

Braga, A., Horst, M., and Traver, R. (2007). "Temperature effects on the infiltration rate through an infiltration basin BMP." *Journal of Irrigation and Drainage Engineering*, 133(6), 593-601.

Davis, A.P., Hunt, W.F., Traver, R.G., and Clar, M. (2009). "Bioretention technology: an overview of current practice and future needs." *Journal of Environmental Engineering*, 135(3), 109-117.

Emerson, C.H. (2008). "Evaluation of Infiltration Practices as a Means to Control Stormwater Runoff". Villanova University.

Emerson, C.H. and Traver, R.G. (2008). "Multiyear and seasonal variation of infiltration from storm-water best management practices." *Journal of Irrigation and Drainage Engineering*, 134(5), 598-605.

Emerson, C.H., Achey, B., Zukowski, Z., Welker, A. (2015). "Long-term performance and as-built infiltration testing of a vegetated SCM." *Proceedings, Pennslyvanai Stormwater Symposium*, Villanova Urban Stormwater Partnership, Villanova, PA.

Fernuik, N. and Huag, M. (1990). "Evaluation of in-situ permeability testing methods." *Journal of Geotechnical Engineer*, 190(2), 297-311.

Gilbert Jenkins, J.K., Wadzuk, B.M., and Welker, A.L. (2010). "Fines accumulation and distribution in a storm-water rain garden nine years post construction." *Journal of Irrigation and Drainage Engineering*, 136(12), 862-869.

Gulliver, J.S, Asleson, B.C., Nestingen, R.S., Nieber, J.L., and Hozalski, R.M. (2008). "Four levels of assessment for LID practices." *Proceedings, 2008 International Low Impact Development Conference*, ASCE, Va., 1-9.

Gulliver, J.S., Erickson, A.J., and Weiss, P.T. (2010). "Stormwater treatment: assessment and maintenance." University of Minnesota, St. Anthony Falls Laboratory. Minneapolis, MN. ⟨http://stormwaterbook.safl.umn.edu/⟩ (April 15, 2016)

Healy, R. W. and Ronan, A.D. (1996). *Documentation of computer program VS2DH for simulation of energy transport in variably saturated porous media-- modification of the U.S. Geological Survey's computer program VS2DT*. U. S. Geological Survey, Water-Resources Investigations Report 96-4230: 36.

Heasom, W., Traver, R.G., and Welker, A. (2006). "Hydrologic modeling of a bioinfiltration best management practice using HEC-HMS." *Journal of the American Water Resources Association*, 42(5), 1329-1347.

Hopmans, J.W. and Dane, J.H. (1985). "Effect of temperature-dependent hydraulic properties on soil water movement." *Soil Science of America Journal*, 49(1), 51-58.

Hopmans, J.W. and Dane, J.H. (1986). "Temperature dependence of soil hydraulic properties." *Soil Science of America Journal*, 50(1), 4-9.

Jennings, A.A., Berger, M.A., and Hale, J.D. (2015). "Hydraulic and hydrologic performance of residential rain gardens." *Journal of Environmental Engineering*, 141(11), 04015033.

Lee, R.S., Traver, R.G., Welker, A. L. (2013). "Continuous modeling of bioinfiltration stormwater control measures using Green and Ampt." *Journal of Irrigation and Drainage Engineering*, 139(12), 1004-1010.

Lee, R.S, Welker, A.L., Traver, R.G. (2015). "Modeling soil matrix hydraulic properties for variably-saturated hydrology analysis." *Journal of Sustainable Water in the Built Environment*, 2(2), 04015011.

Lord, L. (2013). "Evaluation of nitrogen removal and fate within a bioinfiltration stormwater control measure," thesis, presented to Villanova University at Villanova, PA, in partial fulfillment of the requirements for the degree of Master of Science.

Machusick, M., Welker, A., and Traver, R. (2011). "Groundwater mounding at a storm- water infiltration BMP." *Journal of Irrigation and Drainage Engineering*, 137(3), 154-160.

Munoz-Carpena, R., Regalado, C., Alvarez-Benedi, J., Bartoli, Francois (2002). "Field evaluation of the new Philip-Dunne permeameter for measuring saturated hydraulic conductivity." *Soil Science*, 167(1), 9-24.

Nemirovsky, E.M., Lee, R.S., and Welker, A.L. (2015). "Vertical and lateral extent of the influence of a rain garden on the water table." *Journal of Irrigation and Drainage Engineering*, 141(3), 04014053.

Pennsylvania Department of Environmental Protection. (2006). "Pennsylvania Stormwater Best Management Practices Manual." Bureau of Watershed Management. Document Number 363-0300-002.

Philadelphia Water Department (PWD). (2009). "Philadelphia combined sewer overflow long term control plan update, supplemental documentation, volume 5, precipitation analysis." PWD Office of Watershed, ⟨http://www.phillywatersheds.org/ltcpu/Vol05_Precip.pdf⟩ (August 8, 2015).

Philip, J.R. (1998). "Infiltration into crusted soils." *Water Resources Research*, 34(8), 1919-1927.

Prokop, P. (2003). "Determining the effectiveness of the Villanova bio-infiltration traffic island in infiltrating annual runoff," thesis, presented to Villanova University at Villanova, PA, in partial fulfillment of the requirements for the degree of Master of Science.

Richards, L.A. (1931). "Capillary conduction of liquids through porous mediums." *Journal of Applied Physics*, 1(5), 318-333.

Schlea, D., Martin, J.F., Ward, A.D., Brown, L.C., Suter, S.A. (2014). "Performance and water table responses of retrofit rain gardens." *Journal of Hydrologic Engineering*, 19(8), 05014002.

Stander, E., Borst, M., O'Connor, T., and Rowe, A. (2010) "The effects of rain garden size on hydrologic performance". *Proceedings, World Environmental and Water Resources Congress 2010*, ASCE, Va., 3018-3027.

Touloukian, Y.S., Saxena, S.C., Hestermans, P. (1975). "Viscosity thermophysical properties of matter." *TRPC Data Series*, Volume 11, Plenum, NY.

Weiler, M. (2005). "An infiltration model based on flow variability in macropores: development, sensitivity analysis and applications." *Journal of Hydrology*, 310(1-4), 294-315.

Yergeau, S.E. and Obropta, C.C. (2013). "Preliminary field evaluation of soil compaction in rain gardens." *Journal of Environmental Engineering*, 139(9), 1233-1236

Zukowski, Z., Emerson, C., Welker, A., Achey, B. (2016). "Evaluation of Field Hydraulic Conductivity Data: Comparing Spot Infiltrometer Test Data to Continuous Recession Data." *Proceedings*, *Geo-Chicago 2016: Sustainability, Energy and the Geoenvironment*, ASCE, Va.

APPENDIX

APPENDIX A: SOIL DATA
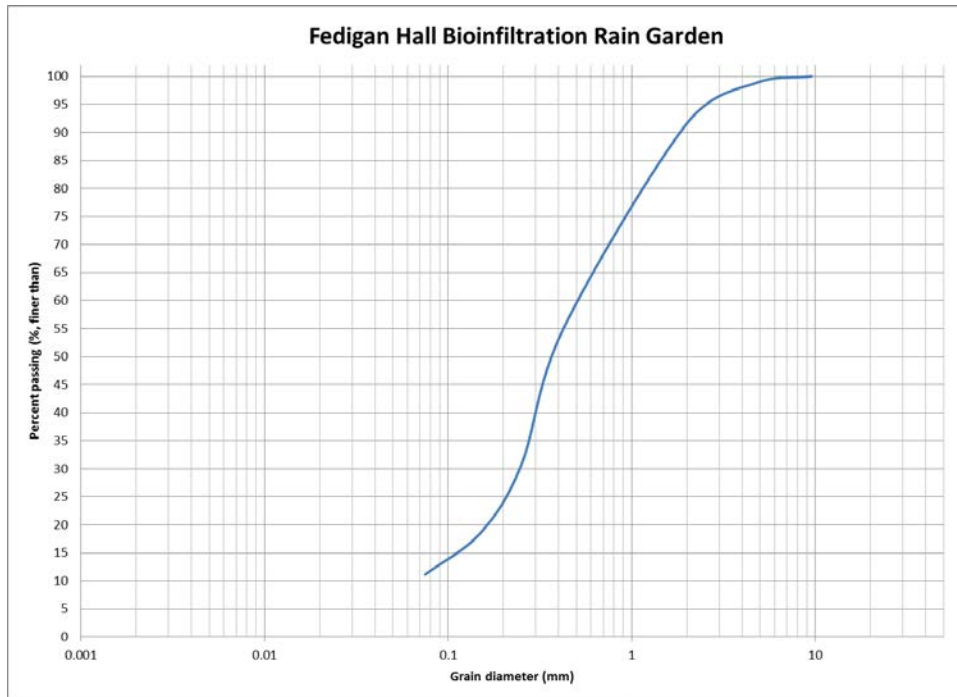
Figure A.1 FRGI grain size distribution
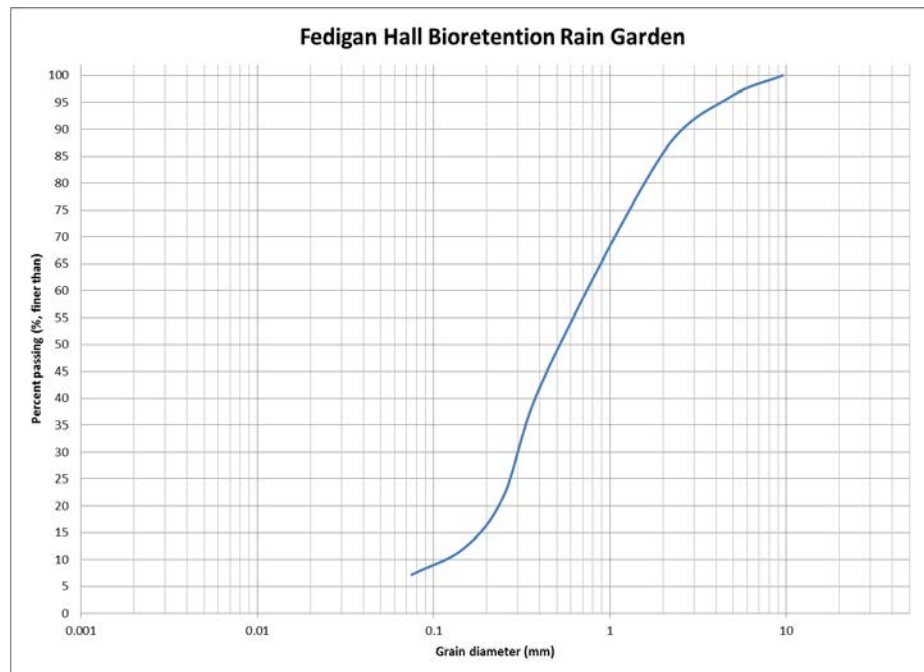
**Figure A.2** FRGR grain size distribution
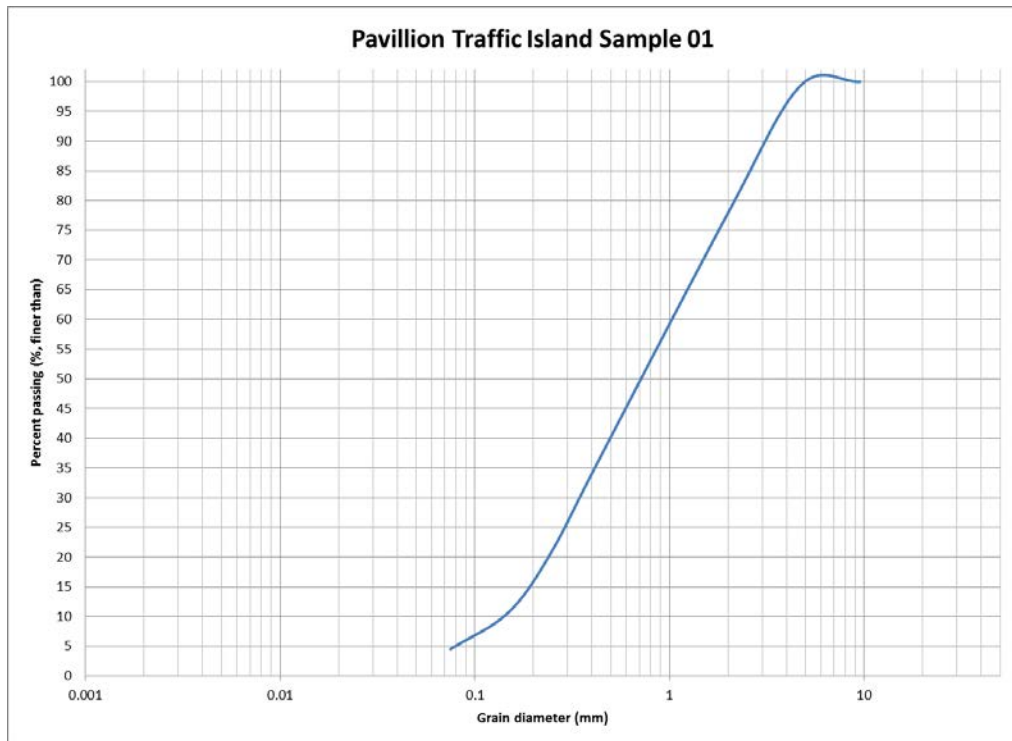
**Figure A.3** PTI sample 1 grain size distribution
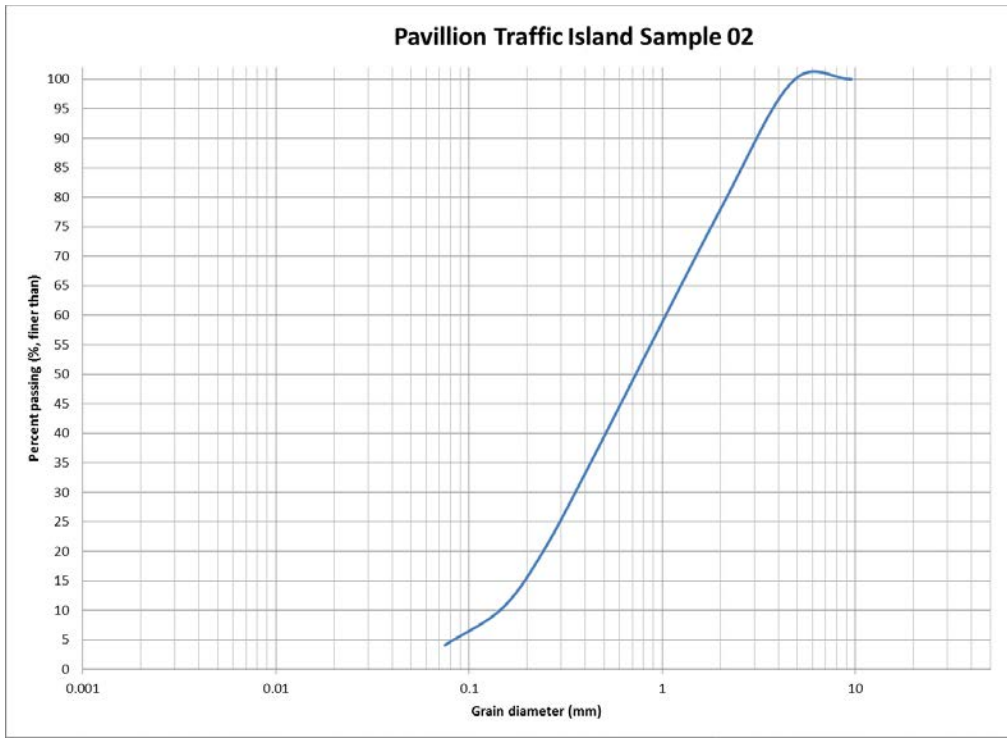
Figure A.4 PTI sample 2 grain size distribution
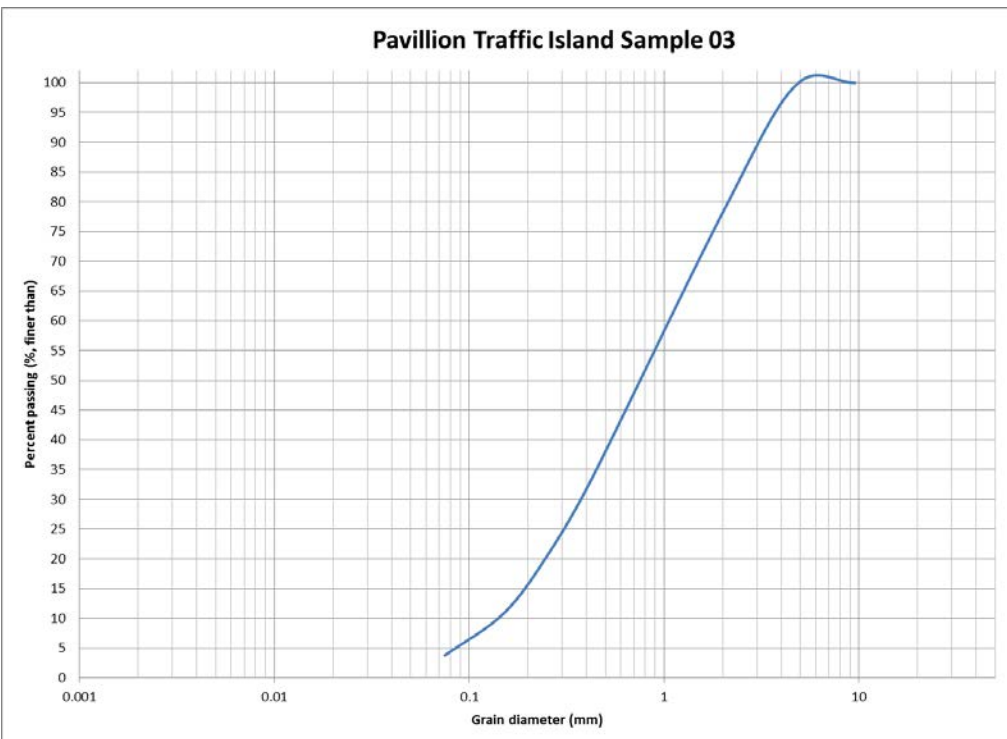
Figure A.5 PTI sample 3 grain size distribution

253

Table A.1. BTI moisture content test data

ASTM D2216						
Moisture Content						
Laboratory Number	20150205xxxxxxx-1	20150205xxxxxxx-2				
Exploration Number	Villanova BTI	Villanova BTI				
Sample Number	S1	S2				
Depth Range	0-2"	2-14"				
Test Method: Method A	x	x				
Method B						
Container/ Lid Number	SR4	SSS				
Container Mass, g (Mc)	14.4	15.1				
Container + Moist Specimen Mass, g (Mcms)	353	771.2				
Date / Time in oven						
Initial Container+Oven Dry Specimen Mass, g	184.3	649.1				
Date / Time out of oven						
Secondary Container+Oven Dry Specimen Mass, g	184.3	649.1				
Date / Time out of oven						
Final Container+Oven Dry Specimen Mass, g, (Mcds)	184.3	649.1				
Date / Time out of oven						
Mass of Water, g, Mw = Mcms – Mcds	168.7	122.1				
Mass of Solids, Ms = Mcds-Mc	169.9	634				
Water Content, %, w = (Mw/Ms)x100	99	19				
Maximum particle size (100% passing)						
3 in						
1½ in						
¾ in						
3/8 in		x				
#4	x					
#10						
< #10						
Tested Maximum Grain Size (mm)	3/8	#4				
Oven Temperature	110.0	110.0				
Remarks						
QA/QC						
Sample Size Check: (grams less)	Adequate	Adequate				
Tested by:	BA	BA				
Data Entry By:	BA	BA				
Data Entry Date:	02/05/15	02/05/15				
Checked By:	BA	BA				
Checked Date:	02/05/15	02/05/15				
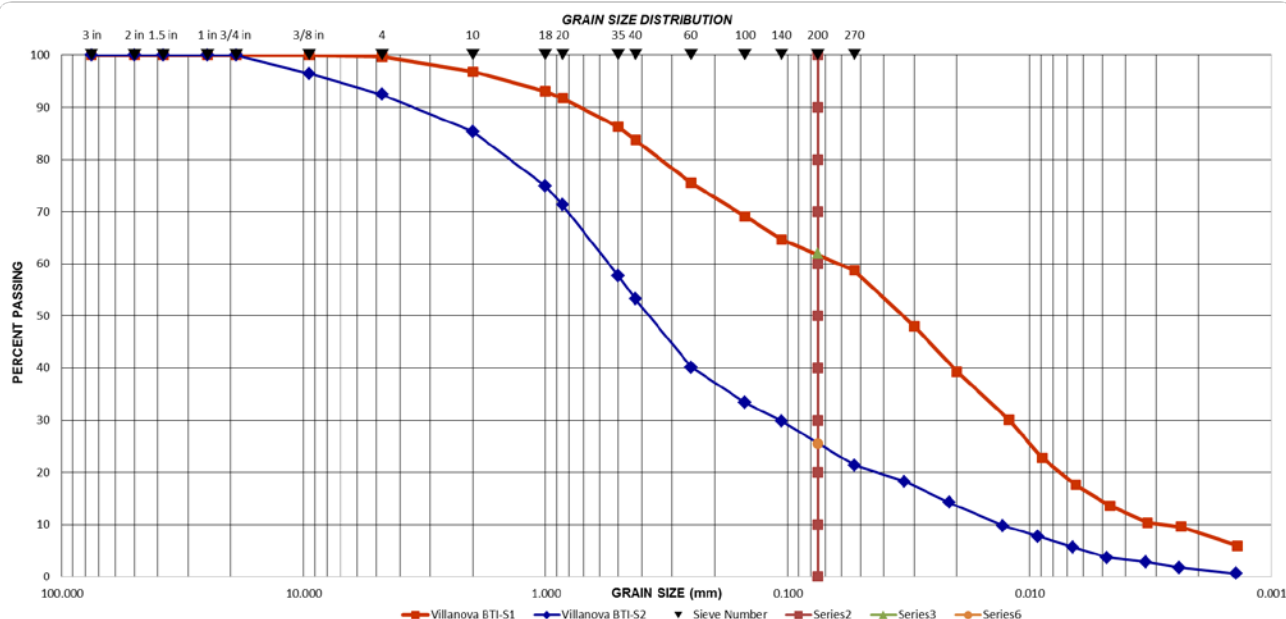
Figure A.6 BTI grain size distribution

254

Table A.2. BTI organic content test data

|			Test Method:		Method A	x	Method C
ASTM D 2974 Moisture, Ash, and Organic Matter of Peat and Other Organic Soils							
					Method B		Method D
Laboratory Number	20150205xxxxxxx-1	20150205xxxxxxx-2					
Exploration Number	Villanova BTI	Villanova BTI					
Sample Number	S1	S2					
Depth Range	0-2"	2-14"					
§ 8.1.1 Test Method A							
§8.1.1.1 Weight of Evaporating Dish (g)							
§8.1.1.3 Weight of Dish and Wet Soil (g)							
§8.1.1.4 Time In oven							
§8.1.1.4 Time out of oven							
§8.1.1.4 Dry Time							
§8.1.1.4 Weight of Dish and Dry Soil (g)							
§ 8.1.2 Test Method A - Results							
A = mass of as received test specimen (g)							
B = mass of oven-dried specimen (g)							
§8.1.2.1 Moisture Content – of Total Mass (%)							
§8.1.2.2 Moisture Content – of Oven-dried Mass (%)							
§ 8.1.3 Test Method B							
§8.1.3.2 Weight of Evaporating pan (g)							
§8.1.3.2 Weight of Pan and Wet Soil (g)							
§8.1.3.2 Begin Air drying							
§8.1.3.2 End Air Drying							
§8.1.3. Time of Air Drying							
§8.1.3.2 Weight of Pan and Dry Soil (g)							
A = mass of as received test specimen (g)							
A1 = mass of air-dried test specimen (g)							
M = moisture removed in air drying (%)							
§8.1.1.1 Weight of Evaporating Dish (g)							
§8.1.1.3 Weight of Dish and Air-dried Soil (g)							
§8.1.1.4 Time In oven							
§8.1.1.4 Time out of oven							
§8.1.1.4 Dry Time							
§8.1.1.4 Weight of Dish and Dry Soil (g)							
§ 8.1.3 Test Method B - Results							
B = mass of oven-dried specimen (g)							
§8.1.2.1 Moisture Content – of Total Mass (%)							
§8.1.2.2 Moisture Content – of Oven-dried Mass (%)							
§ 8.2.1 Test Method C & D							
§8.2.1.1 Weight of Crucible (g)	86.08	164.43					
§8.2.1.2 Weight of Crucible and Oven-dried Soil (g)	111.73	334					
§8.2.1.3 Temperature of furnace (℃)	440	440					
§8.1.1.4 Weight of Dish and Burnt Soil (g)	107.58	330.06					
§ 8.2.3 Test Method C & D - Results							
C = mass of ash, (g)	21.5	165.6					
§8.2.3.1 D = Ash Content (%)	83.8	97.7					
§8.3.1.1 Organic Matter (%)	**16.2**	**2.3**					
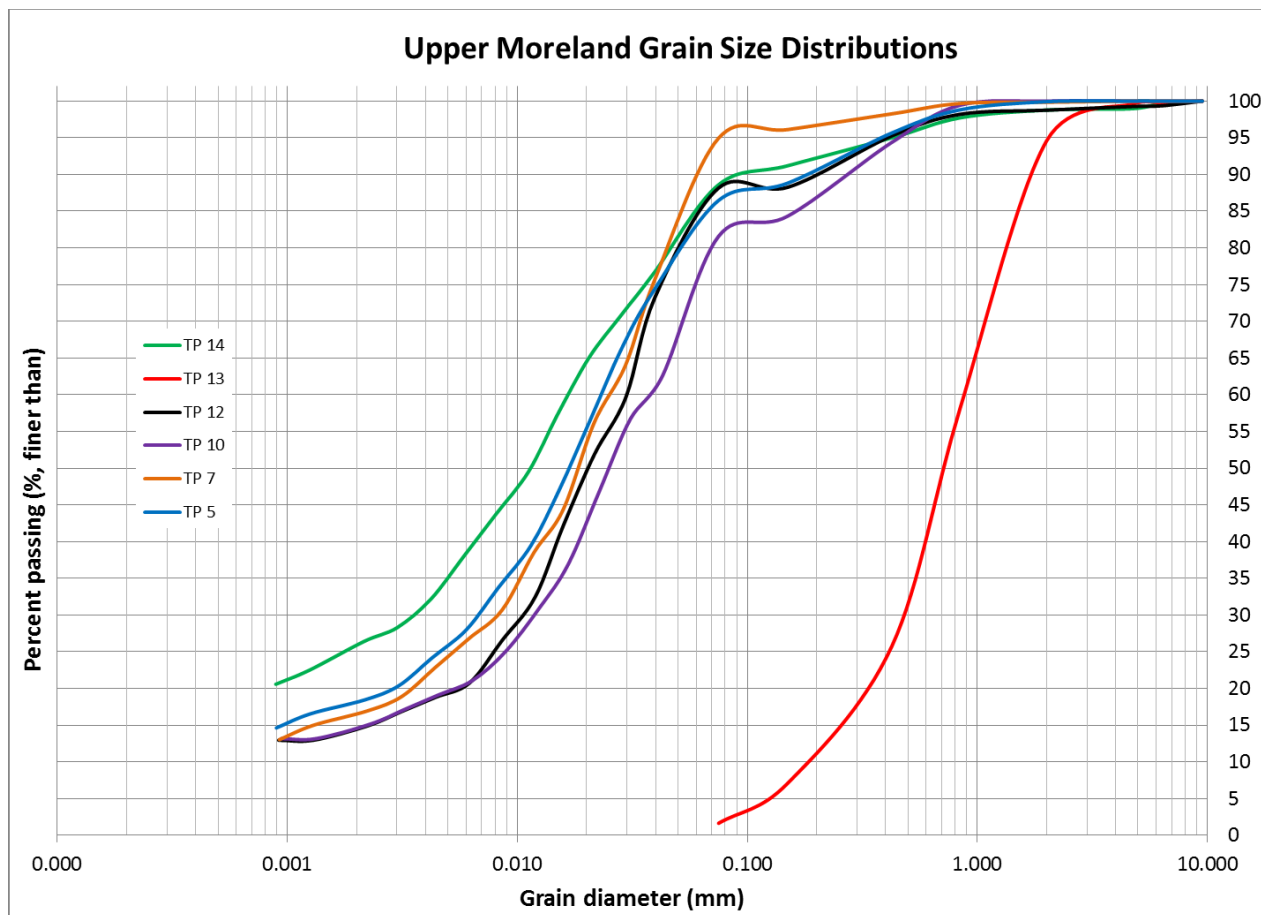
Figure A.7 Upper Moreland grain size distributions

Table A.3. Upper Moreland KSAT and dry unit weight data.

Sample Name	Saturated Unit Weight (g/cm^3)	Dry Unit Weight (g/cm^3)	KSAT (cm/day)	KSAT (in/hr)	Water Content at Saturation	Specific Gravity
TP 14	2.12	1.74	BDL*	BDL*	0.220467001	2.82
TP 13	1.96	1.60	108.864	1.7858	0.22823912	2.52
TP 12	2.05	1.64	1.011	0.0166	0.251160518	2.78
TP 10	2.01	1.60	0.4	0.0066	0.253366584	2.70
TP 7	2.00	1.58	0.703	0.0115	0.270115963	2.75
TP 5	2.17	1.80	BDL*	BDL*	0.208778966	2.87

* BDL = below detection limit

Table A.4. Upper Moreland liquid limit data

	Weight of Tin (g)	Weight of Soil + Tin (g)	Weight of Dry Soil + Tin (g)	Number of Blows	Water Content	Water Content (%)
TP 14 Liquid Limit						
Tin 1	15.5	42.2	36.3	36	0.283653846	28.36538462
Tin 2	16.2	56.9	47.2	25	0.312903226	31.29032258
Tin 3	15.6	50.1	41.8	24	0.316793893	31.67938931
TP 12 Liquid Limit						
Tin 1	16	62.2	53.4	29	0.235294118	23.52941176
Tin 2	11.6	43.7	37.7	31	0.229885057	22.98850575
Tin 3	15.7	51.6	44.3	21	0.255244755	25.52447552
TP 10 Liquid Limit						
Tin 1	15.6	47.7	41.3	35	0.249027237	24.90272374
Tin 2	15.9	52.6	44.8	23	0.269896194	26.98961938
Tin 3	15.5	59.4	50.7	37	0.247159091	24.71590909
TP 5 Liquid Limit						
Tin 1	15.6	52.7	44.8	32	0.270547945	27.05479452
Tin 2	16.2	53.2	45.6	34	0.258503401	25.85034014
Tin 3	15.6	47.9	40.7	28	0.28685259	28.68525896
TP 7 Liquid Limit						
Tin 1	16.1	50.1	42.7	29	0.278195489	27.81954887
Tin 2	16	46.1	39.4	27	0.286324786	28.63247863
Tin 3	15.9	45.6	39.6	35	0.253164557	25.3164557

Table A.5. Upper Moreland plastic limit data

TP 14 Plastic Limit	
Weight of Tin (g)	16.2
Weight of Tin + Soil (g)	27.4
Weight of Tin + Dry Soil (g)	25.3
Plastic Limit	23.07692308
Plasticity Index	8.275576923
TP 12 Plastic Limit	
Weight of Tin (g)	16
Weight of Tin + Soil (g)	26.8
Weight of Tin + Dry Soil (g)	24.9
Plastic Limit	21.34831461
Plasticity Index	3.170685393
TP 10 Plastic Limit	
Weight of Tin (g)	16.1
Weight of Tin + Soil (g)	25.8
Weight of Tin + Dry Soil (g)	24
Plastic Limit	22.78481013
Plasticity Index	3.861189873
TP 5 Plastic Limit	
Weight of Tin (g)	15.4
Weight of Tin + Soil (g)	34.8
Weight of Tin + Dry Soil (g)	31.2
Plastic Limit	22.78481013
Plasticity Index	7.346189873
TP 7 Plastic Limit	
Weight of Tin (g)	15.6
Weight of Tin + Soil (g)	20.6
Weight of Tin + Dry Soil (g)	19.6
Plastic Limit	25
Plasticity Index	4.4705

APPENDIX B: INSTRUMENT CALIBRATION DATA
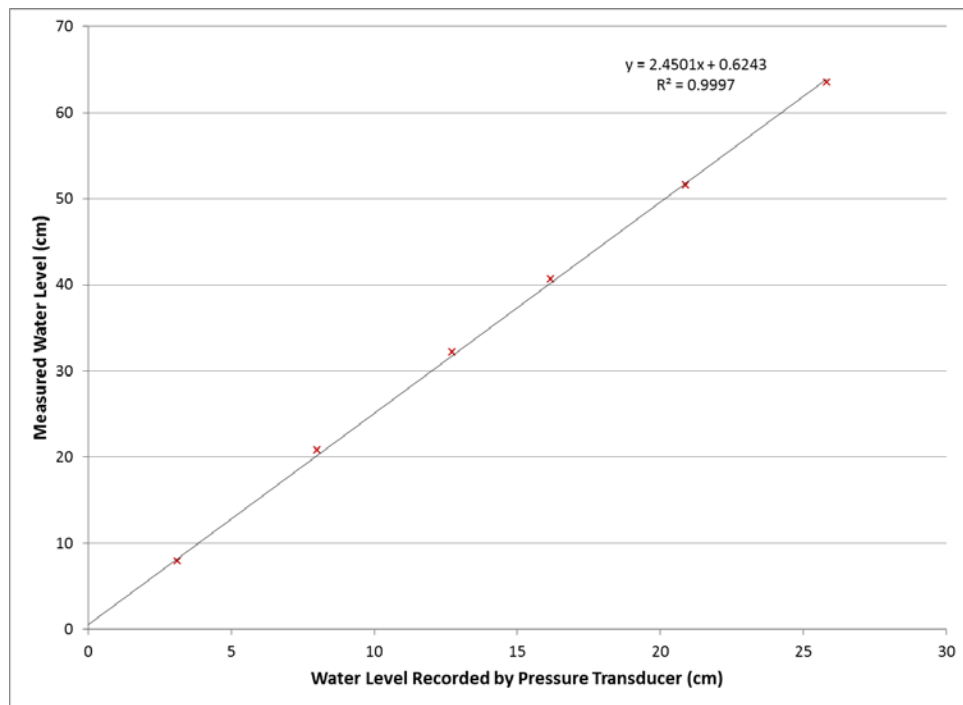
**Figure B.1** FRGI pond pressure transducer calibration
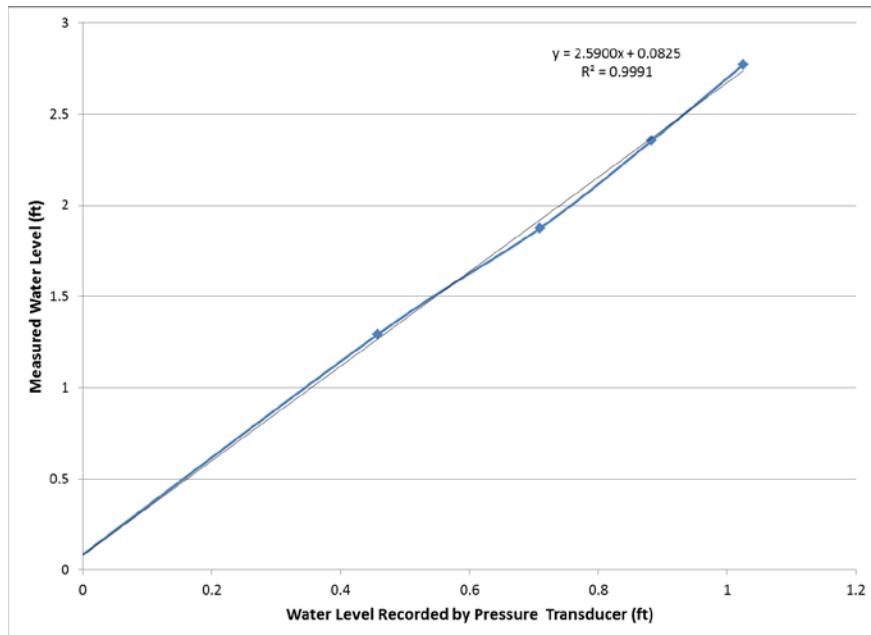

Figure B.2 FRGI overflow pressure transducer calibration
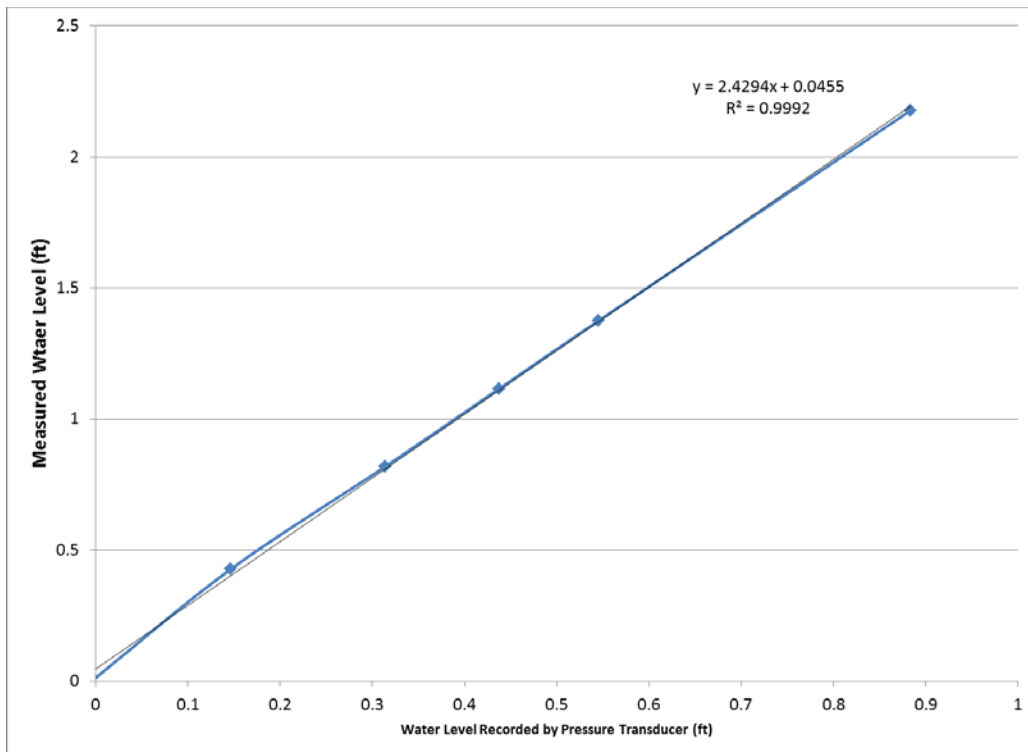
Figure B.3 FRGR pond pressure transducer calibration
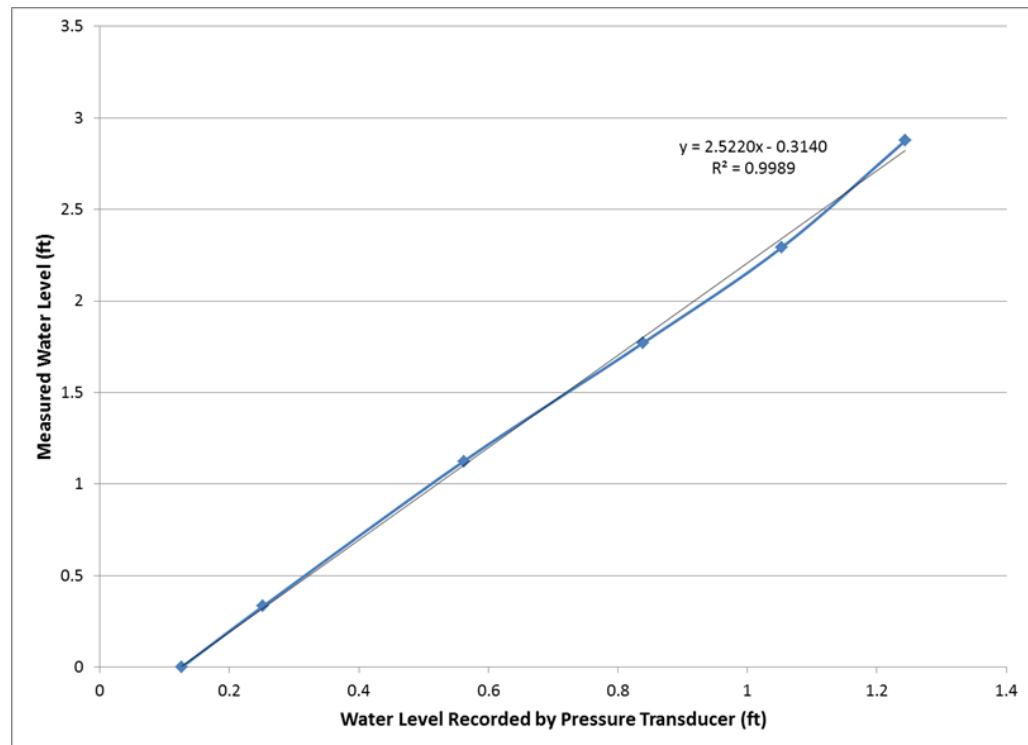

Figure B.4 FRGR overflow pressure transducer calibration

259
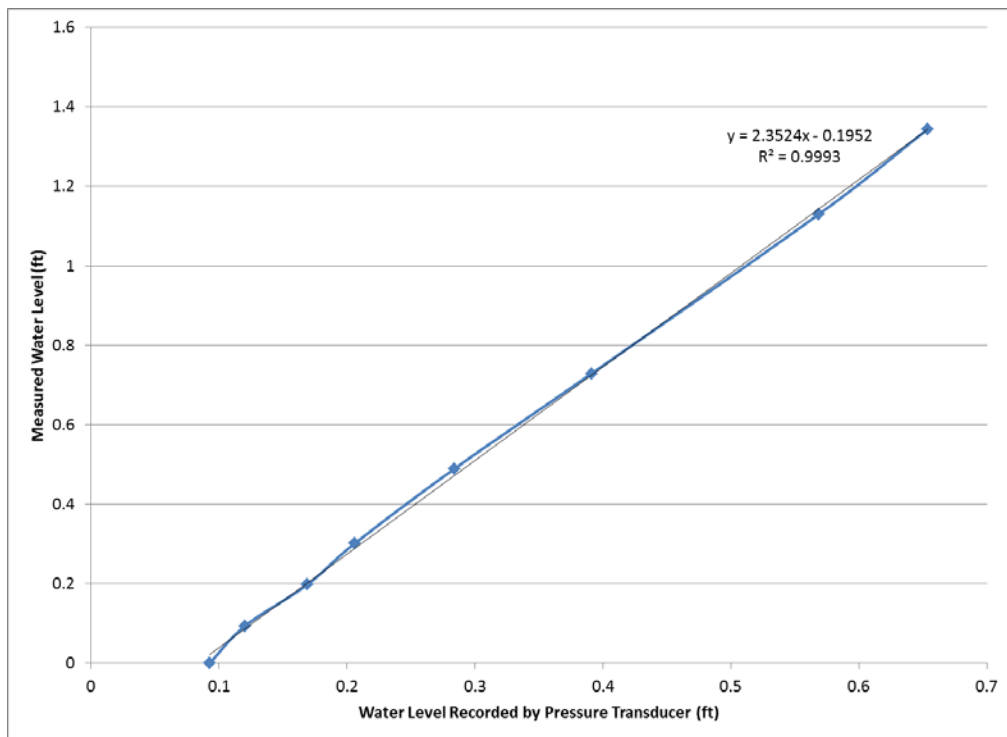
**Figure B.5** FRGI underdrain pressure transducer calibration
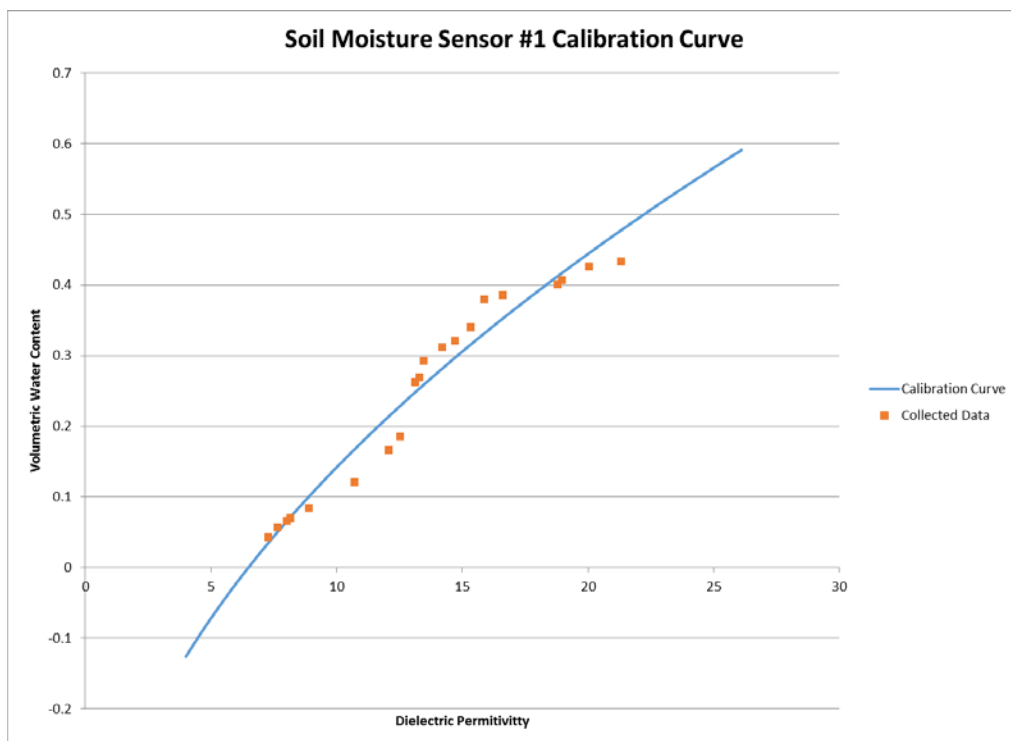
**Figure B.6** FRGI soil moisture sensor 1 calibration curve

260
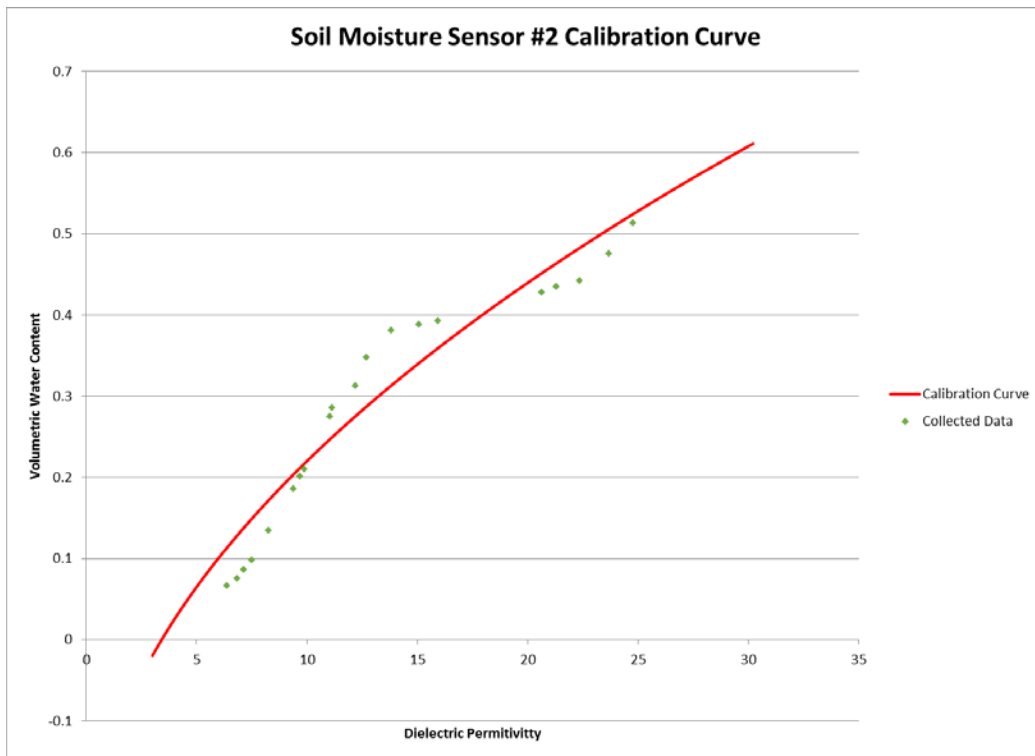
**Figure B.7** FRGI soil moisture sensor 2 calibration curve
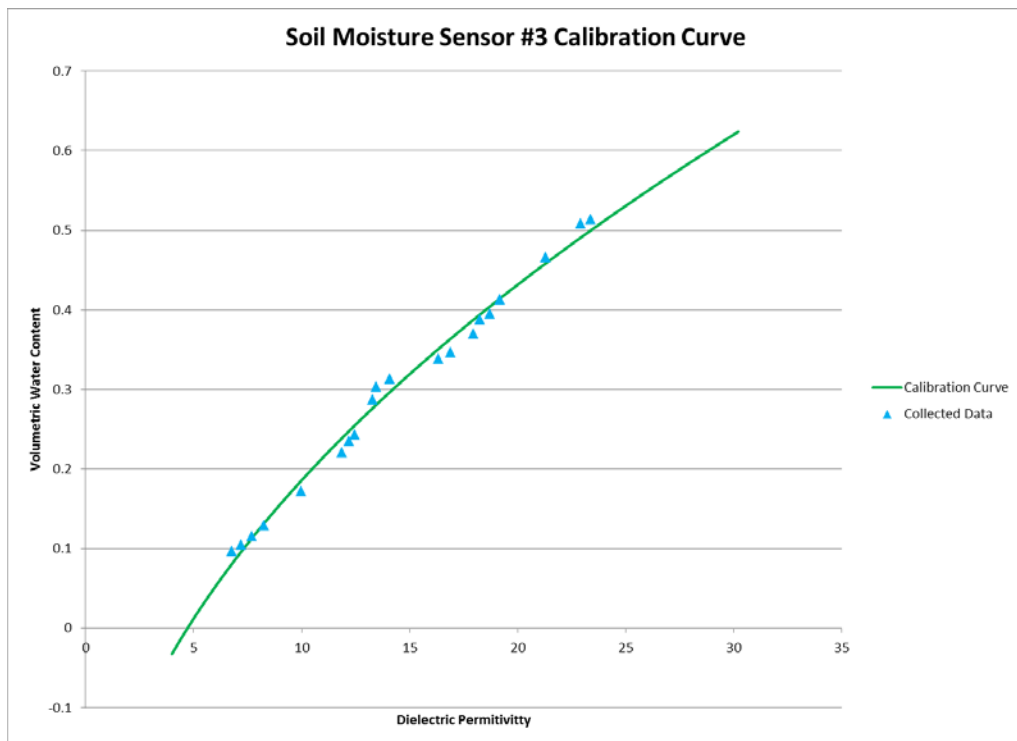
Figure B.8 FRGI soil moisture sensor 3 calibration curve
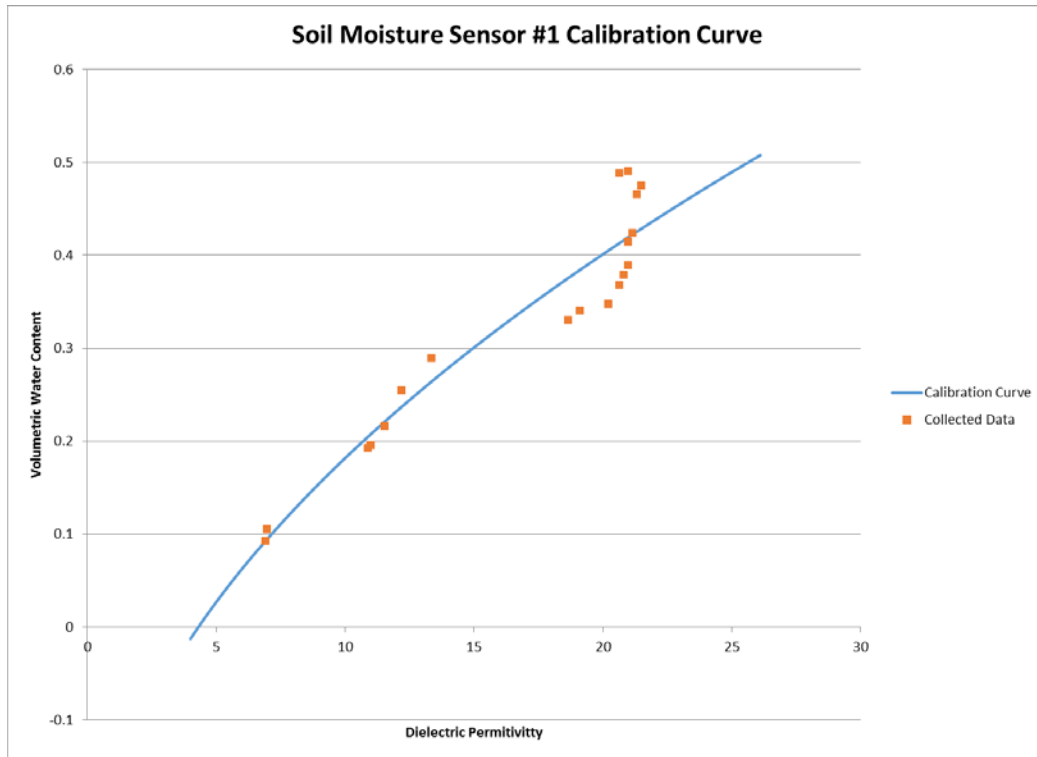
Figure B.9 FRGR soil moisture sensor 1 calibration curve
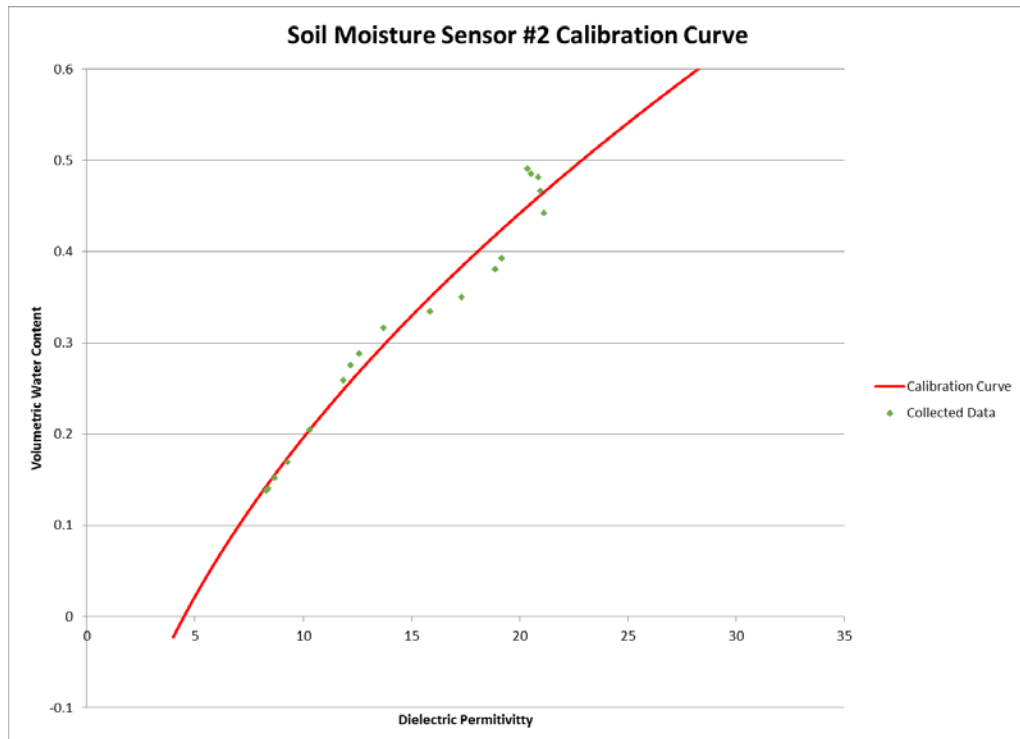
Figure B.10 FRGR soil moisture sensor 2 calibration curve
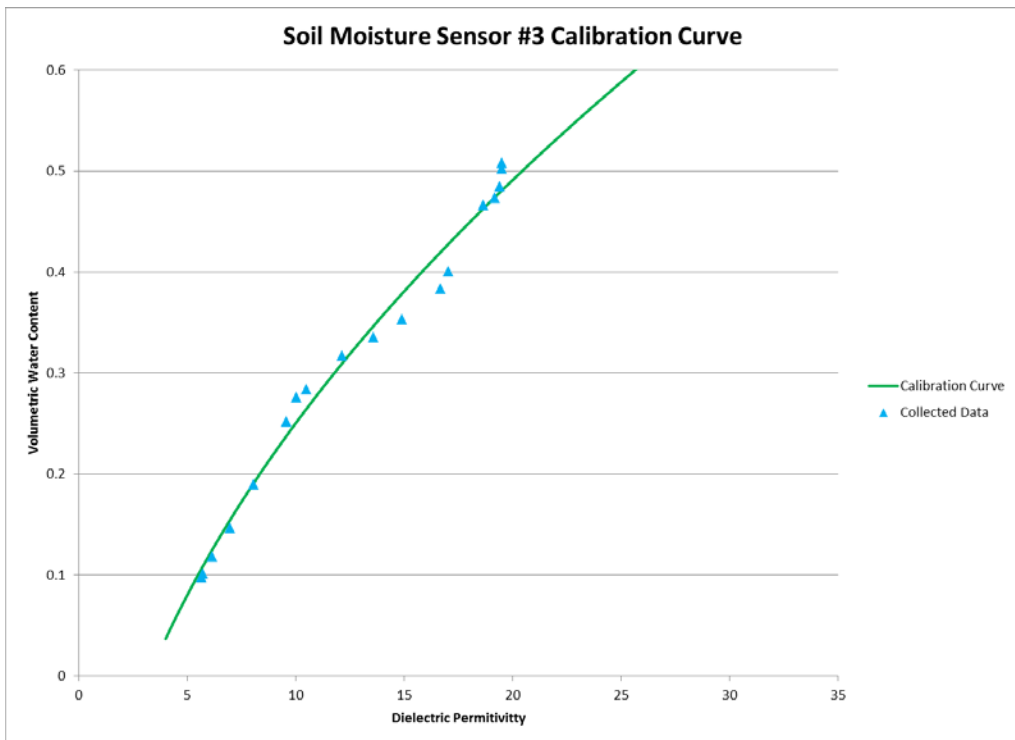
Figure B.11 FRGR soil moisture sensor 3 calibration curve
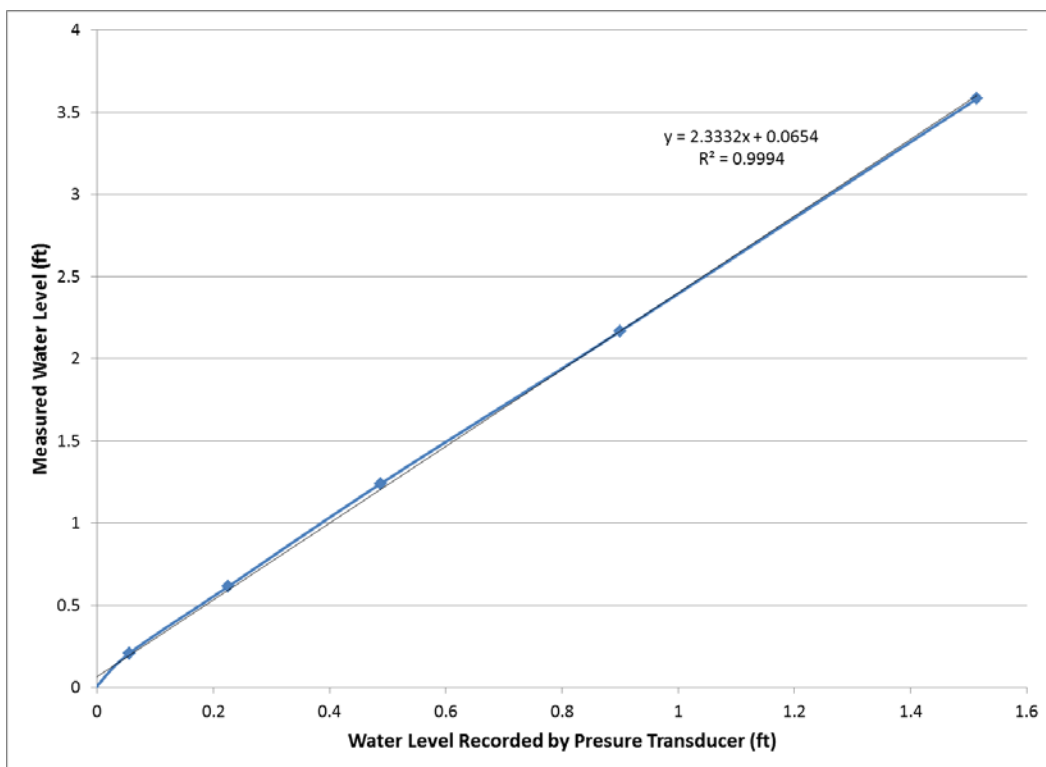
Figure B.12 PTI pond pressure transducer calibration

263
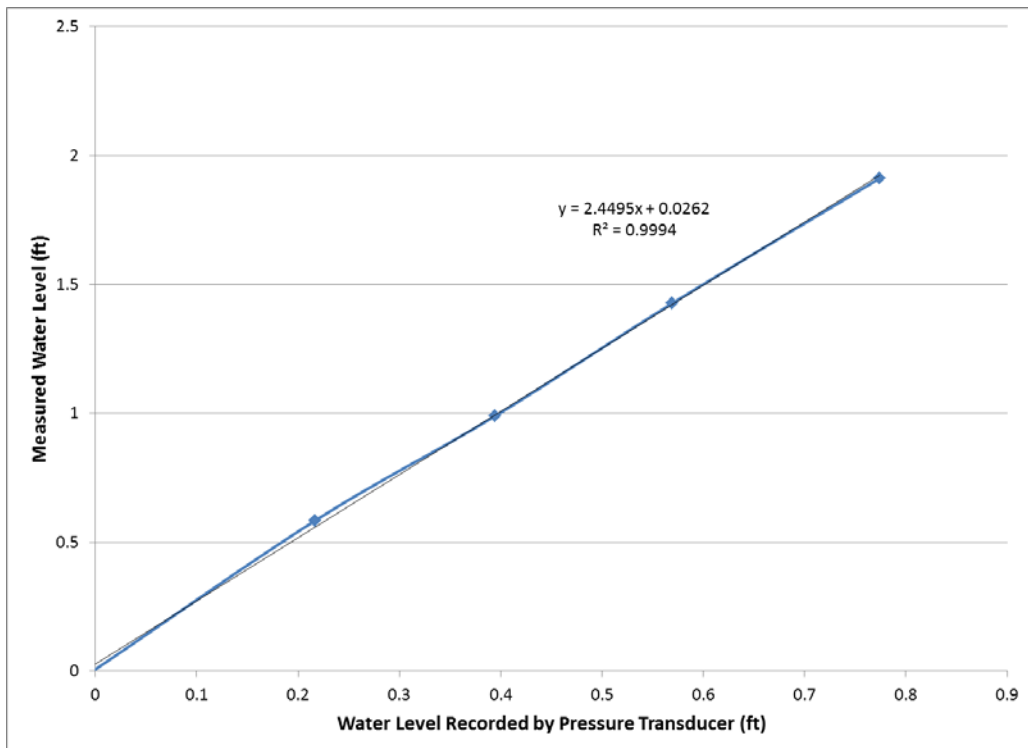
Figure B.13 PTI box pressure transducer calibration
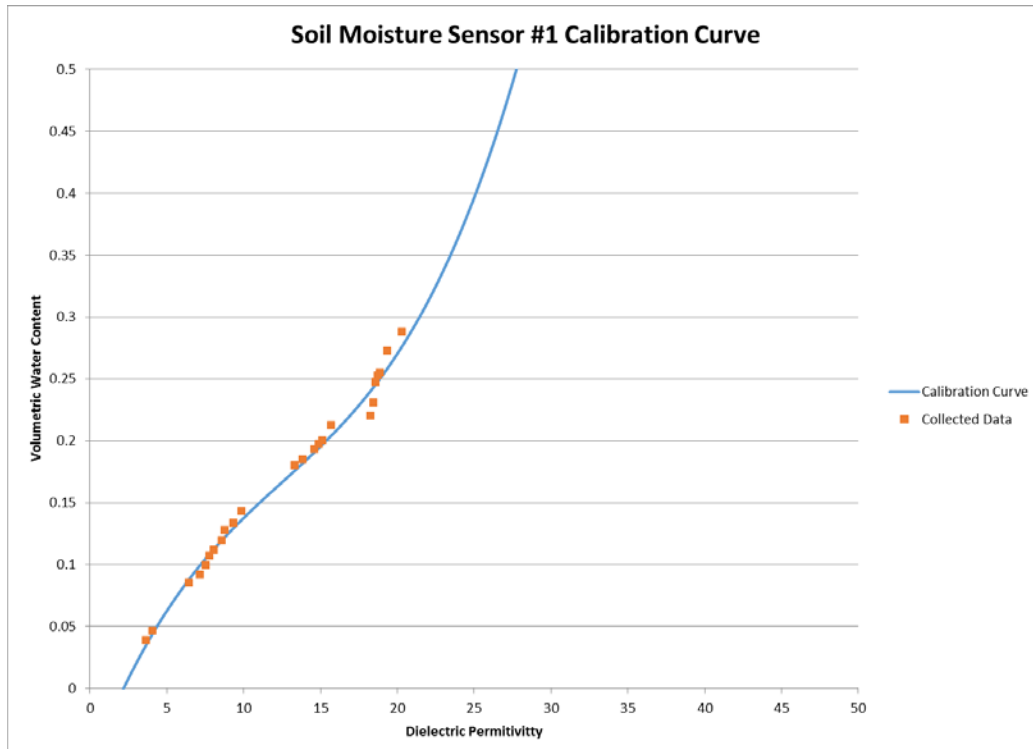
Figure B.14 PTI soil moisture sensor 1 calibration curve
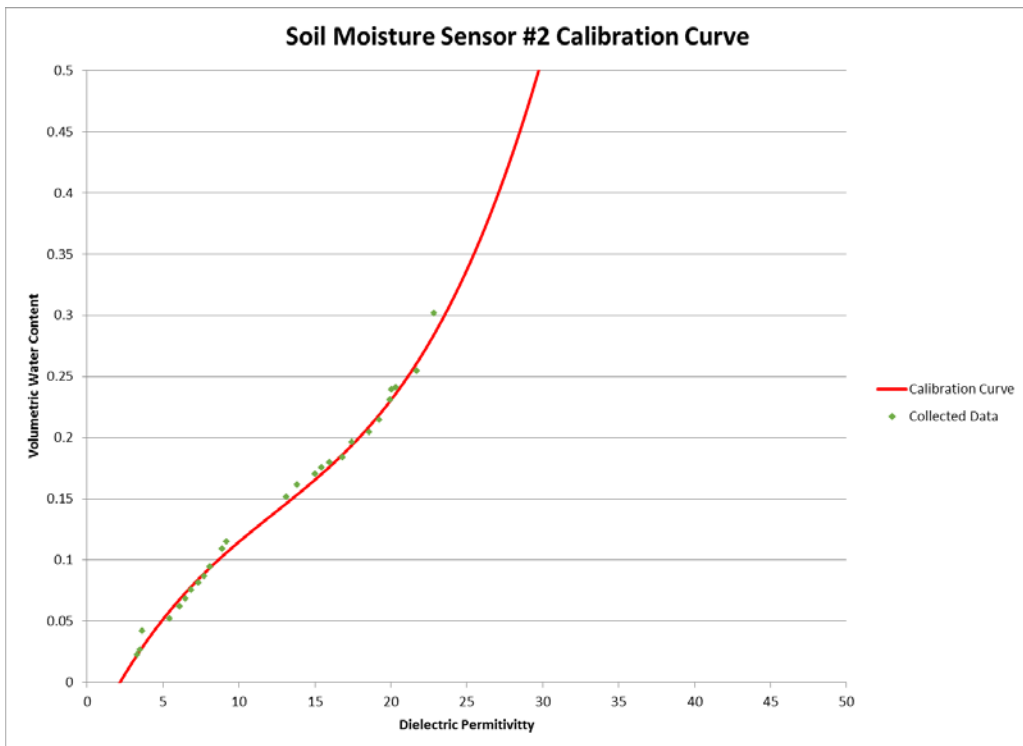
**Figure B.15** PTI soil moisture sensor 2 calibration curve
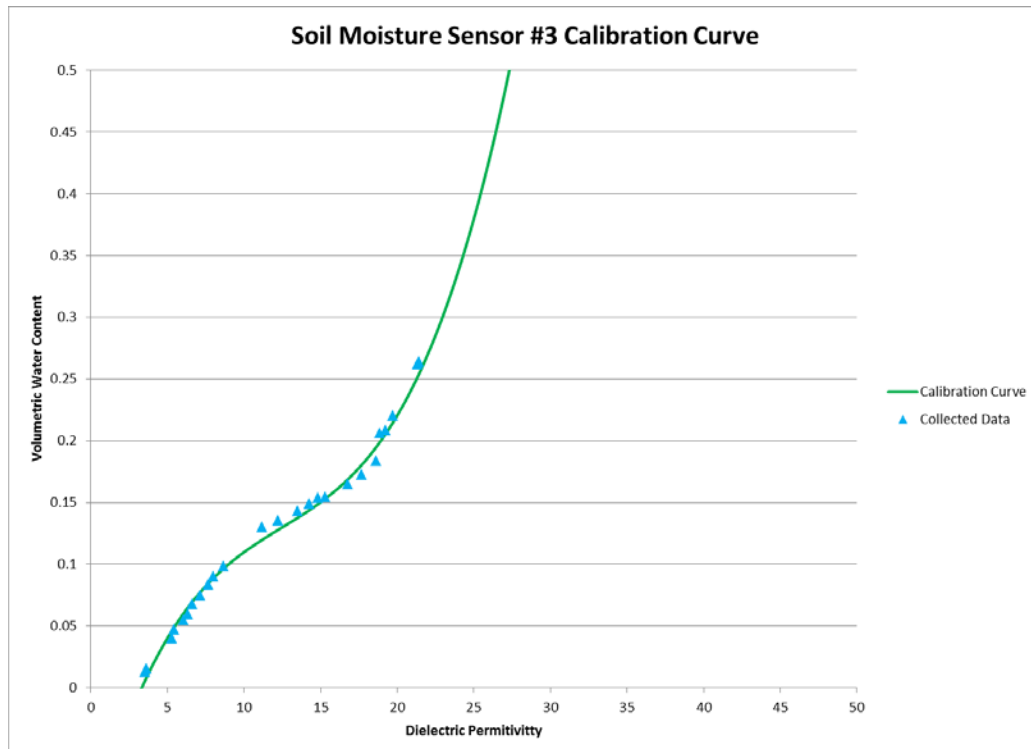
Figure B.16 PTI soil moisture sensor 3 calibration curve
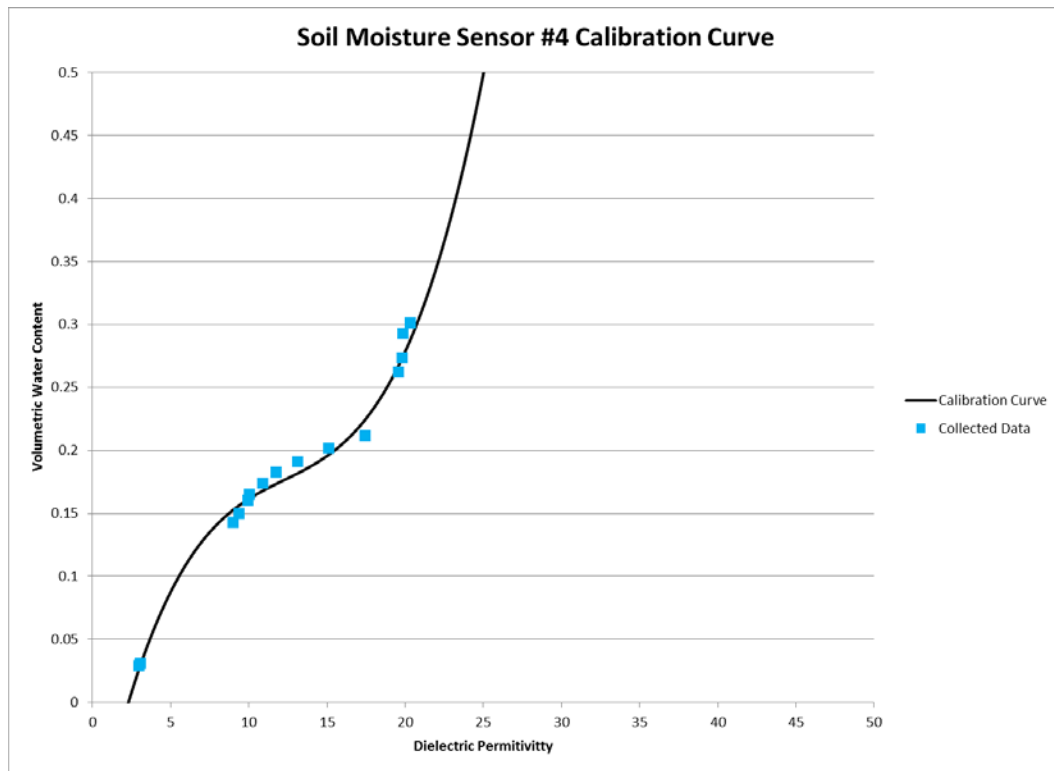
Figure B.17 PTI soil moisture sensor 4 calibration curve
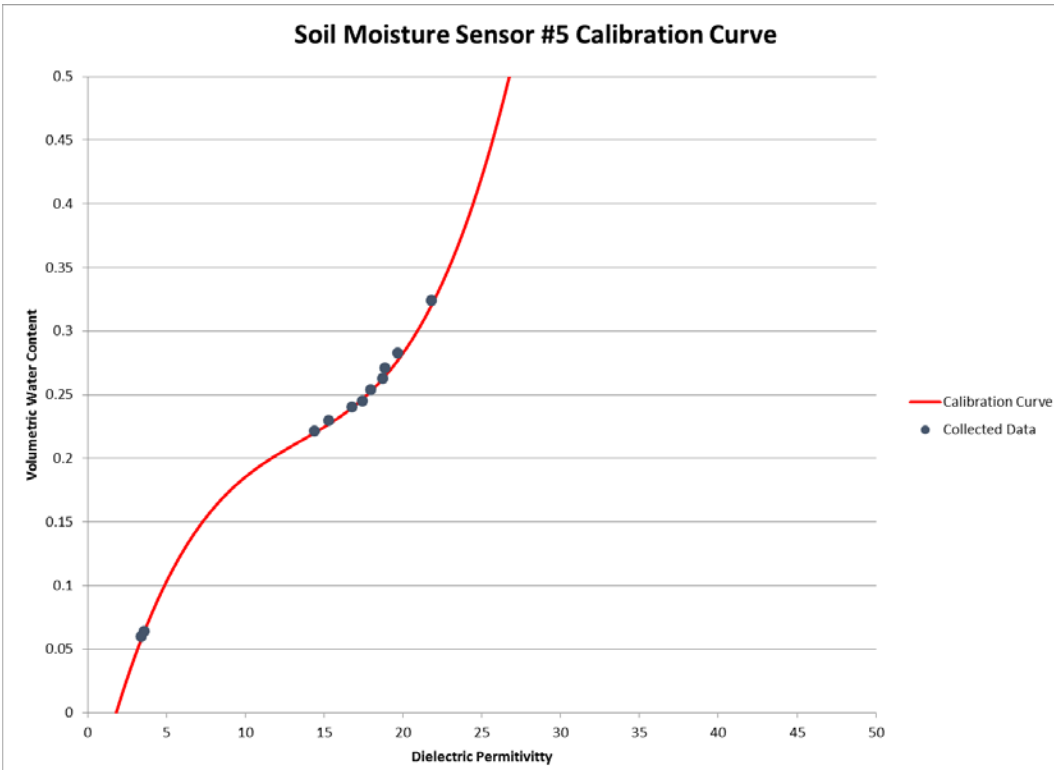
Figure B.18 PTI soil moisture sensor 5 calibration curve

266